

A STUDY OF AN ON-LINE RECURSIVE FILTER

APPLIED TO A MILLING CIRCUIT

by

Ian James Barker, B.Sc.(Eng), M.Sc(Eng)



Submitted in partial fulfilment of the requirements for
the degree of Doctor of Philosophy, in the Department
of Chemical Engineering, University of Natal, in 1975.

DURBAN

DECEMBER 1975

P R E F A C E

I hereby state that this thesis is my own original work, except where specifically indicated to the contrary in the text.

I.J. Barker.

I.J. Barker.

ACKNOWLEDGEMENTS

I wish to express my sincere gratitude and thanks to the many people who have contributed to the project. In particular, I would like to thank the following:

Professor E.T. Woodburn, and the academic, workshop and laboratory staff of Department of Chemical Engineering at the University of Natal, Durban,

Professor R.P. King, my supervisor, for suggesting the project, and for his helpful assistance during the course of the work,

My local supervisors, Dr R.C. Everson and Mr M.F. Dawson for the guidance which they gave,

The National Institute for Metallurgy, who generously provided financial assistance and sponsored the project,

The Phosphate Development Corporation for the supply of crushed rock,

Professor T.S. Mika, who provided a programme for calculation of grinding parameters,

The people who assisted me in operating the pilot-plant, in particular Mr M.F. Dawson, Mr D.G. Hulbert and Mr R.M. Finlayson,

My fellow students, particularly those of the National Institute for Metallurgy research group in the Department,

My typists for this thesis, Allison Hudson and Frances Manson,

My parents and my wife for their patience during the duration of the project.

CONTENTS

	Page
Title page	i
Preface	ii
Acknowledgements	iii
Contents	iv
 <u>Chapter 1 Summary</u>	 1
 <u>Chapter 2 Introduction</u>	 2
2.1 Background	3
2.2 Brief description of filter	4
2.3 Outline of work done and thesis	7
2.4 Units	8
 <u>Chapter 3 Literature survey</u>	 9
3.1 Modelling of grinding	9
3.2 Grinding circuit control	10
3.3 Measurement and control of particle size distribution	12
3.4 Cyclone and classifier modelling	13
3.5 Filtering theory - fundamentals	14
3.6 Applications of filtering	16
3.7 Methods related to the solution of nonlinear filters	17
3.8 Modelling for Kalman filters	18
 <u>Chapter 4 Theory</u>	 19
4.1 Basic filtering theory	19
4.1.1 Linear filtering theory	21
4.1.2 Nonlinear filtering theory	24
4.1.2.1 Extensions to linear filtering theory	24
4.1.2.2 Use of moments/...	

	Page
4.1.2.2 Use of moments	25
4.1.2.3 Orthogonal series approximations	27
4.1.2.4 Use of discretised state space	27
4.1.2.5 Differential quadrature	28
4.2 Modelling of grinding circuit operations	30
4.2.1 Comminution	30
4.2.2 Cyclone modelling	34
4.2.3 Modelling of random processes	36
4.2.4 Determination of noise levels in models	39
4.3 Development of filter for grinding circuit	41
4.3.1 Volumetric filter	42
4.3.2 Checks in volumetric filter	44
4.3.3 Particle size distribution model and filter	47
4.3.4 Solution of particle size distribution filter using moments	50
4.3.5 Conversion to particle size distributions and concentrations	53
4.3.6 Summary of p.s.d. filter	55
4.3.7 Use of filter	55
<u>Chapter 5 Equipment and Experimentation</u>	58
5.1 Milling circuit	58
5.2 'Control Data 1700' computer	64
5.3 Analyses	64
5.4 The ore	68
5.5 Off-line tests	69
5.5.1 Batch milling	69
5.5.2 Cyclone tests	70
5.5.3 Mill outflow characteristics	70
5.5.4 Calibrations of instruments	71
5.6 Runs done on mill for filter	72

Chapter 6 Results

6.1 Batch milling results	75
6.2 Errors in analyses	86
6.3 Cyclone data	89
6.4 Mill overflow characteristics	96
6.5 Results from runs on milling circuit	96
6.5.1 Run A	98
6.5.2 Run B	98
6.5.3 Run C	104
6.5.4 Run D	107
6.6 Values of parameters used in the filter	107
6.7 Results of filter tests on runs	115
6.7.1 Run A filter results	116
6.7.2 Run B filter results	117
6.7.3 Run C filter results	129
6.7.4 Run D filter results	134
6.8 Effects of various factors on filter	139
6.8.1 Efficacy of checks in the volumetric filter	139
6.8.2 Effect of cyclone model parameter errors	140
6.8.3 Effects of errors in grinding model parameters	146
6.8.4 Effect of feed size distribution and softness of rock	147
6.8.5 On-line regression of softness	149
6.8.6 Effects of observation errors	153
6.8.7 Effects of incorrect starting points	157
6.8.8 Frequency response of filter	157
6.8.9 Stability of filter	159
6.8.10 Time requirements	163
6.8.11 Simplified calculations	165
6.9 Results from differential quadrature filter	166

	Page
<u>Chapter 7 Discussion</u>	168
7.1 Results of off-line tests	168
7.1.1 Selections and breakage functions from batch mill tests	168
7.1.2 Cyclone model	169
7.1.3 Mill overflow and transport	169
7.1.4 Runs on milling circuit	170
7.2 Results from the filter tests	171
7.3 Effects of factors on filter	172
7.4 General use of real-time recursive filters	173
7.4.1 Determination of noise levels	173
7.4.2 Presentation of results	174
7.4.3 Advantages of a noisy system	175
7.4.4 Updating a filter	176
7.5 Necessary considerations in designing a filter	176
7.6 Comparison of methods for implementing a filter	177
7.7 Recommended procedure for practical filters	179
7.8 Comment on linear algebra	179
7.9 Estimation of a distribution	180
7.10 Advantages and disadvantages of practical use	180
<u>Chapter 8 Conclusions</u>	182
<u>Appendix A Equations for evolution of moments for the p.s.d. filter</u>	A1
<u>Appendix B Bibliography</u>	B1
<u>Appendix C Listing of programmes used in filter</u>	C1
<u>Appendix D Nomenclature and symbols used</u>	D1

LIST OF FIGURES

	Page
2.1 Basic signal flowchart with filter	3
2.2 Simplified flowchart of milling circuit	4
2.3 Block diagram of the filter which was developed	5
4.1 Block diagram of system	19
4.2 Comparison of Itô and Stratonovich definitions of a stochastic integral	37
4.3 Circuit showing symbols used for volumetric filter	42
4.4 Solids flows in the milling circuit	48
4.5 Filter flowchart	56
5.1 Flowchart of milling circuit	59
Plate 1 Discharge end of mill	61
Plate 2 Instrument cabinet on plant	65
Plate 3 Computer room	67
6.1 Results from batch grinds for runs 30/4 and 20/6	78
6.2 Selection functions for runs 30/4 and 20/6	81
6.3 Breakage functions for runs 30/4 and 20/6	82
6.4 Determination of effects of concentration and charge	85
6.5 Rate scaling factors against volume and concentration	87
6.6 Cyclone classification dependence on feed flow	90
6.7 Cyclone classification dependence on feed concentration	90
6.8 Corrected classifier constants against feed concentration (23/7, 5/8)	91
6.9 Corrected classifier constants against feed concentration (18/10, 23/10)	93
6.10 Dependence of cyclone underflow rate on feed conc and flow	95
6.11 Overflow test on mill	97
6.12 Run A - summary of stored data from run	99
6.13 Run B - summary of stored data from run	101
6.14 Run C/...	

6.14	Run C - summary of stored data from run	105
6.15	Run D - summary of stored data from run	108
6.16	Determination of noise levels in p.s.d. filter	114
6.17	Run A - volumetric filter results	118
6.18	Run A - predictions of cyclone overflow size distribution (softness = 0,2)	119
6.19	Run A - predictions of size distributions in cyclone underflow and mill contents	120
6.20	Run A - predictions and measurements of concentrations	121
6.21	Run A - predictions of cyclone overflow size distribution (softness = 0,5)	122
6.22(a)	Run B - volumetric filter results	123
6.22(b)	Run B - detail from fig. 6.22(a), volumetric filter results	124
6.23	Run B - predictions of cyclone overflow size distribution	125
6.24	Run B - predictions of size distributions in cyclone underflow and mill contents	126
6.25	Run B - predictions and measurements of concentrations	127
6.26	Run C - volumetric filter results	130
6.27	Run C - predictions of cyclone overflow size distribution	131
6.28	Run C - predictions of size distributions in cyclone underflow and mill contents	132
6.29	Run C - predictions and measurements of concentrations	133
6.30	Run D - volumetric results	135
6.31	Run D - predictions of cyclone overflow size distribution	136
6.32	Run D - predictions of size distributions in cyclone underflow and mill contents	137
6.33	Run D - predictions and measurements of concentrations	138
6.34	Volumetric filter without checks (run B data)	141
6.35	Effect of volumetric filter checks on p.s.d. filter predictions of concentrations	142

	Page
6.36 Effect of cyclone model changes	143
6.37 Effect of cyclone model changes	145
6.38 Effect of finer feed on cyclone overflow size predictions	148
6.39 Effect of finer feed on run A data. Size distributions of cyclone overflow and mill contents	150
6.40 On-line regression of softness	152
6.41 Effect of accentuated cyclone overflow concentration measurement	154
6.42 Effect of accentuated cyclone feed concentration measurement	155
6.43 Effect of reduced observation sensitivity in p.s.d. filter	156
6.44 Response from different starting points	158
6.45 Frequency testing of filter	160
6.46 Frequency testing of filter	161
6.47 Frequency testing of filter	162
6.48 Instability caused by wrong starting covariance matrix	164
6.49 Quadrature filter predictions	167

LIST OF TABLES

	Page
5.1 Specifications of milling circuit	60
5.2 Details of ball charges	62
5.3 Details of measurement and control devices	63
5.4 Details and specifications of the computer system used	66
5.5 Approximate data for the ore used	68
6.1 Batch milling results for run 30/4	76
6.2 Batch milling results for run 20/6	77
6.3 Regressed values of selection and breakage function for run 30/4	79
6.4 Regressed values of selection and breakage function for run 20/6	80
6.5 Selection and breakage functions for lumped size groups	84
6.6 Averaged feed size distribution	83
6.7 Typical particle size analysis errors	88
6.8 Corrected classifier functions, runs 23/7 and 5/8	92
6.9 Corrected classifier functions, runs 18/10 and 23/10	92
6.10 Corrected classifier functions, data from all runs	92
6.11 Cyclone flow data	94
6.12 Mill overflow model parameters	96
6.13 Analyses of samples for run A	100
6.14 Analyses of samples for run B	102
6.15 Analyses of samples for run C	106
6.16 Analyses of samples for run D	109
6.17 Standard values of parameters used in filter	110
6.18 Noise levels in volumetric filter	112
6.19 Reduced data for simplified grinding model	146
6.20 Computation times	165

Chapter 1

SUMMARY

The development and testing of a Kalman filter on a typical metallurgical plant is described in this thesis. A ball milling circuit, which was monitored by a medium-sized process control computer, was used.

A two-level filter was developed. The first level processed volumetric data, and estimated volumes and flows from the noisy measurements. The second level used these data and measurements of concentration to predict the masses in each particle size fraction around the circuit. From these, unmeasured variables, such as particle size distributions, were calculated and compared with samples.

Parameters for use in the filter had to be determined experimentally. When the filter was ready, runs were done on the milling circuit to get data, which were then used to do off-line testing of the filter. Once this was working satisfactorily, and its characteristics were understood, it was run in real time on the milling circuit. These results were successful and showed some of the problems associated with the actual application of such a filter in real time.

This thesis gives the development and subsequent testing of the milling circuit filter. It discusses the relevant literature, and goes on to present the theory and how the filter was built. The apparatus and experimentation, both off-line and on-line, are described. The results of the experiments and the filter computations are shown, and the effects of various factors on the filter are displayed. Finally, all the results are discussed in the light of using an on-line filter, and recommendations are made.

Chapter 2.

INTRODUCTION.

Kalman filters have been limited mainly to the aerospace industry in the past, but are potentially useful in a wide variety of industrial applications. The objectives behind this study were:-

- (1) To develop and test recursive Kalman type filters on metallurgical processes.
- (2) To determine and find solutions for the problems associated with their real-time use.
- (3) To devise methods of solving the filter equations in real time.

To do this, a pilot plant milling circuit in the Department of Chemical Engineering at the University of Natal was used. This plant was coupled to a CDC 1700 process control computer for control and data logging purposes. By means of a dynamic stochastic model for the grinding circuit, a filter was written and programmed to take measurements from the plant and predict the state. This gave (inter alia) the particle size distribution at any point in the circuit, which was then checked against samples taken.

Although the development of a useful filter depends on an adequate model of the process, it was not the aim of this investigation to make a detailed study of the modelling of comminution, or to develop optimal automatic control for a grinding circuit.

The use of a filter such as the one outlined here enabled dynamic estimation to be done on a milling circuit, unlike steady state predictions based on linear regressions.

2.1. Background

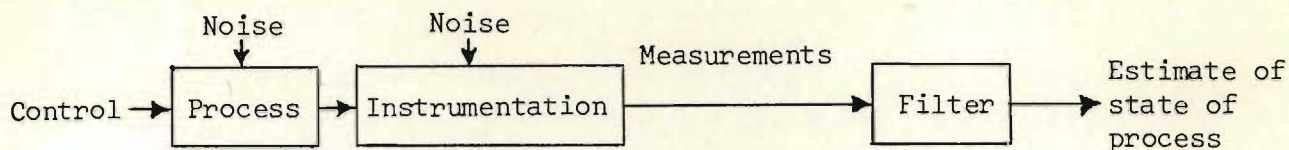


Figure 2.1. Basic signal flowchart with filter

Figure 2.1. shows how a filter is used to estimate the state of a process which cannot be observed directly and noiselessly. The filter cannot predict the state exactly, but rather the probability of a state, and this may be simplified to estimates of the mean and variance. A recursive filter treats the observations from the plant sequentially and, with a computer, observations are taken at discrete points in time. The filter contains a simplified model of the process and corrects its own estimates from the actual observations as the plant is operating.

Since 1960, when Kalman first proposed his form of a recursive filter, a lot of fundamental work in developing the theory has taken place. The aerospace industry has been a profitable area for applications and most of the early reports came from missile guidance applications. The use of recursive estimation and filtering on industrial plants has not been reported as much, but it has been shown to be successful. There are a number of problems associated with plant use, such as the formulation of a filter and its solution in real time for a generally nonlinear problem. There are also operational difficulties which are often overlooked in theoretical or simulated studies. The reason that this project was started was to investigate these problems on an actual plant in real time.

On the metallurgical side, there has been a considerable increase in the use of automatic control and computer control recently. Plant disturbances here are large (compared to aerospace work) and instrumentation on the key variables is often poor or non-existent. On-line estimation is suited to this sort of problem. For example, a milling circuit is a severe test for a filter.

It is subject to disturbances which cannot be measured, such as solids feed variations in hardness or size, a relatively large yet poor model, a state (i.e., masses in each particle size fraction) which cannot be measured directly, and observations of concentrations which are inherently clouded by noise. The pilot plant milling circuit in the Department was a suitable subject for this investigation.

2.2. Brief description of filter

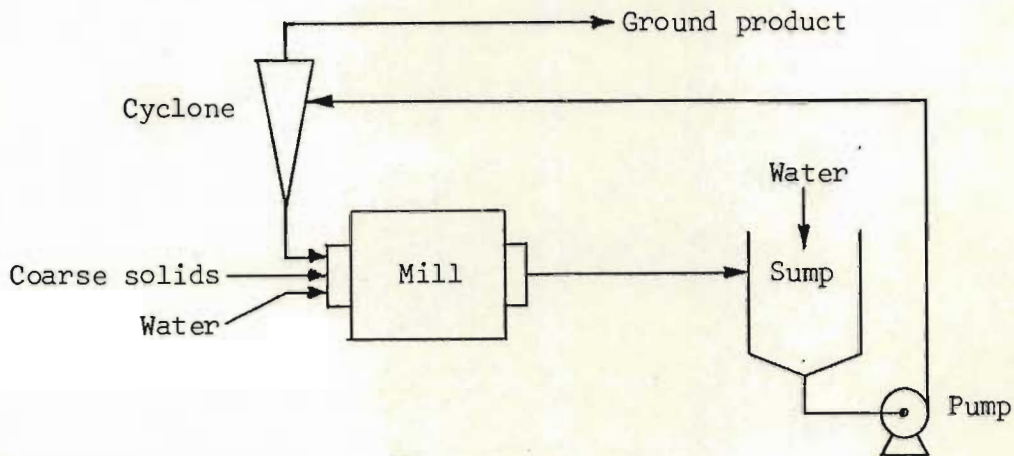


Figure 2.2. Simplified flowchart of milling circuit

The wet ball milling circuit shown in Figure 2.2. was used. It was instrumented and connected to the computer so that all control was D.D.C.* By this means it was possible to store the operating data for subsequent use, as well as having powerful computing facilities available while running the plant.

* D.D.C. = direct digital control.

Figure 2.3./...

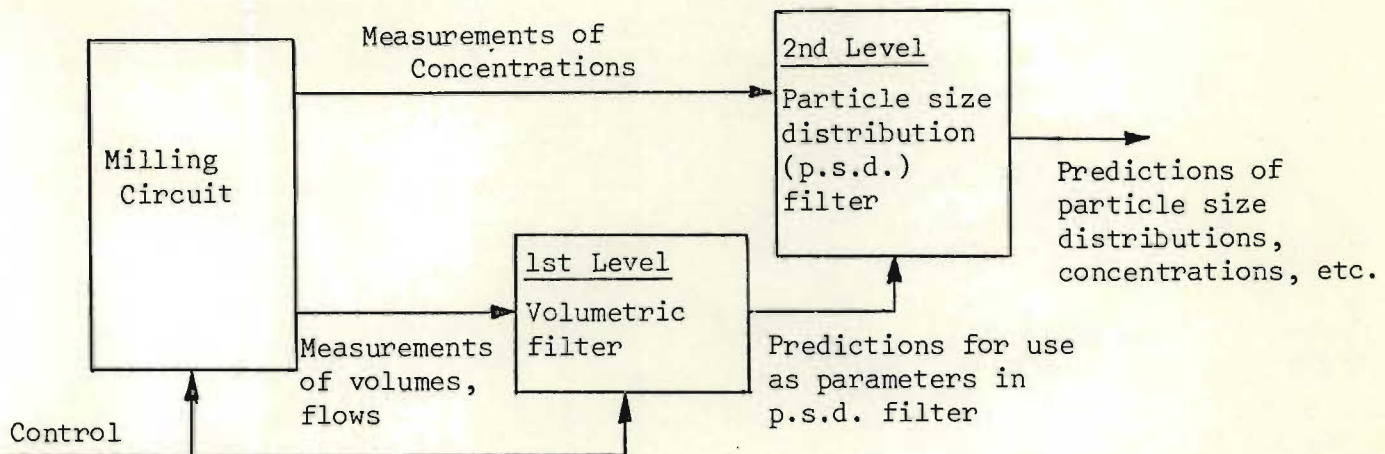


Figure 2.3. Block diagram of the filter which was developed

The signal flowchart of the filter is shown in Figure 2.3. Because a complete model of the milling circuit is highly nonlinear, the filter was split into two levels. This also saved some complexity. The volumetric filter handled only the volumes and volume flows around the plant. The particle size distribution (p.s.d.) filter dealt with the grinding and the classification of the rock carried in the slurry. It took measurements of concentrations of cyclone feed and overflow, and used data from the volumetric filter as parameters, to predict the masses in each size fraction in the mill and sump.

The volumetric filter was a linear Kalman-Bucy continuous-discrete filter. Its state variables were the volumes in the mill and sump, and control parameters were the water additions to the mill and sump, the solids feed (as a volume feed rate), and the sump to cyclone flow rate. Its state model was obtained by writing volume balances over the mill, sump and cyclone. Its observations consisted of single state or control variables, and so they could be handled one at a time.

The volumetric filter was assumed to be independent of the results from the p.s.d. filter, i.e., it was assumed that the volumetric models and measurements were not affected by either quantity or size of the solids present. This was justified sufficiently (see results) to be of use. The errors associated with the volumetric estimates were assumed to be small compared to the errors in the p.s.d. filter, so that the mean values of the volumetric estimates might be used as deterministic parameters in the p.s.d. filter.

The p.s.d. filter was a nonlinear filter. The particle size range was discretised into four size groups, and the masses in each size group in the mill and sump were the state variables (i.e., dimension of state = 8). These masses were random variables with their own probability distribution, which should not be confused with the particle size distribution.

The normal comminution equations for a continuous mill were written as stochastic differential equations with the rates of grinding as the random input. The cyclone model used was a simple one with the reduced classification constants for each size group dependent linearly upon the feed concentration. A mass balance for each group around the sump completed the state model. This formed a set of eight stochastic differential equations. The use of moments was found to be the most practical method of solving the set, although closure approximations were needed. A technique using differential quadrature was also tried, with only limited success.

The observations used in the p.s.d. filter were the cyclone feed and overflow concentrations. Using the cyclone model, these were written in terms of the mass in each size fraction in the sump, and so the observation step of the p.s.d. filter was derived, using a simplified second order extended Kalman filter observation step.

The filter was run/...

The filter was run recursively. The volumetric filter was run first after each observation, and the results from this were then used in the p.s.d. filter. Finally, if it was required to display the results, the distributions and concentrations around the circuit were calculated from the p.s.d. filter results.

This filter was used on data from the mill and was found to have reasonable agreement with the samples taken. These results are discussed at length in this thesis. The cyclone overflow was used most often for samples, as the sizing in this stream is an important criterion for mill operation. The sizing generally agreed well with the predictions, although the concentrations were more scattered than expected.

The effects of a number of factors on the filter were also investigated, and information about its operation was collected to determine what considerations would be important in designing filters such as these in the future. Experience was gained on the practical side of filter application and this is reviewed in the discussion.

2.3. Outline of work done and thesis

At the beginning of this investigation, much of the relevant literature was studied, on both filtering theory and milling. Some stochastic modelling was tried with simulations on the computer, and some elementary filtering theory was tested out in real time on the slurry mixing tanks for the flotation plant.

The pilot plant milling circuit in the Department was instrumented and prepared for use in this project. The milling circuit filter was also developed. A number of preliminary off-line tests were done to get parameters for the filter and calibrations for the instruments. Some simple runs were done on the circuit to test it out and get data for

filtering. From these results, further off-line tests and runs on the circuit were performed. This gave a lot of stored data for evaluating the filter. After determining the effects of various factors in the filter on stored data, the filter was run in real time on the mill and its performance was evaluated.

This thesis concentrates on development of the filter and its subsequent testing. Pertinent literature is surveyed in Chapter 3, and is listed in the bibliography in Appendix B. Chapter 4 develops the filter, and summarises the basic theory on filters and modelling which was used. Details of the equipment used, and the experimental procedure are presented in Chapter 5. This includes details of the milling circuit, computing facilities, and some of the basic software. The test procedure, both off-line and on-line, and methods of analysis are given. The results of all the work are presented in Chapter 6. The results from off-line tests for determining parameters in the model, graphical records and details of the runs done on the mill, and computed results from tests on the filter are given. All the results are discussed in Chapter 7, and the final conclusions are listed in Chapter 8.

2.4. Units

Basic S.I. units have been used throughout (except where quoting nominal sizes of equipment). Slurry concentration (kg solids/m^3 slurry) is used in preference to percent solids by mass, as the latter is nonlinear in the quantity of solids present.

Chapter 3

LITERATURE SURVEY.

This chapter is not intended as an exhaustive survey of all the literature available, but rather as a description of the literature which was used for this investigation. It can be divided into two main classes: the one relates to milling circuit operation and modelling, and the other to filtering theory. An alphabetical list of all the references appears in Appendix B.

3.1 Modelling of Grinding

Early modelling of grinding was based on energy considerations, and gave rise to models such as those of Kick, Rittinger and Bond (see Austin 1973(a), Mular and Bull 1969, Perry 1963, Taggart 1927). At present, the form of model most widely used is based on the sizing analysis and the rates of grinding from one fraction into smaller fractions. This is the selection and breakage function model, originally given by Epstein (Austin 1971/72). Broadbent and Callcott (1956) published the discrete version of this model. Apart from the generally understood fact that the selection for breakage is a random process, (originally proposed by Kolmogorov in 1941 - see Austin 1971/72) there have been very few attempts made to model grinding as a stochastic process. An important paper in this field is by Filippov (1961, see also Goren 1968). It is interesting to note that the handling of the selection function as a random process in some publications is slightly incorrect in the light of stochastic calculus. This is explained in section 4.2.3.

When applying the grinding model to practical problems, it is necessary to know the effects of various operating variables on the basic parameters in

the grinding model/...

the grinding model. The number of publications of use here is large, but the following were found particularly useful:

- (1) A sequence of papers by the division of Chemical Engineering, CSIRO, Australia, on the effects of various parameters in wet ball and rod milling. (Heyes, Kelsall, Stewart 1973(a) and (b), and Kelsall, Reid, Restarick 1967/68, 1968/69, 1969/70, 1973(a) and 1973(b)).
- (2) Austin (1973(b)).
- (3) Herbst and Fuersteneau (1972).
- (4) Clark and Kitchener (1968).
- (5) Herbst and Mika (1973).

Many attempts have been made to obtain a general solution to the grinding equation, suitable for practical use. Analytical solutions usually require rather major restrictive assumptions. An interesting analytical solution to the batch grinding equation is given by King (1972a).

Gardner and Verghese (1975) give a very simple analytical solution to a steady state grinding circuit model, which had already been used indirectly by Herbst and Mika (see below). Luckie and Austin (1972) have published programmes useful for grinding circuit modelling. Austin and Klimpel (private communication) have developed a programme to regress on grinding data. They use functional forms for the selection and breakage functions. Herbst, Grandy, Mika and Fuersteneau (1972) have described another similar programme which they have developed which can fit individual selection functions (see also Herbst and Mika, 1970). Both these programmes were made available to the author during this investigation.

3.2 Grinding Circuit Control

It is only fairly recently that sophisticated control or even simple control has been applied to grinding circuits. The conventional grinding

circuit with a cyclone/...

circuit with a cyclone is open loop stable (except for sump level control) and although the dynamic response is poor, it is slow and amenable to manual control. The number of control strategies which have been tried are enormous, and are evidence of the problem involved. Descriptions of some of the more common methods being used and reports on some specific projects are given by Birch (1972), Stewart (1970), Rowland (1963), Weiss (1960), Cross (1966), Pownall (1964), Williamson (1960), and Draper, Dredge and Lynch (1969).

The advent of computers for control, with their flexibility, has yielded a number of reports of their applications to grinding circuits: Lees (1971), Wiegel (1973), Timm and Williams (1970(a) and 1970(b)), Smith and Lewis (1969), Lewis (1970/71), "The Kloof Concentrator" (1973 - no author given), Fewings (1971), Fewings and Pitts (1973), Lynch and Stanley (1971), Brookes, Cutting, Watson (1970), Peterson, White, Krist (1974), King (1972(d)). Amsden, Chapman and Reading (1972) reported a simple installation on the Ecstall flotation plant which paid for itself in two months. Brittan, see e.g. Brittan and van Vuuren (1973) has achieved remarkable success with off-line optimisation. A useful survey was done by White (1974) to test how industry was responding to instruments and controls in mineral processing works. (See also Kelly 1973) Grinding circuit control also forms part of the control packages being offered by some large companies e.g. Outokumpu Oy. (see Leskinen & Penttilä 1973). Ol'skii (1971) reports similar trends towards computer control in Soviet mining and mineral undertakings.

There have not been many attempts to analyse the control dynamics of grinding circuits on a theoretical basis. This unfortunate position is probably indicative of the gap which exists between the practising metallurgists and control theorists. Brookes, et. al. (1969) modelled the

grinding but controlled the mill separately. Steady state regressions have been used by Watson et. al. (1970) and the group at the University of Queensland, see e.g. Fewings (1971) and Lees and Lynch (1972).

Schonert (1969) attempted to analyse the effects of the classifier characteristics. Woodburn (private communication) is taking a dynamic "black box" approach, and is using multivariable linear control theory to solve the problem. Crosby (1967) discussed mill circuit dynamics rather qualitatively, as did Freeh et. al. (1973).

3.3 Measurement and Control of Particle Size Distribution

Recently, a number of papers have appeared, proposing various methods of on-line particle size measurement. Autometrics are now marketing a unit, the PSM system-100, which uses ultrasonics. Several authors have reported favourably on its use - Diaz and Musgrove (1971), Bassarear and McQuie (1972), Hathaway (1972), Dart and Sand (1973), Webber and Diaz (1973), Lloyd, Atkins and Hind (1974). Unfortunately, it is expensive and very little information on its actual operation is available. Beck, Lee and Stanley-Wood (1973) have developed a technique which monitors the eddies present in a slurry stream and correlates these with the sizes of particles present. Osborne (1970 and 1972) describes an instrument originally developed by the Royal School of Mines, London (see Holland-Batt (1968)). This instrument uses a loop in the pipe to classify the slurry stream and then detects differences in density with a nuclear gauge. Ricci (1970) dilutes the slurry stream and then uses a light scanning device to "see" the particles. Carr-Brion and Mitchell (1967) use an X-ray technique.

No papers or reports have been found which deal directly with the use of on-line filters for the prediction of particle size distribution in a

milling circuit for the purposes of control. Fournier and Smith (1972) at the University of Toronto have been engaged in a programme of developing observers for milling and flotation plants (see also Fournier 1971). The group at the University of Queensland have developed steady state linear regressions relating product particle size to various operating measurements (similar to their cyclone model) and have used these for control (Fewing 1971, see also Peterson et. al. 1974).

3.4 Cyclone and Classifier Modelling

The detailed quantitative modelling of a cyclone has not been taken very far. Kelsall (1952) described the trajectories of single particles in a cyclone. Bloor and Ingham (1973 (a) and (b)) attempted to derive efficiency curves from a model of the fluid dynamics of the system. It is interesting that a stochastic model of the cyclone has been published by Molerus (1967).

Early reports on cyclones generally concentrated on the influence of design variables, e.g. Fontein, van Kooi and Leniger (1962). Bradley (1965) published a book on hydrocyclones, giving general correlations and design criteria.

The group at the University of Queensland have published a number of useful correlations. Two that were used frequently in this investigation were Lynch and Rao (1967) and Lees (1968). Mular and Bull (1969) summarize some of these results in their course. Other references giving useful operating information are Kanungo and Rao (1973), Lynch, Rao and Prisbey (1974), Tarr (1965) and figure 2 in Peterson, et. al. (1974).

Earlier in this investigation, the use of a D.S.M. screen was considered. It is worth recording the reference by Fontein (1965) on sieve bend

performance/...

performance, as this was the only reference on the subject which could be found.

3.5 Filtering Theory - Fundamentals

Kalman (1960) published a paper, and this was followed a year later by Kalman and Bucy (1961), in which a type of filter formulation was proposed which was radically different from earlier filters (associated mainly with Wiener) . These new recursive filters were linear, but their concept was soon extended to cover a wide range of processes, and they became known as Kalman or Kalman-Bucy filters. Much of the development work was due to the aerospace industry, and many papers are oriented towards this field.

The first book to be published on the subject was by Bucy and Joseph (1968). In 1970, Jazwinski published his book on stochastic processes and filtering theory, (Jazwinski, 1970) which was the first comprehensive treatment of the subject with a strong engineering orientation. This was followed by Sage and Melsa's book (1971). A number of recent books on control also feature a chapter on filtering e.g. Åström (1970). Computer and Control Abstracts (published by the IEEE, ref. 75) covers most of the work published in this field.

In this investigation, the accent on researching literature on filters was on finding new ways of solving nonlinear filtering equations. The following is a list of techniques and associated references:

- (1) Extensions of linear filtering theory: Jazwinski (1970) Sage and Melsa (1971), Bejczy and Shridhar (1972)
- (2) Approximations of the probability density using Gaussian Sums: Alspach and Sorenson (1972), Sorenson and Alspach (1971), Alspach (1972), Center (1971).

(3) Power series/...

- (3) Power Series expansions approximating the probability density:
Schilder (1971), Swerling, Goldstein, Arnold (1971).
- (4) Statistical linearisation (series expansions of non linearities with the coefficients determined in some optimal way): Mahalanabis and Farooq (1971), Dessau (1972), Kazakov (1969) (who uses an iterative technique), Heess (1970).
- (5) Discretisation of state space: Tacker and Linton (1970), Center (1971).
- (6) Polynomial approximation of the probability density: Huguen and Vimolvanich (1972), Hecht (1971), Center (1971).
- (7) Multilevel filters and Hierarchical filters: Noton (1971).
- (8) Stochastic Approximation. (This is an extension of linear filtering theory where the gain matrix is approximated): Solov'yev (1970).
- (9) Filtering algorithms for parallel computation: Tse (1971) and Larson and Tse (1971). See also Slotnik (1971) for a description of ILLIAC IV.
- (10) Monte Carlo Techniques: Yoshimura and Soeda (1971), Hammersley and Handscomb (1964), White (1971).
- (11) Expansion of non linearities by series approximations: Swerling (1966(a) and (b)).
- (12) Fading memory nonlinear filter: Sacks and Sorenson (1971).

It is interesting to note that other on-line estimation techniques exist although they were not used here, eg.

- (1) Square root filters: Bierman (1974).
- (2) Deterministic observers (e.g. Luenberger observers): Seborg, Fisher and Hamilton (1974), Crossley and Porter (1971).
- (3) Polynomial filtering: Stubberud and Masenten (1970).

Basañez et. al. (1974) present an interesting technique called stochastic computation. In a number of cases, very simple forms of data smoothing

have been used/...

have been used successfully, e.g. Fertik (1971), Rome (1971). Adaptive control and on-line model identification were not found to be of much use, and so are not reported here.

3.6 Applications of Filtering

Most reports on the implementation of Kalman-Bucy filters are based on simulations. The value of testing them on an actual plant is often underestimated, for it is only then that many unforeseen phenomena occur.

Outside the field of the aerospace industry, the experimental testing of Kalman filters has not been reported much. Some early work was done on papermaking machines (Åström 1970). Wismer and Wells (1972) reported the application to a basic oxygen furnace. A group at the University of Alberta have reported several times on the application to a pilot plant evaporator (Hamilton, Seborg and Fisher 1973, Seborg, Fisher and Hamilton 1974, Fisher and Jacobson 1973). King (1972(c)) achieved success with the application of a nonlinear filter to slurry mixing tanks. Harvey (1972) reported the use of on-line estimation in the control of a cement plant feed proportioning system.

Some useful reports on simulations are given by Goldman and Sargent (1971), Camp (1971), Wells (1971), Bar-Shalom (1972(a)).

A number of authors have reported on the computational requirements of various forms of filter:

- (1) Gura and Bierman (1971) and Singer and Sea (1971) consider the computational efficiency of linear filtering algorithms.
- (2) Kaneko and Liu (1971) and Philips (1972) analyse the error in assimilating and processing data by digital computer.

Several authors/...

Several authors have compared the operating and predicting efficiency of various filters, (there is considerable overlap with conventional estimation here) e.g. Lapa (1970), Saridis (1974), Iserman et. al. (1974), Wasan (1970).

3.7 Methods Related to the Solution of Nonlinear Filters

The following text books were used in this study. They are grouped according to the subject for which they were consulted.

- (1) Probability theory, stochastic calculus and statistics: Cramér (1955), Papoulis (1965), Sveshnikov (1968), Takács (1968), Åström (1970), Himmelblau (1970), Jazwinski (1970), Sage and Melsa (1971).
- (2) Computer methods: Carnahan, Luther and Wilkes (1969), Ralston and Wilf, vols. I and II (1967), Knuth (1969). For time-series data processing, Robinson (1967), and Bendat and Piersol (1971).
- (3) Nonlinear analysis: Bellman (1973).
- (4) Orthogonal Polynomials and general tables: Abramowitz and Stegun (1964/65).
- (5) Orthogonal functions: Sansone (1959).
- (6) Monte Carlo methods: Schreider et. al. (1966).

The following papers were also used. They are similarly grouped according to subject:

- (1) Stochastic Calculus and solutions of stochastic differential equations (S.D.E.'s): King (1971(a)), King (1971(b)), Åström (1965) who gives interesting simulations, King (1972(b)), Wong (1964) who relates typical distributions to corresponding S.D.E.'s.
- (2) Simulations of random processes and generation of pseudorandom numbers: Muller (1959).

- (3) Use of polynomial expansions to approximate probability density functions: Wong and Thomas (1962).

3.8 Modelling for Kalman Filters

The models used in a Kalman filter are stochastic. For the purposes of achieving observability and simplicity in solution, the models must be carefully chosen, and an understanding of the physical interpretations of stochastic calculus is essential. Clark (1966) deals with the problem of modelling real processes by diffusion processes, and the approximation of noise inputs by "white noise". Wong and Zakai (1965(a) and (b)) show that the Stratonovich definition of a stochastic integral is more realistic than Itô. Anderson and Kailath (1971) prove a conjecture of Kalman that the best linear model is the one with the "smallest" error covariance matrix. Mahalanabis (1972) briefly discusses a problem in reducing model dimensions. See also Galiana, Schweppe and Fiechter (1974), Bar-Shalom (1972(b)).

The handling of distributed variables in a filter is developed by Meditch (1970), Meditch (1971), Atre and Lamba (1972), Dubenko (1972), Nomura and Nakamura (1972), and Tzafestas (1972) who deals with poisson disturbances.

Chapter 4

THEORY

This chapter is divided into three main sections. The first section deals with basic filtering theory. It is not intended to be rigorous or thorough, but to cover the theory which is needed ahead. The next section discusses several theoretical topics in modelling grinding circuits. Finally, the filter used in this investigation is developed. Nomenclature is given in appendix D.

4.1 Basic Filtering Theory

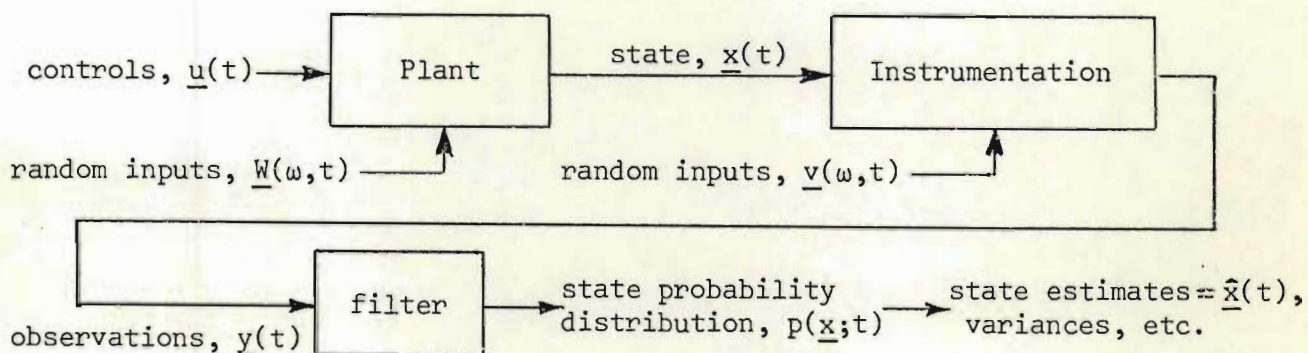


Figure 4.1 Block diagram of system.

In figure 4.1, it is assumed that we have a plant which may be described by the following stochastic differential equation. (For a more comprehensive treatment than the following, see e.g. Jazwinski, 1970)

$$d\underline{x}(t) = \underline{f}(\underline{x}, \underline{u}, t).dt + \underline{g}(\underline{x}, \underline{u}, t).d\underline{W}(\omega, t) \quad (4.1.1)$$

Where $\underline{x}(t)$ is the state vector of dimension n_s

$\underline{u}(t)$ is the control parameter vector of dimension n_u

$\underline{W}(\omega, t)$ is a vector of random Wiener processes of dimension n_w ,

as defined, for example, by Jazwinski(1970)

$\underline{f}, \underline{g}$ are functions/...

\underline{f} , \underline{g} are functions as shown.

The discrete observations are clouded by noise and may be modelled by:

$$\underline{y}_k = \underline{y}(t_k) = \underline{m}(\underline{x}, \underline{u}, t_k) + \underline{v}(\omega, k) \quad (4.1.2)$$

Where $\underline{y}(t_k)$ is the observation vector of dimension n_o at time t_k

$\underline{v}(\omega, k)$ is a normally distributed noise vector, $E\underline{v}(\omega, k) = \underline{0}$,

$$E\underline{v}(\omega, k) \cdot \underline{v}^T(\omega, j) = \underline{R} \cdot \delta_{kj}.$$

We will refer to Y_k as the set of discrete observations up to and including time t_k ,

$$Y_k = \{\underline{y}_i, i = 1, 2, \dots, k\}$$

We will also drop the vector and matrix notation, except in cases where clarity is needed.

The state and observations are random variables, and the filter describes these in terms of probability distribution densities. The continuous-discrete filter, as it is called, is then given by the following equations, (4.1.3) and (4.1.4).

At an observation, the probability distribution density of the state is updated from the value of the observation, y_k , by Bayes' rule:

$$p(x; t_k | Y_k) = \frac{p(x; t_k | Y_{k-1}) \cdot p(y_k | x; t_k, Y_{k-1})}{p(y_k | Y_{k-1})} \quad (4.1.3)$$

Where $p(x; t_k | Y_k)$ is the probability density function of x at time t_k given the set of observations Y_k , (i.e. after observation y_k)

$p(x; t_k | Y_{k-1})$ is the probability density function of x at time t_k given the observations Y_{k-1} , (i.e. before observation y_k)

$p(y_k | x; t_k, Y_{k-1})$ is the probability density function of observation y_k given the state x at time t_k and the observation set, Y_{k-1}

(This is from the statistics of $v(\omega, k)$ in equation (4.1.2))

$p(y_k | Y_{k-1})$ is the integral of the numerator in (4.1.3) over the state space

Between the observations, the distribution of the state evolves according to the Fokker-Plank or Kolmogorov forward equation associated with equation (4.1.1). Let $p(x;t|Y_k) = p_x$, where $t_{k+1} \geq t \geq t_k$, then

$$\frac{\partial p_x}{\partial t} = - \sum_{j=1}^{n_s} \frac{\partial \alpha_{1j} p_x}{\partial x_j} + \frac{1}{2} \sum_{j=1}^{n_s} \sum_{k=1}^{n_s} \frac{\partial^2 \alpha_{2jk} p_x}{\partial x_j \partial x_k} \quad (4.1.4)$$

where $\alpha_{1j} = f_j(x,u,t)$, $j=1,2,\dots,n_s$ (using Itô calculus) (4.1.5)

$$\alpha_{2jk} = \sum_{l=1}^{n_s} g_{jl}(x,u,t) \cdot g_{kl}(x,u,t) \quad (4.1.6)$$

If the control parameters are constant between observations but uncertain, we may include them as augmented state variables in defining equation (4.1.4), but with their corresponding f_j and g_{jl} set equal to zero.

From the results of the filter we may calculate more meaningful quantities such as the estimated mean of the state,

$$\hat{x}(t) = \int_{-\infty}^{+\infty} x \cdot p(x;t|Y_k) dx \quad (4.1.7)$$

The major problem in implementing the above filter is to solve the equations, particularly (4.1.4), and to do so in real time.

4.1.1 Linear Filtering Theory

The linear Kalman-Bucy filter is a special case of the above when the plant and observation equations are linear and all distributions are Gaussian. For practical purposes, it is convenient to write the model equations as follows. (For symbols, see nomenclature, appendix D)

Plant model:

differential form: $\underline{dx} = (\underline{F} \cdot \underline{x} + \underline{D} \cdot \underline{u} + \underline{c}').dt + \underline{G} \cdot dW$ (4.1.8)

difference form: $\underline{x}_{k+1} = \underline{\Phi} \cdot \underline{x}_k + \underline{\Psi} \cdot \underline{u}_k + \underline{c} + \underline{\Gamma} \cdot \Delta W$ (4.1.9)

(The conversion from the differential to the difference form is shown in most texts on state space control.)

observation model/...

observation model:
$$\underline{y}_k = \underline{M} \cdot \begin{pmatrix} \underline{x}_k \\ \underline{u}_k \end{pmatrix} + \underline{v}_k \quad (4.1.10)$$

For Gaussian distributions we need consider only the mean vector and covariance matrix to characterise the distribution completely. Define $\hat{\underline{x}}_{k-}$, \underline{P}_{k-} as the means and covariances immediately before the observation \underline{y}_k . Similarly define $\hat{\underline{x}}_{k+}$, \underline{P}_{k+} immediately after the observation. The filter equations then simplify to the following:

From the equation (4.1.4) we get

evolution of means:
$$\hat{\underline{x}}_{k+1-} = \underline{\Phi} \cdot \hat{\underline{x}}_{k+} + \underline{\Psi} \cdot \hat{\underline{u}}_k + \underline{c} \quad (4.1.11)$$

evolution of covariances:
$$\begin{aligned} \underline{P}_{k+1-} &= \underline{\Phi} \cdot \underline{P}_{k+} \cdot \underline{\Phi}^T + \underline{\Psi} \cdot \underline{U}_k \cdot \underline{\Psi}^T \\ &+ \underline{\Phi} \cdot \underline{C} \underline{u}_k \cdot \underline{\Psi}^T + \underline{\Psi} \cdot \underline{C} \underline{u}_k^T \cdot \underline{\Phi}^T + \underline{\Gamma} \cdot \underline{Q} \cdot \underline{\Gamma}^T \end{aligned} \quad (4.1.12)$$

where \underline{U}_k = covariance matrix of \underline{u}_{k+}

$\underline{C} \underline{u}_k$ = covariance matrix between \underline{x}_{k+} and \underline{u}_{k+}

\underline{Q} = noise covariance matrix = $\underline{E} \Delta \underline{W} \cdot \Delta \underline{W}^T$

From equation (4.1.3) we get at an observation:

update of means:
$$\begin{pmatrix} \hat{\underline{x}}_{k+} \\ \hat{\underline{u}}_{k+} \end{pmatrix} = \begin{pmatrix} \hat{\underline{x}}_{k-} \\ \hat{\underline{u}}_{k-} \end{pmatrix} + \underline{K}_k \cdot (\underline{y}_k - \underline{M} \cdot \begin{pmatrix} \hat{\underline{x}}_{k-} \\ \hat{\underline{u}}_{k-} \end{pmatrix}) \quad (4.1.13)$$

where
$$\underline{K}_k = \underline{P}_{Ak-} \cdot \underline{M}^T (\underline{M} \cdot \underline{P}_{Ak-} \cdot \underline{M}^T + \underline{R})^{-1}, \quad (4.1.14)$$

= the Kalman gain matrix

$$\underline{P}_A = \text{augmented covariance matrix} = \begin{pmatrix} \underline{P} & \underline{C} \underline{u} \\ \underline{C} \underline{u}^T & \underline{U} \end{pmatrix}$$

$$\underline{R} = \text{observation noise covariance matrix} = \underline{E} \underline{v}_k \cdot \underline{v}_k^T$$

update of covariances:
$$\underline{P}_{Ak+} = \underline{P}_{Ak-} - \underline{K}_k \cdot \underline{M} \cdot \underline{P}_{Ak-} \quad (4.1.15)$$

or:
$$\underline{P}_{Ak+} = (\underline{I} - \underline{K}_k \cdot \underline{M}) \cdot \underline{P}_{Ak-} \cdot (\underline{I} - \underline{K}_k \cdot \underline{M})^T + \underline{K}_k \cdot \underline{R} \cdot \underline{K}_k^T \quad (4.1.16)$$

or:
$$\underline{P}_{Ak+}^{-1} = \underline{P}_{Ak-}^{-1} + \underline{M}^T \cdot \underline{R}^{-1} \cdot \underline{M} \quad (4.1.17)$$

In addition, controller changes may be included in the formulation. These are shown in section 4.3.1, but are not normally included in the standard

linear filter.

The following points regarding linear filters were made use of in the volumetric filter:

- (1) Jazwinski (p270) explains that equation (4.1.16) is to be preferred for computational stability to equation (4.1.15). Consequently, equation (4.1.16) was used in the volumetric filter to update the covariances at the observation step.
- (2) When the \underline{R} matrix is diagonal, the observations are independent and may be treated separately, one at a time. This simplifies the calculations and shortens the time required, mainly through the saving in time required to compute an inverse matrix.
- (3) When the matrix \underline{M} consists of zeroes with only one 1 per row, and if \underline{R} is a diagonal matrix, then equations (4.1.14) and (4.1.15) simplify to row and column manipulations. For example, $\underline{M} \times \underline{P}$ would be a matrix consisting of rows in \underline{P} as marked out by ones in \underline{M} . This occurs when direct observations are made of state variables. Far fewer arithmetical operations are needed, and the time saved is considerable.
- (4) Generally after a few observations, the covariances in the linear filter tend to steady values. The Kalman gain matrix is then constant, and it is only necessary to update the means from the observations. The evolution of the means is the only evolution step. This is then called the stationary Kalman filter, and all the covariances and the Kalman gain may be pre-computed and stored, with a large saving in time and storage during execution.

During this investigation, generalised programmes were written for doing filter calculations for most of these types of filters at varying levels of complexity.

4.1.2 Nonlinear Filtering Theory.

When either a plant model or an observation model is nonlinear, the problem of implementing a filter becomes more complicated. Some usable form of solution to the Kolmogorov equation must be obtained which can be solved in real time. This is by far the most difficult problem. The observation step is not usually as complicated, but it should be quick to compute if control is to be implemented as soon as possible after taking the observations. The following is a list of techniques which were considered for this investigation. This list is by no means complete as far as nonlinear filters are concerned. Many other techniques (as listed in the literature survey section 3.5) are important but were not considered usable, and so are not listed here.

4.1.2.1 Extensions to Linear Filtering Theory.

Several methods based on linearisation of the equations exist. See any text, e.g. Jazwinski, or Sage and Melsa, for details of the following.

- (a) Linearised Kalman filter. This linearises all the equations around a fixed trajectory and observation, then uses the standard Kalman-Bucy filter.
- (b) Extended Kalman filter and iterated extended Kalman filter. Here the nominal trajectory moves with the mean of the filter. All the standard Kalman-Bucy equations apply (as given in section 4.1.1) except for the evolution of the means equation, which is nonlinear.
- (c) The truncated and Gaussian second order filters. Both these filters expand the nonlinearities to the second order. The truncated filter ignores all moments higher than the second, while the Gaussian filter approximates fourth order moments in terms of second order moments as they would be for a Gaussian distribution. Modified second order filters simplify calculations considerably by ignoring terms of minor importance

in the covariance /...

in the covariance observation step. Finally, there is a minor term in the denominator of the Kalman gain, which not only differs between the two types of second order filter, but is of opposite effect. A simplified second order filter, which ignores this term, has the following observation step (compare this with equations (4.1.13), (4.1.15), and (4.1.2)). Based on the observation model in equation (4.1.2), we have:

$$\begin{pmatrix} \hat{x}_{k+} \\ \hat{u}_{k+} \end{pmatrix} = \begin{pmatrix} \hat{x}_{k-} \\ \hat{u}_{k-} \end{pmatrix} + K_k \cdot (y_k - m(\hat{x}_{k-}, \hat{u}_{k-}) - \frac{1}{2}(P_{Ak-} \partial^2 m)) \quad (4.1.18)$$

$$P_{Ak+} = P_{Ak-} - K_k \cdot m_x \cdot P_{Ak-} \quad (4.1.19)$$

$$K_k = P_{Ak-} \cdot m_x^T \cdot (m_x \cdot P_{Ak-} \cdot m_x^T + R)^{-1} \quad (4.1.20)$$

where m_x = matrix with elements $i, j = \frac{\partial m_i(x, u_{k-})}{\partial x_j}$

$$i = 1, \dots, n_o, \quad j = 1, \dots, n_s$$

$$P \partial^2 m = \text{vector with element } i = \sum_{j=1}^{n_s} \sum_{k=1}^{n_s} P_{jk} \cdot \frac{\partial^2 m_i(x, u_{k-})}{\partial x_j \cdot \partial x_k}, \quad (4.1.21)$$

$$i = 1, \dots, n_o$$

These observation step equations are also suitable for any filter using moments, and were used in the particle size distribution filter (section 4.3.4).

4.1.2.2 Use of Moments

When the functions f and g given in equation (4.1.1) can be written as polynomials in x , then the use of moments is a convenient technique for solving the filter. We shall derive the evolution equations for the first and second moments $\mu_1(x_i)$ and $\mu_2(x_i, x_m)$ respectively, as these were used in the grinding circuit filter. Multiplying the Kolmogorov equation (4.1.4) through by x_i and integrating over the region in state space, we get:

$$\frac{d}{dt} \mu_1(x_i) / \dots$$

$$\begin{aligned}
\frac{d}{dt} \mu_1(x_i) &= \int x_i \cdot \frac{\partial p}{\partial t} \cdot dx \\
&= - \sum_{j=1}^{n_s} \int x_i \cdot \frac{\partial \alpha_{1j} p_x}{\partial x_j} \cdot dx + \frac{1}{2} \sum_{j=1}^{n_s} \sum_{k=1}^{n_s} \int x_i \cdot \frac{\partial^2 \alpha_{2jk} p_x}{\partial x_j \cdot \partial x_k} \cdot dx \\
&= \int \alpha_{1i} \cdot p_x \cdot dx + 0 \quad (4.1.22a)
\end{aligned}$$

$$\begin{aligned}
\frac{d}{dt} \mu_2(x_i x_m) &= \int x_i x_m \cdot \frac{\partial p}{\partial t} \cdot dx \\
&= - \sum_{j=1}^{n_s} \int x_i x_m \frac{\partial \alpha_{1j} p_x}{\partial x_j} \cdot dx + \frac{1}{2} \sum_{j=1}^{n_s} \sum_{k=1}^{n_s} \int x_i x_m \frac{\partial^2 \alpha_{2jk} p_x}{\partial x_j \cdot \partial x_k} \cdot dx \\
&= \int x_i \alpha_{1m} p_x \cdot dx + \int x_m \alpha_{1i} p_x \cdot dx + \int \alpha_{2im} p_x \cdot dx \\
&= \int (x_i \alpha_{1m} + x_m \alpha_{1i} + \alpha_{2im}) p_x \cdot dx \quad (4.1.22b)
\end{aligned}$$

The second central moments $m_2(x_i x_m)$ can be derived from the above as follows:

$$\begin{aligned}
\frac{d}{dt} m_2(x_i x_m) &= \frac{d}{dt} \mu_2(x_i x_m) - \mu_1(x_i) \frac{d}{dt} \mu_1(x_m) - \mu_1(x_m) \frac{d}{dt} \mu_1(x_i) \\
&= \int ((x_i - \bar{x}_i) \alpha_{1m} + (x_m - \bar{x}_m) \alpha_{1i} + \alpha_{2im}) p_x \cdot dx \quad (4.1.22c)
\end{aligned}$$

If the α functions, which are related to f and g in equation (4.1.1) by equations (4.1.5) and (4.1.6), are polynomials in x , then these equations ((4.1.22a) to (4.1.22c)) will be a set of ordinary differential equations for the moments in terms of other moments. If in equation (4.1.1), \underline{f} and \underline{g} are polynomials in x of order greater than one, then the differential equations for the moments form an open set, and closure approximations are needed. The closure approximations used in this study are given in section 4.3.4.

For the observation step, if up to only second order moments are considered, equations (4.1.18) to (4.1.21) may be used. Jazwinski gives formulae for

updating higher order moments at an observation.

Moments give a very convenient solution to the filtering problem, provided the problem is not highly nonlinear. Usually only the first and second moments are considered, as they are the most meaningful and are usually sufficient. Solution via moments should not be confused with the approximate linear filters. Although moments take longer to programme, they are usually quicker and more accurate.

4.1.2.3 Orthogonal Series Approximations.

After the success that King (1972(c)) and others had had, the use of this technique was tried. The probability distribution density is approximated as an orthogonal series, and is written:

$$p(x;t) \approx f_0(x) \sum_{i=1}^I a_i(t) \cdot f_i(x) \quad (4.1.23)$$

where the $f_i(x)$, $i = 1, \dots, I$ are I terms of an orthogonal set of functions with normalising function $f_0(x)$.

Substituting this into equation (4.1.4), we get a set of I ordinary differential equations in the coefficients a_i . Depending upon the set chosen, so various properties are apparent. The observation step also depends upon the set of orthogonal functions chosen.

The major disadvantage of this technique is that the equations for the coefficients usually have to be worked out by hand, and only small dimensional problems are feasible. One generally needs at least 3^{ns} coefficients in the expansion.

4.1.2.4 Use of Discretised State Space

This technique lumps the probability density at a number of discrete points in the state space, x_i , $i = 1, \dots, I$. The derivatives w.r.t. x in the Kolmogorov equation (4.1.4) are put in a discrete form, and this yields a

set of ordinary differential equations in time. The discrete form of the observation step (from Bayes' rule) is as follows:

$$p(x_i; t_k | Y_k) = p(x_i; t_k | Y_{k-1}) \cdot p(y_k | x_i; t_k, Y_{k-1}) / K' ,$$

$$i = 1, \dots, I \quad (4.1.24)$$

where $K' = \sum_{i=1}^I p(x_i; t_k | Y_{k-1}) \cdot p(y_k | x_i; t_k, Y_{k-1})$

Again the disadvantage of this technique is the large number of points required for anything larger than about a two dimensional system. It can, however, handle highly nonlinear systems. It also forms the basis for our next technique.

4.1.2.5 Differential Quadrature

This technique was originally proposed by Bellman (see Bellman 1973) as a means of solving nonlinear partial differential equations using a discretised space. The method is suited to highly nonlinear problems with small dimensions. It was tried on the 8-dimensional particle size distribution (p.s.d.) filter (see ahead) as an experiment, and although it did not perform well, it was interesting to see the results.

The method is given below. Only an outline of the method is shown here, as the actual implementation was simple and involved much repetitive work.

The state space was discretised as in section 4.1.2.4 above, and the probability density, $p(\underline{x}, t)$, was lumped at these points, p_i , $i = 1, \dots, I$. The differential quadrature assumed that the derivatives of $p(\underline{x}, t)$ could be approximated by weighted sums of the p_i , i.e.:

$$\frac{\partial p}{\partial x_j} \text{ at point } i \approx \sum_{m=1}^I \theta_{jim} \cdot p_m \quad (4.1.25)$$

Second derivatives were written similarly.

In the Kolmogorov equation (4.1.4), the terms containing the derivatives w.r.t. the state were expanded as shown below for the first term in

equation (4.1.4), at point i

$$\begin{aligned}
 \sum_{j=1}^{n_s} \frac{\partial \alpha_{1j} \cdot p_x}{\partial x_j} &= \sum_{j=1}^{n_s} \left(\frac{\partial \alpha_{1j}}{\partial x_j} \cdot p_x + \alpha_{1j} \cdot \frac{\partial p_x}{\partial x_j} \right) \\
 &= \sum_{j=1}^{n_s} \left(\frac{\partial \alpha_{1j}}{\partial x_j} \cdot p_i + \alpha_{1j} \sum_{m=1}^I \theta_{jim} \cdot p_m \right) \\
 &= \sum_{m=1}^I \left[\sum_{j=1}^{n_s} \left\{ \frac{\partial \alpha_{1j}}{\partial x_j} \cdot \delta_{im} + \alpha_{1j} \cdot \theta_{jim} \right\} \right] \cdot p_m \\
 &= \underline{K}_i^T \times p \quad \quad \quad (4.1.26)
 \end{aligned}$$

The expression in square brackets (making up the elements of \underline{K}_i) was calculated beforehand. Terms with second order derivatives were treated similarly, and although more complicated, had the same format. The Kolmogorov equation then simplified to a linear matrix equation for the p_i ,

$$\frac{dp}{dt} = \underline{T} \cdot p \quad \quad \quad (4.1.27)$$

The p.s.d. filter had the \underline{T} as a function of two parameters,

$$\underline{T} = \underline{T}_0 + \underline{T}_1 \cdot u_1 + \underline{T}_2 \cdot u_2 \quad \quad \quad (4.1.28)$$

The observation step followed the usual discrete solution of the nonlinear filter shown in equation (4.1.24) above.

The p.s.d. filter had 8 states, and so the points were chosen on a rectangular grid, along the lines of a two level factorial design with a centre point. The maximum number of points which could be handled by the CDC 1700 computer was $16+1 = 17$. This gave some aliasing between second derivatives, and it would have been desirable to have considerably more. The coefficients θ_{jim} in equation (4.1.25), and similar coefficients for second derivatives, were obtained by a linear regression done on a Gaussian distribution with a comparable variance to the distribution given by the solution with moments (as shown in the results, chapter 6). Suitable levels for the states were

also chosen from the solution with moments. It was found necessary to limit the elements of \underline{p} to be not negative.

A programme was written to implement the above filter. This programme read in data for the filter including the plant and observation models, then converted these into the \underline{T} matrices in equation (4.1.28), and into observation values at each point. It then ran the filter recursively, following the procedure below:

- (1) Values of the observations were used in equation (4.1.24) to update \underline{p} .
- (2) The \underline{p} was evolved using the linear equations (4.1.27) and (4.1.28) with the precomputed matrices and values of the parameters read in.
- (3) The values of \underline{p} were converted into means of the state variables and thence into the concentrations and particle size distributions.

Another programme extended the above programme to work on real data. The results of this are shown in section 6.9.

4.2 Modelling of grinding circuit operations

4.2.1 Comminution

To model grinding, we describe an assembly of particles in terms of the mass of particles in each of a number of size ranges. Let $p(d_i) = p_i$ be the mass fraction in size group i with mean size d_i . The particles in group i break with a rate constant S_i into a number of smaller size groups. Let b_{ji} be the mass fraction of products from breakage of size group j which are in group i .

S_i is called the selection function, and b_{ji} the individual breakage function.

It is customary to number size groups sequentially from the largest, 1, to the smallest, n_p . Note $S_{n_p} = 0$. The equation governing the rate of grinding for a batch of rock is then :

$$\frac{dp_i}{dt} / \dots$$

$$\frac{dp_i}{dt} = -S_i \cdot p_i + \sum_{j=1}^{i-1} S_j \cdot b_{ji} \cdot p_j, \quad i = 1, \dots, n_p \quad (4.2.1)$$

(Where the sum is zero for the case $i = 1$.)

Let P_i be the cumulative mass fraction $= \sum_{j=1}^{n_p} p_j$. Similarly define the cumulative breakage function $B_{ji} = \sum_{k=i}^{n_p} b_{jk}$. Then equation (4.2.1) can also be written:

$$\frac{dP_i}{dt} = \sum_{j=1}^{i-1} S_j \cdot B_{ji} \cdot (P_{j+1} - P_j), \quad i = 2, \dots, n_p \quad (4.2.2)$$

For continuous distributions, $p(d)$ and $P(d)$, we have equivalent equations

$$\frac{dp(d;t)}{dt} = -S(d) \cdot p(d;t) + \int_d^{\infty} S(y) \cdot b(y,d) \cdot p(y;t) \cdot dy \quad (4.2.3)$$

and

$$\frac{dP(d;t)}{dt} = \int_d^{\infty} S(y) \cdot B(y,d) \cdot dP(y;t) \quad (4.2.4)$$

Where $S(d)$, $b(y,d)$, $B(y,d)$ are the continuous selection function, and individual and cumulative breakage functions respectively.

For continuous milling (as opposed to batch milling), feed and discharge terms must be included in these equations.

The above equations (4.2.1) to (4.2.4) are the basis for most of the studies done on grinding. To implement them, some assumptions must be made, e.g.:

- (1) Generally the equations are assumed to be linear (i.e. the selection and breakage functions are not functions of the masses in each fraction), and deterministic.
- (2) Although each size interval may cover a range of sizes, the selection and breakage functions are assumed constant over each range.
- (3) In order to obtain estimates of the parameters in the model from experimental data, the breakage function and sometimes the selection

function are described by a simple functional form on d , the particle size.

In this investigation, experimental batch grinding tests were the source of data used to determine the parameters in the grinding model, and their dependence on experimental conditions. This data was in the form of the particle size distribution (p.s.d.) at a number of times during the batch grind, as well as the p.s.d. at a fixed time (in this case 20 minutes) for high and low slurry densities and high and low total slurry charge.

The selection and breakage functions were calculated using a programme called "GRIND". This generalised programme was written by Herbst and Mika, and was lent to the author during a visit to the department by Prof. T. S. Mika, who also assisted in running the programme. This fitted discrete values of the selection function and a three parameter breakage function of the form:

$$B_{ji} = \alpha_1 \cdot (d_i/d_j)^{\alpha_2} + (1 - \alpha_1) \cdot (d_i/d_j)^{\alpha_3} \quad (4.2.5)$$

The programme used a Gauss-Newton type of search to optimise a quadratic performance criterion. A full description of the programme is given by Herbst, Grandy, Mika and Fuersteneau (1972).

It was necessary in the filter to know the effects of slurry solids concentration and total slurry charge on the selection and breakage functions. To avoid doing extensive tests, the following method was used. It was assumed that the main effect would be a uniform scaling of the selection function (i.e. scaling the rates of breakage by the same factor in each size fraction). From the sequence of particle size distributions over the range of batch grinding times done under standard conditions, graphs of D_{25} , D_{50} , and D_{75} against time were drawn, where D_{25} , D_{50} , and D_{75} were the particle sizes corresponding to 25%, 50%, and 75% cumulative mass percent respectively, and were functions of time (refer to graph 6.4).

On these lines, the D_{25} , D_{50} and D_{75} of the runs done using high and low values

of density/...

of density and charge (all done for the same grinding time of 20 minutes), were plotted, to give equivalent grinding times, t_e . The assumption that the selection function scaling was the major effect was reasonably justified, as the t_e values at D_{25} , D_{50} and D_{75} were almost the same for any given set of conditions. The rate scaling factors for the selection function for each variation in conditions were calculated from

$$\text{scaling factor} = t_e / 20 \quad (t_e \text{ in minutes}) \quad \underline{(4.2.6)}$$

To scale up the selection function for a larger mill, the scaling factor $\left(\frac{\text{diameter}_1}{\text{diameter}_2}\right)^{0.6}$ was used (see Austin 1973(b)). The breakage function was assumed to be unaffected.

To condense the grinding parameters into fewer size groups for use in the filter, the following method was used.

Let: S_i be the selection function	}	as defined above, for the
b_{ij} be the individual breakage function		larger number of narrower size classes.
S'_k be the selection function	}	for the reduced system, with
b'_{kl} be the individual breakage function		a smaller number of wider classes.

n_k = number of smaller classes in larger class k .

Also let $i \in k$ mean that size group i forms a part of larger group k .

Also assume that all the narrower classes which together form a wider class have the same mass of solids in each.

S'_k and b'_{kl} are distributed variables, the mean of which can be found by writing equation (4.2.1) for this smaller system and then expanding each term. This gives:

$$E S'_k = \sum_{\text{all } i \in k} S_i \times \left[\sum_{\text{all } j \in k} b_{ij} \right] / n_k \quad \underline{(4.2.7)}$$

$E b'_{kl} / \dots$

$$E b'_{kl} = \sum_{\text{all } j \in l} \left(\sum_{\text{all } i \in k} b_{ij} \cdot S_i / (S'_k \cdot n_k) \right) \quad (4.2.8)$$

A variance of the S'_k due to this reduction may be calculated from:

$$\sigma_{S'_k}^2 = \sum_{\text{all } i \in k} \left[S_i \times \left(\sum_{\text{all } j \neq k} b_{ij} \right) - E S'_k \right]^2 / n_k \quad (4.2.9)$$

(Note that we divide by n_k and not $n_k - 1$.)

In this study, 17 size groups were condensed into 4 for the filter.

4.2.2 Cyclone Modelling

Two parts were needed to model the cyclone:

- (1) The volumetric flow split model. This gave the dependence of the exit flows on feed flow, concentration, and particle size distribution.
- (2) The solids size split model.

The most successful modelling work on cyclones which has been published so far is by the group at the University of Queensland, as given in the literature survey. Their models have been mostly simple linear correlations. The solids size split model is in terms of the reduced corrected classifier function. The D_{50} , or size corresponding to 50% on the corrected classifier function curve, is then written as a linear function of the operating variables.

Particular points which were found in the literature and verified experimentally, were:

- (1) The size split is very dependent on feed concentration, but far less on feed flow or pressure. The split is also affected by the specific gravity of the rock being handled. Provided the cyclone does not rope badly, the linear model is reasonably good.
- (2) The underflow volume rate is nearly constant. It is only slightly affected (within a reasonable operating range) by the feed flow, concentration, and size distribution. The small functional dependence on these variables

is not/...

is not properly understood.

The volumetric split was finally modelled by the following equation:

$$Q_U = Q_{U0} + \epsilon_U \quad (4.2.10)$$

Where Q_{U0} is a constant, independent of feed flow or concentration.

ϵ_U is a random error term, $E \epsilon_U = 0$, $E \epsilon_U^2 = \sigma_\epsilon^2$.

The particle size split model required the corrected classifier functions for each particle size group as a function of feed concentration. This meant that the models from the literature could not be used directly in the filter, but only as rough checks on the experimental data. The following linear classifier model was then chosen:

$$cc_i = cc_{0i} + cc_{1i} \cdot C_F \quad (4.2.11)$$

Where cc_i = the corrected classifier function for size group i ,

cc_{0i} , cc_{1i} are constants for size group i ,

C_F = cyclone feed solids concentration.

The actual classifier function, c_i , was calculated from the corrected classifier function as follows:

$$c_i = \frac{Q_{UW}}{Q_{SW}} + \frac{Q_{SW} - Q_{UW}}{Q_{SW}} \cdot cc_i \quad (4.2.12)$$

Where Q_{UW} = water-only flow in the underflow,

Q_{SW} = water-only flow in the feed coming from the sump.

We can thus write:

$$c_i = c_{0i} + c_{1i} \cdot C_F \quad (4.2.13)$$

Where

$$c_{0i} = \frac{Q_{UW}}{Q_{SW}} + \frac{Q_{SW} - Q_{UW}}{Q_{SW}} \cdot cc_{0i}$$

$$c_{1i} = \frac{Q_{SW} - Q_{UW}}{Q_{SW}} \cdot cc_{1i}$$

4.2.3 Modelling of Random Processes

A problem which is associated with nonlinear filtering is that of stochastic calculus and the modelling of random processes. A common way of modelling noise is as shown in equation (4.1.1).

The stochastic integral, $\int_a^{t_b} g(x(t)).dW(t)$ has two common definitions. The Itô definition is:

$$\int_a^{t_b} g(x(t)).dW(t) = \lim_{\substack{n \rightarrow \infty \\ \Delta t \rightarrow 0}} \sum_{i=0}^{n-1} g(x(t_i)).(W(t_{i+1}) - W(t_i)) \quad (4.2.14)$$

and the Stratonovich definition is

$$\int_a^{t_b} g(x(t)).dW(t) = \lim_{\substack{n \rightarrow \infty \\ \Delta t \rightarrow 0}} \sum_{i=0}^{n-1} g\left(\frac{x(t_i) + x(t_{i+1})}{2}\right) \cdot (W(t_{i+1}) - W(t_i)) \quad (4.2.15)$$

The two definitions are not equivalent, and there have been a lot of papers in recent years on the subject of which is more realistic.

To "get a feel" for the problem, and to determine how to model plant noise quantitatively, a study was made of a simple one-dimensional equation of a form similar to that encountered in the particle size distribution filter:

$$dx = (1 - x).dt + x.dW \quad (4.2.16)$$

The theoretical stationary distributions for the Itô and Stratonovich definitions are plotted in figure 4.2. They are markedly different. Sample paths were then simulated in the computer using a normally distributed random number generator. Two types of equivalent difference equation were tried, one in the form of the Itô definition,

$$x_{k+1} = x_k + (1 - x_k). \Delta t + x_k. \Delta W \quad (4.2.17)$$

and the other in the form of the Stratonovich definition,

$$x_{k+1} = x_k + \left(1 - \frac{x_k + x_{k+1}}{2}\right) \Delta t + \left(\frac{x_k + x_{k+1}}{2}\right) \Delta W \quad (4.2.18)$$

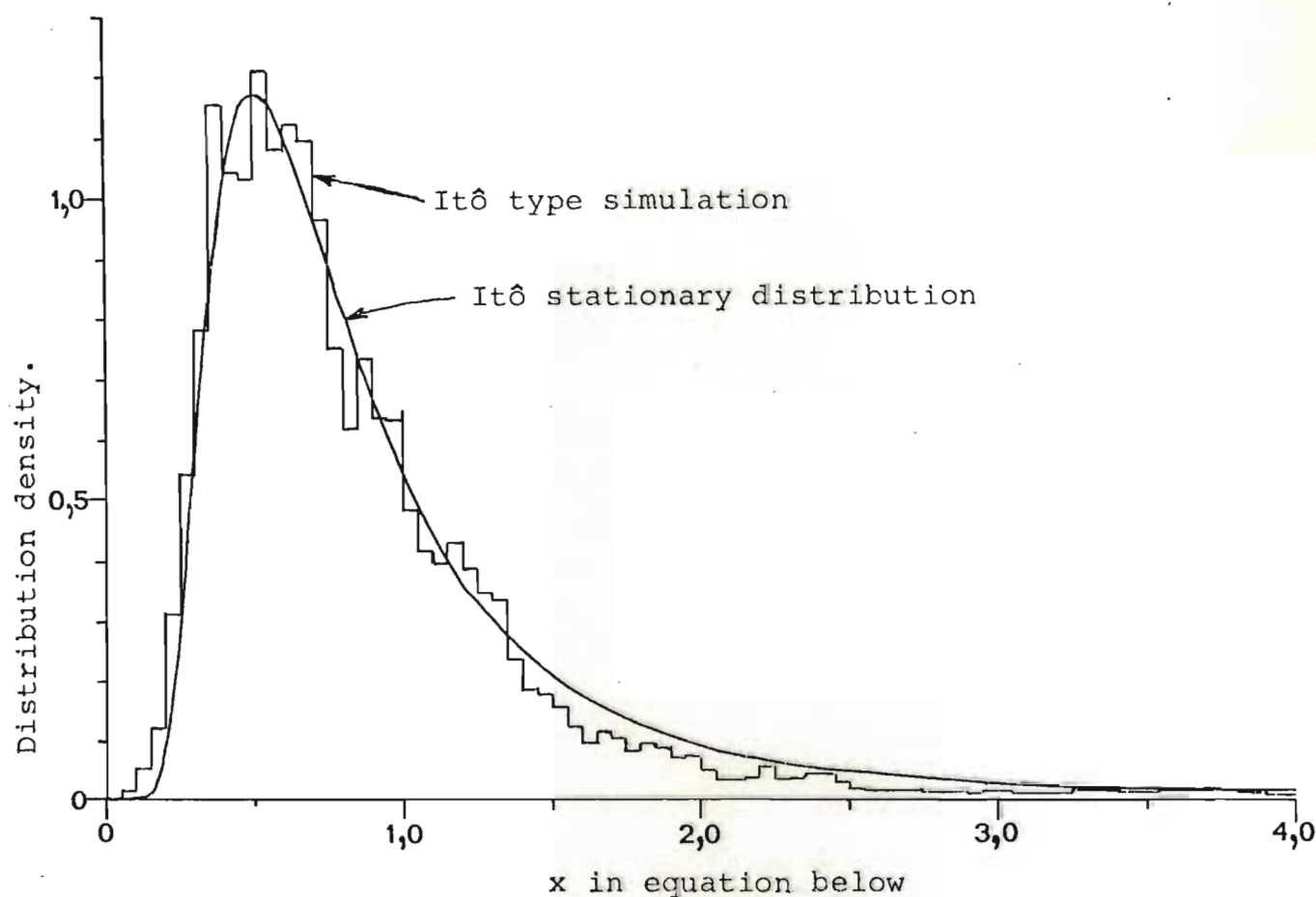
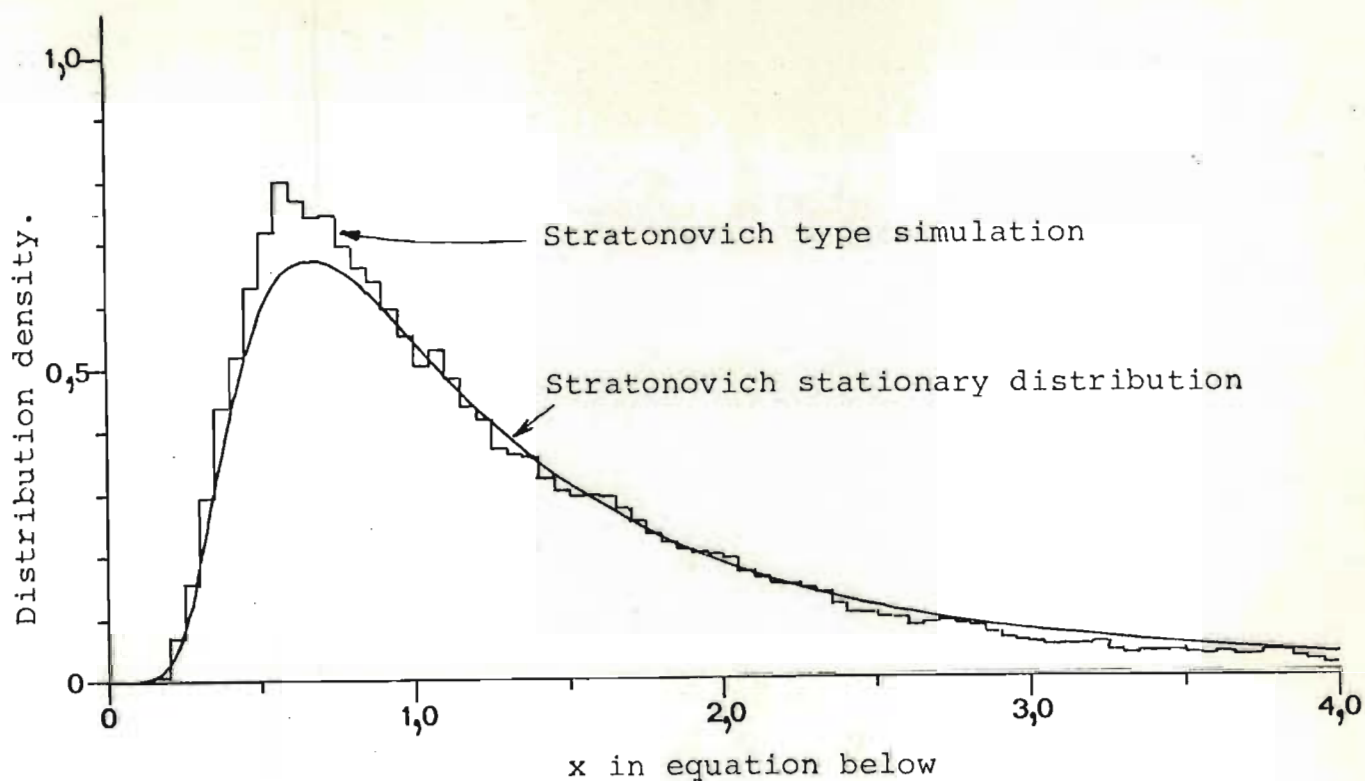


Figure 4.2 Comparison of Itô and Stratonovich definitions of a stochastic integral. Theoretical stationary distributions and simulation histograms shown for equation

$$dx = (1-x)dt + x.dW$$

Histograms were drawn up from these sample paths showing the fraction of the total time spent by the path in each small interval along the x-axis. These histograms are also shown in figure 4.2. They too, are markedly different, but agree closely with their corresponding stationary distribution curves.

From this it can be seen that the modelling of processes and the fixing of noise levels in the model depend on the type of stochastic calculus used, and are not uniquely determined by the differential equation alone. This is important to remember, as it is unlike deterministic, or linear stochastic, modelling. This also means that some of the grinding models being used, which assume that the selection functions are random, but which continue by using the mean values, may be wrong. The error in a large collection of particles is small, however. Throughout the rest of this investigation, Itô calculus was used as it is simpler to apply in most cases.

The form of equations (4.1.1) and (4.1.2) allows one to model a large variety of realistic noise processes. One can easily fit desired probability distributions and power spectra (see Sveshnikov 1968, Wong 1964). This usually requires at least one extra variable per noise input, and so it is not desirable because of the extra complexity of the filter. A number of workers (e.g. Galiana et al 1974, Clark 1966) have reported that sophisticated noise models are often an unnecessary complication, and that an equivalent simple Wiener process is satisfactory in terms of model response. It appears (see Goldman and Sargent 1972, and section 6.8.5) that models requiring extra state variables often degrade filter performance by producing larger differences between predictions and actual values, or by making the filter unstable. The use of simplified noise models often result in apparently unrealistically high noise levels in a model. This is particularly the case with correlated observation noises.

4.2.4 Determination of Noise Levels in Models

The assigning of values to noise levels in a filter model is a problem, particularly on real plants (unlike simulations). The noise levels can seldom be measured beforehand, and consequently methods are needed which enable one to make a careful guess based on whatever information is available.

For a linear filter, one can consider all factors which are likely to contribute to each noise, measure or guess the effects of each factor, and then calculate the total resulting noise. Generally this is sufficient, but it may be checked by running the filter on the actual plant, and comparing the residuals of the actual observations about the predicted observations to their statistics (see Jazwinski, p271). The covariance matrix for these residuals, \underline{V}_k , is given by:

$$\underline{V}_k = \underline{M} \cdot \underline{P}_{Ak} \cdot \underline{M}^T + \underline{R} \quad (4.2.19)$$

This method was used for the volumetric filter. The resulting noise levels used are given in section 6.6. This statistical check does not require a knowledge of the actual state, but if this is also available (say from samples), it enables the \underline{P}_A and \underline{R} matrices to be checked separately.

For nonlinear systems, there is no way of specifying noise levels in the plant model solely from a consideration of the factors involved. This is because noise levels depend on the definition of the stochastic integral, and are only physically meaningful when their effects on the state variables are known. There are two alternative techniques to determine noise levels:

(1) The first method is to run the complete filter on a set of synthetic data. This set consists of average values of the parameters and measurements, and the filter is run until an almost stationary state is reached. The

predicted errors on the state variables are then compared to measured or guessed values on the actual plant. Other noise levels are tried, and the filter responses to step changes in some of the parameters and measurements are also measured. From these tests, noise levels can be obtained which produce the desired output. This method has the advantage that it is the closest to reality.

(2) The second method is to run only the evolution part of the filter, until a stationary state is obtained (if this can be done) which is the state of the system without any observations. Again the predicted errors on the estimates are compared to measured or guessed values on the actual plant. These errors are the uncertainties in the state of operation of the real plant when inputs are fixed and no other measurements are taken. From tests done at various noise levels, values can be chosen for the noise levels to produce the desired output. This method was used for the p.s.d.filter.

Observation errors, even for nonlinear observations, can generally be obtained directly from measurements, or from guesses based on a knowledge of the plant instrumentation.

If it is found that noises cannot be uniquely determined, it is possible that the plant has been over modelled, so that a model simplification (if it is possible) will help.

In this investigation, noise levels in the p.s.d. filter were determined beforehand using the second method above, based on carefully guessed error levels, but with a slightly erroneous plant model. These values were used until after the filter had been debugged and was running normally. They were then rechecked using the same method with the new model and found to be satisfactory (see graph 6.16, section 6.6).

4.3 Development of Filter for Grinding Circuit

The formulation of a suitable particle size distribution filter proved to be a problem and considerable time was spent on it. Initial problems were mostly on the mathematical side, formulating a model which had a reasonable solution, and which could be solved in real time. Realisation that the filter could be split into two levels helped considerably. Later modifications and improvements were made in the light of operating experience on the milling circuit.

Modelling a full grinding circuit required a large number of nonlinear differential equations. In this investigation, the filter was broken down into two levels, thereby removing some of the nonlinearities and simplifying the problem, at the expense of some precision and resulting in slightly suboptimal estimates. These two sections of the filter were as follows:

- (1) The volumetric filter. This part of the filter estimated the volumes and volumetric flows in the grinding circuit from measurements of flows and levels. It was basically a stationary linear filter with a control step, and was assumed (with reasonable justification - see results, chapter 6) to be independent of the solids concentrations or size distributions.
- (2) The particle size distribution filter (p.s.d. filter). This part of the filter operated at a higher level (i.e. it was dependent on the results from the volumetric filter) and estimated the masses in each particle size fraction around the circuit and hence the size distributions and solids concentrations, from a knowledge of solids feed and concentration measurements from the gamma-ray density gauges. It was a nonlinear filter, based on the grinding model. Estimates of the mean volumes and flows from the volumetric filter were used as parameters in the p.s.d. filter, without regard for their estimation variances.

4.3.1 Volumetric Filter

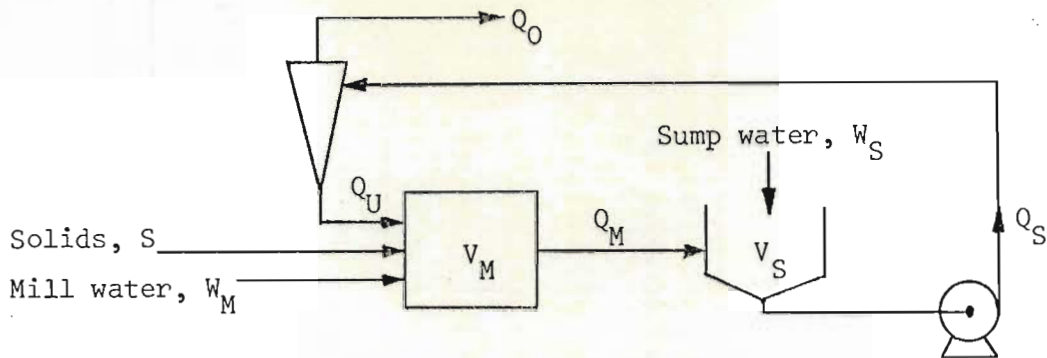


Figure 4.3 Circuit showing symbols used for volumetric filter.
(Also see figure 5.1.)

Let V denote volume, and Q volumetric flow.

Subscripts M refer to mill, S to sump, O to cyclone overflow, U to cyclone underflow.

Volume balances over the mill and sump yielded:

$$\left. \begin{aligned} \frac{dV_M}{dt} &= S/\rho_S + W_M + Q_U - Q_M \\ \frac{dV_S}{dt} &= Q_M + W_S - Q_S \end{aligned} \right\} \quad (4.3.1)$$

It was assumed (see section 5.5.3) that the mill outflow could be modelled by

$$Q_M = k_1 \cdot (V_M - V_{M0}) \quad (4.3.2)$$

and the cyclone (section 4.2.2) by

$$Q_U = Q_{U0} + \epsilon_U \quad (4.3.3)$$

where ϵ_U was an unknown constant, to describe the uncertainty in the model.

Putting equations (4.3.2) and (4.3.3) into (4.3.1), and grouping the terms, we get:

$$\frac{dV_M}{dt} = /....$$

$$\begin{array}{rcll}
 \frac{dV_M}{dt} & = & -k_1 V_M & + W_M + S/\rho_S & + k_1 \cdot V_{M0} + Q_{U0} & + \epsilon_U \\
 \frac{dV_S}{dt} & = & +k_1 V_M & + W_S - Q_S & -k_1 \cdot V_{M0} & 0
 \end{array} \left. \vphantom{\begin{array}{rcll} \frac{dV_M}{dt} \\ \frac{dV_S}{dt} \end{array}} \right\} \quad (4.3.4)$$

state
control parameters
constants
errors

We now have a linear equation, and defining

$$\begin{aligned}
 \underline{x} &= (V_M, V_S)^T \\
 \underline{u} &= (Q_S, S, W_M, W_S)^T \\
 \underline{c} &= (k_1 \cdot V_{M0} + Q_{U0}, -k_1 \cdot V_{M0})^T \\
 \underline{N} &= (\epsilon_U, 0)^T
 \end{aligned}$$

we may write the volumetric model, equation (4.3.4), as

$$d\underline{x} = (\underline{F} \cdot \underline{x} + \underline{G} \cdot \underline{u} + \underline{c} + \underline{N}) \cdot dt \quad (4.3.5)$$

Instruments were available to take uncorrelated observations of S , W_M , Q_S , V_S and W_S directly. The observation model was thus

$$\underline{y} = \underline{M} \cdot \begin{pmatrix} \underline{x} \\ \underline{u} \end{pmatrix} + \underline{v} \quad (4.3.6)$$

which can be written

$$y_i = \left[\begin{pmatrix} \underline{x} \\ \underline{u} \end{pmatrix} \right]_{m_i} + v_i, \quad i = 1, \dots, 5 \quad (4.3.7)$$

where: \underline{M} is a matrix of 1s and 0s, and $E \underline{v} \cdot \underline{v}^T$ is diagonal.

Subscript m_i implies the m_i th element from the augmented state and control parameter vector.

Equation (4.3.7) was for use when handling observations individually.

Directly after each observation step, each of the control parameters underwent control changes:

$$\underline{u}_{k+1-} = \underline{u}_{k+} + \underline{\Delta u}_k \quad (4.3.8)$$

During operation of the plant, the control changes which were sent out to the controllers/...

the controllers were known, but the instrument responses were uncertain. Thus $\underline{\Delta u}_k$ was not known exactly, and so was written as the sum of the mean, $\underline{\Delta \hat{u}}_k$, and an error with covariance $\underline{\Delta U}$. The control step in the filter was then

$$\underline{\hat{u}}_{k+1-} = \underline{\hat{u}}_{k+} + \underline{\Delta \hat{u}}_k \quad (4.3.9)$$

$$\underline{U}_{k+1-} = \underline{U}_{k+} + \underline{\Delta U} \quad (4.3.10)$$

Depending on the length of time, t_{ci} , taken to change controller i , so an average value of the control over the next interval, $\bar{u}_{k,i}$, was calculated for use in the evolution step from

$$\bar{u}_{k,i} = \hat{u}_{k+,i} \cdot \left(\frac{t_{ci}}{2T} \right) + \hat{u}_{k+1-,i} \cdot \left(1 - \frac{t_{ci}}{2T} \right) \quad (4.3.11)$$

where T is the observation interval.

With equation (4.3.5) as a plant model, equation (4.3.7) as an observation model, and equation (4.3.8) as a controller model, a linear Kalman-Bucy filter was developed for the volumetric filter (section 4.1.1). The unknown constant, \underline{N} , in equation (4.3.5) was treated as an uncertain parameter but without an update at the observations (see Jazwinski, page 285).

4.3.2 Checks in the Volumetric Filter

If a plant which is being monitored is upset, or if for some other reason the measurements reaching a filter are incorrect, the predictions will be wrong. Faulty predictions from the volumetric filter were found to upset the p.s.d. filter, and so the following three checks were built into the volumetric filter.

(1) Check against faulty observations.

$$\text{Define } \Delta y_i \triangleq y_i - \begin{bmatrix} \hat{x}_{k-} \\ \hat{u}_{k-} \end{bmatrix}_{m_i}, \quad i = 1, \dots, 5 \quad (4.3.12)$$

$$\text{and } S = \sum_{i=1}^5 (\Delta y_i)^2 / \sigma_{\Delta y_i}^2$$

where the residual Δy_i is the difference between the actual and the predicted i th observation. The $\sigma_{\Delta y_i}^2$ is given by the i th diagonal element of \underline{V}_k in equation (4.2.19).

S has approximately a χ^2 distribution with 5 degrees of freedom, as the Δy_i are approximately normally distributed. S was calculated at each observation step (it did not require much extra programming), and checked against some criterion, S_{crit} (here the 99% confidence limit was used). This determined whether the observations were satisfactory. If they were, then the filter continued unchanged. If they were not, then the Δy_i were scaled in proportion to $\sqrt{S/S_{\text{crit}}}$ before updating the means in equation (4.1.13). This was equivalent to scaling down the Kalman gain matrix when there was a faulty observation.

This check protected against outlying points, as caused by, say, faulty instruments, and also protected against the actual observations behaving differently from the observation model.

(2) Check against undetectable plant upsets.

If, at an observation, we check a measure of the difference between the predicted observation at the end of the previous interval and that observation, to the difference between the predicted observation at the beginning of the previous interval and the same observation, we should find that the latter is larger if the plant and plant model are in agreement. This was done in the following way.

$$\text{Define } \left. \begin{aligned} \underline{\Delta y}_a &= y_k - \underline{M} \cdot \begin{bmatrix} \hat{x}_{k-1+} \\ \hat{u}_{k-1+} \end{bmatrix} \\ \underline{\Delta y}_b &= y_k - \underline{M} \cdot \begin{bmatrix} \hat{x}_{k-} \\ \hat{u}_{k-} \end{bmatrix} \end{aligned} \right\} \quad (4.3.13)$$

$$\text{and} \quad \left. \begin{aligned} S_a &= \sum_{i=1}^5 (\Delta y_{ai})^2 / \sigma_{\Delta y_i}^2 \\ S_b &= \sum_{i=1}^5 (\Delta y_{bi})^2 / \sigma_{\Delta y_i}^2 \end{aligned} \right\} \quad (4.3.14)$$

Then if the plant were operating as the filter would expect,

$$E(S_a - S_b) > 0$$

If this difference, $S_a - S_b$, was greater than zero at an observation, then the error in the filter would be greater if the previous evolution step was accepted as correct. In this case it would be better to use

$\hat{x}_{k-} = \hat{x}_{k-1+}$ and $\hat{u}_{k-} = \hat{u}_{k-1+}$. The following procedure was used at an observation:

- (i) Calculate S_a and S_b for the observation, using equation (4.3.14).
- (ii) If $S_a < S_b$, set $\hat{x}_{k-} = \hat{x}_{k-1+}$, $\hat{u}_{k-} = \hat{u}_{k-1+}$, $S_b = S_a$.
- (iii) Use S_b in the observation check outlined in (1) above.
- (iv) Perform the observation step.

These were not sure checks against plant mishaps, but they reduced the risk of an upset, and were suitable for detecting when a control action was not having the desired effect. Their practical use is shown in section 6.8.1.

(3) Checks against variables out of range.

This check was used to prevent the sump volume becoming too small and giving integration difficulties in the p.s.d. filter. The minimum volume of the sump was limited to 0.008 m^3 at all times.

All these checks were conservative: they kept near to the state which they were at when an unexpected observation was received from the plant. This was a desirable characteristic in the two level filter, and also probably for any subsequent control algorithms.

4.3.3 Particle Size Distribution Model and Filter

The first problem encountered with any particle size distribution (p.s.d.) filter is how to represent a particle size distribution as a random variable. Let $p(d_i)$ and $P(d_i)$ (also denoted p_i and P_i) be the individual and cumulative mass fractions respectively of a discrete particle size distribution. Both are random variables. We can now define the probability distributions:

$$H_I(\tilde{p}_i, i = 1, \dots, n_p) = \text{Prob}\{p_i \leq \tilde{p}_i, i = 1, \dots, n_p\} \quad (4.3.15)$$

$$H_C(\tilde{P}_i, i = 1, \dots, n_p) = \text{Prob}\{P_i \leq \tilde{P}_i, i = 1, \dots, n_p\} \quad (4.3.16)$$

Also let

$$h_I(p_i, i = 1, \dots, n_p) = \frac{\partial^{n_p}}{\partial p_1 \dots \partial p_{n_p}} H_I(p_i, i = 1, \dots, n_p) \quad (4.3.17)$$

$$h_C(P_i, i = 1, \dots, n_p) = \frac{\partial^{n_p}}{\partial p_1 \dots \partial p_{n_p}} H_C(P_i, i = 1, \dots, n_p) \quad (4.3.18)$$

Discrete grinding models can now be handled if there is a random input to the system. The individual form was used in this investigation. Continuous particle size distributions were not easily handled, and no satisfactory filter in the form of either equation (4.2.3) or (4.2.4) was developed.

To model the mill behaviour for use in the filter, it was necessary to find the sources of random disturbances, and model them. A list of the major noise sources which were encountered, is given below.

- (1) The solids feed rate and size distribution to the mill.
- (2) The hardness of the rock affecting the rate of grinding.
- (3) Perturbations in operating conditions affecting the rate of grinding.
- (4) Cyclone operating and modelling errors.
- (5) Slurry flow behaviour causing fluctuations, particularly in the sump.
- (6) Modelling errors, particularly as a result of simplifications.

Variations in the rate of grinding were perhaps the largest source of

noise. Because all the above causes were dependent upon the mass of solids present in each size fraction, it was assumed that the perturbations were directly proportional to the mass in each fraction. Thus it was chosen to lump all the causes together and model the noise input as a variation in the S_i in equation (4.2.1). The following model was written:

$$S_i \cdot dt = S_{i0} \cdot K_L \cdot K_S \cdot (dt + \phi_i \cdot dW_i) \quad (4.3.19)$$

where S_{i0} is the deterministic selection function calculated from off-line tests,

K_L is a load factor which depended on the slurry charge in the mill,

K_S is a softness factor (reciprocal of hardness) which could be estimated on line, if desired,

ϕ_i is a noise attenuation factor,

dW_i is a normalised Wiener process associated with size fraction i .

This meant, in effect, that S was a white noise process with a non-zero mean (section 4.2.3).

We now consider the flow of solids around the grinding circuit:

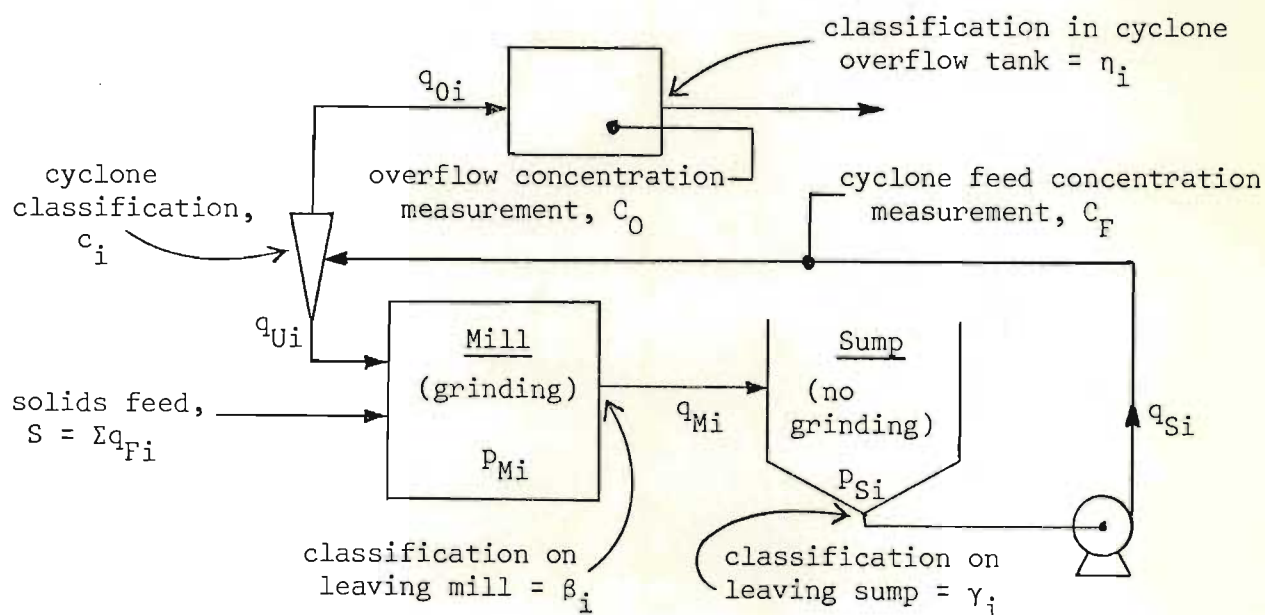


Figure 4.4 Solids flows in the milling circuit.

The mill and sump were regarded as fully mixed vessels, but with classification occurring at the output as shown. Thus,

$$q_{Mi} = \frac{Q_M}{V_M} \cdot \beta_i \cdot p_{Mi} \quad (4.3.20)$$

$$q_{Si} = \frac{Q_S}{V_S} \cdot \gamma_i \cdot p_{Si} \quad (4.3.21)$$

The cyclone model was written as

$$q_{Ui} = q_{Si} \times c_i = q_{Si} \cdot (c_{0i} + c_{1i} \cdot C_F) \quad (4.3.22)$$

where C_F was the cyclone feed concentration, and

$$C_F = \frac{1}{V_S} \cdot \sum_{i=1}^{n_p} \gamma_i \cdot p_{Si} \quad (4.3.23)$$

Material balances for the mill and sump were written for size group i , based on the individual grinding model, equation (4.2.1), giving:

$$dp_{Mi} = (q_{Fi} + q_{Ui} - q_{Mi} - S_i \cdot p_{Mi} + \sum_{j=1}^{i-1} S_j \cdot b_{ji} \cdot p_{Mj}) \cdot dt \quad (4.3.24)$$

$$dp_{Si} = (q_{Mi} - q_{Si}) \cdot dt \quad (4.3.25)$$

Substituting equations (4.3.19) to (4.3.23) into (4.3.24) and (4.3.25) gave:

$$\begin{aligned} dp_{Mi} = & \left(q_{Fi} + \frac{Q_S}{V_S} \cdot \left(c_{0i} + \frac{c_{1i}}{V_S} \cdot \sum_{j=1}^{n_p} \gamma_j \cdot p_{Sj} \right) \cdot \gamma_i \cdot p_{Si} - \frac{Q_M}{V_M} \cdot \beta_i \cdot p_{Mi} \right. \\ & \left. - S_{i0} \cdot K_L \cdot K_S \cdot p_{Mi} + \sum_{j=1}^{i-1} S_{j0} \cdot K_L \cdot K_S \cdot b_{ji} \cdot p_{Mj} \right) \cdot dt \\ & - S_{i0} \cdot K_L \cdot K_S \cdot \phi_i \cdot p_{Mi} \cdot dW_i + \sum_{j=1}^{i-1} S_{j0} \cdot K_L \cdot K_S \cdot \phi_j \cdot b_{ji} \cdot p_{Mj} \cdot dW_j, \\ & i = 1, \dots, n_p \end{aligned} \quad (4.3.26)$$

$$dp_{Si} = \frac{Q_M}{V_M} \cdot \beta_i \cdot p_{Mi} - \frac{Q_S}{V_S} \cdot \gamma_i \cdot p_{Si}, \quad i = 1, \dots, n_p \quad (4.3.27)$$

Equations (4.3.26) and (4.3.27) formed the plant model for the p.s.d.

filter. Note that for n_p particle size groups, there were $2n_p$ state

variables, p_{Mi} , p_{Si} , $i = 1, \dots, n_p$. All other variables of interest were

calculated/....

calculated from these state variables.

At observations, the concentrations of the feed to the cyclone and the overflow from the cyclone were measured. Thus, for the observation model:

$$\text{feed conc., } y_1 = \frac{1}{V_S} \cdot \sum_{i=1}^{n_p} \gamma_i \cdot P_{Si} + v_1 \quad (4.3.28)$$

$$\begin{aligned} \text{overflow conc., } y_2 = \frac{Q_S}{V_S(Q_S - Q_U)} \cdot \sum_{i=1}^{n_p} (1 - c_{0i} - \frac{c_{1i}}{V_S} \cdot \sum_{j=1}^{n_p} \gamma_j \cdot P_{Sj}) \gamma_i \eta_i P_{Si} \\ + v_2 \end{aligned} \quad (4.3.29)$$

In this investigation, 4 particle size groups were used. This was about the largest number which could be handled, and about the smallest number which would model the process adequately. This also reduced the problem of observability which might have occurred if there were two nearly equal size groups. The size ranges chosen were 0 to 75 μ m, 75 to 212 μ m, 212 to 850 μ m, and 850 to 9500 μ m. The choice of 75 and 212 μ m was because these are two commonly quoted sizes, and with 850 μ m, they divide up the size spectrum into suitable ranges.

4.3.4 Solution of Particle Size Distribution Filter, Using Moments.

Several methods of solving the filter equations were considered. The most successful was the method of moments. Other methods failed either because of over-complexity with the large dimension, or because of excessive core or time requirements in implementation. Differential quadrature was also tested as explained in section 4.1.2.5.

The solution by moments was carried out as explained in section 4.1.2.1, and 4.1.2.2, with the plant model given by equations (4.3.26) and (4.3.27), and the observation model given by equations (4.3.28) and (4.3.29). Only the first and second moments were considered, partly because of the difficulty with large dimensions, and partly because most of the information is

contained in the first and second moments. The calculations were done using central second order moments or covariances because these were more directly usable. With 4 size groups, there were 8 state variables, which had 8 means and 36 variances and covariances, the latter being most easily written as a symmetric 8x8 matrix (i.e. 64 elements). To estimate softness, another state variable, K_S , was added (see section 4.1), which required one extra mean and a further 8 covariances. K_S could then be estimated on line together with the masses in each fraction.

Appendix A lists the differential equations for the evolution of the moments as used in the filter, based on the plant model equations (4.3.26) and (4.3.27). The problem of closure occurred using moments. This was handled by ignoring all third order central moments, as though the distribution were Gaussian, i.e. (using the notation in appendix A):

$$\mu_3(ABC) = m_2(AB).m_1(C) + m_2(AC).m_1(B) + m_2(BC).m_1(A) \quad (4.3.30)$$

and writing fourth order moments as

$$\begin{aligned} \mu_4(ABCD) = & m_1(A).m_1(B).m_1(C).m_1(D) + m_2(AB).m_2(CD) \\ & + m_2(AC).m_2(BD) + m_2(AD).m_2(BC) \end{aligned} \quad (4.3.31)$$

This approximation was not the best for fourth order moments, but it was short and sufficiently accurate.

Subroutine IBCDRV was written to compute the derivatives given in appendix A. This is listed in appendix C.

For integration of the moment equations, both simple trapezoidal rule and Euler half step integration were tried. These are, respectively, for moments \underline{m} :

$$\underline{m}(t_{k+1-}) = \underline{m}(t_{k+}) + \Delta t. \frac{d\underline{m}}{dt}(\underline{m}(t_{k+}), t_{k+}) \quad (4.3.32)$$

$$\left. \begin{aligned} \underline{m}(t_{k+\frac{1}{2}}) &= \underline{m}(t_{k+}) + \frac{1}{2} \Delta t. \frac{d\underline{m}}{dt}(\underline{m}(t_{k+}), t_{k+}) \\ \underline{m}(t_{k+1-}) &= \underline{m}(t_{k+}) + \Delta t. \frac{d\underline{m}}{dt}(\underline{m}(t_{k+\frac{1}{2}}), t_{k+\frac{1}{2}}) \end{aligned} \right\} \quad (4.3.33)$$

The time required for the evaluation of the derivatives (see section 6.8.10), made it uneconomic to try higher order integration methods with the time interval used. Equation (4.3.33) was used for all results given in this thesis.

For the observation step, the simplified second order filter observation step which was outlined in section 4.1.2.1(c) was used, with the model in equations (4.3.28) and (4.3.29). This observation step was handled by subroutine IBPOBS. This subroutine used the concentration measurements of the cyclone feed and overflow from each observation k , as the vector y_k in equation (4.1.18), with the function, m , in this equation given by the first terms on the right hand sides of equations (4.3.28) and (4.3.29):

$$\underline{m} = \begin{bmatrix} \frac{1}{V_S} \cdot \sum_{i=1}^{n_p} \gamma_i \cdot p_{Si} \\ \frac{Q_S}{V_S(Q_S - Q_U)} \cdot \sum_{i=1}^{n_p} (1 - c_{0i} - \frac{c_{1i}}{V_S} \cdot \sum_{j=1}^{n_p} \gamma_j \cdot p_{Sj}) \cdot \gamma_i \cdot p_{Si} \end{bmatrix}$$

and the P_A matrix consisting of the second central moments of p_{Mi} , p_{Si} , $i = 1, \dots, 4$, and K_S . From this observation step, the means and variances (\hat{x} and P_A respectively in equations (4.1.18) to (4.1.21)), of the masses in each fraction in the mill and sump were updated, and if desired, the softness factor, K_S , was simultaneously estimated (as a parameter \hat{u} in equation (4.1.18)). Normally the softness was kept fixed.

It should be noted here how the filter is able to estimate variables which are not measured directly. During the evolution step, the plant model (equations (4.3.26) and (4.3.27)) causes the variables in the model to become correlated through the covariance matrix P_A . This part is described by the evolution for the covariances given in appendix A. At an observation k , the Kalman gain matrix K_k in equation (4.1.18) is calculated from equation (4.1.20), using the covariance matrix P_A as shown. The elements of matrix K_k are effectively correction factors for each variable from each observation

error, based on the expected correlations. Thus the softness parameter, K_S , for example, may be included in the estimation by augmenting it to the state variables as a parameter u , with equations for the evolution of the state and softness (as given in appendix A), and with u included in the observation step (equations (4.1.18) to (4.1.21)).

4.3.5 Conversion to Particle Size Distributions and Concentrations

Presenting the output from a filter was found to be a problem because of the large amount of information produced. For the p.s.d. filter, it was found easiest to convert the raw data (i.e. the masses in each fraction) into quantities such as particle size distributions and concentrations, and to display these graphically. The conversions were done as shown below.

Let \underline{x} be the state vector of the p.s.d. filter (consisting of the masses in each fraction in the mill and sump) and let \underline{f} be the vector of individual mass fractions in the stream under consideration. Now, $f_i = f_i(\underline{x})$, and expanding the function to second order, we get:

$$\text{mean of } f_i = \bar{f}_i \approx f_i(\bar{\underline{x}}) + \frac{1}{2} \sum_{j=1}^8 \sum_{k=1}^8 \frac{\partial f_i}{\partial x_j \partial x_k} \cdot m_2(x_j x_k) \quad (4.3.34)$$

$$\text{covariance of } f_i f_j = m_2(f_i f_j) \approx \sum_{k=1}^8 \sum_{l=1}^8 \frac{\partial f_i}{\partial p_k} \cdot m_2(x_k x_l) \cdot \frac{\partial f_j}{\partial p_l} \quad (4.3.35)$$

where $m_2(x_j x_k)$ is the covariance of x_j and x_k as used in appendix A.

(The similarity of equation (4.3.34) to the observation step, equations (4.1.18) and (4.1.21), should be noted.)

The cumulative fractions, F_i , were the sum of the individuals, i.e.:

$$F_i = \sum_{j=i}^4 f_j \quad (4.3.36)$$

Hence,

$$\text{mean of } F_i = \bar{F}_i = \sum_{j=i}^4 \bar{f}_j \quad (4.3.37)$$

$$\text{covariance of } F_i, F_j = m_2(F_i F_j) = \sum_{k=i}^4 \sum_{l=j}^4 m_2(f_k f_l) \quad (4.3.38)$$

Similarly for a concentration $C_i = C_i(\underline{x})$ in stream i , we have:

$$\text{mean of } C_i = \bar{C}_i \approx C_i(\bar{x}) + \frac{1}{2} \sum_{j=1}^8 \sum_{k=1}^8 \frac{\partial f_i}{\partial x_j \partial x_k} \cdot m_2(x_j x_k) \quad (4.3.39)$$

$$\text{variance of } C_i = m_2(C_i^2) \approx \sum_{j=1}^8 \sum_{k=1}^8 \frac{\partial C_i}{\partial x_j} \cdot \sigma_{x_j x_k}^2 \cdot \frac{\partial C_i}{\partial x_k} \quad (4.3.40)$$

For example, for the cyclone overflow concentration,

$$C_O = K_0 \cdot \sum_{i=1}^4 \gamma_i \cdot (1 - c_{0i} - c_{1i} \cdot C_F) \cdot p_{Si} \quad (4.3.41)$$

$$\text{where } K_0 = \frac{Q_S}{V_S(Q_S - Q_U)} \quad \text{and} \quad C_F = \frac{1}{V_S} \cdot \sum_{i=1}^4 \gamma_i \cdot p_{Si}$$

so that

$$\bar{C}_O = \bar{K}_0 \cdot \sum_{i=1}^4 \gamma_i \cdot (1 - c_{0i} - c_{1i} \cdot \bar{C}_F) \cdot m_1(p_{Si}) - \frac{\bar{K}_0}{2} \cdot \sum_{i=1}^4 \sum_{j=1}^4 \frac{\gamma_i \gamma_j (c_{1i} + c_{1j})}{V_S} \cdot m_2(p_{Si} p_{Sj}) \quad (4.3.42)$$

and

$$m_2(C_O^2) = \bar{K}_0^2 \cdot \sum_{i=1}^4 \sum_{j=1}^4 \gamma_i \gamma_j \cdot (1 - c_{0i} - \frac{1}{V_S} \cdot \sum_{k=1}^4 \gamma_k \cdot (c_{1i} + c_{1k}) \cdot \bar{p}_{Sk}) \times \\ (1 - c_{0j} - \frac{1}{V_S} \cdot \sum_{k=1}^4 \gamma_k \cdot (c_{1j} + c_{1k}) \cdot \bar{p}_{Sk}) \cdot m_2(p_{Si} p_{Sj}) \quad (4.3.43)$$

Subroutine IBPTOF was written to calculate the means and variances of the size distributions of the product stream (cyclone overflow), the cyclone underflow and mill contents, as well as the concentrations around the circuit. This took a long time to compute (see section 6.8.10) and so a simplified subroutine, IBSIMP, was written to calculate concentrations and distributions without taking variances into account. This used equations (4.3.34) without the second term, (4.3.36), and (4.3.39) without the second term. Its accuracy is discussed in section 6.8.11.

4.3.6 Summary of p.s.d. Filter.

The particle size distribution filter developed here estimated the first moments and second central moments of the masses in each size fraction in the mill and sump. Four particle groups were used. The softness of the rock could also be estimated on line through the filter if desired.

To do this, an evolution step and an observation step were developed. The evolution step used subroutine IBCDRV, which calculated the derivatives of the means and variances of the estimates given in appendix A, to integrate over the interval between observations. At the observations (after running the volumetric filter), the concentration measurements were used to update the estimates with subroutine IBPOBS.

From the means and variances of the state in the p.s.d. filter, the predictions of the actual particle size distributions were calculated using IBPTOF or IBSIMP.

4.3.7 Use of the Filter

A simple flowchart for the full filter is shown in figure 4.5.

Before running the filter, by means of programme IBPRPC, the values of the constants and starting values for use in both filters were read in. Matrices for the volumetric filter were calculated, and all the necessary data were stored on a disc file. The data were then read back when the filter started. Two main programmes were written to coordinate the filter calculations, IBMFLC for off-line work, and IBOLMF for real time work. The following steps were then performed after each observation from the plant.

(1) Measurements from the instruments were taken and converted to values of the variables S , W_M , Q_S , V_S , W_S , C_F and C_O at time t_k on the operating

plant./....

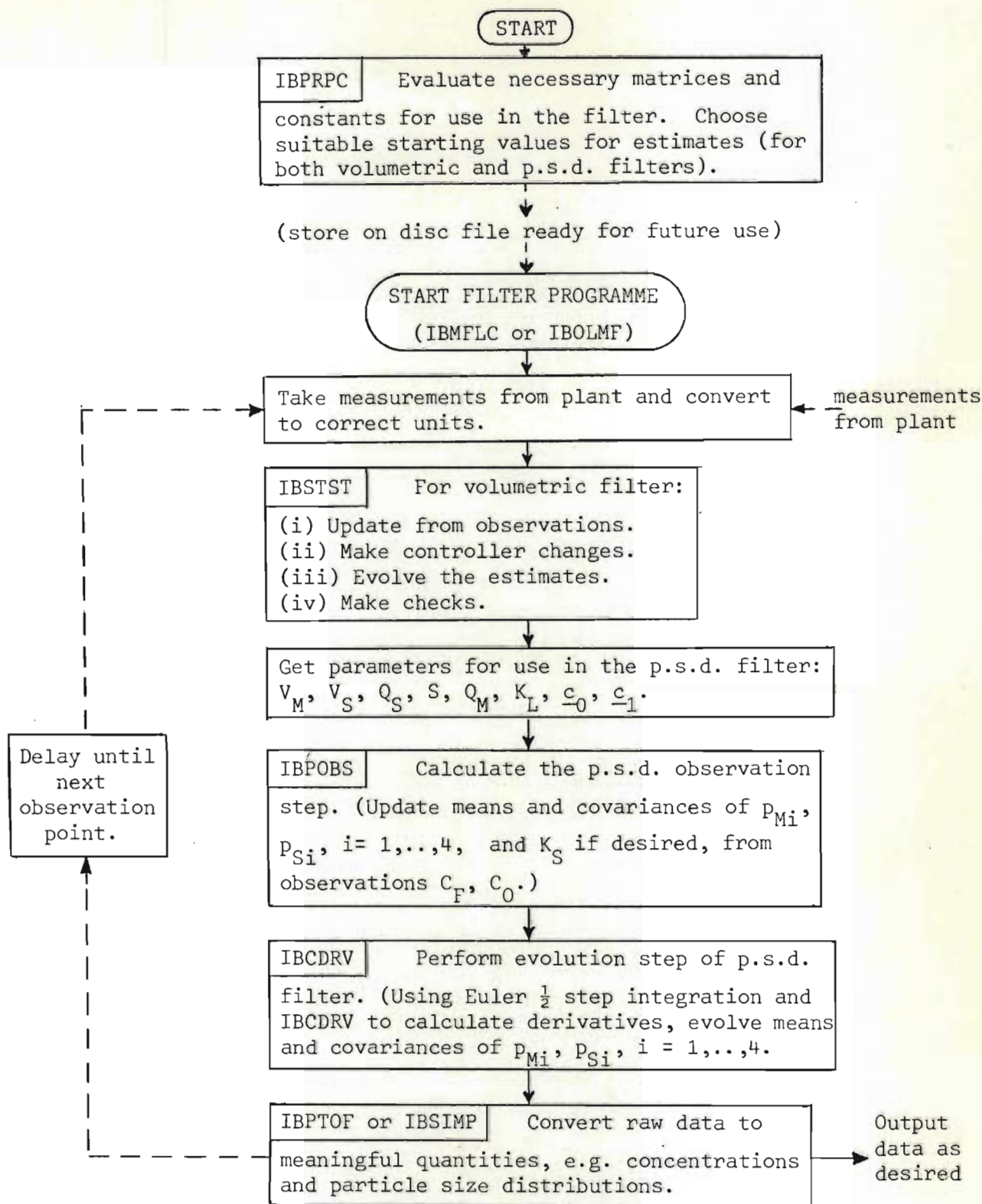


Figure 4.5 Filter Flowchart.

This shows basic signal flows and sequencing of calculations.

(See section 4.3.7.)

plant.

- (2) The volumetric filter, outlined in sections 4.3.1 and 4.3.2, was implemented using subroutine IBSTST. This gave estimates of V_M , V_S , Q_S , S , W_M and W_S . From these, Q_M , K_L and the actual classifier constants, c_0 and c_1 , were calculated for use in the p.s.d. filter.
- (3) The p.s.d. filter observation step given in section 4.3.4 was taken using IBPOBS.
- (4) The p.s.d. filter evolution step was taken using Euler half step integration with the derivatives calculated by IBCDRV.
- (5) The p.s.d. state was then converted to the size distributions and concentrations using IBPTOF for off-line runs, and IBSIMP for real-time work. At this point, all the estimates were available for the following interval. For off-line tests, these were stored on another disc file, and the programme went back to step(1) to continue. For on-line work, these were also made available for control, and the programme then waited for the next observation.

The main subroutines used in the filter, IBSTST, IBCDRV, IBPOBS, IBPTOF, and IBSIMP are listed in appendix C. The preparation programme, IBPRPC, the off-line filter programme IBMFLC, and the on-line filter programme, IBOLMF, are also shown.

Chapter 5

EQUIPMENT AND EXPERIMENTATION

Most of the work done was on the pilot plant milling circuit or the Control Data 1700 computer in the Department. The batch grinding tests were done on a separate batch grinding machine, and use was made of the research group's analytical equipment for doing the analyses of samples. Other off-line experiments were done on the milling circuit. The Burroughs B5700 computer at the University of Natal, Durban computer centre was also used for some of the computations.

5.1. Milling circuit

Figure 5.1 shows details of the milling circuit. It was a wet ball mill with a nominal capacity of one tonne per hour. Solids were fed from a storage bin by means of a variable speed belt to the mill, where water was added before entry. The mill overflowed into a sump which was stirred. After dilution, the slurry was pumped with a variable speed pump to the cyclone. The coarse cyclone underflow returned to the mill, while the finer overflow discharged into a small stirred tank where its concentration was measured before it left the plant as the product stream. Table 5.1 gives specifications of the circuit. Plate 1 shows a general view of the equipment.

Two different ball charges were used, and these are shown in Table 5.2. The initial charge was found to be too fine for grinding larger stones. The coarser charge was used for all full scale runs quoted here, but scaled down versions of both were used for the batch runs.

The instrumentation is also shown in Figure 5.1. All the instrumentation was connected to the CDC 1700. All control was of the signal to change type D.D.C. with manual override, which gave great flexibility. Table 5.3

Analogue instrument signals to computer

- A1. Solids feed-belt speed setting
- A2. Mill water feed valve setting
- A3. Sump water feed valve setting
- A4. Recirculation rate
- A5. Sump level
- A6. Recirculation concentration
- A7. Product conc.
- A8. Mill power
- A9. Solids hopper weight

Control signals

- C1. Solids feed belt
- C2. Mill water feed
- C3. Sump water feed
- C4. Recirculation rate.

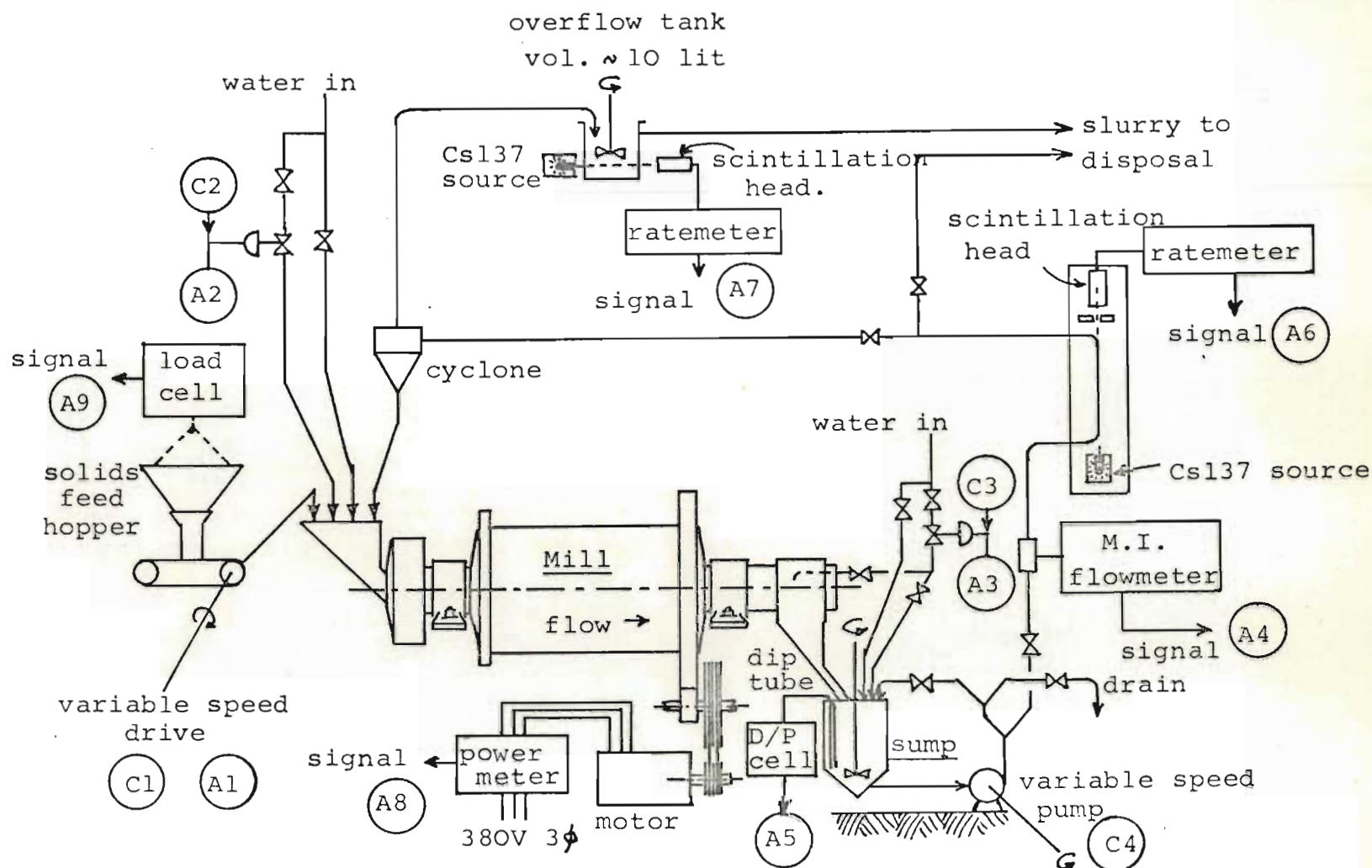


Figure 5.1 Flowchart of milling circuit.

Table 5.1Specifications of Milling Circuit.

<u>Mill type:</u>	Allis Chalmers, nominal size 3ft x 4ft with overflow discharge
<u>Internal dimensions:</u>	1,22m long, 0,762m mean diameter 7 lifters, wave $\pm 1,27$ cm about mean diameter 0,217m overflow diameter
<u>Mill speed:</u>	30 r.p.m. (= 62% of critical)
<u>Sump capacity:</u>	originally 0,18 m ³ max. (unstirred) subsequently 0,025 m ³ max. (stirred) (The former was used only for the mill outflow characteristics.)
<u>Cyclone:</u>	150mm diameter 20°, type S.I. cyclone (made by R.J. Spargo) 50mm (i.d.) vortex finder diameter 25mm x 75mm inlet 12,5 mm spigot diameter
<u>Variable speed pump:</u>	1½/1B Warman pump 810 to 2430 r.p.m. speed range nominal flow of 1 l/s

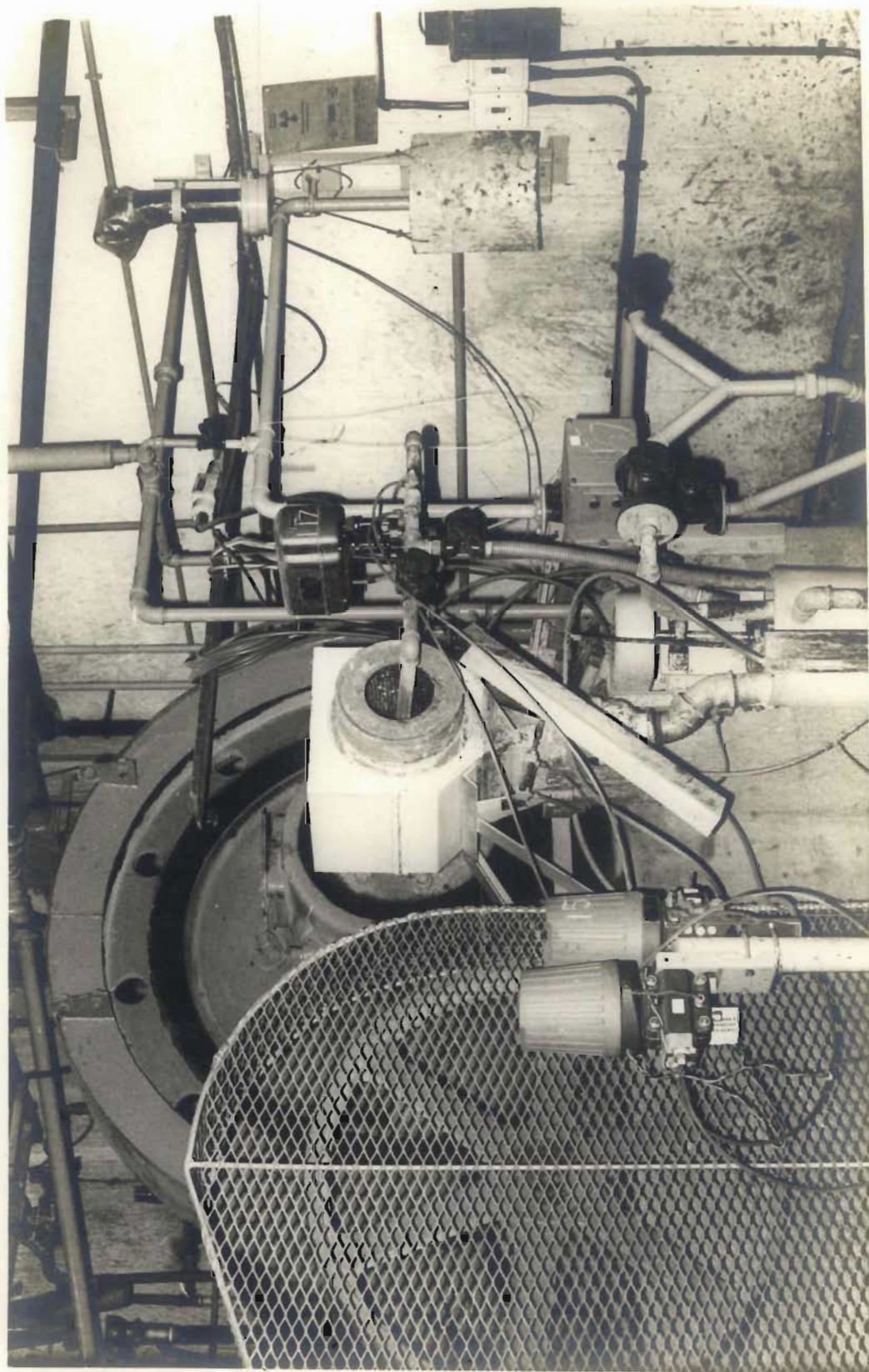


Plate 1 Discharge end of mill showing some associated instrumentation.

Table 5.2

Details of ball charges used in the pilot plant mill and corresponding batch tests.

Ball size mm (nominal)	Mean mass per ball kg	First load				Second load			
		Mass loaded		Mass used for batch test 30/4		Mass loaded		Mass used for batch test 20/6	
		kg	%	kg	%	kg	%	kg	%
30	0,126	570	63,0	23,1	63,3	63,4	6,9	2,60	7,1
40	0,263	335	37,0	13,4	36,7	145,2	15,9	5,70	15,7
50	0,589	-	-	-	-	312,9	34,4	12,25	33,7
60	0,956	-	-	-	-	245,0	26,9	9,65	26,6
70	1,545	-	-	-	-	145,0	15,9	6,15	16,9
Totals =		905	100	36,5	100	911,5	100	36,35	100

Table 5.3

Details of Measurement and Control Devices.

Solids feed rate: calculated from actuator setting on variable speed belt, (weight of solids feed hopper also available).

Mill water: calculated from setting of actuator on valve.

Sump to cyclone flow: measured with M.I. flowmeter (Altometer type) and corrected for magnetite content from concentration.

Sump volume: measured with bubble tube and electric D/P cell, and corrected for S.G. from concentration.

Sump water flow: measured with orifice plate and electric D/P cell.

Concentrations: measured by γ -ray absorption using Cs137 source, and Philips detection heads and ratemeters.

Sump to cyclone concentration: situated along a vertical section of the sump to cyclone line (approx. 0.5m long, flow downwards).

Cyclone overflow concentration: situated across the discharge tank from the cyclone overflow (stirred).

Mill power: 3 ϕ power meter on supply to mill motor.

Controls: all controls of the signal-to-change type, controlled directly by computer, with manual override.

Sump pump control: Variable speed pulley drive with actuator
Actuator time = 40,5 s for full range.

Solids feed control: Variable speed belt with actuator
Actuator time = 145,0 s for full range.

Mill water control: Logarithmic control valve with actuator
(Philips ND16 valve, 15mm nominal diameter)
Actuator time = 91,5 s for full range.

Sump water control: Needle valve with Rotork type 1F actuator
Actuator time = 30,7 s for full range.

lists the details of the instrumentation and how each variable was measured or controlled. One of the remote typewriters from the computer was available at the plant for communications. Plate 2 shows the instrument cabinet on the plant.

5.2. "Control Data 1700" computer

This was a process control computer installed in the Department and used for batch processing, real-time data logging, and control of pilot plants. Details of the system are listed in Table 5.4. Part of the system is shown in Plate 3. The computer was basically for control, and operated on a time sharing basis to process several programmes or parts of programmes together. Programmes were written in Fortran IV with extra statements for real-time work (mainly input/output and timing). Data could be stored in a file on a disc for later re-use. Towards the end of this project, hardware was fitted for doing floating point arithmetic, which speeded up filter computations considerably (see results, section 6.8.10).

5.3. Analyses

Sampling of slurry streams was done using a bucket and stopwatch. These samples were then weighed, filtered, dried and weighed again to determine flows and densities.

Samples for particle size analyses were then lightly crushed to break up the lumps, and split using a Jones riffler into suitable quantities for screening. These were wet deslimed on a 38 μm sieve and re-dried before sieving using standard metric 200 mm sieves on an Endecotts sieve shaker. For the batch milling analyses, about 200 to 250 grams of sample were used and the sieving was done in two stacks into 17 size fractions forming the usual $\sqrt{2}$ progression from 6300 μm to 850 μm and then from 600 μm to 53 μm . For the samples from the continuous mill and cyclone, about 100 to 150 grams were used and sieving

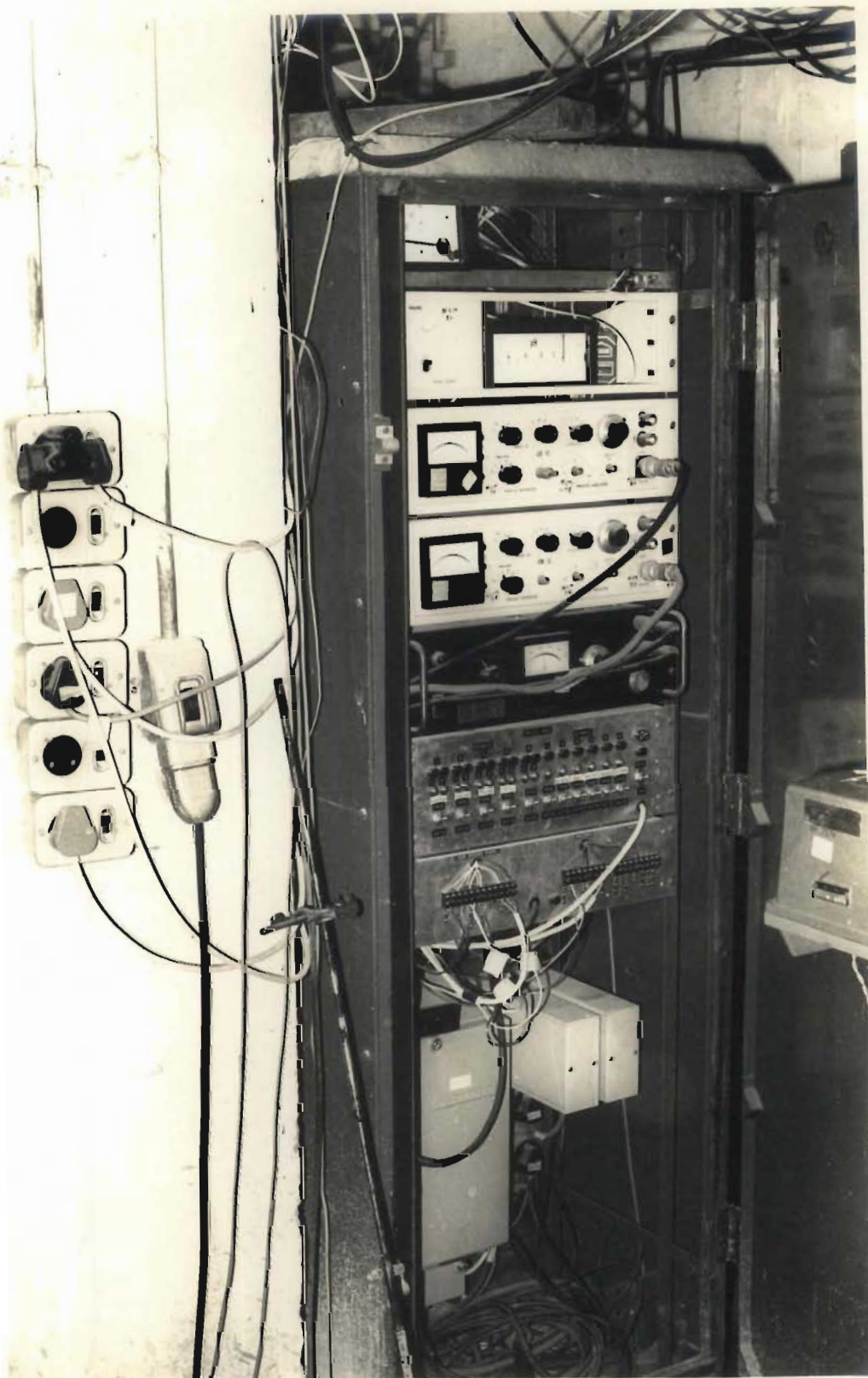


Plate 2 Instrument cabinet on plant showing ratemeters,
control relay box, flowmeter and power supplies.

Table 5.4Details and Specifications of the Computer System Used

- (1) A central processor (1,5 μ s cycle time) with 32K of core, (each word 16 bits + 1 parity + 1 protect) and built-in clock.
- (2) Two disc drives, and a selection of discs each 3M words storage.
- (3) A line printer (150 lines/minute)
- (4) A main teletype.
- (5) Four remote typewriters for communication with the computer from pilot plants.
- (6) A card reader (300 cards/minute)
- (7) An incremental graph plotter.
- (8) A display storage c.r.t. with an associated remote terminal.
- (9) A range of signal input/output devices consisting of
 - (i) 128 Analogue inputs multiplexed to an A/D converter
 - (ii) 8 Analogue outputs
 - (iii) 128 Digital inputs (contact closure)
 - (iv) 96 Digital outputs (relay changeover)
 - (v) 4 event counters
 - (vi) 16 external interrupt lines



Plate 3 Part of the departmental computer centre with CDC 1700 control computer.
From left: C.P.U., teletype, line printer, plotter, display 'scope, card reader.

was done on one stack following a progression of 2 from 3350 μm to 425 μm and then $\sqrt{2}$ down to 53 μm . For the results of the runs on the milling circuit, only condensed particle size analyses are given in this thesis. These used the same 4 groups as the filter, i.e. sizes 0, 75, 212 and 850 μm .

Where densities were measured, an air pycnometer was used to measure the actual volume of dry powder. The density was calculated from the mass and volume, and in the results is expressed as specific gravity (S.G.).

5.4. The ore

The ore used throughout this investigation was an apatite-calcite-magnetite-olivine mixture from the Phalaborwa complex in the north eastern Transvaal, commonly known as "Phoscorite". The approximate analysis is given in Table 5.5.

Table 5.5. Approximate data for the ore used

Apatite	20% (by mass)
Calcite (+ minor MgCO_3)	16% "
Magnetite	34% "
Serpentine-Olivine (+ minor mica)	30% "
Average S.G.	3,37
Range of S.G. in constituent minerals	2,71 to 5,18
Range of hardness in constituent minerals	3 to 6 (Moh's scale)
Average Bond Work Index	~13

A problem encountered with this ore, and perhaps typical of many ores in practice, is the variation in hardness and density between constituents. This resulted in an increase of magnetite in the circulating load in the milling circuit (giving an S.G. up to 3,7 in the cyclone underflow).

Although not unimportant, this was ignored in most cases, and most tests were done using the average rock at that point in the circuit. This caused some scatter in the results, and is discussed in Chapter 7.

The rock supplied by the Phosphate Development Corporation had been crushed to -9,5 mm. This was then fed directly from storage to the milling circuit.

5.5. Off-line tests

The following off-line tests were done:

- 1) Batch milling experiments to get parameters for the grinding model.
- 2) Cyclone tests to get classification and flow behaviour data.
- 3) Mill overflow characteristics, for transport model.
- 4) Calibrations of instruments.

5.5.1. Batch milling

Two sets of runs, 30/4 and 20/6, were done on a batch mill to determine selection and breakage function data. The data from both of these runs are presented in the results, although only run 20/6 data were used in the filter. A 30,5 cm by 30,5 cm batch mill was used. Quantities in the large mill were scaled down in proportion to volume, and the percent of critical speed was kept approximately the same. Each set of runs consisted of a sequence of samples ground for different times to determine the selection and breakage functions corresponding to normal operation, and a set of grinds with varying slurry density and charge to determine the effects of these two variables. These latter grinds were all done for twenty minutes with the total slurry charge and density put separately at two levels, equally spaced each side of the mean. After doing set 30/4, the ball load in the pilot plant was altered, and the second set 20/6 was then done on the new load. Ball charges used are given in Table 5.2.

A fairly representative sample of fresh ore was drawn off from the solids feed system and split into 16 equivalent lots using a Jones riffler. Each sample was then rounded off by hand addition or removal to the desired mill load. A separate sample of solids was used for each grind, and the mill was completely washed out between grinds.

5.5.2. Cyclone tests

The filter required details for two models involving the cyclone, one giving the volumetric split and the other the solids classification for each particle size group. The cyclone was tested in situ in the milling circuit. Perturbations were deliberately added to get data over a wide range. Two sets of runs were done solely to collect cyclone data, and further data were added from samples taken during other runs.

The ore used was not homogeneous. To simplify the model it was assumed that the solids would behave in some "average" way for classification, but variations in solids S.G. between feed, overflow and underflow were taken into account in analysing the results.

The size of a cyclone required for a pilot plant scale milling circuit means that the cyclone operates under near limiting conditions. This makes the useful range of operation smaller, as well as making the cyclone operation noisy and potentially troublesome. Some earlier work (not reported here) was needed to get the cyclone operating properly.

5.5.3. Mill outflow characteristics

In the filter model, the mill and sump were assumed to behave as ideal stirred tanks, and the mill was assumed to have first order outflow characteristics (Section 4.3.1.). An experiment was done to check this and obtain the constant in the overflow equation.

The mill was put/...

The mill was put into normal closed circuit operation. At a given time, all feeds to the mill and sump, and the sump withdrawal were stopped. The mill, which had been overflowing normally, continued to overflow and fill the sump, and the volume in the sump was recorded as a function of time. Finally, the mill was stopped and rolled back so that the charge was horizontal. The total volume of water overflowed was added to the calculated remaining volume of the charge, to get the operating volume of the mill.

5.5.4. Calibrations of instruments

Because the filter required actual values of variables on the plant, a large number of calibrations were required. It was also found to be necessary to continually re-calibrate as instruments drifted, or as they failed and were repaired, or as plant changes were made. A minor change would often mean a major re-calibration. As well as calibrating between sensing elements and the computer, the characteristics of the control devices were determined from actuator time to position and then to value of controlled variable.

The calibrations of most of the devices were simple, and usually linear. Solids feed rate was calculated very approximately from the variable speed belt setting, using a quadratic equation. The mill water valve was logarithmic and had a noticeable hysteresis, which was included in the calibration. The sump pump controller was not calibrated as it was dependent on the slurry being pumped, but the actual flow was measured with a magnetic induction flowmeter and then corrected slightly for the magnetite content from the concentration measurement. Concentrations from the nuclear gauges were calculated by

$$\text{Concentration} = K \times \ln \left(\frac{\text{water reading} - \text{background}}{\text{present reading} - \text{background}} \right) \quad (5.1)$$

where K is/...

where K is a constant dependent on the system

background = background count rate (without source)

water reading = count rate with only water in the system.

5.6. Runs done on mill for filter

The data from four runs which totalled over ten hours of useful operation, were used for testing the filter. Because of the cost of the ore it was not possible to run for a long time, and so the circuit was deliberately perturbed over as wide a range as possible during the runs. Some short runs were done earlier for debugging the system and programmes, but they were found to be of no use for detailed studies.

A control programme, IBMILL, was written to control the plant, log data on a disc file, and write out data on the remote typewriter. Another programme was written for communicating with the control programme to alter set points, controller settings, etc. The first two runs, 18/10 and 23/10, (coded "A" and "B" respectively) were done to get data, without the filter operating in real time. After the filter had been tested off-line on these stored data, it was modified to run on-line as programme IBOLMF. IBMILL was extended to operate with this filter. Runs 16/4 and 18/4 (coded "C" and "D" respectively) were done with the filter operating in real time.

Controller settings were made deliberately slack, so that natural fluctuations would be large for tracking by the filter. The D.D.C. control scheme used was as follows:

- 1) Control the sump water from the cyclone feed concentration.
- 2) Control the sump pump from the pump flow (a fast loop), where the flow set point was controlled from sump level.
- 3) Control the solids feed from the solids flow to the cyclone, calculated from the flow and concentration.

- 4) Control the mill water in proportion to the solids feed.
- 5) If the sump level goes too low, increase the sump water regardless of other control.
- 6) If the cyclone feed concentration was low, (e.g. during start-up) control the sump water from the level and keep the pump flow set point fixed. Otherwise control remained the same. Settings were made to give a smooth change-over to normal control.
- 7) During runs C and D, if it was desired to control from the filter results, the mill feed solids could be controlled from the predicted underflow concentration, and the sump water from the predicted -75 μm fraction in the overflow product. Otherwise the control remained the same. Some difficulty was experienced in setting the controller constants here.

Although control was automatic, at least one assistant was required when doing runs in case of a breakdown. Start-up and shutdown were performed manually. Several hours before a run the ratemeters were switched on, and a quick check was made that the circuit was ready. Sample buckets were also prepared. The other instruments were switched on when the run was ready to start, and the ratemeter water counts were checked and entered in the control programme. The mill was started in open circuit, and extra water was added to the sump during startup. The mill control programme could be scheduled at any time, and the sump control switched to automatic immediately. The circuit was closed by re-routing the sump withdrawal to the cyclone, and all controls were then put on automatic.

Samples were taken during the runs at approximately 5 to 10 minute intervals. These samples were for use in checking the filter, and so it was attempted to take them more frequently when more detailed data were needed. During runs A and B, and up to 90 minutes in run C, the overflow was sampled at the outflow of the density tank. Thereafter the cyclone discharge was sampled directly.

A few underflow samples were taken directly at the cyclone spigot.

Shutdown was the reverse of startup, and was generally faster. After each run, the samples were analysed, and a plot on the computer graph plotter was drawn up of the main variables, using the stored data.

Chapter 6

RESULTS

The results from this study form two main groups, the experimental data and the filter results. The experimental data comprise the off-line tests and the raw data from the runs on the milling circuit. In the results from the filter, the filter predictions for each of the runs are shown and compared with the sampled values, and the effects of various factors in the filter are demonstrated. Finally, the real time requirements of the filter are examined, and the use of a quadrature filter is shown.

6.1. Batch milling results

The results of the two sequences of batch grinds (runs 30/4 and 20/6) are listed in Tables 6.1 and 6.2 respectively, and are displayed for comparison in Figure 6.1. In this figure, the cumulative mass percent has been plotted on a linear axis against particle size on a log axis, to give nearly equal weighting to each fraction. The effect of the difference between the two ball loads is clearly visible.

The regression on these data to get selection and breakage functions was done as explained in the theory, Section 4.2.1. The initial values of the model parameters to be used in the regression were estimated in various ways, but were fairly close to the calculated best fit values and so one may assume that the final regressed values were reasonably optimal. Tables 6.3 and 6.4 summarise the results. Reasonably good fits were obtained as shown by the lines in Figure 6.1, even though the ore was not homogeneous. In Figure 6.2 the selection functions are plotted against particle size, and in Figure 6.3 the breakage functions are plotted together with the breakage function of Broadbent and Callcott for comparison.

To use these data/...

Table 6.1 Batch milling results for run 30/4

Table of individual mass fractions per size group for each grind time.

		Grind time, minutes						
		0	5	10	15	20	30	40
size fractions, range in microns	6300 to 9500	0,0984	0,0795	0,0810	0,0667	0,0416	0,0255	0,0084
	4750 to 6300	0,2071	0,1134	0,0757	0,0780	0,0456	0,0147	0,0042
	3350 to 4750	0,1940	0,1221	0,0821	0,0450	0,0347	0,0111	0,0035
	2360 to 3350	0,1369	0,0835	0,0471	0,0233	0,0158	0,0039	0,0014
	1700 to 2360	0,0767	0,0450	0,0278	0,0143	0,0093	0,0033	0,0014
	1180 to 1700	0,0596	0,0432	0,0233	0,0103	0,0068	0,0022	0,0009
	850 to 1180	0,0397	0,0376	0,0216	0,0114	0,0070	0,0024	0,0010
	600 to 850	0,0325	0,0428	0,0309	0,0175	0,0102	0,0032	0,0014
	425 to 600	0,0247	0,0451	0,0418	0,0288	0,0174	0,0053	0,0019
	300 to 425	0,0223	0,0548	0,0649	0,0587	0,0429	0,0161	0,0064
	212 to 300	0,0201	0,0612	0,0869	0,1002	0,0961	0,0595	0,0284
	150 to 212	0,0152	0,0516	0,0797	0,1041	0,1218	0,1175	0,0894
	106 to 150	0,0118	0,0403	0,0629	0,0827	0,1032	0,1324	0,1275
	75 to 106	0,0111	0,0392	0,0618	0,0815	0,1036	0,1405	0,1620
	53 to 75	0,0089	0,0288	0,0447	0,0590	0,0732	0,0982	0,1178
	38 to 53	0,0065	0,0212	0,0329	0,0409	0,0527	0,0710	0,0892
	-38	0,0379	0,0908	0,1346	0,1777	0,2182	0,2933	0,3551

Table 6.2 Batch milling results for run 20/6

Table of individual mass fractions per size group for each grind time.

		Grind time, minutes							
		0	2	5	10	15	20	30	40
Size fractions, range in microns	6300 to 9500	0,0762	0,0708	0,0358	0,0168	0,0033	0,0055	0,0000	0,0000
	4750 to 6300	0,1589	0,0736	0,0573	0,0193	0,0079	0,0000	0,0000	0,0000
	3350 to 4750	0,1438	0,1191	0,0663	0,0219	0,0083	0,0007	0,0000	0,0000
	2360 to 3350	0,1131	0,1013	0,0694	0,0137	0,0031	0,0001	0,0000	0,0000
	1700 to 2360	0,0893	0,0846	0,0610	0,0197	0,0026	0,0003	0,0000	0,0000
	1180 to 1700	0,0694	0,0771	0,0729	0,0321	0,0070	0,0009	0,0002	0,0002
	850 to 1180	0,0537	0,0639	0,0710	0,0555	0,0160	0,0029	0,0002	0,0002
	600 to 850	0,0460	0,0616	0,0755	0,0856	0,0474	0,0138	0,0014	0,0004
	425 to 600	0,0379	0,0531	0,0702	0,1013	0,0910	0,0474	0,0078	0,0025
	300 to 425	0,0372	0,0520	0,0729	0,1101	0,1316	0,1169	0,0448	0,0157
	212 to 300	0,0350	0,0503	0,0725	0,1098	0,1453	0,1623	0,1277	0,0777
	150 to 212	0,0266	0,0384	0,0564	0,0880	0,1181	0,1437	0,1616	0,1396
	106 to 150	0,0210	0,0294	0,0423	0,0630	0,0827	0,1010	0,1314	0,1421
	75 to 106	0,0192	0,0271	0,0396	0,0592	0,0773	0,0942	0,1223	0,1398
	53 to 75	0,0151	0,0210	0,0293	0,0429	0,0550	0,0668	0,0851	0,1004
	38 to 53	0,0118	0,0169	0,0202	0,0303	0,0407	0,0493	0,0688	0,0814
	-38	0,0460	0,0597	0,0874	0,1305	0,1626	0,1941	0,2485	0,2998

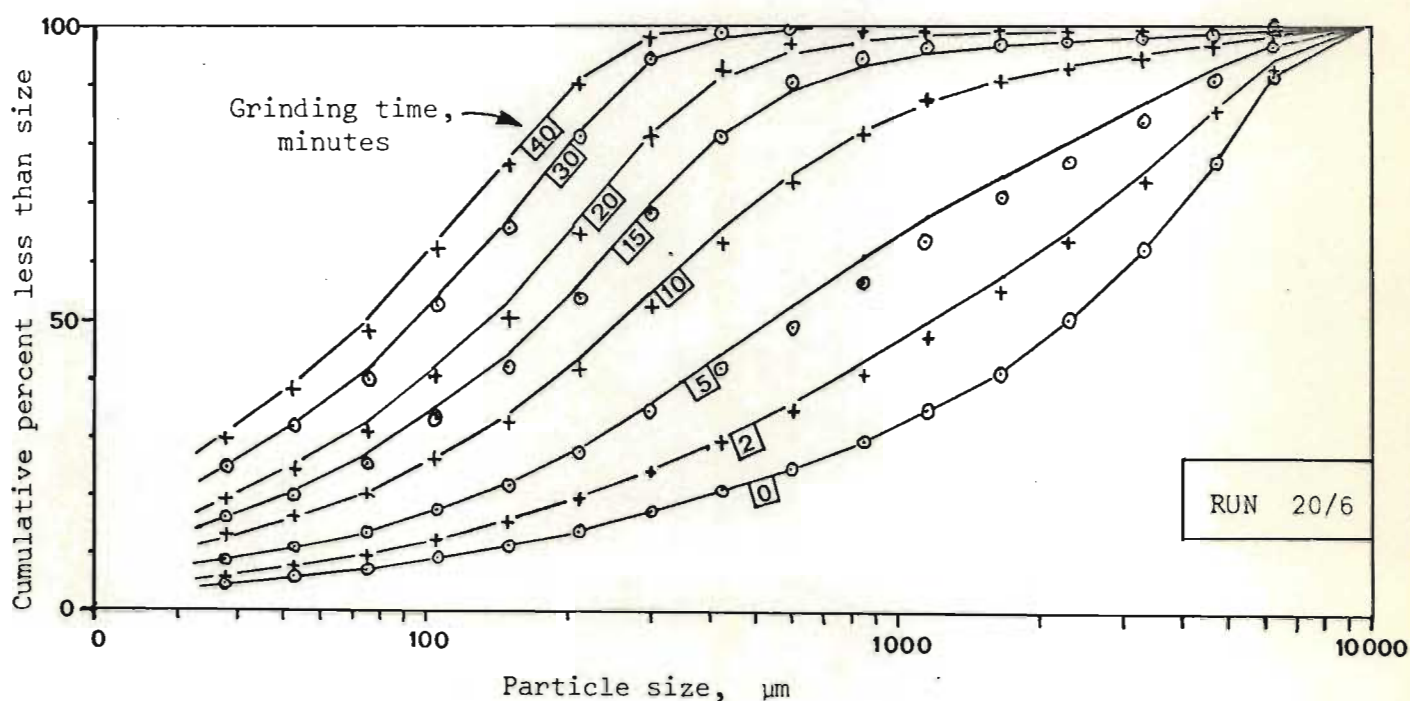
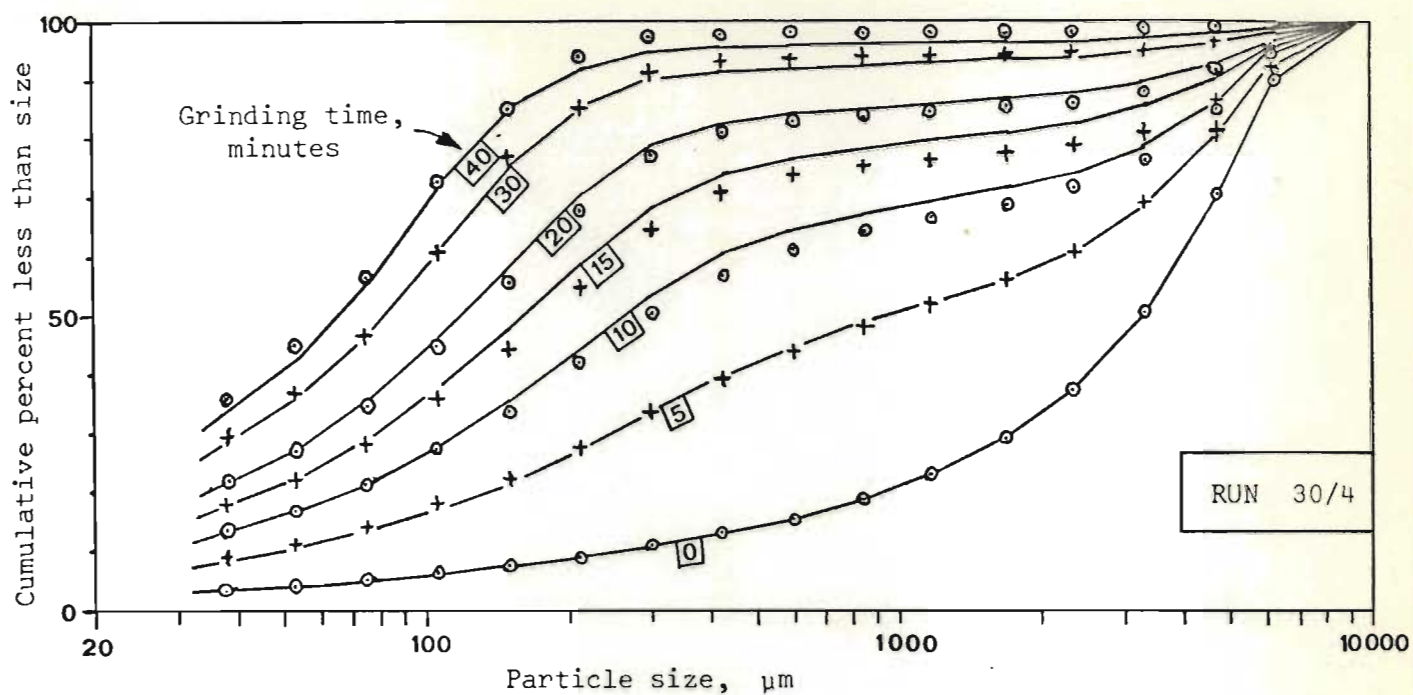


Figure 6.1 Results from batch grinds for runs 30/4 and 20/6.

Cumulative size distributions at grind times shown.
Points are experimental values. Lines are regressed best fits.

Table 6.3

Regressed values of selection and breakage function for run 30/4 in batch mill. (Smaller mean ball size in mill.)

Particle size group		Selection function min^{-1}	Breakage function from 1st size group (individual)
number	range in μm		
1	6300 - 9500	0,0397	0
2	4750 - 6300	0,1061	0,5949
3	3350 - 4750	0,1743	0,1004
4	2360 - 3350	0,2887	0,0741
5	1700 - 2360	0,4771	0,0530
6	1180 - 1700	0,5561	0,0448
7	850 - 1180	0,6208	0,0305
8	600 - 850	0,5068	0,0248
9	425 - 600	0,3975	0,0186
10	300 - 425	0,2295	0,0143
11	212 - 300	0,1175	0,0108
12	150 - 212	0,06622	0,0082
13	106 - 150	0,04024	0,0062
14	75 - 106	0,01283	0,0047
15	53 - 75	0,005957	0,0036
16	38 - 53	0,007743	0,0026
17	0 - 38	0	0,0086
Parameters for breakage function (equation (4.2.5))			
$\alpha_1 = 0,4964$ $\alpha_2 = 18,27$ $\alpha_3 = 0,7957$			

Table 6.4

Regressed values of selection and breakage functions for run 20/6 in batch mill.
(Larger mean ball size in mill.)

Particle size group		Selection function \min^{-1}	Breakage function from 1st size group (individual)
number	range in μm		
1	6300 - 9500	0,1464	0
2	4750 - 6300	0,3667	0,6661
3	3350 - 4750	0,3839	0,0966
4	2360 - 3350	0,4350	0,0583
5	1700 - 2360	0,4885	0,0414
6	1180 - 1700	0,4412	0,0349
7	850 - 1180	0,4056	0,0237
8	600 - 850	0,2948	0,0192
9	425 - 600	0,2158	0,0144
10	300 - 425	0,1321	0,0110
11	212 - 300	0,07445	0,0083
12	150 - 212	0,04838	0,0063
13	106 - 150	0,03892	0,0048
14	75 - 106	0,02161	0,0036
15	53 - 75	0,01627	0,0027
16	38 - 53	0,01263	0,0020
17	0 - 38	0	0,0066
Parameters for breakage function (equation (4.2.5))			
$\alpha_1 = 0,6071$ $\alpha_2 = 12,0$ $\alpha_3 = 0,8004$			

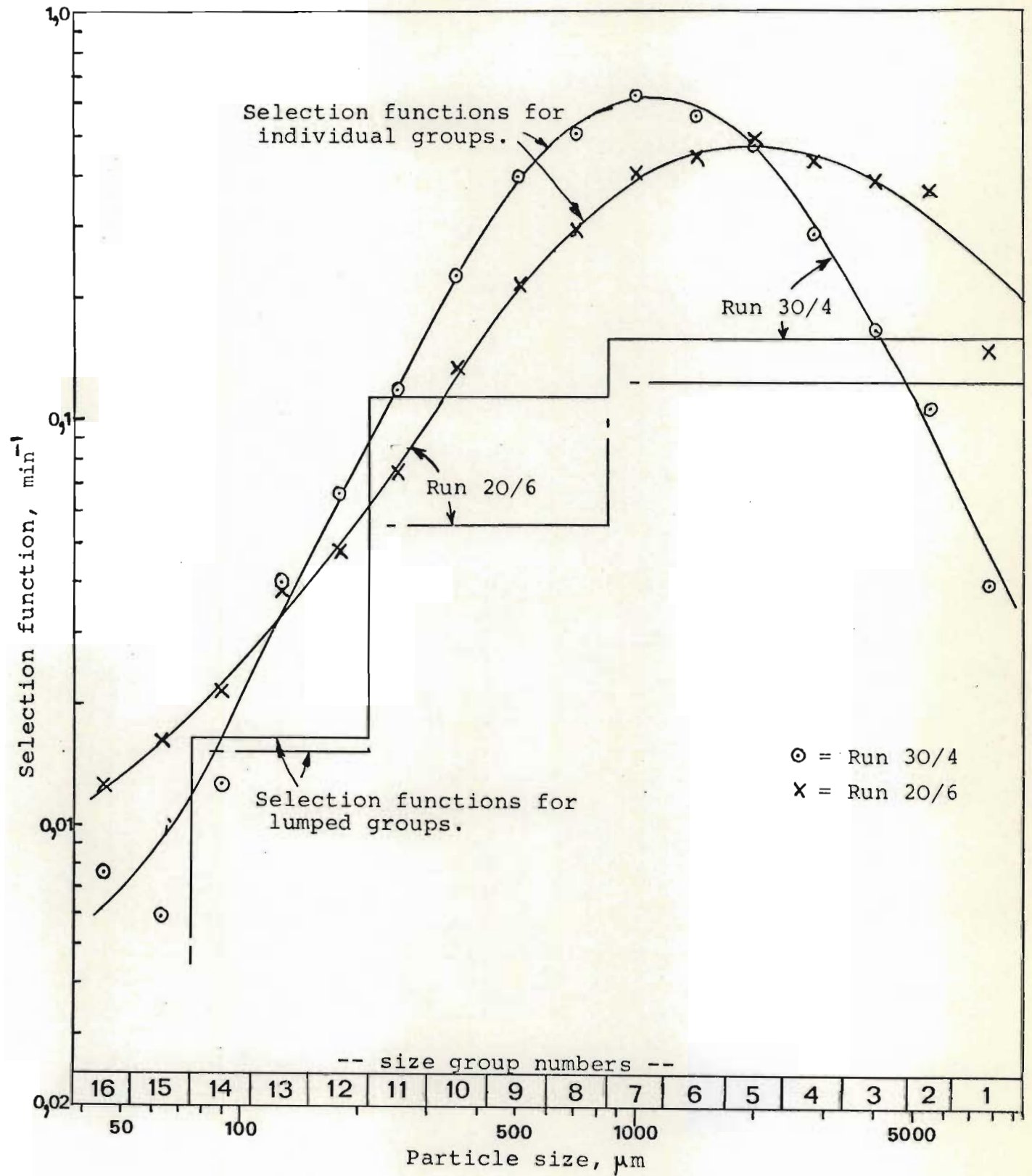


Figure 6.2 Regressed selection functions and lumped selection functions for runs 30/4 and 20/6.

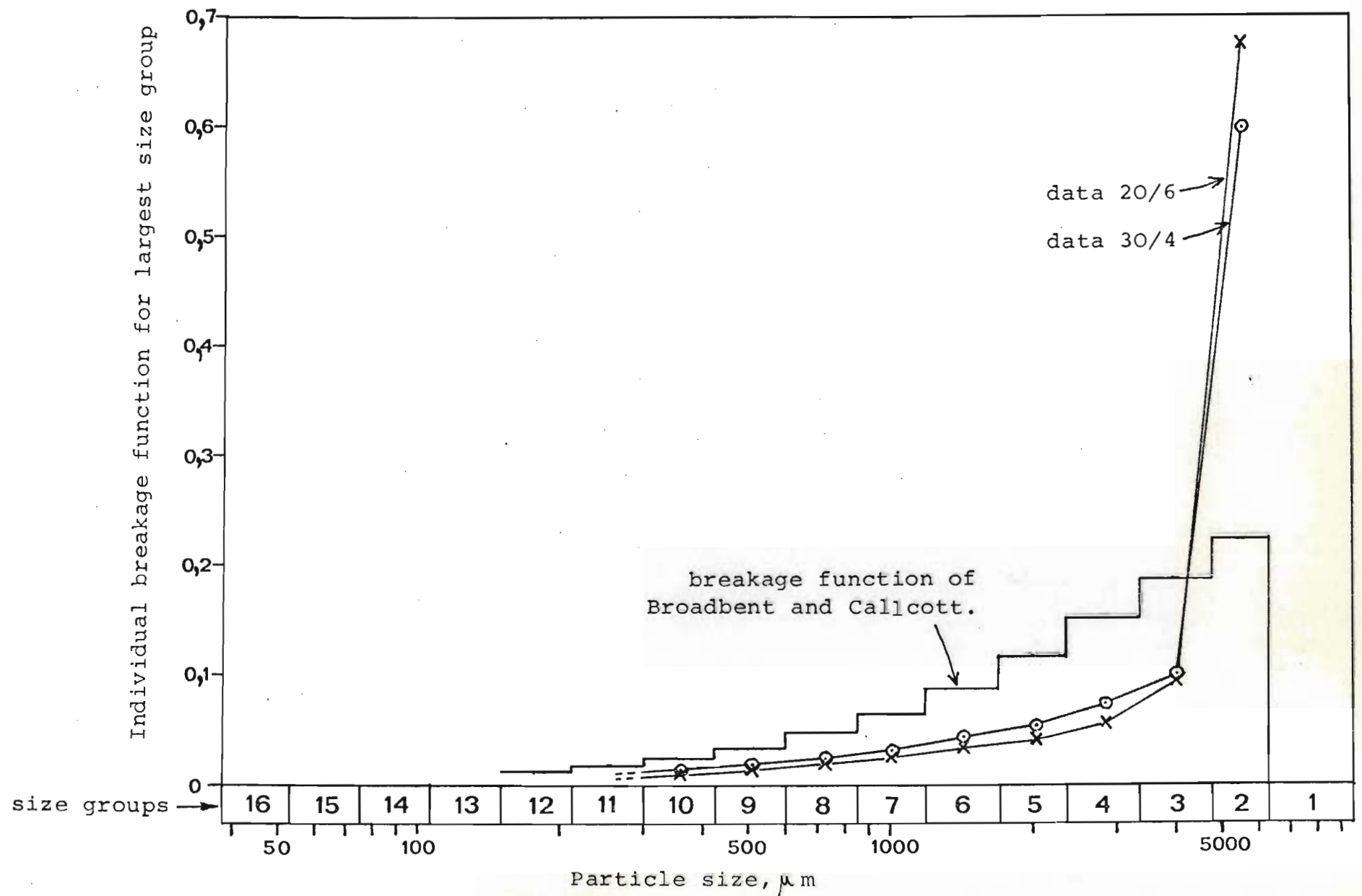


Figure 6.3 Regressed breakage functions from runs 30/4 and 20/6 compared to the breakage function of Broadbent and Callcott.

To use these data, it was necessary to recalculate the parameters for the four size fractions used in the filter, as explained in Section 4.2.1, equations (4.2.7) to (4.2.9). The results of this data compression are given in Table 6.5. The lumped selection functions are also included in Figure 6.2. The calculated standard deviation due to lumping together of the particle size groups, equation (4.2.9), is also given, although the actual error is not likely to be as great. The error is particularly large where the selection function curve is decreasing with particle size. Fortunately, this is associated with a large mean, and is hence not the rate controlling step in grinding from coarse to fine rock. The reduced data from run 20/6 were used directly for all the filter computations shown in this thesis, as they matched the ball load distribution used. They were used in the p.s.d. filter as the values of the S and b functions in the grinding model.

The size analyses of the two feed samples used for the batch grinds were averaged to obtain a mean value of the mill feed for use in the filter. This analysis is shown in Table 6.6.

Table 6.6. Averaged feed size distribution

Size range, μm	Percentage in range
850 - 9 500	75,7
212 - 850	12,8
75 - 212	5,25
0 - 75	6,25

The grinds which were done with the varying slurry concentration and total charge were used to determine the effects of these factors on the grinding model as explained in the theory, Section 4.2.1. These grinds were all done for 20 minutes. Figure 6.4 shows the graphs of the D_{25} , D_{50} and D_{75} against time for the two sequences of batch grinds. On these lines, the

Table 6.5

Selection and breakage functions for lumped size groups

Results of data compression on grinding data for runs 30/4 and 20/6

$$\text{*Rate scaling factor} = \left(\frac{D_1}{D_2}\right)^{0,6} = 1,733$$

Run 30/4

Particle size group		Selection functions min ⁻¹			Breakage functions, fractions into			
Num-ber	range μm	mean	std. devs. due to lumping	scaled mean for big mill*	Group 1	Group 2	Group 3	Group 4
1	850-9500	0,1582	0,2028	0,2740	-	0,7545	0,1378	0,1077
2	212-850	0,1121	0,0112	0,1942	-	-	0,6152	0,3848
3	75-212	0,01644	0,00300	0,02848	-	-	-	1,0000
4	0-75	-	-	-	-	-	-	-

Run 20/6

Particle size group		Selection functions min ⁻¹			Breakage functions, fractions into			
Num-ber	range μm	mean	std. devs. due to lumping	scaled mean for big mill*	Group 1	Group 2	Group 3	Group 4
1	850-9500	0,1212	0,1237	0,2099	-	0,7651	0,1324	0,1025
2	212-850	0,05562	0,01135	0,09634	-	-	0,6544	0,3456
3	75-212	0,01536	0,00447	0,02661	-	-	-	1,0000
4	0-75	-	-	-	-	-	-	-

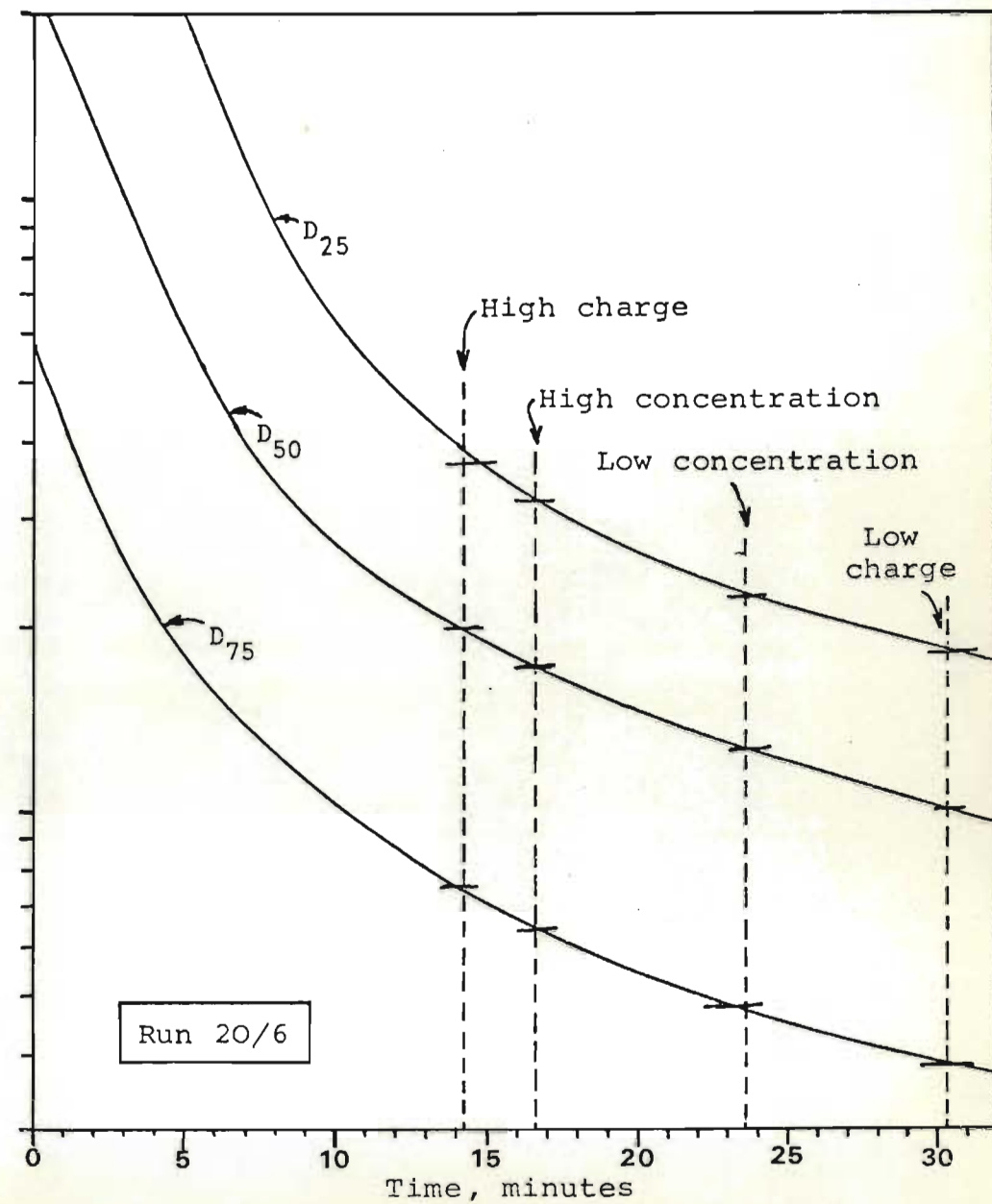
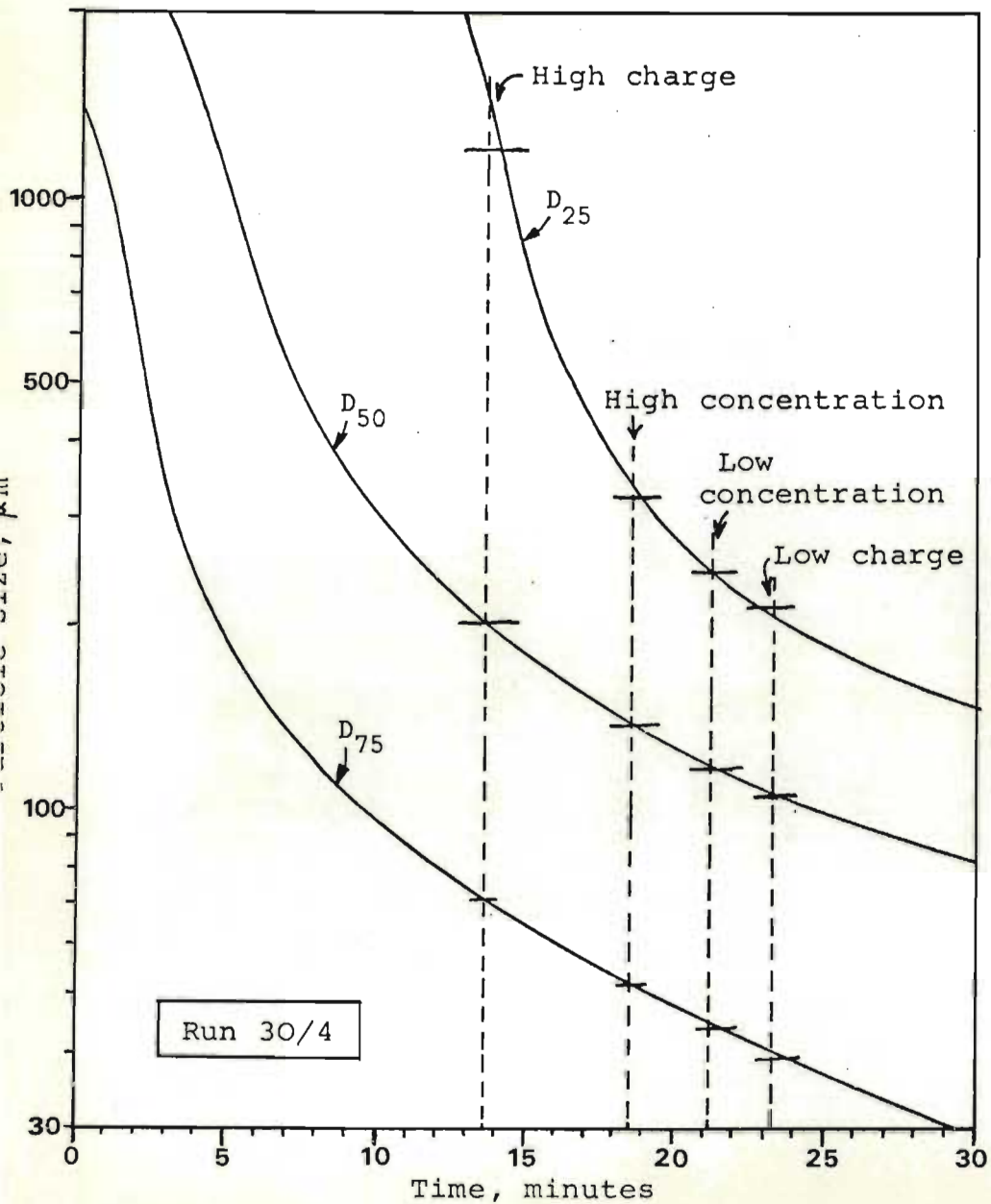


Figure 6.4 Determination of effects of concentration and charge on rates of grinding.

D₂₅, D₅₀, D₇₅ as functions of time from batch tests, with points for high and low concentrations and charges marked in. (See section 6.1 and graph 6.5)

D_{25} , D_{30} and D_{75} for the varying charge and concentration runs have been plotted, and a line corresponding to a mean time has been drawn for each set of three points, to give the equivalent grinding time, t_e . From these results, the rate scaling factors were calculated using equation (4.2.6).

These rate scaling factors are plotted in figure 6.5. The difference between the ball charges is noticeably different, but the general trends are the same. Approximate linear relationships from these graphs, scaled for the pilot plant mill, were:-

$$K_L = 1,0 - 10,0 \times (V_M - 0,1435) \quad (6.1)$$

$$K_C = 1,0 - 6,34 \times 10^{-4} \times (C_M - 1500) \quad (6.2)$$

where K_L , K_C are the rate scaling factors for load and concentration respectively

V_M is the actual volume in the pilot plant mill (m^3)

C_M is the actual concentration in the pilot plant mill (kg/m^3)

Because the effect of concentration was more difficult to incorporate in the filter, only equation 6.1 was used, even though the total effects were about the same in the normal operating range. This scaling factor was evaluated each time after the volumetric filter to account for the effect of changes in the mill volume on the rates of grinding in the p.s.d. filter.

6.2. Errors in analyses

The feed sample for the first sequence of batch tests (30/4) was split and analysed as four separate samples to get an estimate of the repetition error in the sample analyses. Table 6.7 shows these results for the 17 size fractions, and condenses these into the four size fractions used in the filter.

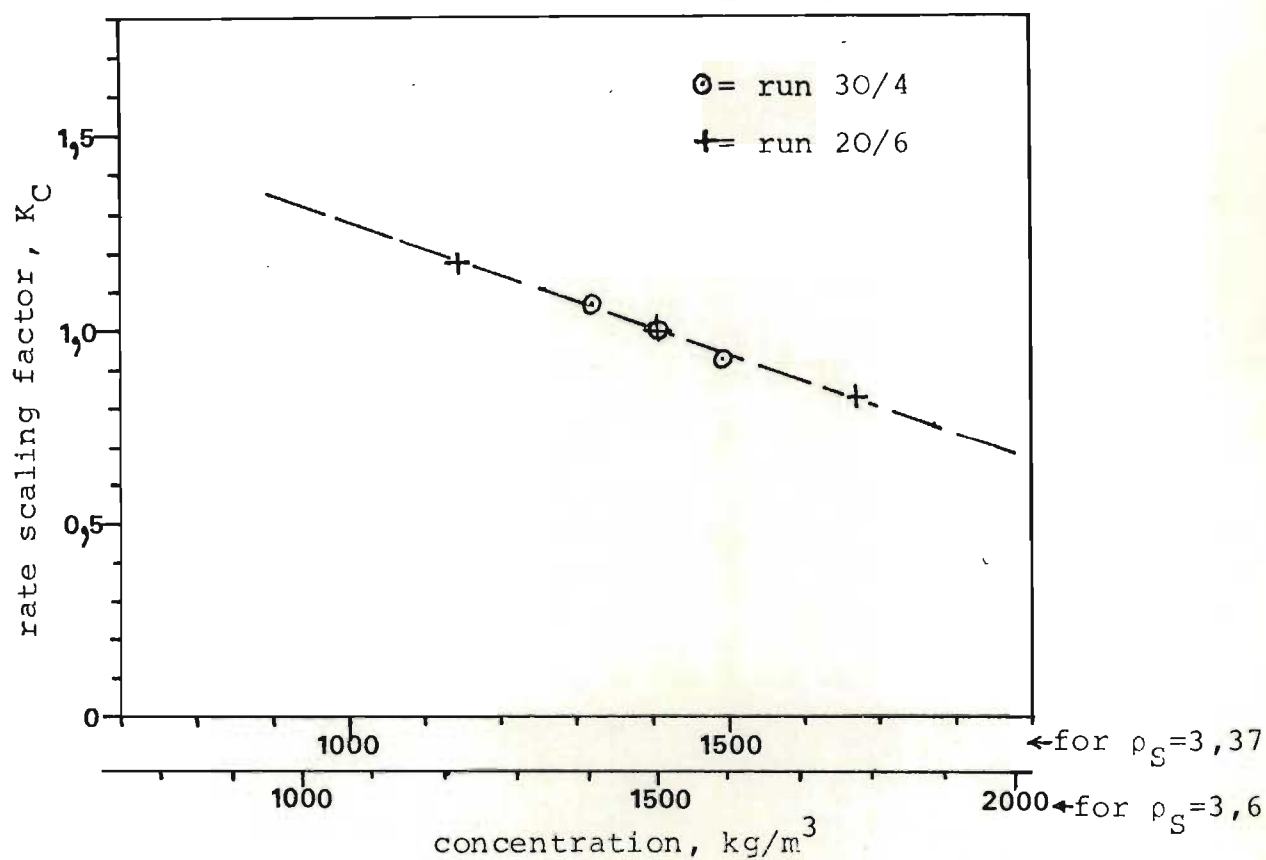
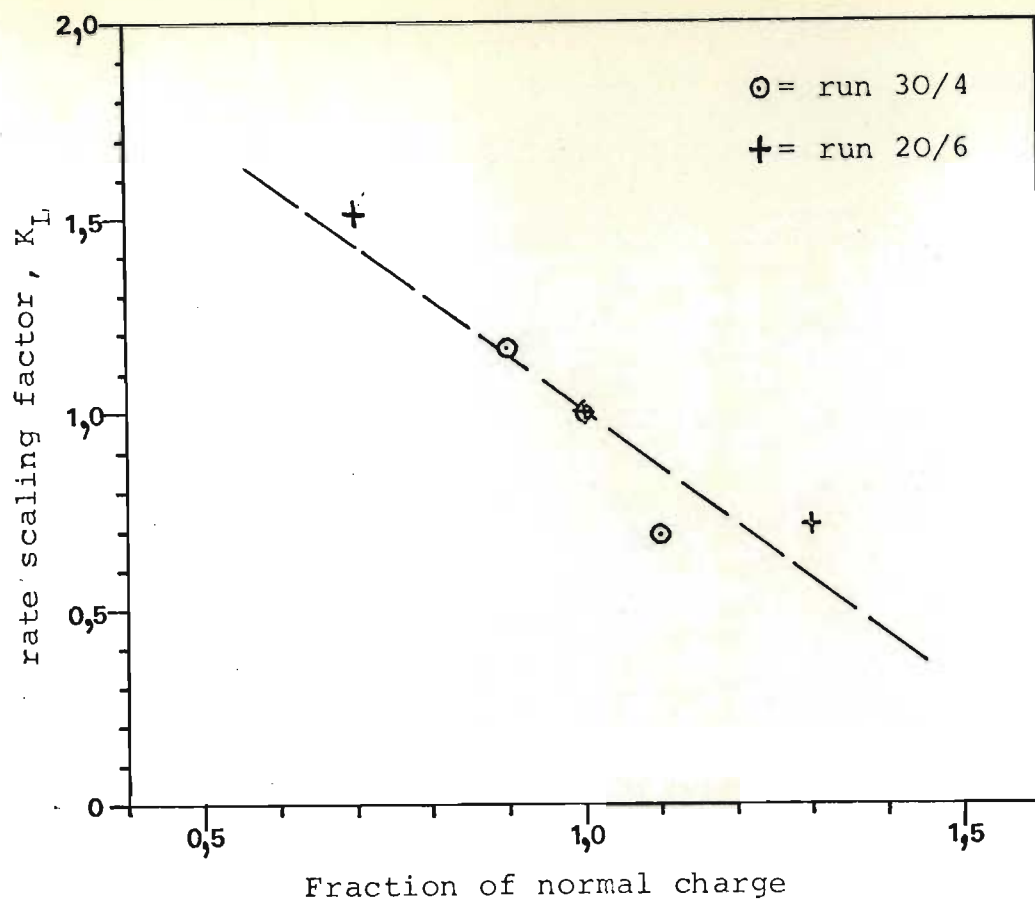


Figure 6.5 Rate (selection function) scaling

factors against charge volume and concentration, in usual operating region. Data from runs 30/4 and 20/6.

Table 6.7

Typical Particle Size Analysis Errors

(feed sample for experiment 30/4)

Particle size range, microns	Average mass % in group	Standard Deviation of mass %	C.V. = $\frac{\text{std.dev.}}{\text{mean}}$
0 - 38	3,70	0,11	0,031
38 - 53	0,64	0,02	0,035
53 - 75	0,85	0,05	0,053
75 - 106	1,14	0,06	0,050
106 - 150	1,19	0,04	0,029
150 - 212	1,52	0,04	0,025
212 - 300	2,03	0,05	0,025
300 - 425	2,22	0,03	0,013
425 - 600	2,47	0,08	0,032
600 - 850	3,26	0,09	0,027
850 - 1180	4,04	0,12	0,030
1180 - 1700	5,96	0,14	0,024
1700 - 2360	7,69	0,25	0,033
2360 - 3350	13,45	0,23	0,017
3350 - 4750	19,80	1,06	0,054
4750 - 6300	19,30	1,75	0,091
6300 - 9500	10,75	1,96	0,182
0 - 75	5,19	0,14	0,027
75 - 212	3,85	0,12	0,030
212 - 850	9,98	0,25	0,025
850+	80,98	0,47	0,006

6.3. Cyclone data

The results from the cyclone show considerable scatter. Several reasons for this were outlined in Section 5.5.2, but the main causes were the use of a mixed ore, the scale of operation, and a poor model. It is an obvious area for further development of the filter.

Initially, two sets of runs, 23/7 and 5/8, were done, each giving 7 pairs of overflow and underflow samples. From these, graphs of classifier characteristics were drawn and the D_{50} corrected was read. These D_{50} corrected were then plotted against feed rate and feed concentration to check against the results quoted in literature. They are shown in Figures 6.6 and 6.7 respectively. Also shown in Figure 6.7 are two correlations for D_{50} corrected against concentration from sources in literature as indicated. Similar trends can be seen in the experimental points above the scatter. The allowable operating region for the feed flow in Figure 6.6 was limited, but no trends can be seen. We may therefore assume that the cyclone could be adequately modelled either by fixed classifier constants, or slightly better by linear functions of feed concentration.

The filter required classification parameters for each of the four size groups separately, so the cyclone data were also calculated in this form. The results of runs 23/7 and 5/8 are shown in Figure 6.8 as the corrected classifier functions against feed concentration for each size group. Linear regressions were done on these to fit equation (4.2.11), and the results are given in Table 6.8.

When runs A and B were done on the milling circuit to collect data for filtering, it was found from samples of the overflow and underflow taken together that the cyclone behaviour had changed slightly. From these new samples, corrected classifier functions were calculated and are shown in Figure 6.9 against feed concentration. These points were insufficient to

do a full linear/...

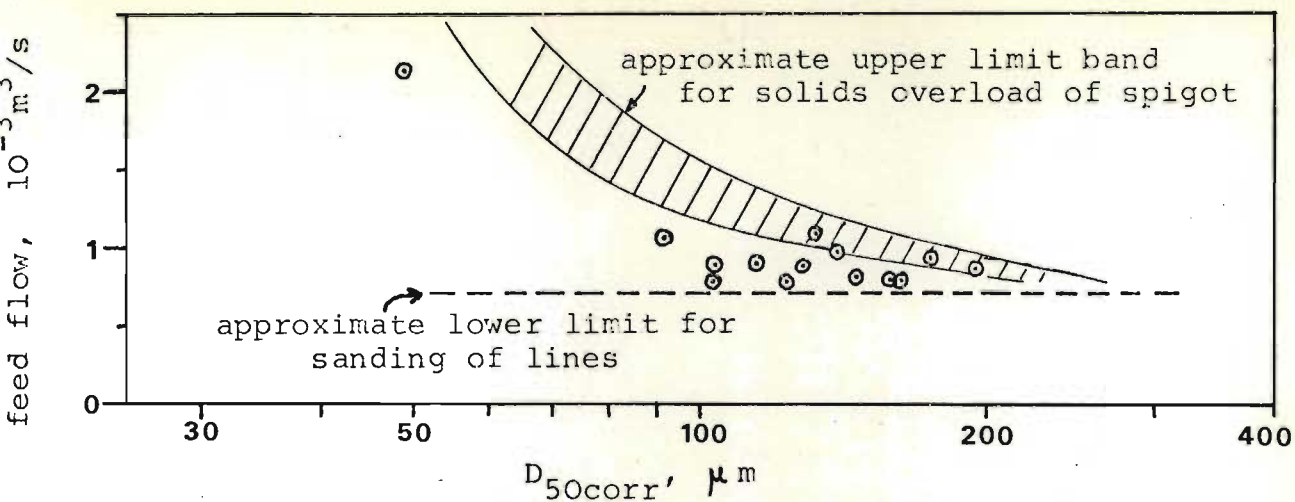


Figure 6.6 Cyclone classification dependence on feed flow.

Corrected D_{50} against feed flow, showing experimental points and operating limits.

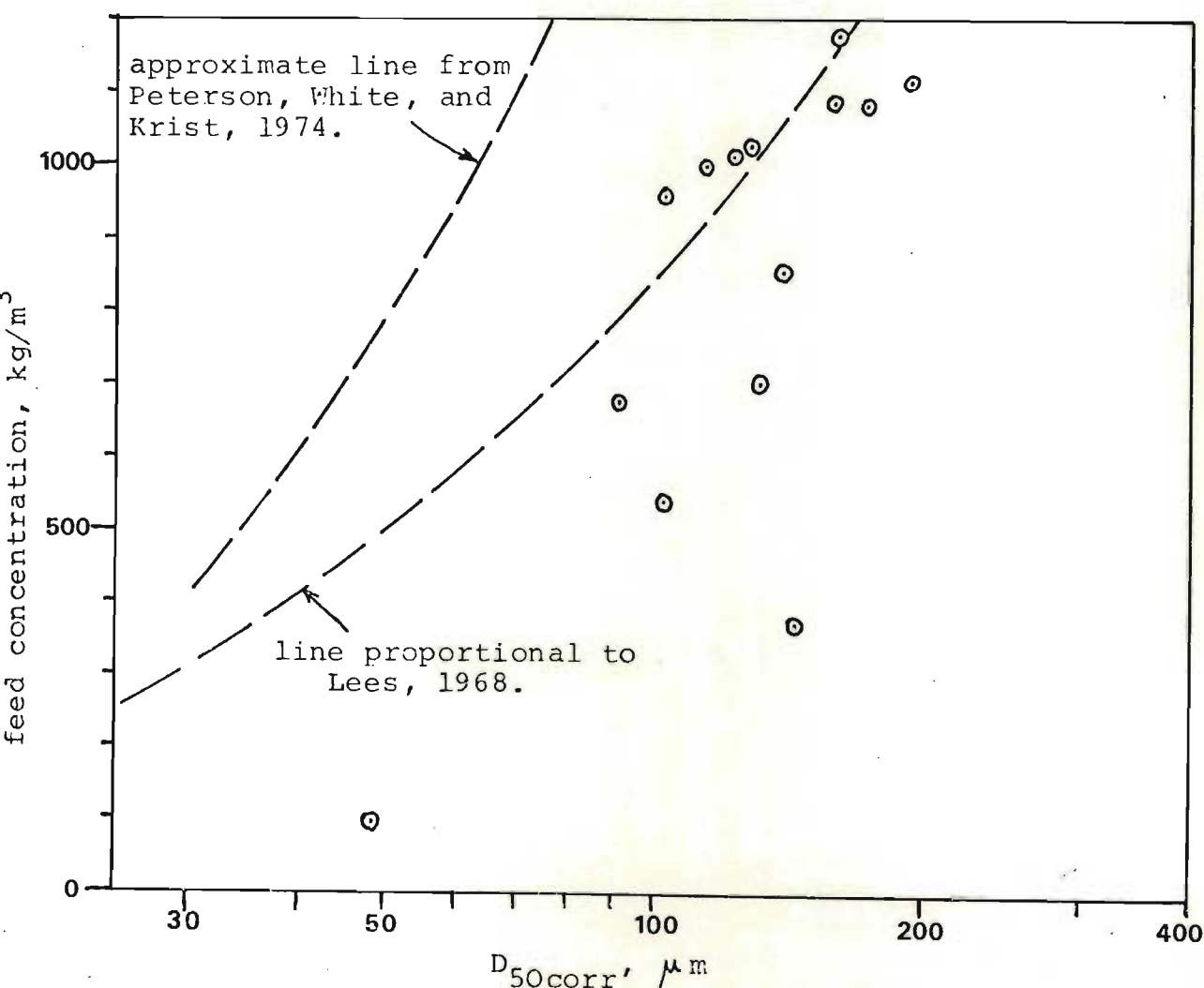


Figure 6.7 Cyclone classification dependence on feed concentration.

Corrected D_{50} against feed concentration, with two correlations from literature for comparison.

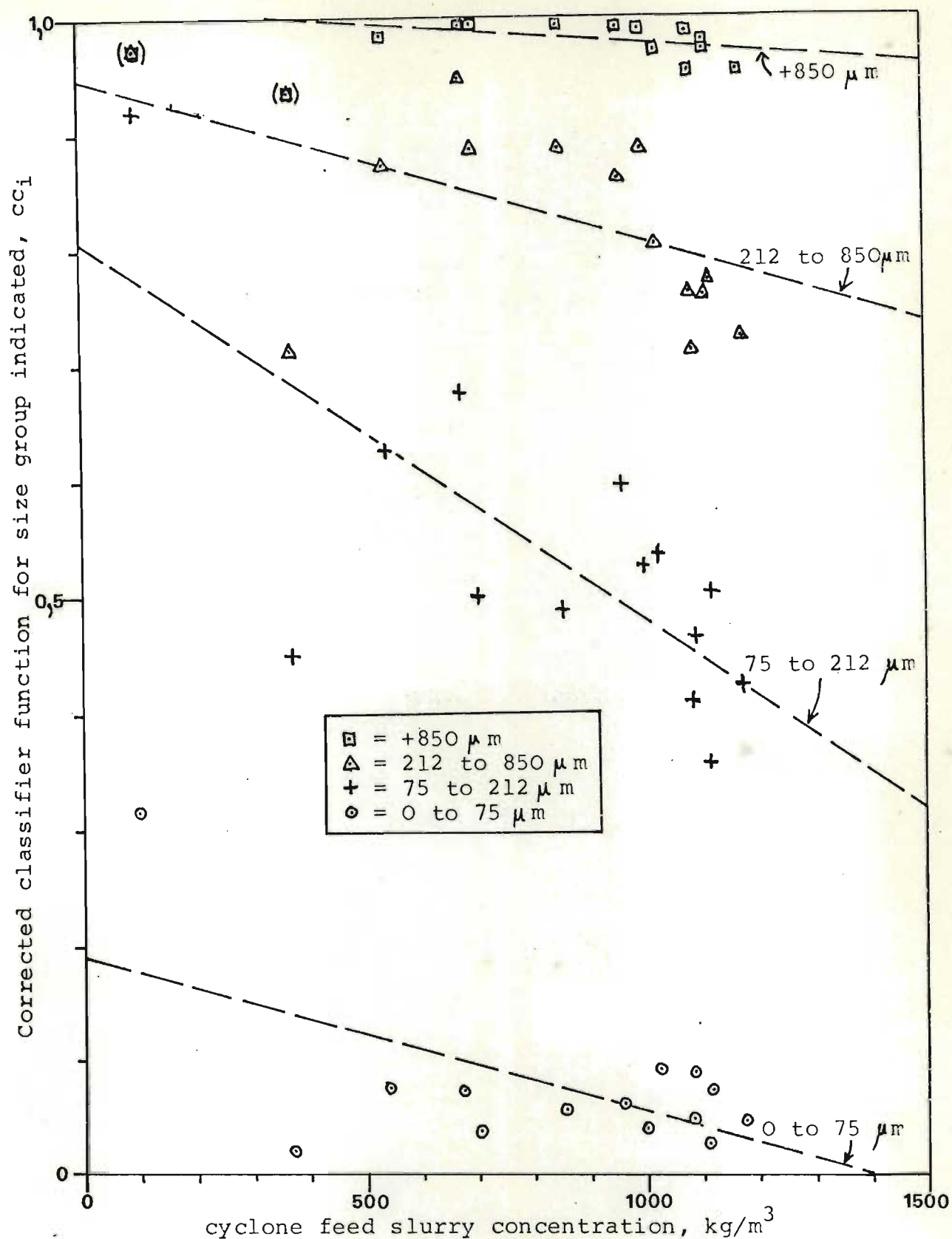


Figure 6.8 Corrected classifier constants against feed concentration for runs 23/7 and 5/8. (Table 6.8)

Sample points and regressed lines shown.

Table 6.8 Corrected classifier functions for individual size groups, from runs 23/7 and 5/8

Particle size range, μm	linear classifier functions of feed conc.	
	cc_{0i}	cc_{1i}
850 to 9500	1,0073	$-0,2894 \times 10^{-4}$
212 to 850	0,9479	$-1,4582 \times 10^{-4}$
75 to 212	0,8088	$-3,276 \times 10^{-4}$
0 to 75	0,1904	$-1,364 \times 10^{-4}$

Table 6.9 Corrected classifier functions for individual size groups, from runs 18/10 and 23/10

Particle size range μm	mean corrected classifier constants, \overline{cc}_i	linear classifier functions of feed conc.	
		cc_{0i}	cc_{1i}
850 to 9500	0,9351	0,9543	$-0,2894 \times 10^{-4}$
212 to 850	0,6660	0,7629	$-1,458 \times 10^{-4}$
75 to 212	0,3516	0,5694	$-3,276 \times 10^{-4}$
0 to 75	0,0144	0,1051	$-1,364 \times 10^{-4}$

Table 6.10 Corrected classifier functions for individual size groups, data from all runs.

Particle size range, μm	linear classifier functions of feed conc.	
	cc_{0i}	cc_{1i}
850 to 9500	0,96229	$+0,0614 \times 10^{-4}$
212 to 850	0,78381	$-0,0826 \times 10^{-4}$
75 to 212	0,60516	$-1,6883 \times 10^{-4}$
0 to 75	0,11496	$-0,7623 \times 10^{-4}$

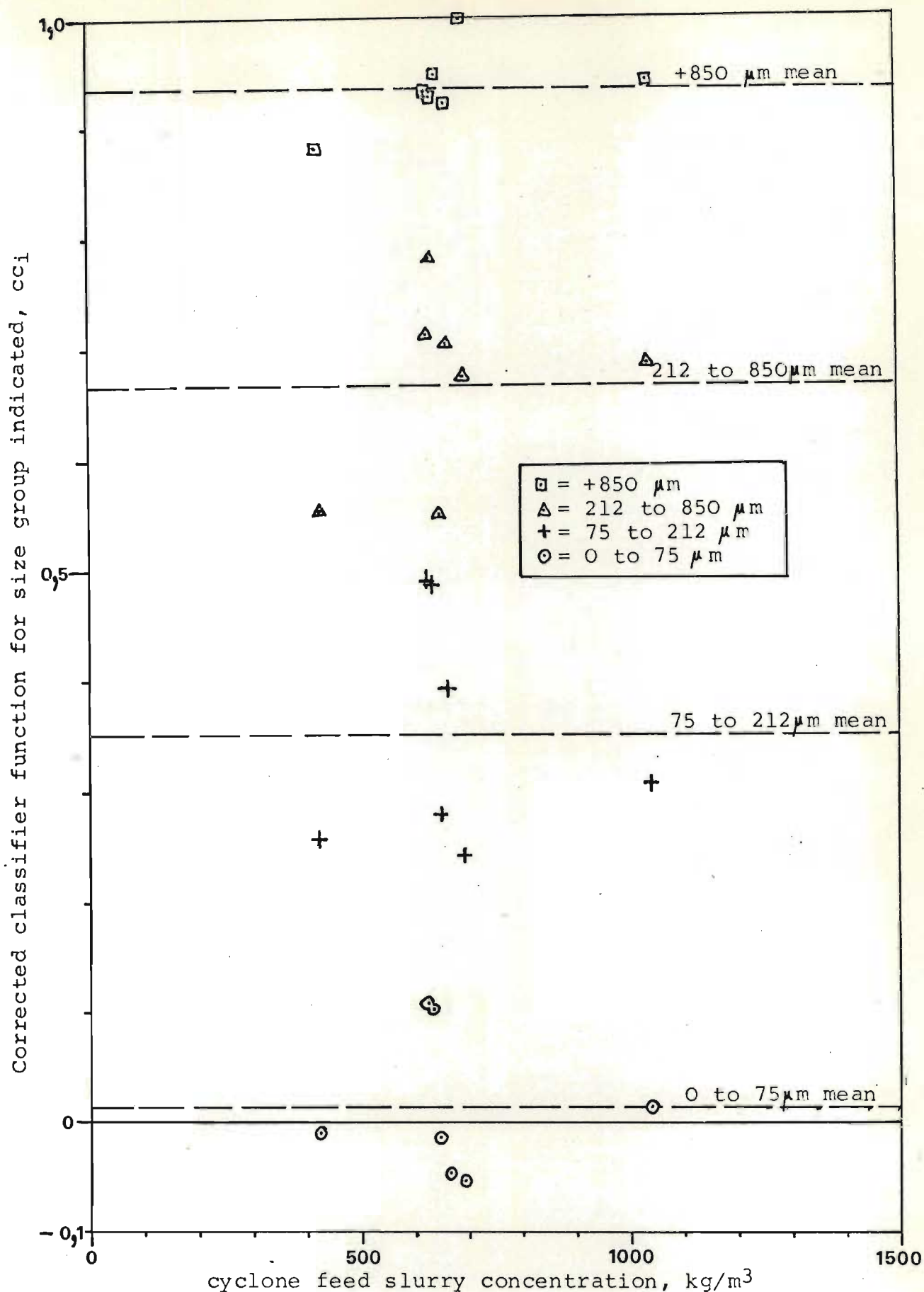


Figure 6.9 Corrected classifier constants against feed concentration for runs 18/10 and 23/10. (Table 6.9)

Sample points and means shown.

do a full linear regression, and so the slopes of the lines from the previous regressions (Table 6.8) were put through the averages of the new points to obtain the classification parameters shown in Table 6.9.

The values of cc_{0i} and cc_{1i} given in Table 6.9 were used for all the filtering tests. They were used in the p.s.d. filter. From the volumetric filter, and the predicted concentrations in the p.s.d. filter from the previous step, the flow split in the cyclone was calculated. From this and the corrected classifier constants in Table 6.9, the actual classifier constants were calculated as explained in Section 4.2.2.

Finally, as shown in Section 6.8.2, different values of classifier functions were used to test the effects of this factor. To get values for this, all the data from runs 23/7, 5/8, 18/10 (run A) and 23/10 (run B) were put in a regression, and the results are shown in Table 6.10. The values of cc_{0i} and cc_{1i} in this table were only used for this one test, and represented a generally finer cut than the average.

The flow model for the cyclone assumed that the underflow was fairly constant over the range of operation, independent of the feed flow or concentration (equation (4.2.10)). The data from runs 23/7 and 5/8 were plotted as underflow volume flow rate against feed concentration and feed flow rate. These two graphs are shown in Figure 6.10. Although there is scatter, there is no noticeable dependence on either feed flow or concentration, and the points are fairly constant. From these data, the average and variance were calculated and are shown in Table 6.11.

Table 6.11 Cyclone flow data (equation 4.58)

$$\text{Mean underflow rate, } Q_{U0} = 0,4073 \times 10^{-3} \text{ m}^3/\text{s}$$

$$\text{Error variance, } \sigma_{\epsilon}^2 = 0,383 \times 10^{-8} \text{ m}^6/\text{s}^2$$

$$\text{Error standard deviation, } \sqrt{\sigma_{\epsilon}^2} = 0,619 \times 10^{-4} \text{ m}^3/\text{s}$$

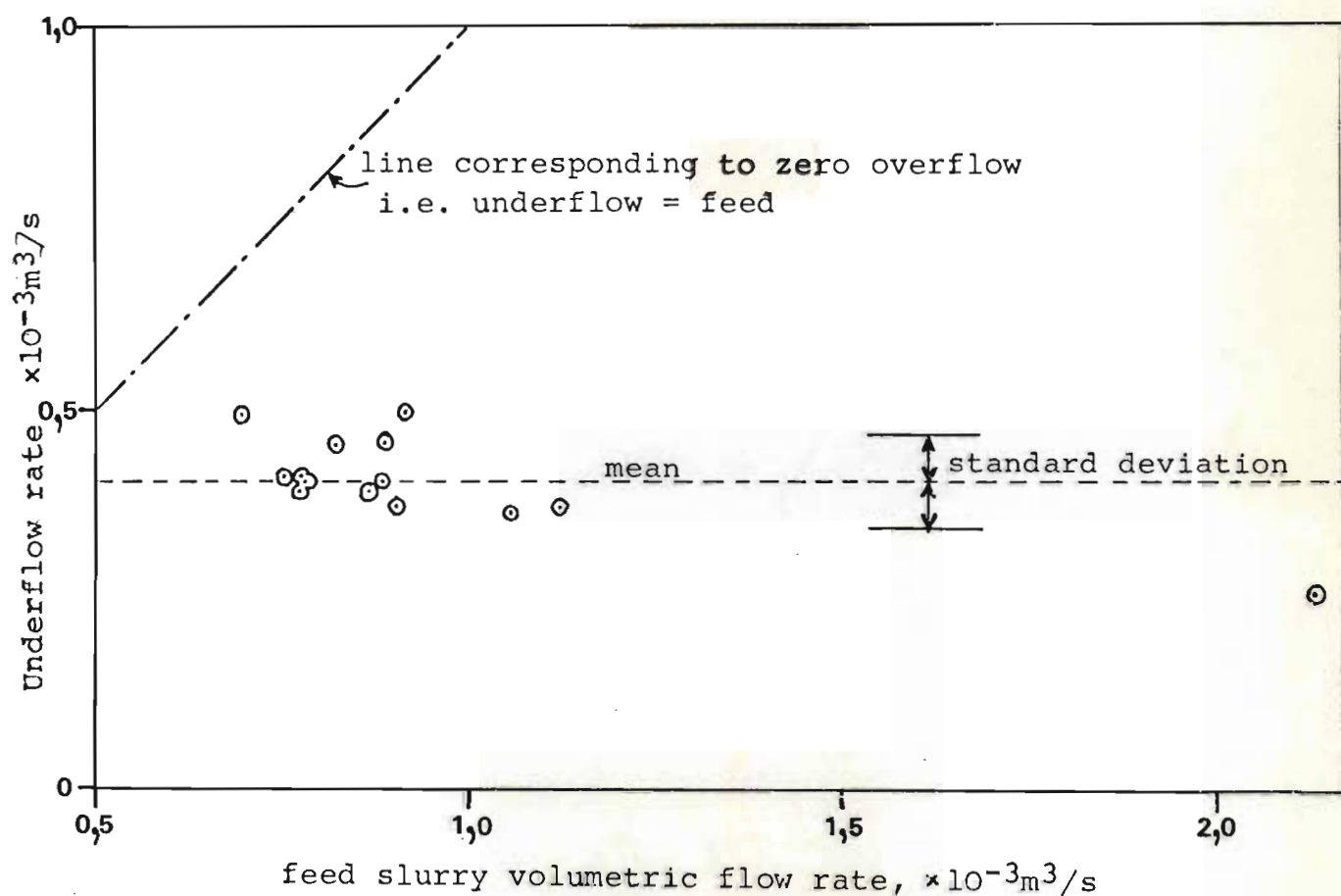
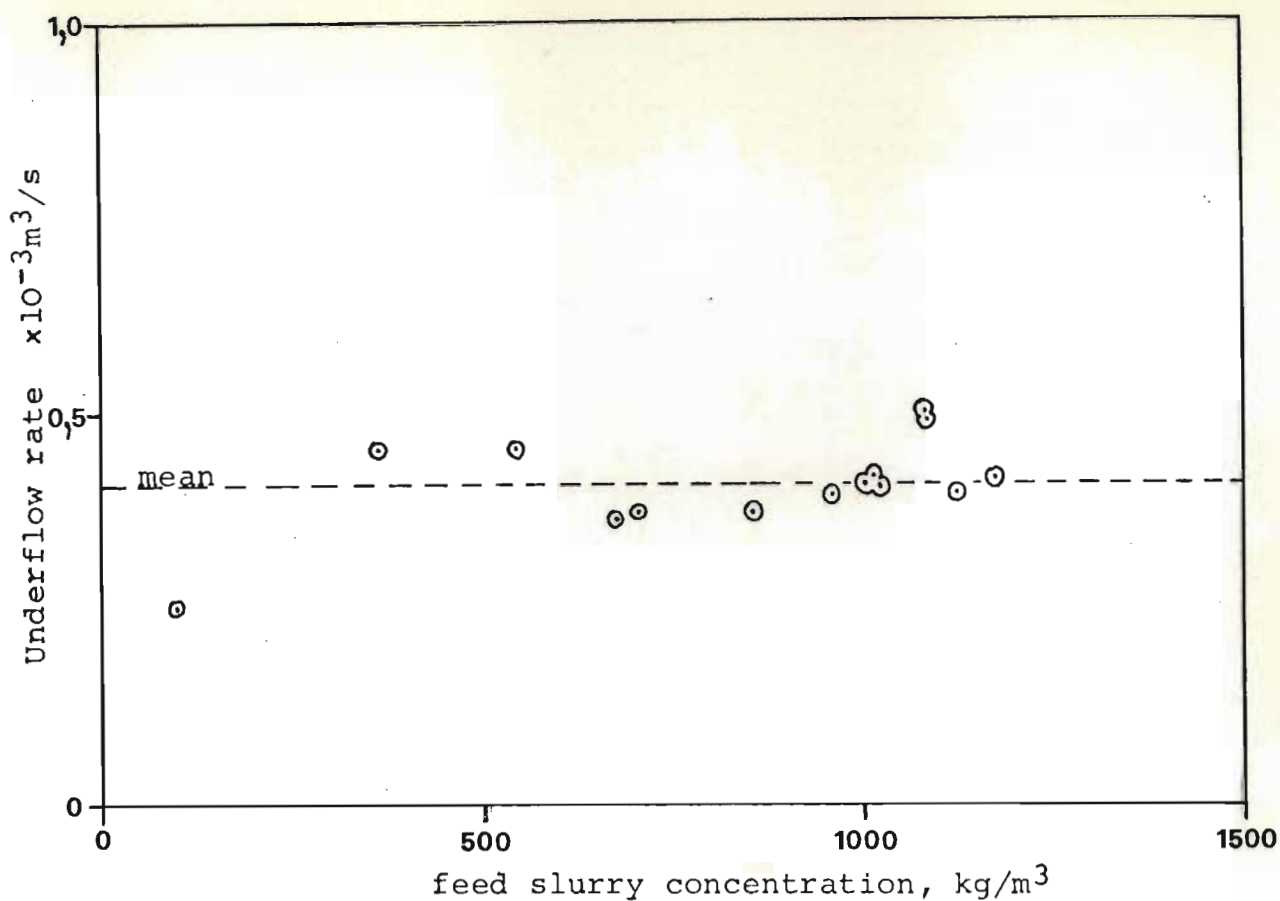


Figure 6.10 Dependence of cyclone underflow rate on feed concentration and flow. (Data from runs 23/7 and 5/8)

The values in Table 6.11 for the cyclone flow model were used in the volumetric filter as parameters.

6.4. Mill overflow characteristics

The results from the overflow test on the mill are shown in Figure 6.11. The graph shows the volume in the sump as the mill overflowed into it, plotted against time (as explained in Section 5.5.3). It seemed reasonable to assume that the overflow characteristics were first order, and that equation (4.3.2) would apply. From the slope of the curve at the start, the flow rate through the mill was determined. The operating volume of the mill, V_M , and the minimum volume, V_{MO} , were calculated as explained in Section 5.5.3. From these, the parameters in Table 6.12 were calculated for equation (4.3.2).

Table 6.12 Mill overflow model parameters

Model: $Q_M = k_1(V_M - V_{MO})$	(4.3.2)
$V_{MO} = 0,0935 \text{ m}^3$	
$k_1 = 0,01 \text{ s}^{-1}$	

These values were used in the volumetric filter in the mill flow model.

6.5. Results of runs on milling circuit

Runs coded "A" and "B" (18/10 and 23/10 respectively) were done on the milling circuit to get data for testing the filter. Runs coded "C" and "D" (16/4 and 18/4 respectively) were done with the filter running in real time. The data from all runs were stored on a disc file. Run B was the most successful, and it was used for doing most of the off-line tests.

The graphs of/...

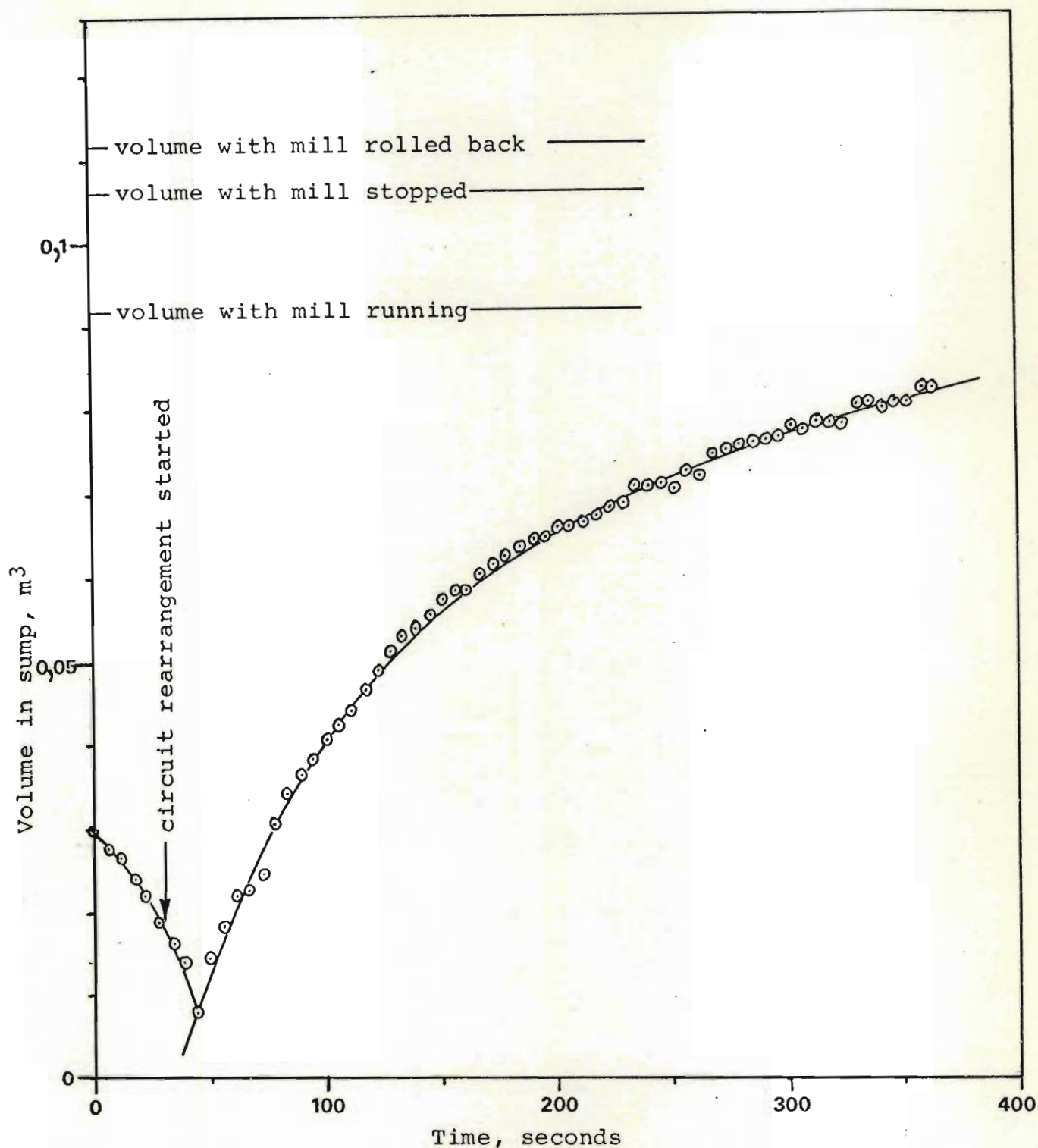


Figure 6.11 Overflow test on mill.

Volume in sump as mill overflowed, after stopping mill feeds and sump withdrawal.

The graphs of the raw data from each run shown ahead are intended as summaries of how the main variables behaved during the runs. Greater detail is shown in the filter results. The complete set of data was kept on a disc file on the CDC-1700.

The particle size analyses for these runs, although done as explained in Section 5.3, are quoted only in a condensed form for the sizes used in the filter. The times at which the samples were taken are shown in each graph.

6.5.1. Run A

The graphs of the measurements taken during this run are shown summarised in Figure 6.12. Twelve samples were taken of the cyclone overflow, and one of the underflow. Summarised analyses of these samples are given in Table 6.13.

During the run, the mill concentration rose so high that the stones which were discharged overloaded the cyclone after about 48 minutes. This gave a very coarse cut and the overflow tank sanded up, resulting in abnormally high overflow concentration measurements. The sump ran low as a result of the decreased circulating load, and the control on the sump water cycled while trying to bring the level up. The run terminated shortly afterwards.

6.5.2. Run B

Figure 6.13 shows the graphs for this run, and Table 6.14 gives the analyses of the samples. 28 overflow samples and 6 underflow samples were taken.

This run continued for over three hours and gave much useful data. During this time, conditions varied over a wide range and only two minor upsets were experienced. A fuse blew in the controller box at about 55 minutes, but was quickly repaired. The second upset occurred when the line to the cyclone blocked at about 100 minutes, but this was also quickly cleared. The cyclone behaved well and operated around a fast rope to a spray discharge throughout the run. Some large stones were discharged from the mill towards the end, but they did not cause any trouble. During the run, the cyclone feed concentration set point was deliberately lowered for a period of about 40 minutes to provide a perturbation on the

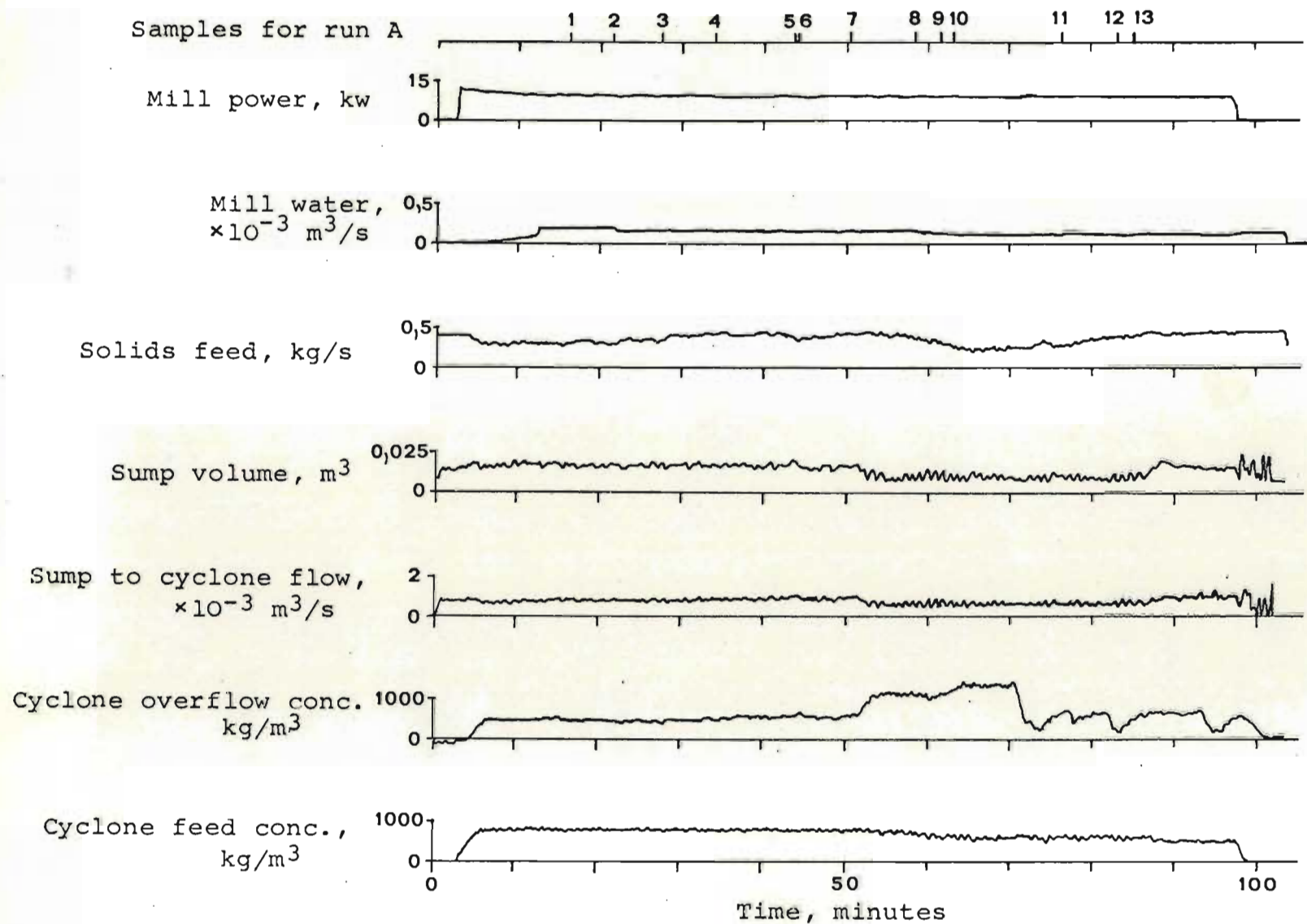


Figure 6.12 Run A - Summary of stored data from run, showing trends.

Table 6.13

Analyses of Samples for Run A.

Sample No.	Sample Type	Volumetric flow $\times 10^{-3} \text{ m}^3/\text{s}$	Concentration, kg solids/ m^3 slurry	Cumulative Particle Size Analyses		
				-75 μm %	-212 μm %	-850 μm %
A1	O/F	0,535	536	37,67	70,56	98,62
A2	O/F	0,402	477	37,74	70,05	98,72
A3	O/F	0,618	476	34,61	69,26	98,83
A4	O/F	0,600	505	30,99	65,54	98,04
A5	U/F	0,387	1690	5,75	18,97	71,02
A6	O/F	0,475	505	29,49	59,95	97,04
A7	O/F	0,549	532	22,65	46,34	88,21
A8	O/F	0,732	538	20,36	46,00	88,55
A9	O/F	0,664	269	31,21	60,02	94,82
A10	O/F	0,495	343	33,85	61,16	95,50
A11	O/F	0,466	415	29,05	59,81	97,30
A12	O/F	0,620	365	27,71	54,85	95,46
A13	O/F	0,819	358	25,99	55,05	93,82

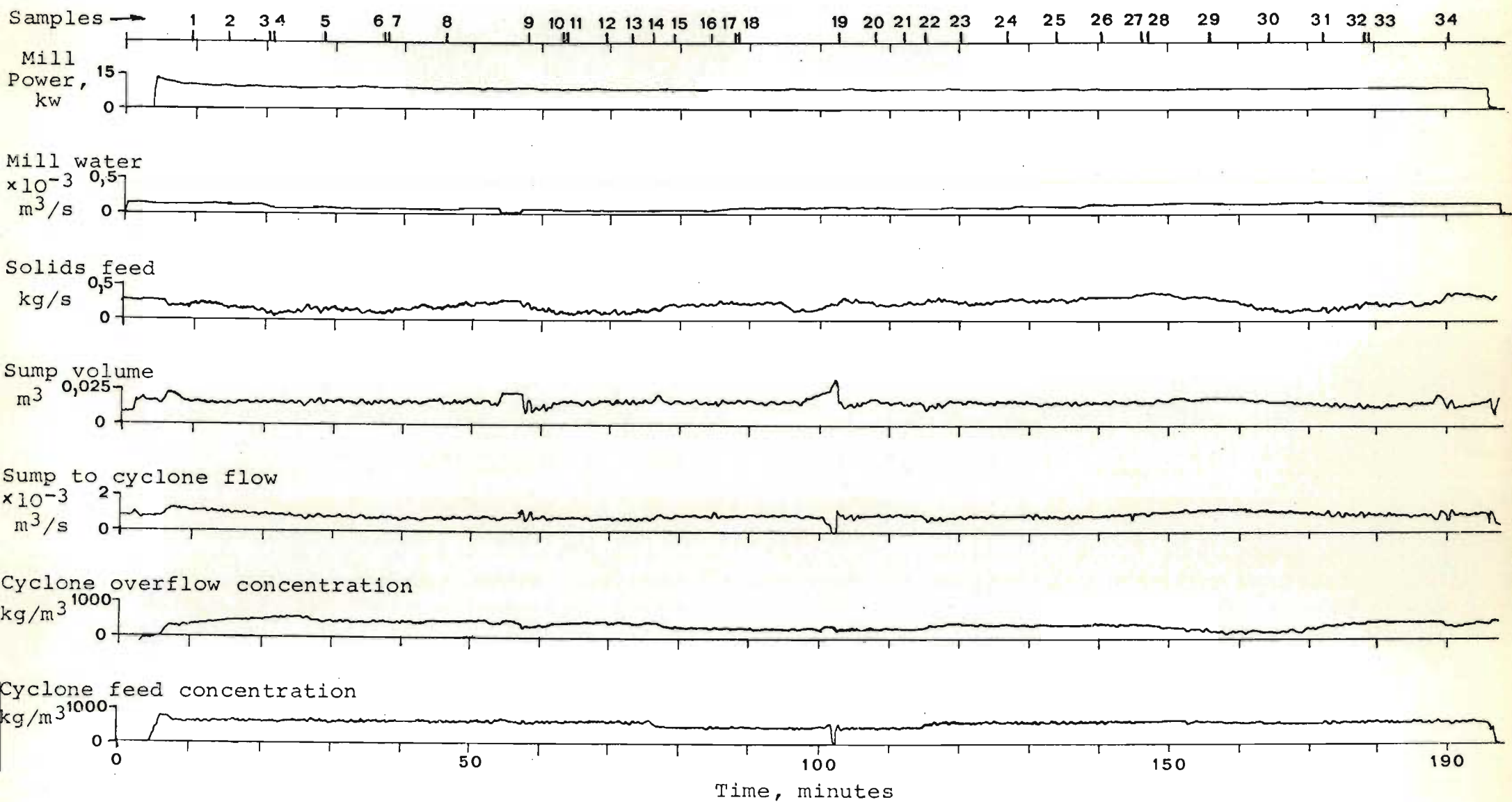


Figure 6.13 Run B - Summary of stored data from run showing trends.

Table 6.14

Analyses of Samples for Run B.

Sample No.	Sample Type	Volumetric flow $\times 10^{-3} \text{ m}^3/\text{s}$	Concentration kg solids/ m^3 slurry	Cumulative Particle Size Analyses		
				-75 μm %	-212 μm %	-850 μm %
B1	O/F	0,735	325	35,00	70,11	99,03
B2	O/F	0,551	349	36,80	72,02	99,28
B3	U/F	0,440	810	16,10	50,00	98,40
B4	O/F	0,246	398	38,96	76,87	99,76
B5	O/F	0,253	465	37,25	75,66	99,76
B6	U/F	0,488	692	25,50	63,07	98,83
B7	O/F	0,241	468	43,98	84,09	99,85
B8	O/F	0,261	472	44,76	82,09	99,81
B9	O/F	0,318	437	41,99	78,62	99,59
B10	U/F	0,473	701	25,72	61,37	98,77
B11	O/F	0,148	479	40,80	78,04	99,79
B12	O/F	0,194	474	42,20	80,80	99,84
B13	O/F	0,506	355	43,32	80,62	99,78
B14	O/F	0,449	310	47,08	83,38	99,89
B15	O/F	0,559	327	45,99	83,82	99,85
B16	O/F	0,675	271	43,57	80,86	99,74
B17	U/F	0,440	570	21,43	56,63	97,93
B18	O/F	0,584	315	42,53	79,76	99,66
B19	O/F	0,588	323	39,46	76,22	99,62
B20	O/F	0,620	284	40,10	75,96	99,58
B21	O/F	0,417	423	39,39	76,30	99,63
B22	O/F	0,503	440	38,98	75,60	99,56

- continued overleaf -

Table 6.14 (contd.) (Run B sample analyses)

Sample No.	Sample Type	Volumetric flow $\times 10^{-3} \text{ m}^3/\text{s}$	Concentration kg solids/ m^3 slurry	Cumulative Particle Size Analysis		
				-75 μm %	-212 μm %	-850 μm %
B23	O/F	0,470	403	36,39	70,52	98,92
B24	O/F	0,478	362	39,88	72,73	99,25
B25	O/F	0,607	342	37,26	71,06	99,04
B26	O/F	0,838	339	34,55	68,89	98,59
B27	U/F	0,375	1605	5,60	26,43	83,11
B28	O/F	0,995	265	35,09	69,41	97,65
B29	O/F	1,001	229	34,30	67,63	97,85
B30	O/F	0,812	215	37,47	70,33	99,25
B31	O/F	0,790	302	33,28	68,18	99,23
B32	U/F	0,373	1189	9,53	39,18	95,06
B33	O/F	0,656	324	34,18	69,53	99,39
B34	O/F	0,816	301	34,37	69,07	98,98

system. Around 150 to 170 minutes, the sump pump was running near the maximum of its range.

6.5.3. Run C

The plots for this run are shown in Figure 6.14, and the sample analyses in Table 6.15. 15 overflow samples were taken but no underflow samples were collected. At the beginning, the samples were taken after the cyclone overflow tank, but from sample 9 onwards the overflow was sampled directly at the cyclone discharge.

This was the first run done to test the filter on line, and it performed satisfactorily. (Filter results are shown ahead.) Some time-sharing difficulties had been experienced earlier while debugging the programme, caused by the complexity and size of the on-line filter, but these were removed before doing the run.

At the beginning, the potentiometer on the solids feed actuator came loose, and some of the readings were below the actual value, giving a low solids feed rate. This was repaired after 50 minutes, and the run continued. After 42 minutes, and again after 95 minutes, it was attempted to control the plant from the filter, as explained in Section 5.6, but the controller settings were too high, and instability resulted, particularly on the sump water. (Note that the control strategy was not written into the filter, but control changes were entered after each observation as part of the volumetric filter. Consequently, a change in control strategy such as this would not require a reformulation of the filter.) Both times the plant was put back on normal control after a few minutes. The measurements of the sump volume were found to have a slight uniform offset throughout the run (later found to be caused by the instrument), and so the set point was set to $0,020 \text{ m}^3$ in place of the normal $0,016 \text{ m}^3$. Otherwise the circuit and the filter worked well. The cyclone operated with a fast rope most of the time, except when the oscillations from the filter control caused it to block

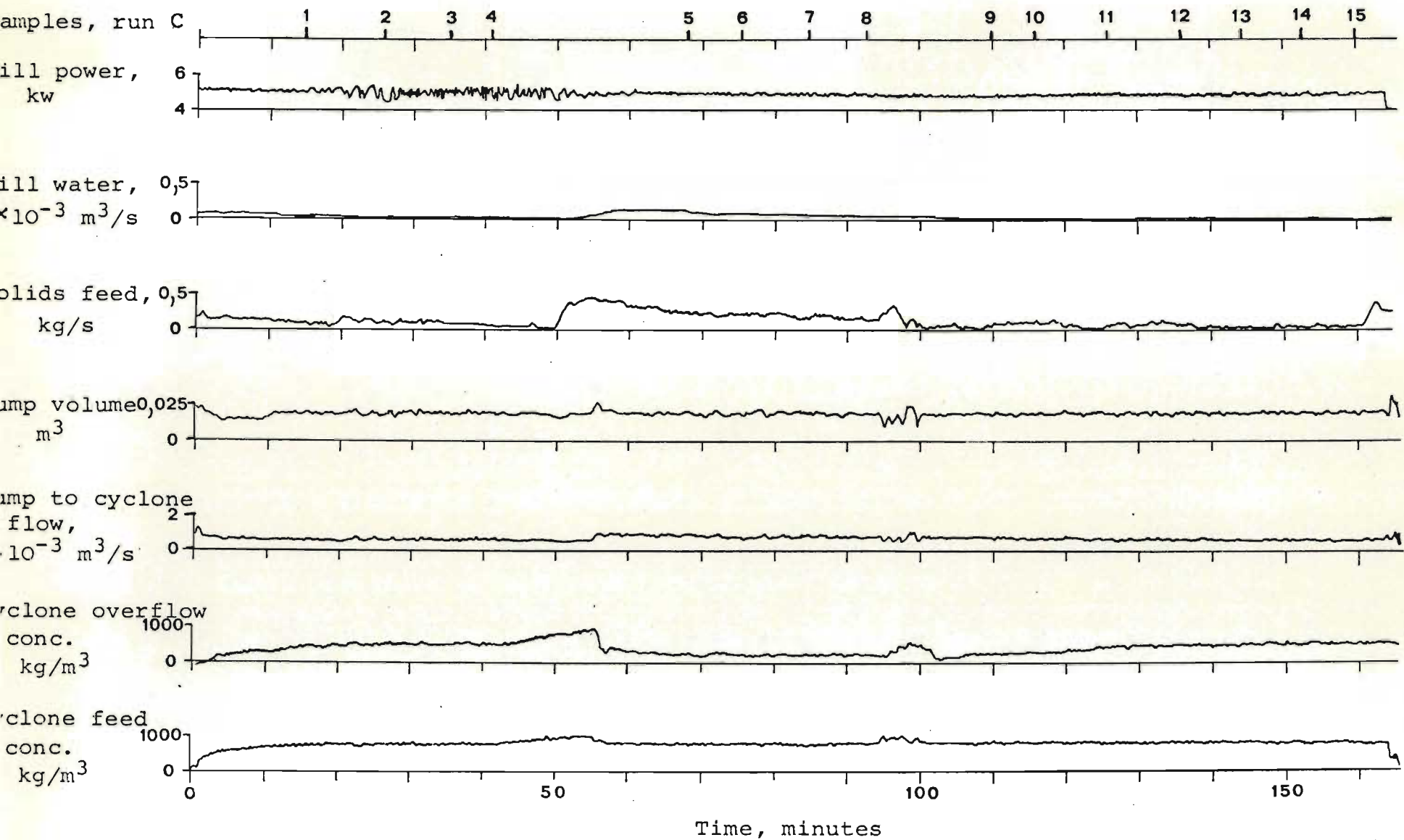


Figure 6.14 Run C - Summary of stored data from run, showing trends.

Table 6.15

Analyses of Samples for Run C.

All samples of cyclone overflow.

Sample No.	Volumetric flow, $\times 10^{-3} \text{ m}^3/\text{s}$	Concentration kg solids/ m^3 slurry	Cumulative Particle Size Analysis		
			-75 μm %	-212 μm %	-850 μm %
C1	0,082	642	44,90	84,21	99,85
C2	0,207	756	43,68	82,38	99,78
C3	0,194	735	44,61	81,51	99,68
C4	0,136	792	44,13	80,16	99,54
C5	0,563	380	48,39	84,80	99,85
C6	0,499	324	44,32	77,70	99,18
C7	0,585	340	40,68	75,99	99,47
C8	0,490	352	39,07	71,99	99,09
C9	0,395	316	46,83	79,16	99,71
C10	0,296	386	47,82	82,82	99,88
C11	0,287	525	37,80	78,04	99,85
C12	0,123	581	43,51	82,30	99,93
C13	0,148	776	38,79	82,97	99,92
C14	0,089	647	46,66	86,00	99,94
C15	0,104	754	45,90	86,64	99,94

6.5.4. Run D

Figure 6.15 shows the plots of the data from this run, and the analyses of the 15 overflow samples are given in Table 6.16. All samples were taken at the cyclone discharge.

The operating conditions did not fluctuate much during this run. From 55 to 80 minutes it was attempted to control from the filter results using new controller settings but, while this was less erratic than run C, it did not work well. The sump overflowed slightly from 75 to 80 minutes. Nevertheless, control was achieved as desired. To attempt to perturb the circuit, two manual increases were made on the solids feed controller at 83 and 138 minutes. The equipment behaved well throughout the run.

6.6. Values of parameters used in the filter

The values of the parameters summarised in Table 6.17 were the standard values used for the tests done on the filter. Their explanation is as follows. (Where non-standard values were used in a test, the reason is given in the section dealing with that test.)

(1) The grinding data (selection and breakage functions), cyclone data (\underline{cc}_0 , \underline{cc}_1 , Q_{UO} , σ_ϵ^2), feed size distribution, and mill overflow parameters were determined from off-line experiments as explained already in Sections 6.1 to 6.4. The rate scaling factor K_C was kept constant at 1.0, while K_L was calculated from equation 6.1. The units of the selection function were also changed from min^{-1} to s^{-1} .

(2) The classification parameter vectors, $\underline{\beta}$, $\underline{\gamma}$, and \underline{n} for the mill, sump and cyclone overflow tank respectively, were all given values of unity, except where a different value could be adequately justified. Thus, in the coarsest size fraction, the mill parameter β_1 was given a value of 0.1 as this fraction was generally held back in the mill. Earlier tests seemed to

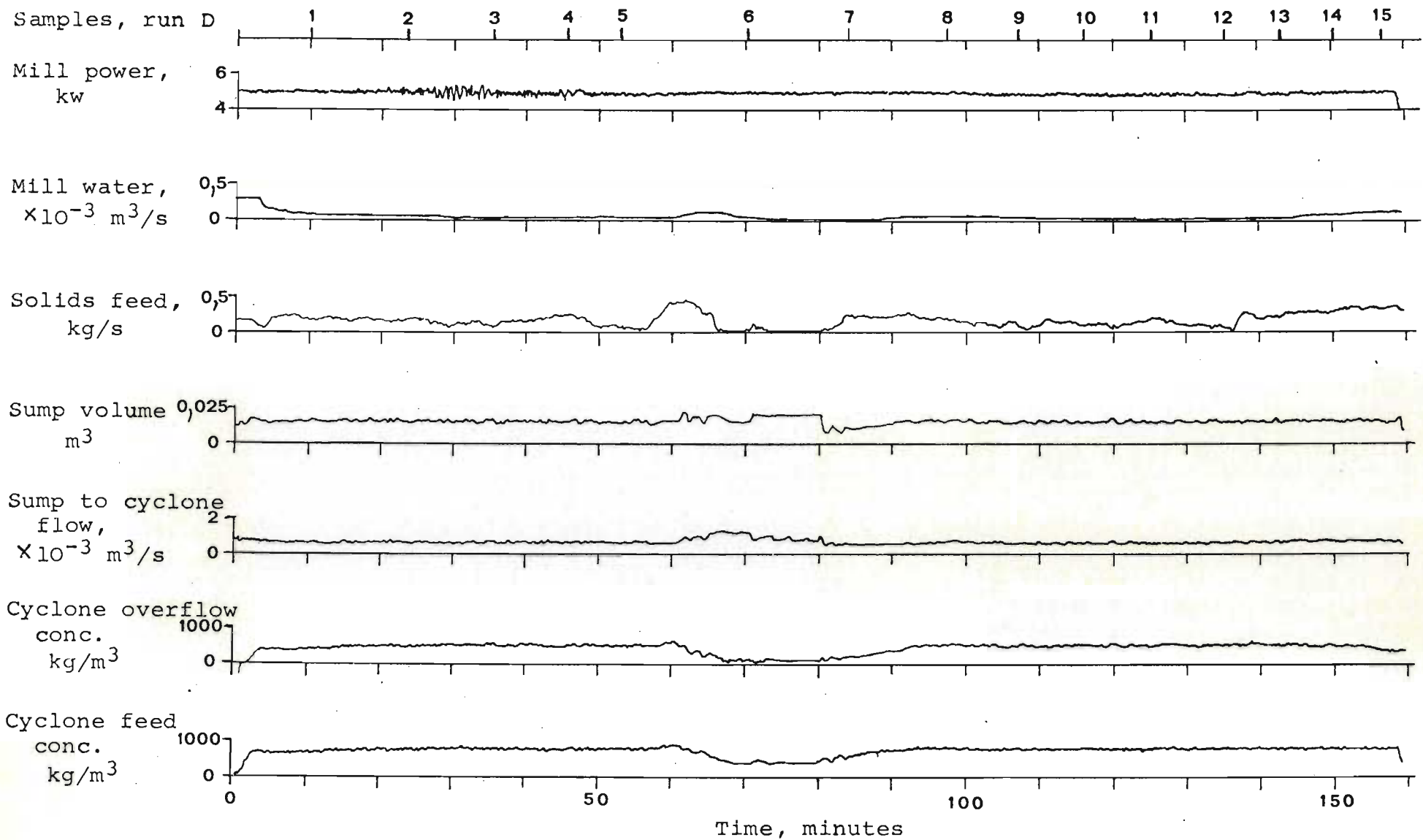


Figure 6.15 Run D - Summary of stored data from run, showing trends.

Table 6.16

Analyses of Samples for Run D

All samples of cyclone overflow.

Sample No.	Volumetric flow $\times 10^{-3} \text{ m}^3/\text{s}$	Concentration kg solids/ m^3 slurry	Cumulative Particle Size Analysis		
			-75 μm %	-212 μm %	-850 μm %
D1	0,139	671	46,79	86,88	99,90
D2	0,235	525	45,30	82,27	99,77
D3	0,262	796	42,86	81,14	99,76
D4	0,126	759	45,93	80,07	99,69
D5	0,136	767	45,32	80,05	99,68
D6	0,869	222	46,80	81,12	99,60
D7	0,052	379	55,05	90,96	99,95
D8	0,152	849	41,51	79,89	99,70
D9	0,186	844	42,00	79,98	99,67
D10	0,141	764	43,53	79,29	99,73
D11	0,135	815	42,79	79,48	99,76
D12	0,112	903	44,05	79,75	99,73
D13	0,212	865	44,60	80,76	99,61
D14	0,262	748	44,84	79,48	99,50
D15	0,352	540	53,10	85,01	99,61

Table 6.17

Standard values of parameters
used in the filter.

Parameter	Value
Observation interval	5,0 seconds
Mean cyclone underflow rate, Q_{U0}	$0,4073 \cdot 10^{-3} \text{ m}^3/\text{s}$
Standard deviation of cyclone underflow rate	$0,0619 \cdot 10^{-3} \text{ m}^3/\text{s}$
Mill overflow constant	$0,01 \text{ s}^{-1}$
Mill minimum charge volume, V_{M0}	$0,0935 \text{ m}^3$
Specific gravity of solids	3,37
Softness factor, K_S	0,9
Variance of softness, $\sigma_{K_S}^2$	0,02025
Selection function vector, \underline{S}_0) as given in) Table 6.5
Breakage function matrix, \underline{b}	
Mill exit classification vector, $\underline{\beta}$	$(0,1 \ 1,0 \ 1,0 \ 1,0)^T$
Sump exit classification vector, $\underline{\gamma}$	$(1,0 \ 1,0 \ 1,0 \ 1,0)^T$
Cyclone overflow tank classification vector, $\underline{\eta}$	$(10,0 \ 1,0 \ 1,0 \ 1,0)^T$
Noise vector for grinding model, $\underline{\phi}$	$(2,5 \ 0,5 \ 0,5 \ 0,5)^T$
Cyclone classifier functions, \underline{cc}_0 and \underline{cc}_1	as in table 6.9
Feed solids size distribution	as in table 6.6
Standard deviation of cyclone overflow concentration	$400,0 \text{ kg/m}^3$
Standard deviation of cyclone feed concentration	$200,0 \text{ kg/m}^3$

indicate that this was a reasonable value, although it varied considerably depending on the pulp viscosity. Similarly, the cyclone overflow tank tended to retain coarse particles, and so η_1 was given a value of 10,0. Neither of these two values was very critical in the normal filter performance.

(3) If the scale-up of the selection function from the batch tests were exact, then the softness of the rock would be 1,0. The normal operating mill was observed to have an increased magnetite content in the circulating load, which produced higher solids specific gravities (typically 3,6 to 3,7) and harder rock for grinding. It was attempted to calculate the difference in softness from a knowledge of the increased magnetite content calculated from the specific gravity, but there were insufficient reference data available. Instead, Run B was used to find the value of softness giving the best predictions, and this was the value of 0,9 in Table 6.17. This value is fairly critical, but could not be found more accurately, as it could vary slightly depending on the mill charge. The filter was also able to estimate softness, but this was not found to be very satisfactory, as shown in Section 6.8.5, and so K_S was normally kept constant.

(4) The noise levels for the volumetric filter were chosen as explained in Section 4.2.4. for a linear filter. Only the variance of the underflow rate and the control change errors were calculated from data; the remaining noise levels were guessed. Table 6.18 details the noise levels used in the process, measurement, and controller models, and gives the resulting error variances for the stationary state predictions (see Section 4.3.1). Comparing the variances of the predictions with the observation variances, this table shows clearly how the use of even a simple filter can reduce the errors in measured variables, as well as predict variables which cannot be measured. Also shown here are the variances of the actual observations given the a priori observation predictions, which were used for checking the error levels as explained in Section 4.2.4, and for on-line checking of the

Table 6.18

Noise levels in volumetric filter.

(All units are S.I.)

Variance of error on $Q_U = 3,83 * 10^{-9}$

Variables		Measurement error variances (diag \underline{R})	Control change variances (diag $\underline{\Delta U}$)	Variances of predic- tions after observation (diag \underline{P}_A)	Variances of observa- tions given predictions (diag \underline{V}_k)
STATE VARIABLES	Mill volume, V_M	-	-	$7,67 * 10^{-7}$	-
	Sump volume, V_S	$2,5 * 10^{-7}$	-	$8,22 * 10^{-8}$	$3,99 * 10^{-7}$
CONTROL VARIABLES	Sump withdrawal rate, Q_S	$1,6 * 10^{-9}$	$1,44 * 10^{-10}$	$3,34 * 10^{-10}$	$2,08 * 10^{-9}$
	Solid feed rate, S	$9,0 * 10^{-4}$	$2,5 * 10^{-5}$	$1,38 * 10^{-4}$	$1,06 * 10^{-3}$
	Mill feed water, W_M	$1,0 * 10^{-10}$	$1,96 * 10^{-10}$	$7,29 * 10^{-11}$	$3,69 * 10^{-10}$
	Sump dilution water. W_S	$4,0 * 10^{-10}$	$4,0 * 10^{-10}$	$2,39 * 10^{-10}$	$1,04 * 10^{-8}$

reliability of the measurements as explained in Section 4.3.2. Graph 6.22(b) (see Section 6.7.2) shows a detail from run B with the actual measurements of sump flow compared to the predictions. The standard deviation of the observations about the predictions, $= \sqrt{\sigma_{\Delta y_i}^2}$, is shown as a band on each side of the predictions. This was used (see Section 4.2.4) as a check on the noise levels used in the filter.

(5) The noise levels in the p.s.d. model ($\underline{\phi}$ and $\sigma_{K_S}^2 = m_2(K_S)$) were chosen by running the evolution only as explained in Section 4.2.4., method (ii) on a grid of noise levels to determine the best point. The vector $\underline{\phi}$ was guessed, from a consideration of the results of the errors in calculating grinding parameters for the smaller number of size groups (see Section 6.1, Table 6.5) and other sources of error (see Section 4.2.4), to be a scalar multiple of $(5 \ 1 \ 1 \ 0)^T$. The other noise level was the variance of softness, $\sigma_{K_S}^2$. Figure 6.16 shows the effects of 3 different levels of both of these variables on the predicted standard deviations of mill concentration, sump concentration and the percentage in the finest size fraction in the product. Each pair of graphs in this figure shows the data plotted firstly as a function of $\underline{\phi}$ for each level of $\sigma_{K_S}^2$, and secondly as a function of $\sigma_{K_S}^2$ for each level of $\underline{\phi}$.

From Figure 6.16, $\underline{\phi}$ affected the concentrations more than the product size, and $\sigma_{K_S}^2$ was the other way round. The values of the estimation errors which were guessed from a knowledge of the plant are shown below:

Variable	Range of values during normal plant operation	Guessed value of approximate standard deviation at stationary state
Mill concentration	1000 to 1800 kg/m ³	150 kg/m ³
Sump concentration	400 to 800 "	50 "
-75 μ m fraction in product	30 to 50%	4%

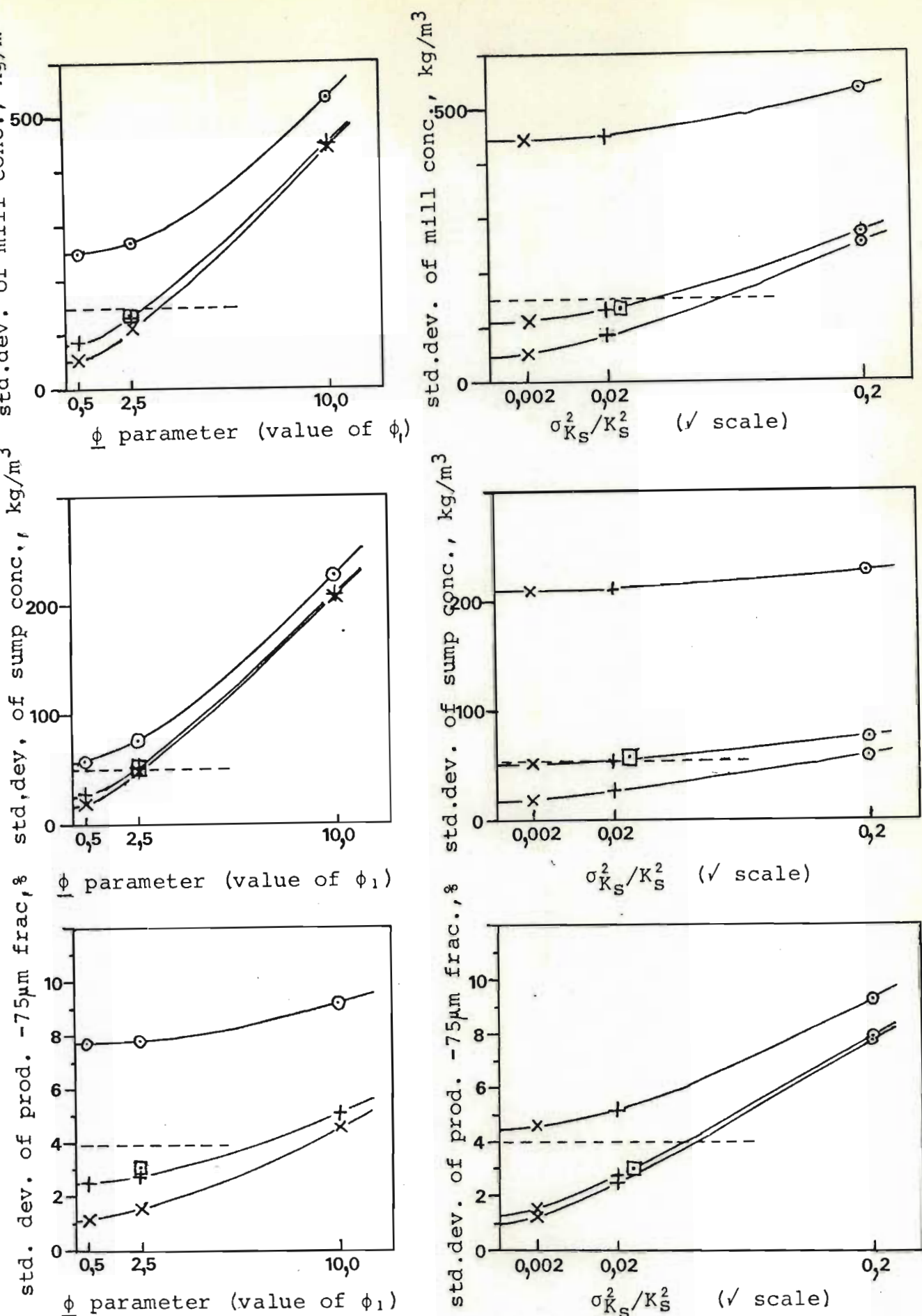


Figure 6.16 Determination of noise levels in p.s.d. filter.

Effect of varying noise levels on standard deviations of predictions. (Without observation step in filter.) Three level grid used. Left hand graphs show effects of ϕ with softness as parameter, right hand graphs show corresponding effects of softness with ϕ as parameter. Values of parameters in the graphs are at points on the grid. \square are points corresponding to values used (table 6.17). Horizontal dotted

Horizontal dotted lines in Figure 6.16 are shown corresponding to these values. The values of the parameters used in the filter (Table 6.17) are shown as squared points, \blacksquare , on the graphs. These points had been chosen earlier (as explained in Section 4.2.4) to agree with the chosen error levels. In retrospect though, it may have been better to have used a larger ϕ , as the concentration predictions were not as accurate as anticipated, while the size predictions were reasonable.

The observations in the p.s.d. filter were measurements of concentrations. These were particularly noisy, and often had slight zero offsets, and so their noise levels in the filter were made particularly high (see Table 6.17). This meant that the results did not depend very much on the observation measurements.

Although the original choices of noise levels were only carefully guessed, in most cases they were found to be satisfactory for use in the filter. The p.s.d. filter measurement errors were examined as one of the factors affecting the filter, and the results are given in Section 6.8.6. There were too many error parameters for all to be carefully calculated and their individual performances evaluated in this way. This determination of noise levels is a difficulty which affects all filters, and it is essential to put much effort into obtaining well estimated values from the start.

6) Average values were used for starting the filter, and a diagonal covariance matrix of suitable size was used for the p.s.d. filter. (This is discussed in Section 6.8.7.)

6.7. Results of filter tests on runs

Graphs 6.17 to 6.33 show the results of the filter applied to each of the runs A, B, C and D. State variables from the p.s.d. filter were not plotted directly, because they were found to be difficult to interpret visually.

Instead, they were/...

Instead, they were reformed into variables that were more meaningful, as explained in Section 4.2.1. For each of the runs,

(1) One graph shows the results of the volumetric filter with the predictions compared to the measurements, for all states and parameters as indicated. Predictions shown are the values of the estimates after each observation step.

(2) Another graph shows the predictions of the cyclone overflow particle size distributions from the p.s.d. filter, with the results from samples taken plotted for comparison. This graph shows the cumulative percentage for the distribution at 75, 212 and 850 microns, against time. Each group of 3 lines is the mean and the mean \pm standard deviation for the prediction of the percent less than the size indicated.

(3) The particle size distribution predictions for the mill contents and cyclone underflow are shown as two separate graphs on a third page.

(4) The predicted concentrations of the mill, sump (i.e. cyclone feed), cyclone overflow and cyclone underflow are shown on the same axes on a fourth graph. The actual measurements recorded are also drawn as dotted lines, and sampled concentrations are plotted as points.

All the plots were calculated from the predictions after each observation step. The volumetric parameters were calculated from the averages over each interval. There were no large differences between the estimates before and after each observation step, except when there was a plant upset.

The details of each of these runs are given below:

6.7.1. Run A filter results

The upsets during this run were too great for the filter to operate very well. The high solids concentration in the mill (see graph 6.20) made the slurry too viscous, and the rate of grinding decreased so that the rock behaved as if it

were harder. A softness factor of 0,2 was needed to get predictions in the correct order of magnitude, and these are shown in Figures 6.17 to 6.20. For comparison, the predicted product particle size distribution shown in Figure 6.21 used a softness of 0,5, and was too fine.

The volumetric predictions in Figure 6.17 closely followed the plant measurements up to the time of the upset. After 48 minutes, the checks built into the volumetric filter found that the plant was not operating properly, and limited the sensitivity to observations. This can be seen clearly in the sump volume, sump water, and sump outflow graphs.

Figures 6.18 and 6.21 show that the softness of the rock appeared to decrease during the run. Up to 30 minutes the grind was finer than a softness of 0,5 predicted. From 30 to 50 minutes, the softness was between 0,5 and 0,2. This correlates with the increase in mill concentration shown in Figure 6.20. After 50 minutes the cyclone had choked and, although the softness appeared to have decreased further, the abnormal operation made the results doubtful.

This run shows that the filter can be made to operate even though the plant is greatly upset. It does not show much about the normal operation of the filter. The predictions followed the correct trends, while the range covered could be explained by a change in softness, caused by a high mill concentration.

6.7.2. Run B filter results

Run B was the most successful in showing how the filter operated. The results are shown in graphs 6.22 to 6.25. The standard values of the parameters were used, and the filter was started 5 minutes after the beginning of the run.

The volumetric filter measurements agreed well with the predictions (Figures 6.22 a and b). The checks in the filter came into operation at 55 to 60

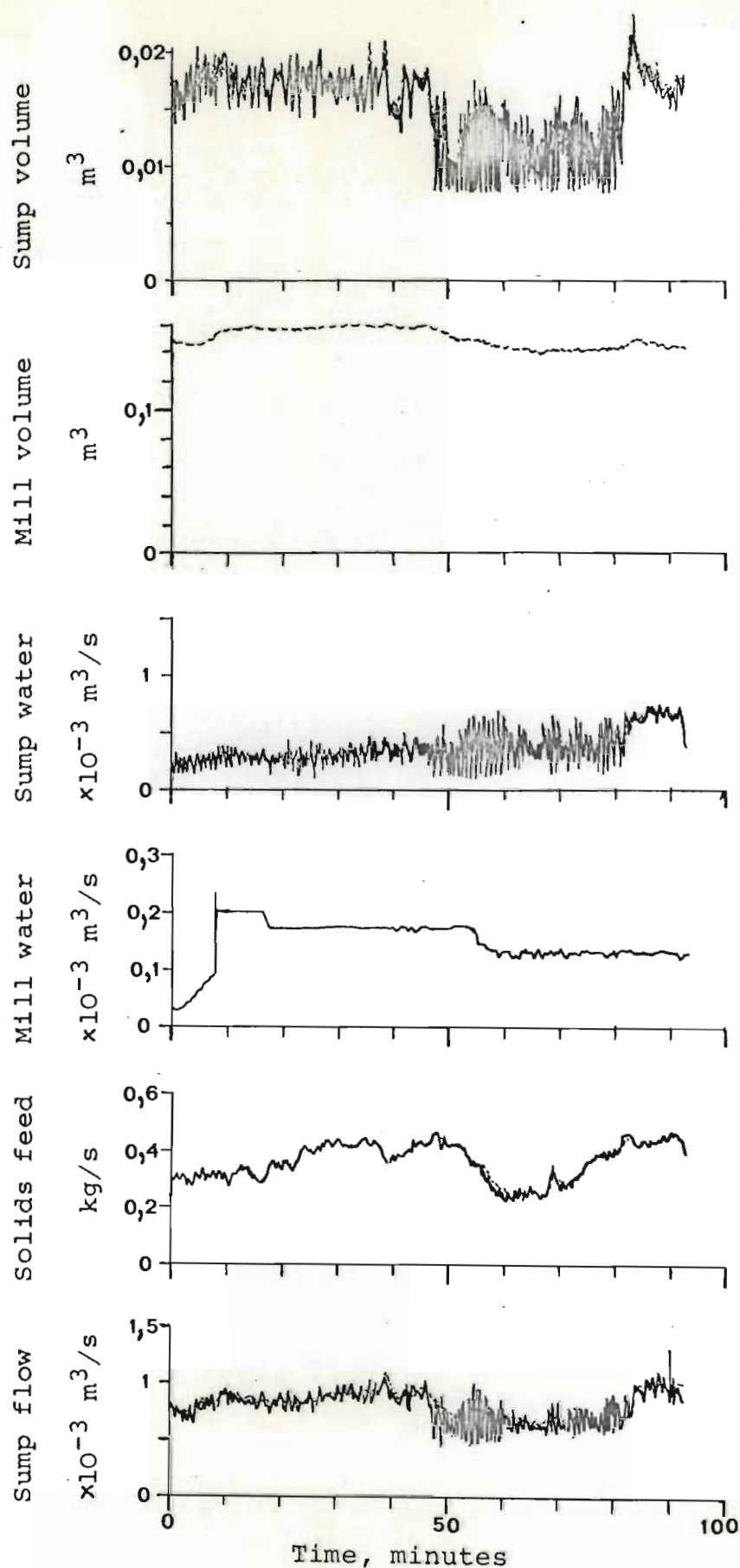


Figure 6.17 Run A - Volumetric filter results.

Predictions shown dotted (----) and instrument measurements shown continuous (—).

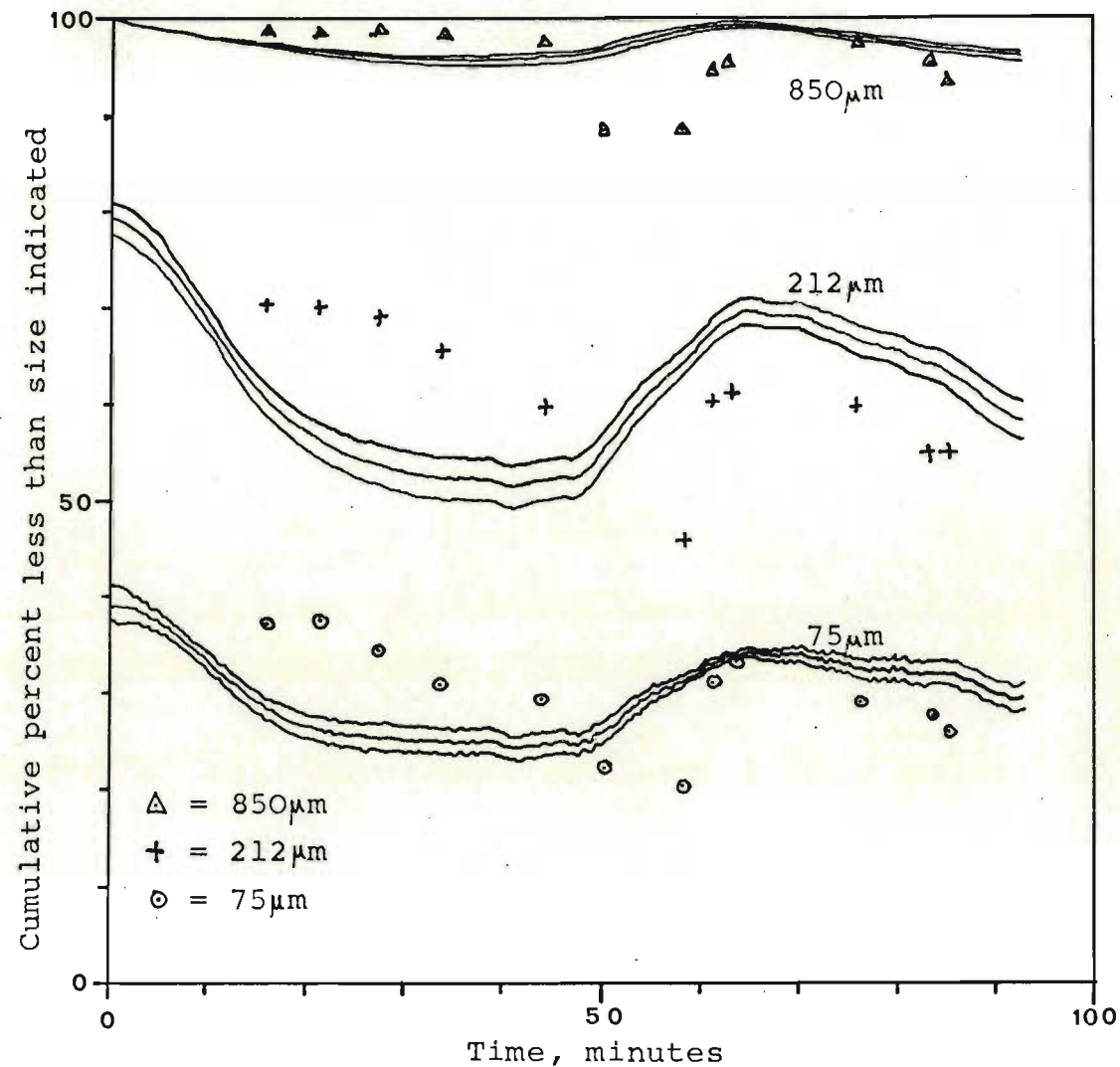


Figure 6.18 Run A - Filter predictions of cyclone overflow
cumulative particle size distribution (softness = 0,2), with actual sample points
plotted for comparison.

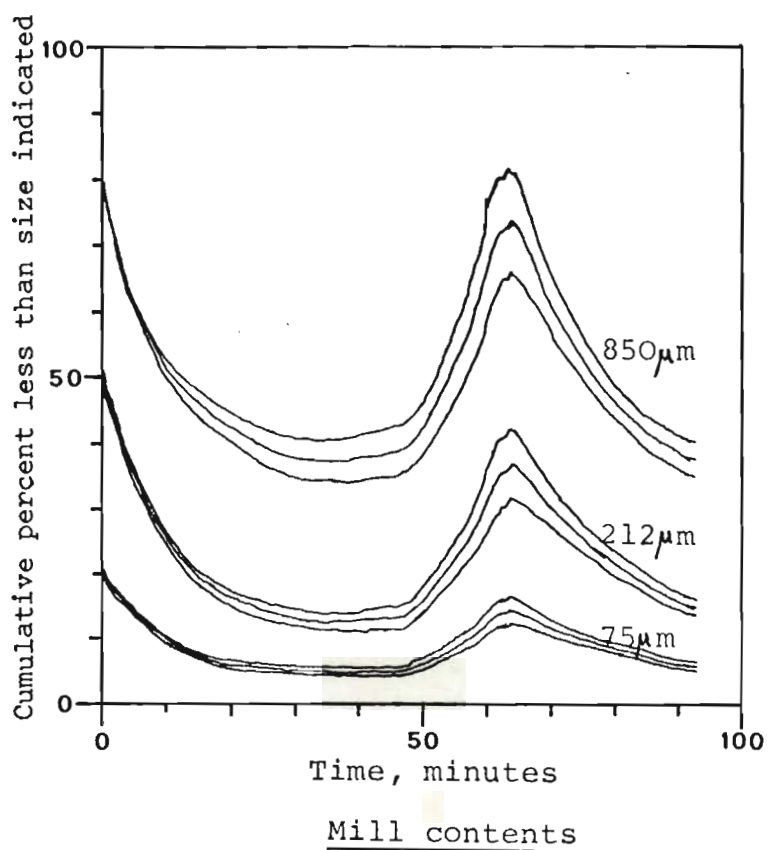
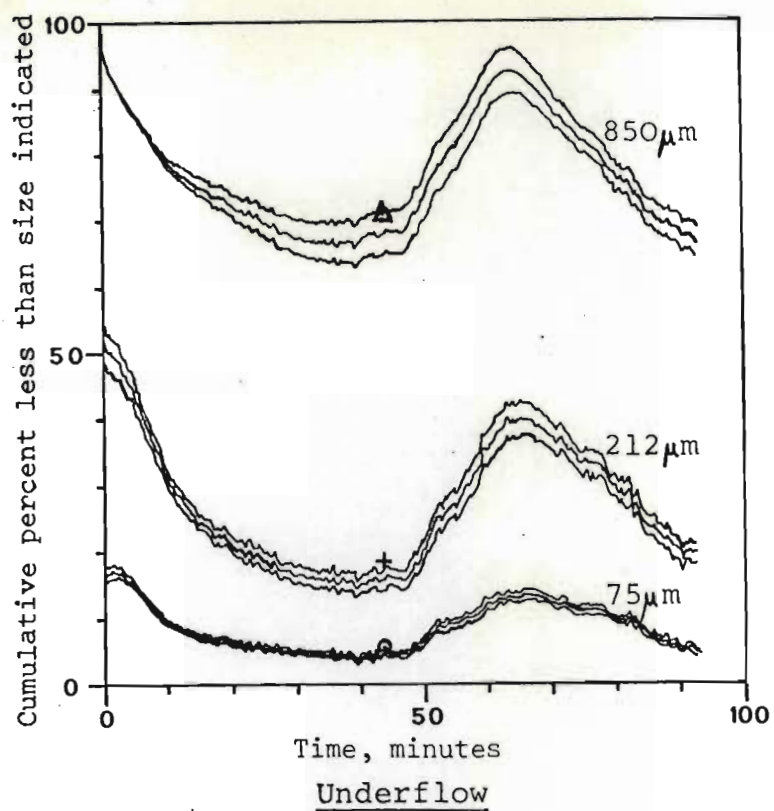


Figure 6.19 Run A - Filter predictions of particle size distributions in the cyclone underflow and mill contents as shown.

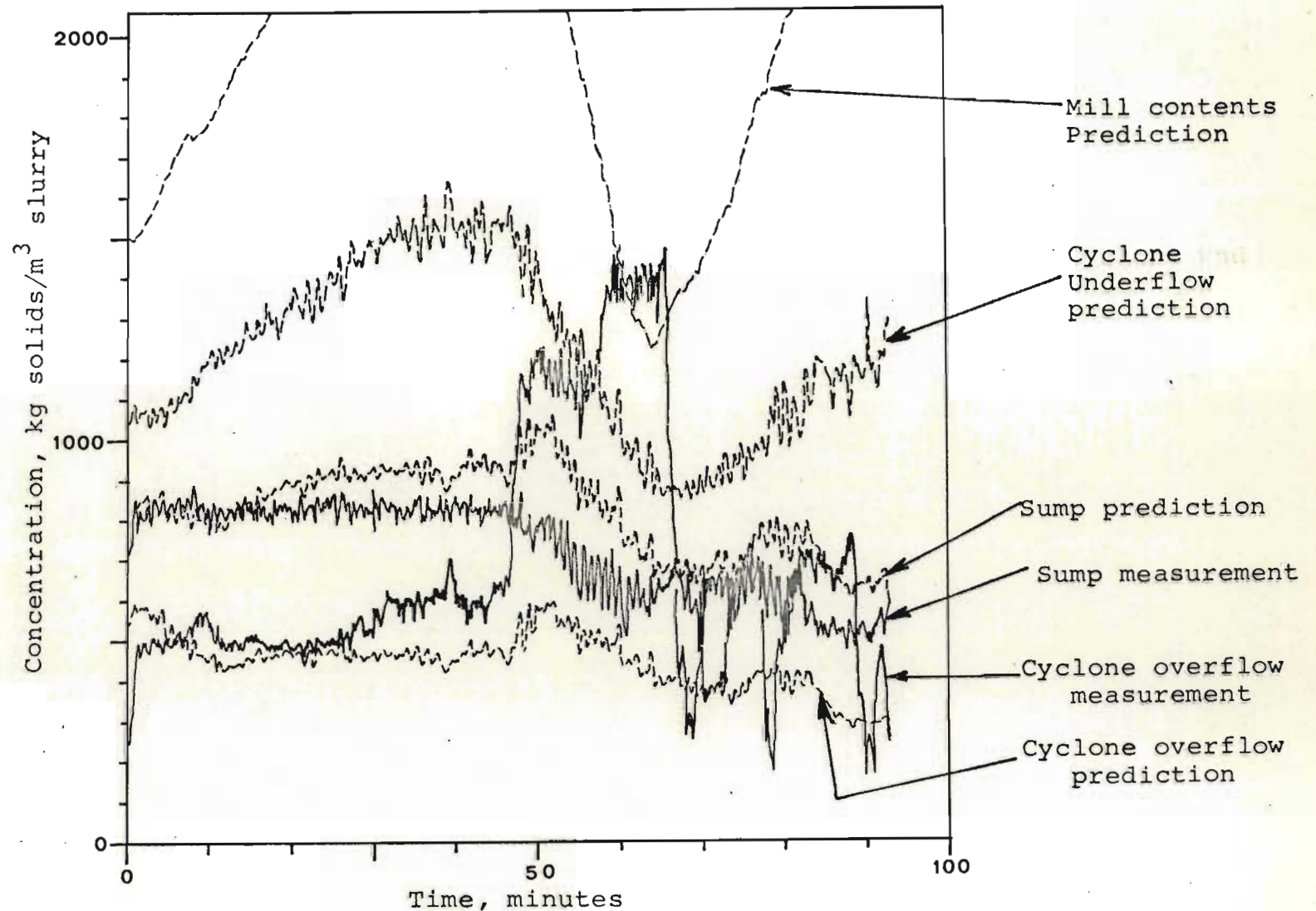


Figure 6.20 Run A - Filter predictions and measurements of concentrations.

Predictions shown dotted and instrument measurements shown continuous. Cyclone overflow concentration measurement wandered during run because of blocked overflow tank (see text).

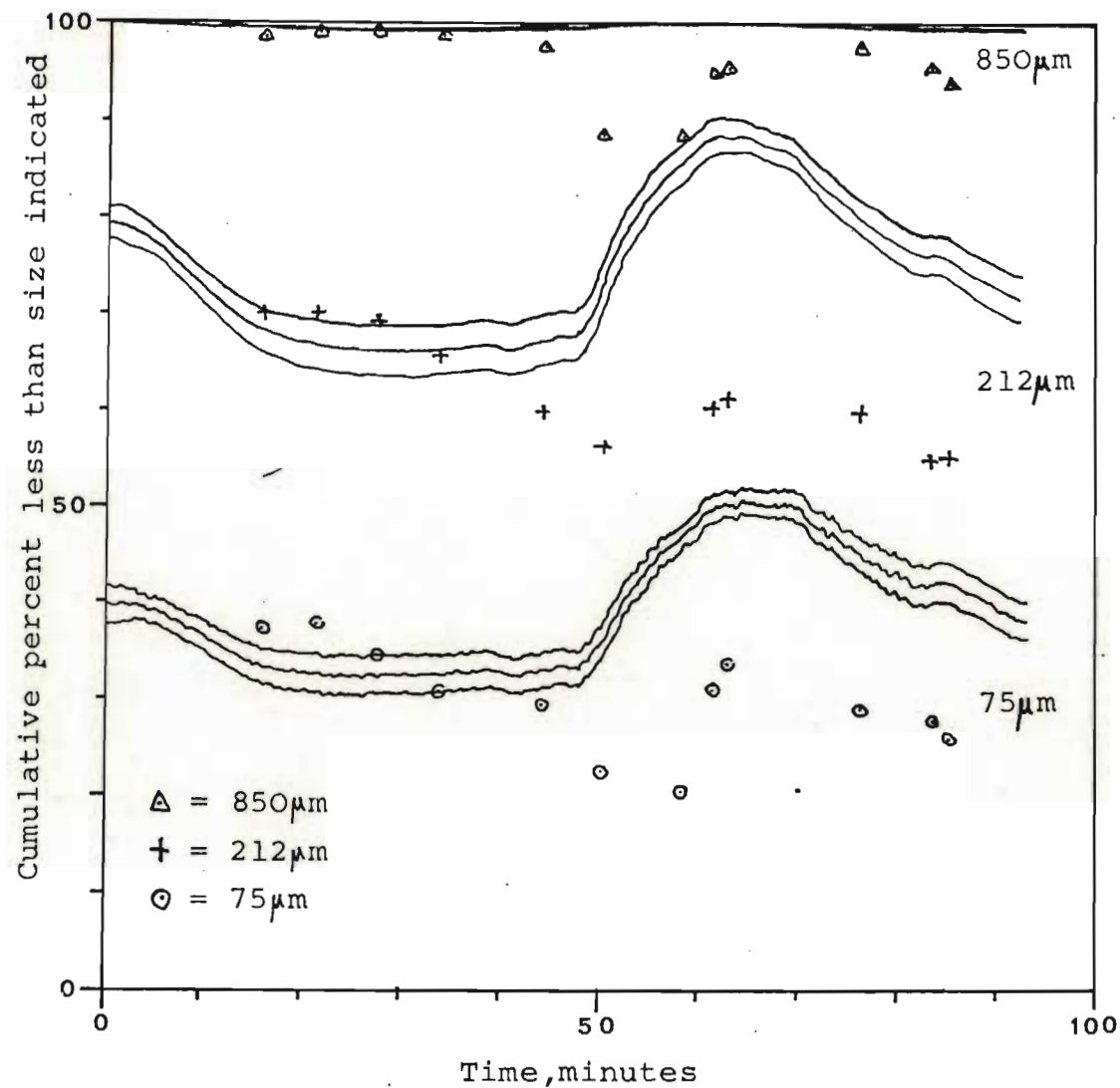


Figure 6.21 Run A - Filter predictions of cyclone overflow
cumulative particle size distribution (softness = 0,5), with actual sample points
plotted for comparison.

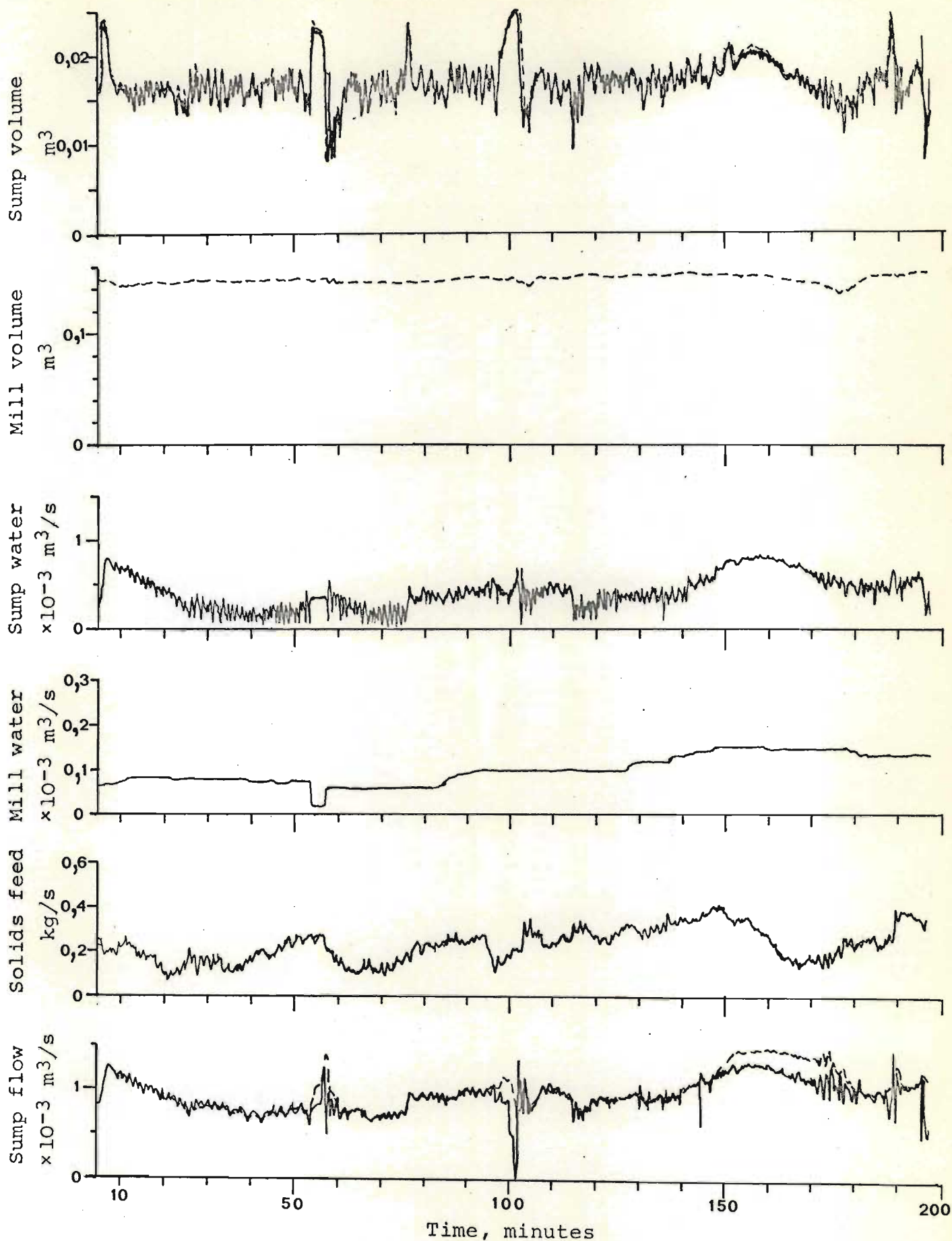


Figure 6.22(a) Run B - Volumetric results.

Predictions shown dotted (-----) and instrument measurements shown continuous (———).

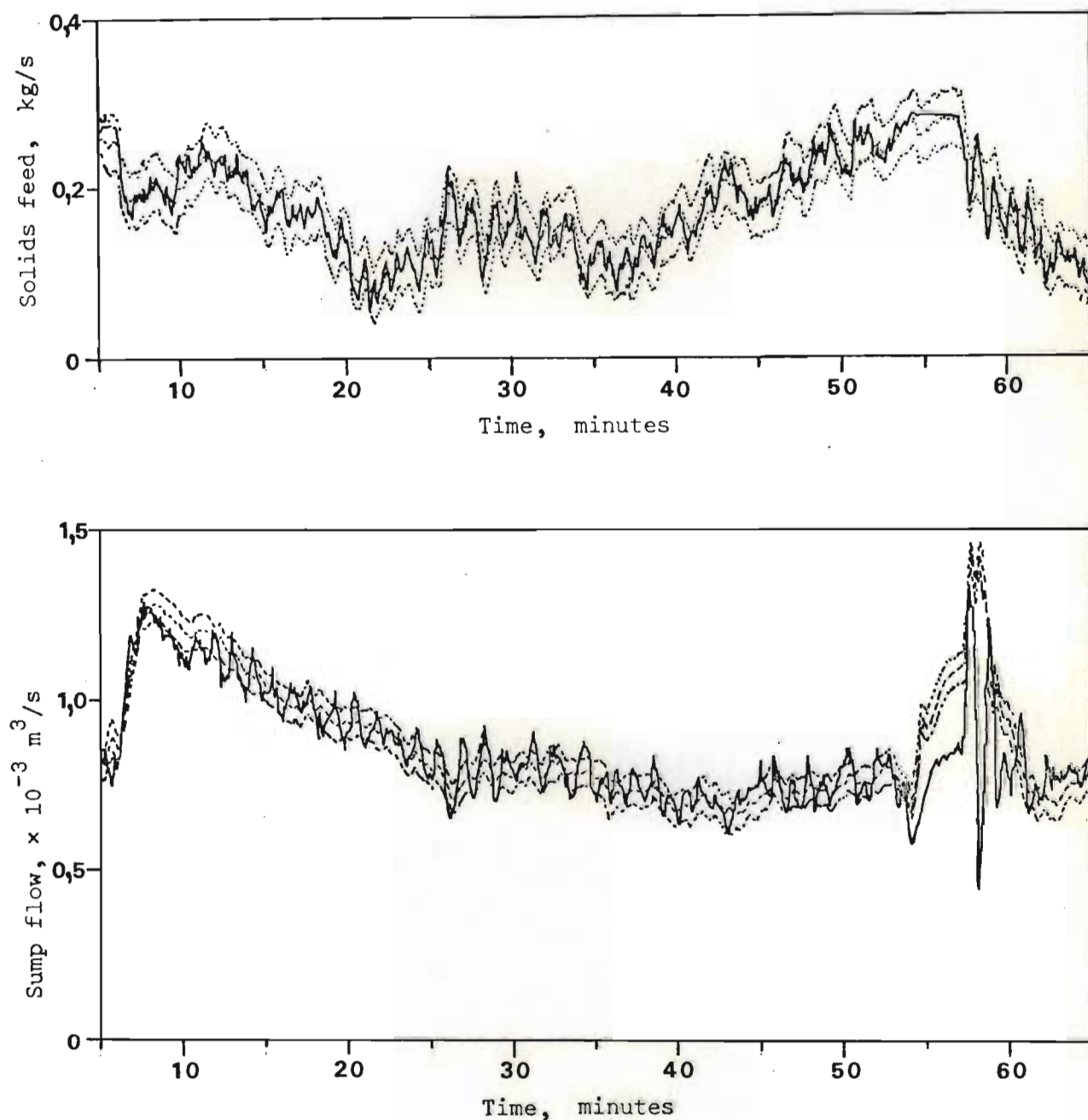


Figure 6.22(b) Detail from figure 6.22(a). Volumetric filter results for

Run B.

First 60 minutes of sump flow and solids feed measurements and predictions. Measurements shown continuous (—). Dotted lines (.....) are the predicted means and the predicted one standard deviation band of the observation errors about the predicted means.

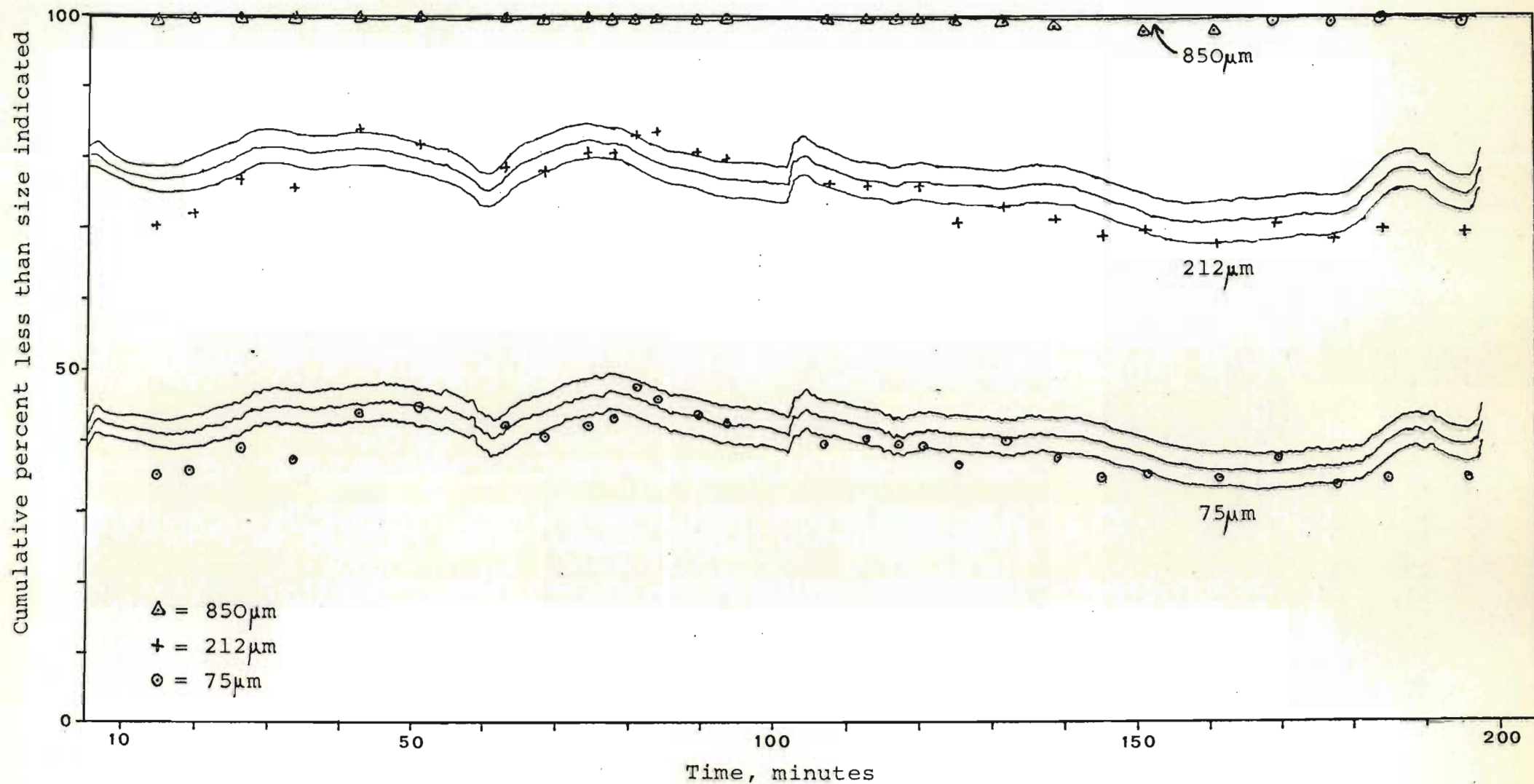


Figure 6.23 Run B - Filter predictions of cyclone overflow cumulative particle size distribution, with actual sample points plotted for comparison.

Each set of three lines are mean and mean +/- standard deviation.

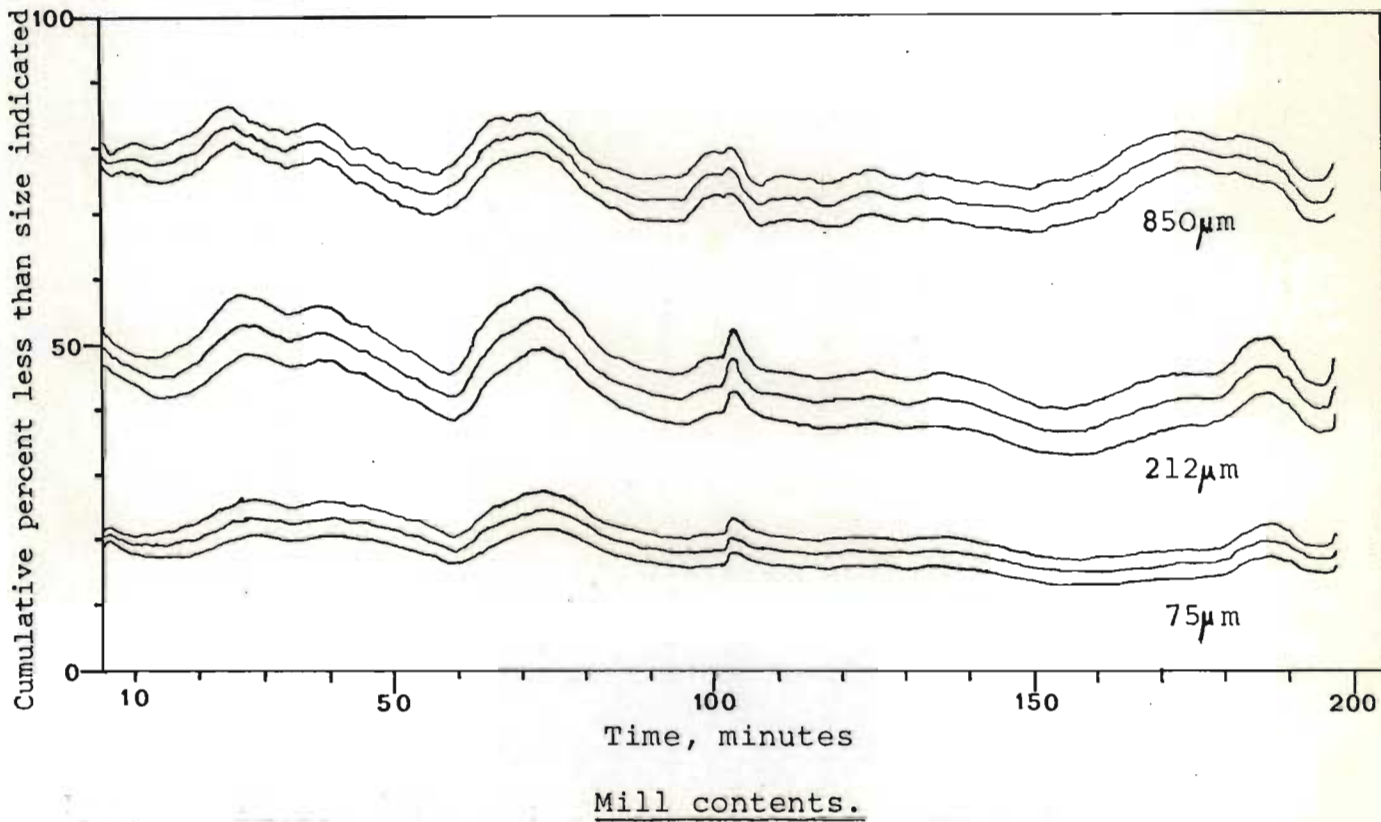
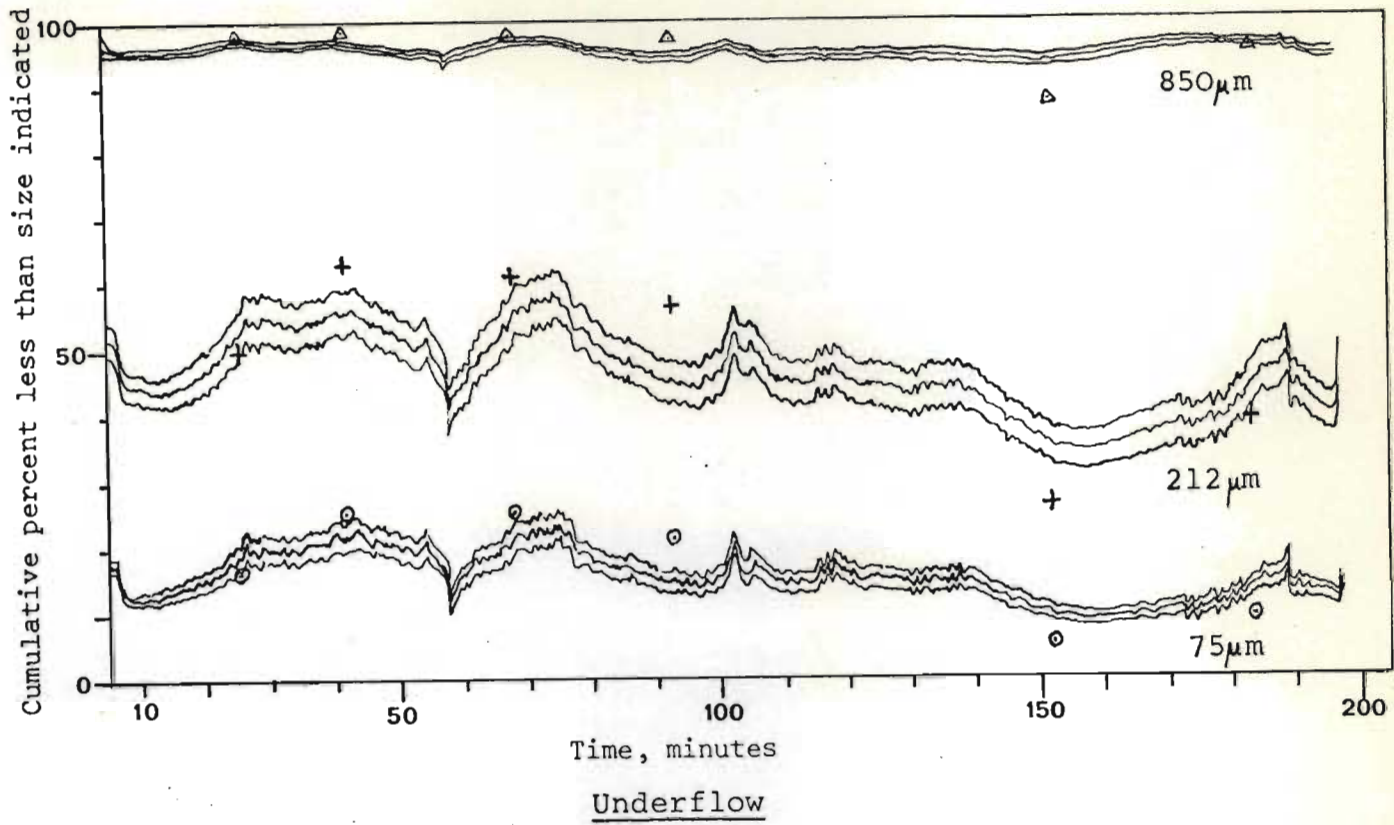


Figure 6.24 Run B - Filter predictions of particle size distributions in the cyclone underflow and mill contents as shown.

Each set of lines is mean and mean \pm standard deviation.

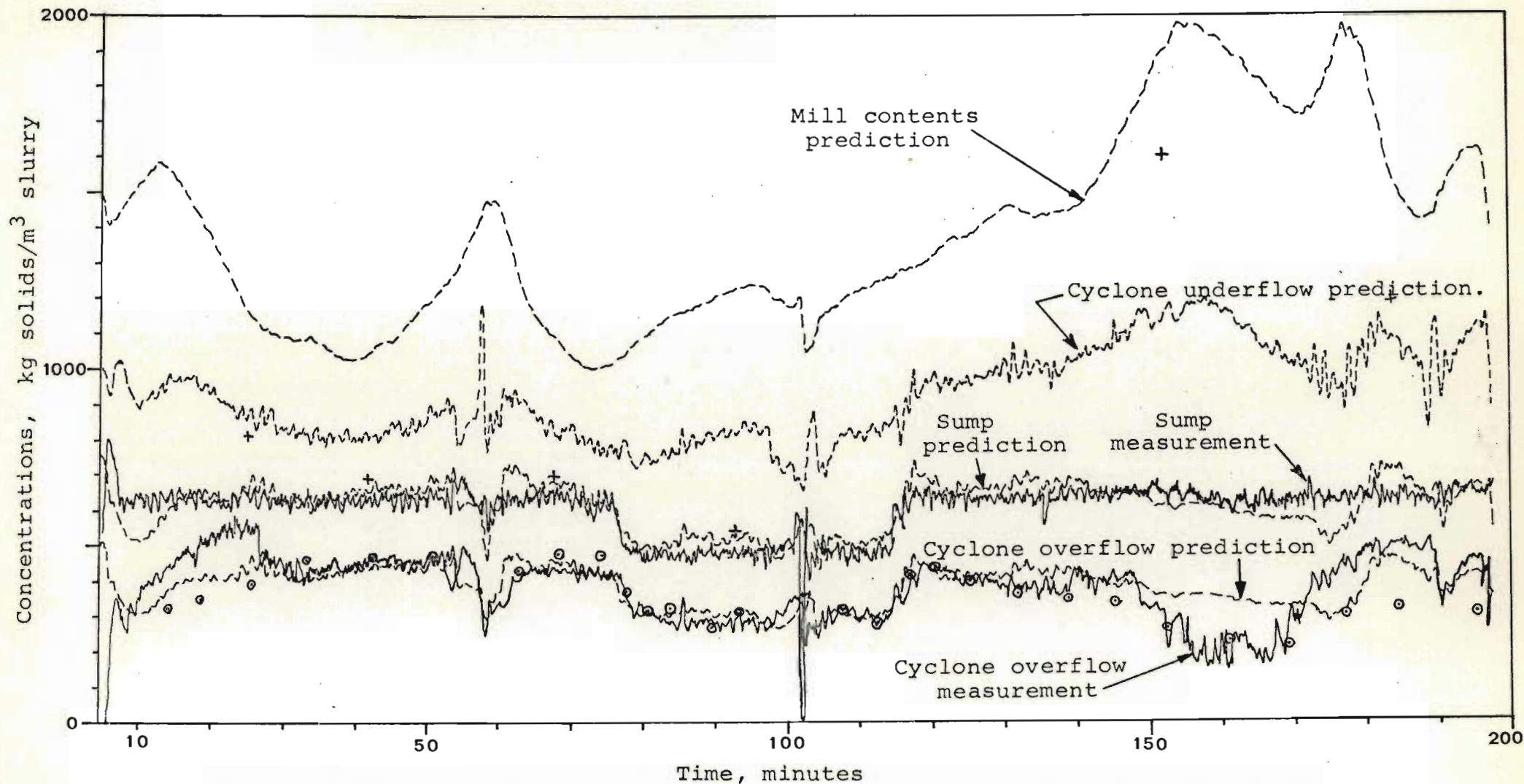


Figure 6.25 Run B - Filter predictions and measurements of concentrations.

Predictions shown dotted and instrument measurements shown continuous. Underflow samples marked + and overflow samples marked o

minutes when the fuse blew, at 100 to 105 minutes when the cyclone line choked, and from 150 to 180 minutes when the sump pump was operating near maximum. The effectiveness of these checks is discussed ahead.

The large number of samples taken of the cyclone overflow size distribution all agreed well with the predictions shown in Figure 6.23. The range covered by the samples was wide for a particle size distribution, from 33,28% to 47,08% for the -75 μm fraction. It can be seen in this plot that the filter tends to predict ahead of the samples by up to 7 or 8 minutes. This is also discussed ahead.

If one assumes that the errors in the particle size distribution predictions are approximately normally distributed, then 68% should lie within the band: mean-standard deviation to mean+standard deviation. Of the -75 μm and -212 μm sample points, 25 out of 56 (45%) lay within the band. (The +850 μm fraction is too small to measure properly.) For a normal distribution, the 45% acceptance limit corresponds to 0,61 x standard deviation on each side of the mean. This meant that the actual standard deviations of the size predictions were approximately 1,64 ($\approx 1/0,61$) times greater than predicted. The original choice of noise levels in the filter would affect these predicted errors, but other factors such as sampling errors could also have an effect.

Underflow samples were of the same order of magnitude as the predicted values shown in Figure 6.24, but were not as accurate as the overflow samples. The underflow predictions were rougher, and the +850 μm fraction was the least accurate.

Concentration predictions agreed well with the overflow samples, when compared with those in runs C and D, but the underflow samples varied considerably more than did the predictions. These large differences between sampled and predicted concentrations could be partly attributed to the volumetric model of the cyclone underflow. From Table 6.11, $Q_{U0} = 0,4073 \times 10^{-3} \text{ m}^3/\text{s}$ and

$\sqrt{\sigma_{\epsilon}^2} = 0,619 \times 10^{-4} \text{ m}^3/\text{s}$, which gives a coefficient of variation for $Q_U = 0,15$.

If the mass flow of solids in the cyclone underflow were to remain fixed, the underflow concentration would then have a coefficient of variation of 0,15.

The poor classification model would also explain some of the errors, especially in the cyclone underflow distribution and concentration (see Section 6.8.2).

6.7.3. Run C filter results

The standard set of parameter values was used to obtain the results shown in Figures 6.26 to 6.29 for run C. The filter was run in real time, although the results shown here were recomputed afterwards, as there was insufficient time during the run to log enough data.

Although the solids feed measurement was faulty up to 50 minutes, and the system cycled from 95 to 100 minutes when a different control was tried, there were no major upsets during the run. As a result of this, the volumetric filter predictions did not deviate much from the measurements, as can be seen in figure 6.26.

The cyclone overflow size predictions in Figure 6.27 show general agreement except for a section from samples C5 to C10. There were two possible explanations for this. The first is that, when the solids feed actuator was repaired at 50 to 55 minutes, and when the different control was tried at 95 to 100 minutes, the system was upset in some way that produced a finer grind. Samples C5 to C8 seem to show that the system was recovering towards the predicted values. The second explanation is that the rock may have hardened during the run perhaps as a result of the increased magnetite in the circulating load, but at the beginning the faulty potentiometer may have given low measurements resulting in predictions that were too fine. The overall result would then be that the predictions appeared to agree up to the time that the actuator was repaired, thereafter the difference was

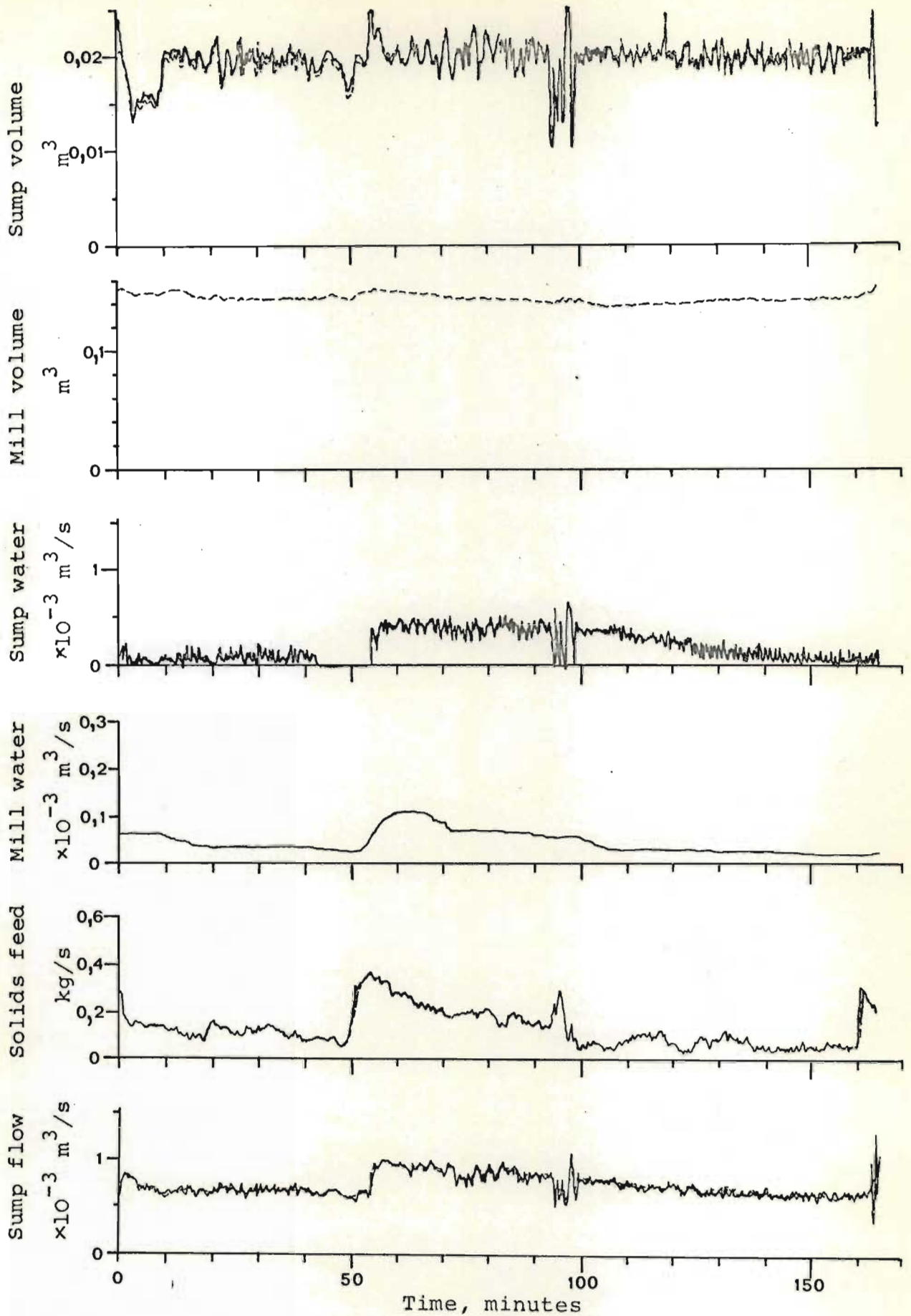


Figure 6.26 Run C - Volumetric results

Predictions shown dotted (---) and instrument measurements shown continuous (—).

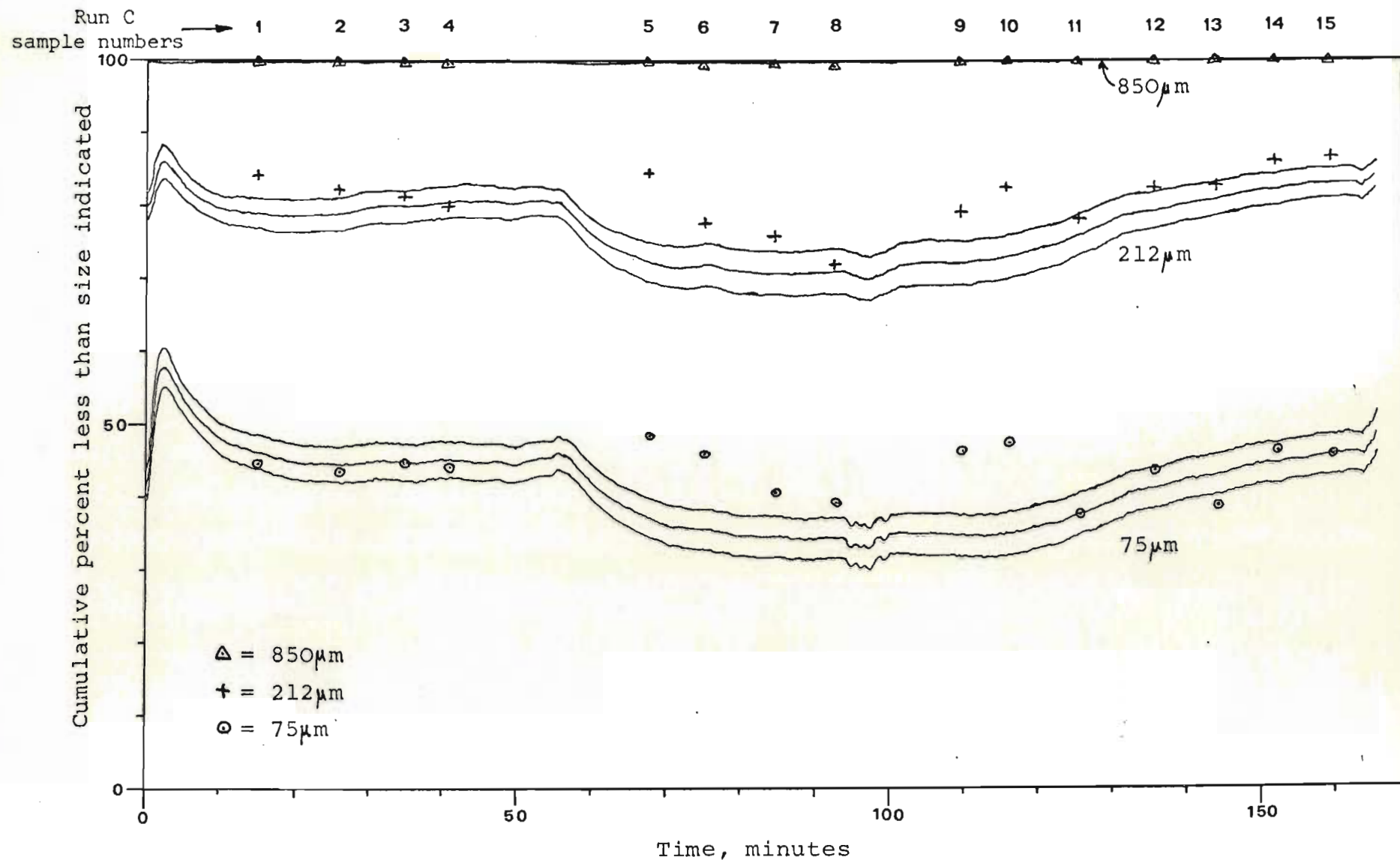


Figure 6.27 Run C - Filter predictions of cyclone overflow cumulative particle size distribution, with actual sample points plotted for comparison.

Each set of three lines are mean and mean +/- standard deviation.

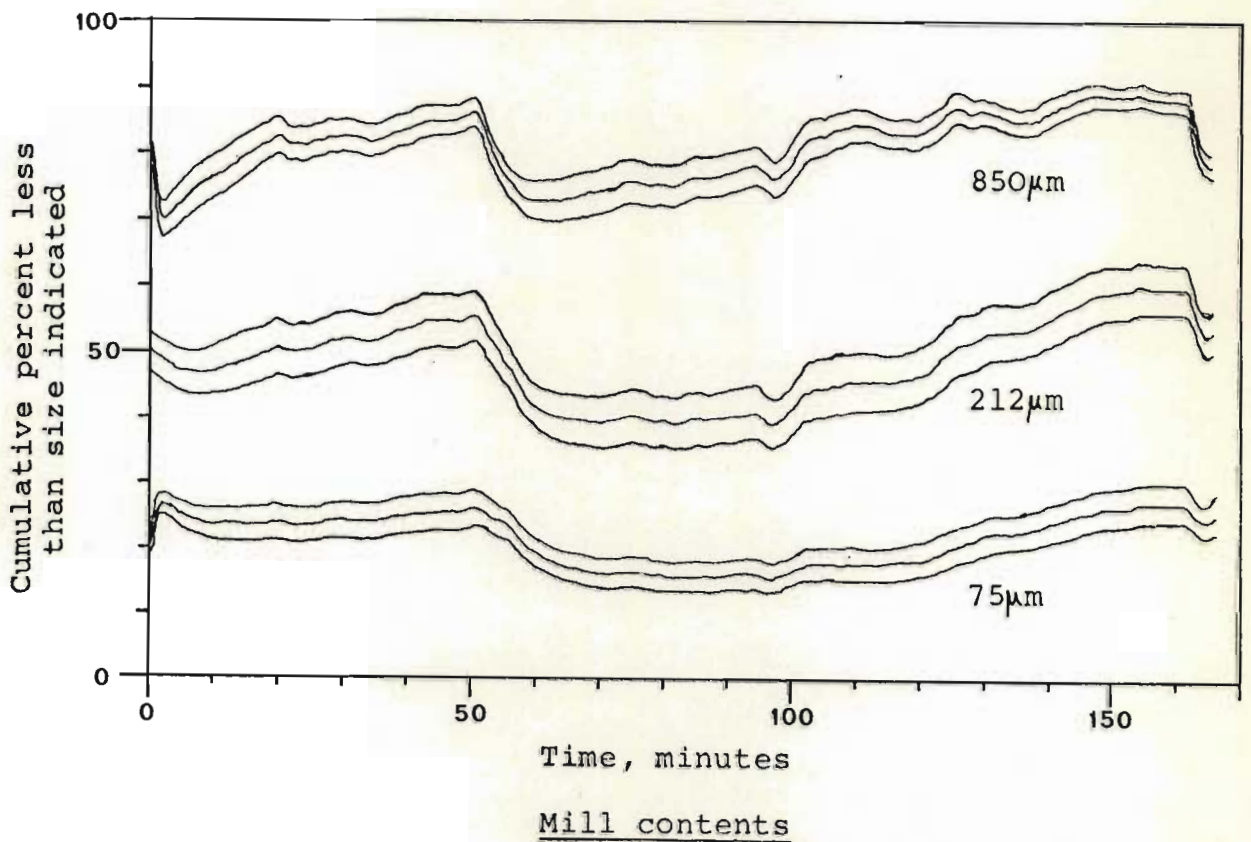
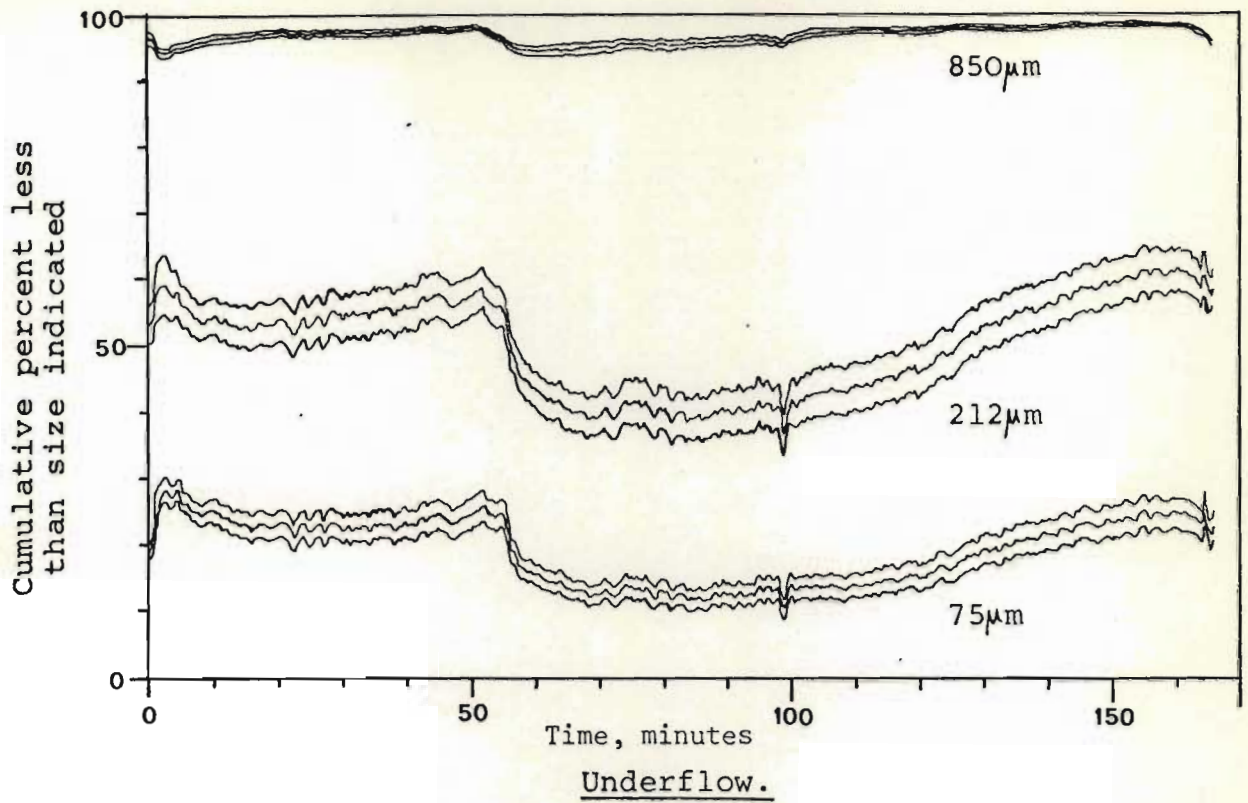


Figure 6.28 Run C - Filter predictions of particle size

distributions in the cyclone underflow and mill contents as shown.

Each set of three lines is mean and mean \pm standard deviation.

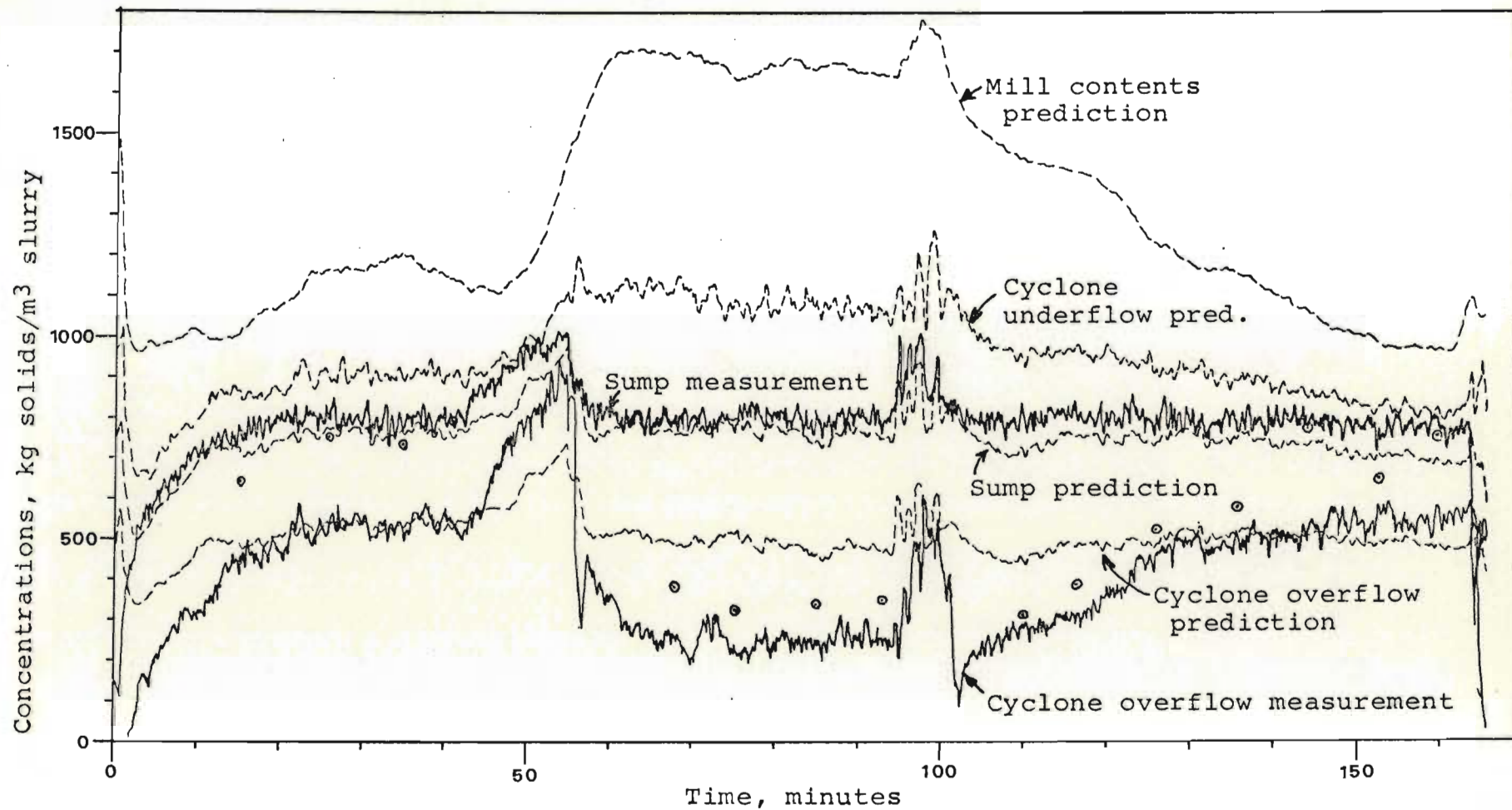


Figure 6.29 Run C - Filter predictions and measurements of concentrations.

Predictions shown dotted and instrument measurements shown continuous. Overflow samples = ○

noticeable, but gradually decreased. In either case, the same trends are seen in both the predicted and the actual values, but again the predictions are ahead. Figure 6.28 of the underflow and mill contents size distributions reveal little information without samples.

In Figure 6.29, the predictions of the cyclone feed concentration agree well with the measurements, but the overflow concentration predictions show poor agreement with both samples and measurements. Again, this is caused mainly by the poor cyclone model, as explained for run B, since the measurements and samples are in greater agreement. The overall higher values of the samples were probably caused by poor operation of the ratemeter measuring the concentration. The higher concentration in the mill during the middle of the run may also have contributed to giving a coarser grind. It is suspected that the actual mill concentration may have been higher around 45 to 55 minutes (caused by the faulty solids actuator) as the cyclone feed concentration measurement was noticeably higher than the predicted values.

6.7.4. Run D filter results

Run D results are shown in Figures 6.30 to 6.33. The standard values of the parameters were used. Again the filter was run in real time, although the results shown here were recomputed afterwards.

The results of this run did not fluctuate much, except from 55 to 80 minutes when it was attempted to control from the filter as explained earlier.

Consequently this was the only major upset and the results were otherwise fairly steady. The volumetric predictions shown in Figure 6.30 agree with the measurements, except during the upset when the sump overflowed from 70 to 80 minutes, and after the manual increases in the solids feed at 83 and 138 minutes.

The cyclone overflow size prediction in Figure 6.31 was also fairly steady and only two of the sample points were away from the predictions. The first

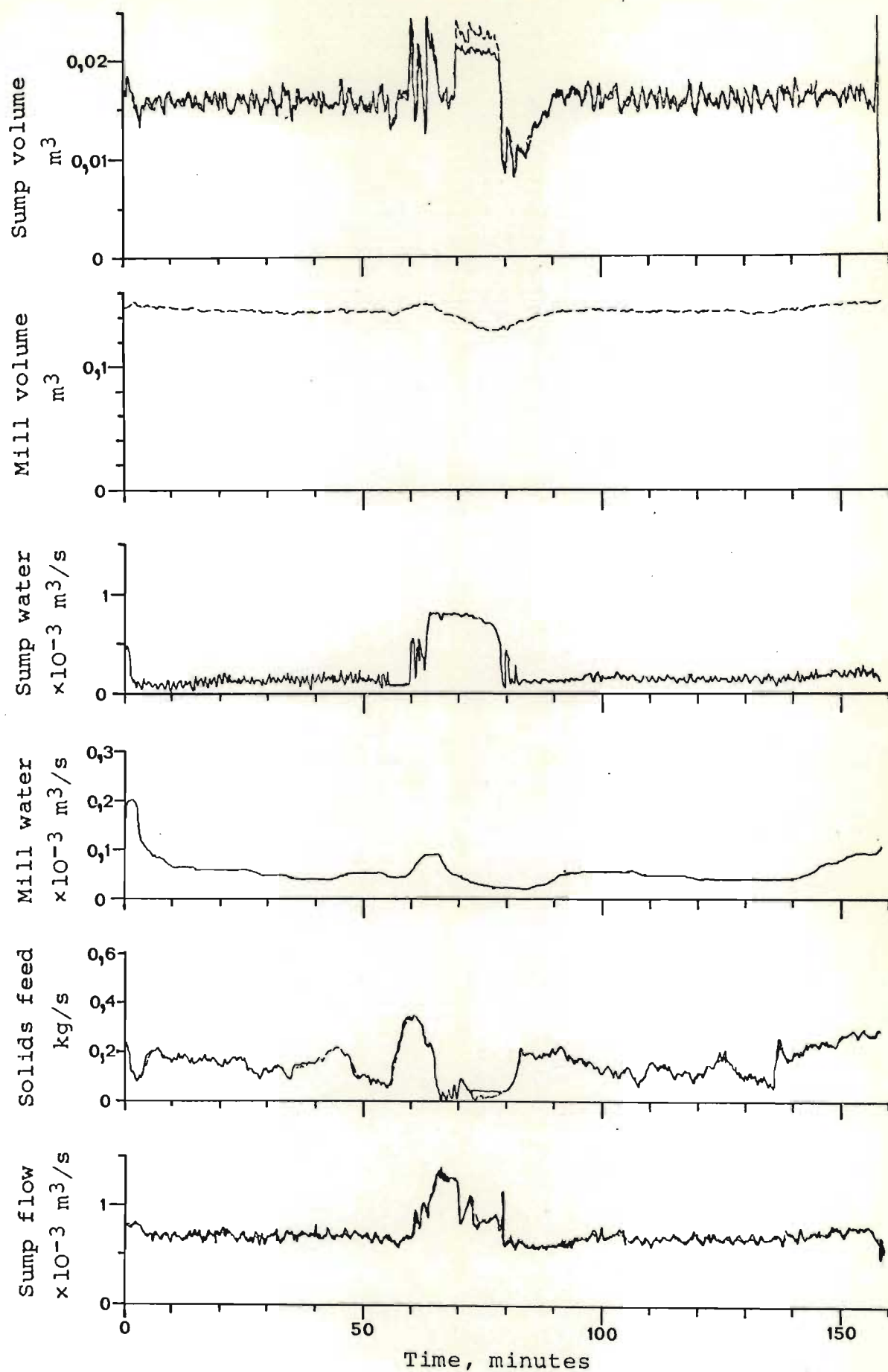


Figure 6.30 Run D - Volumetric results.

Predictions shown dotted (----) and instrument measurements shown continuous (——).

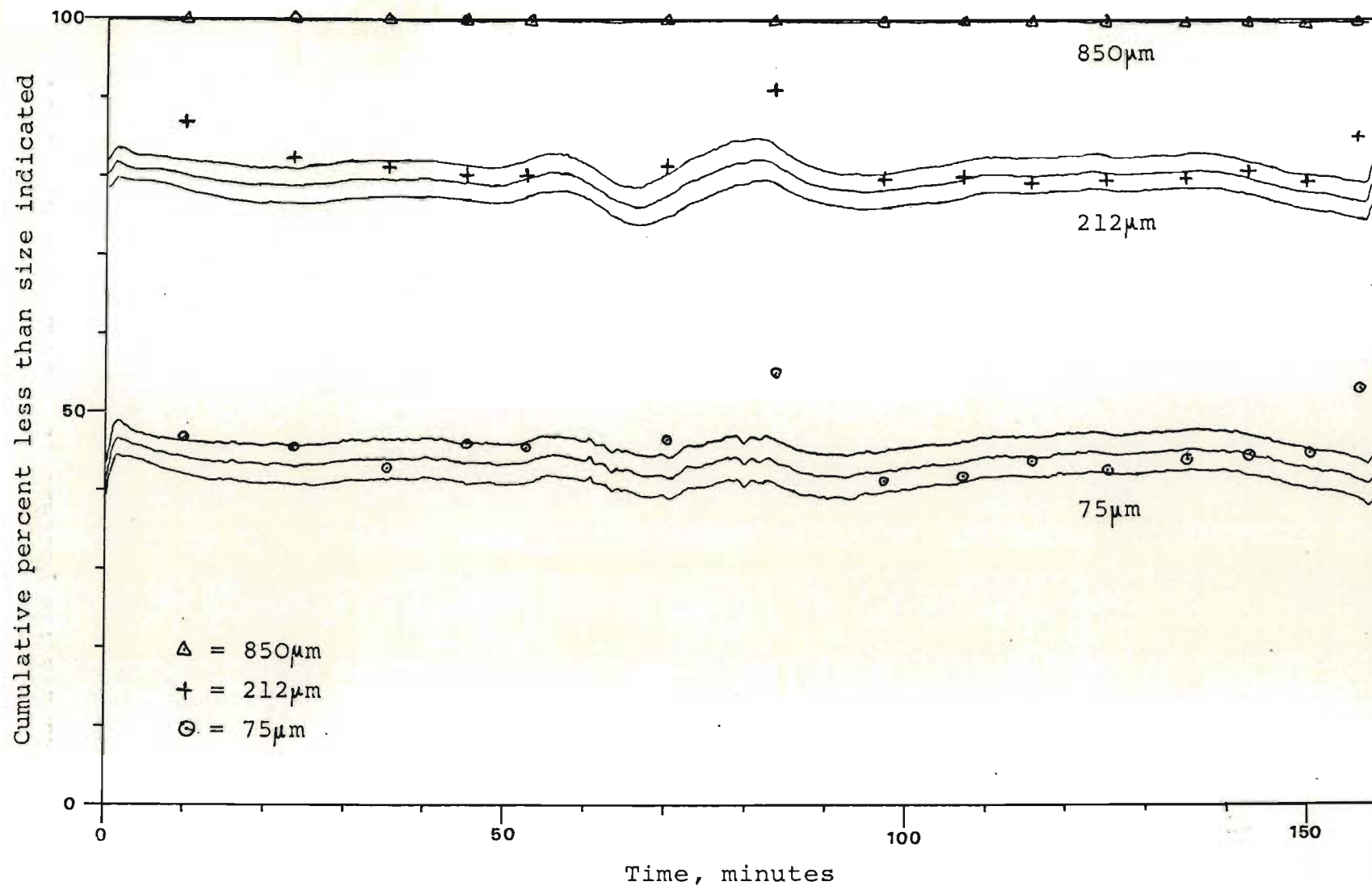


Figure 6.31 Run D - Filter predictions of cyclone overflow cumulative particle size distribution, with actual sample points plotted for comparison.

Each set of three lines are mean and mean +/- standard deviation.

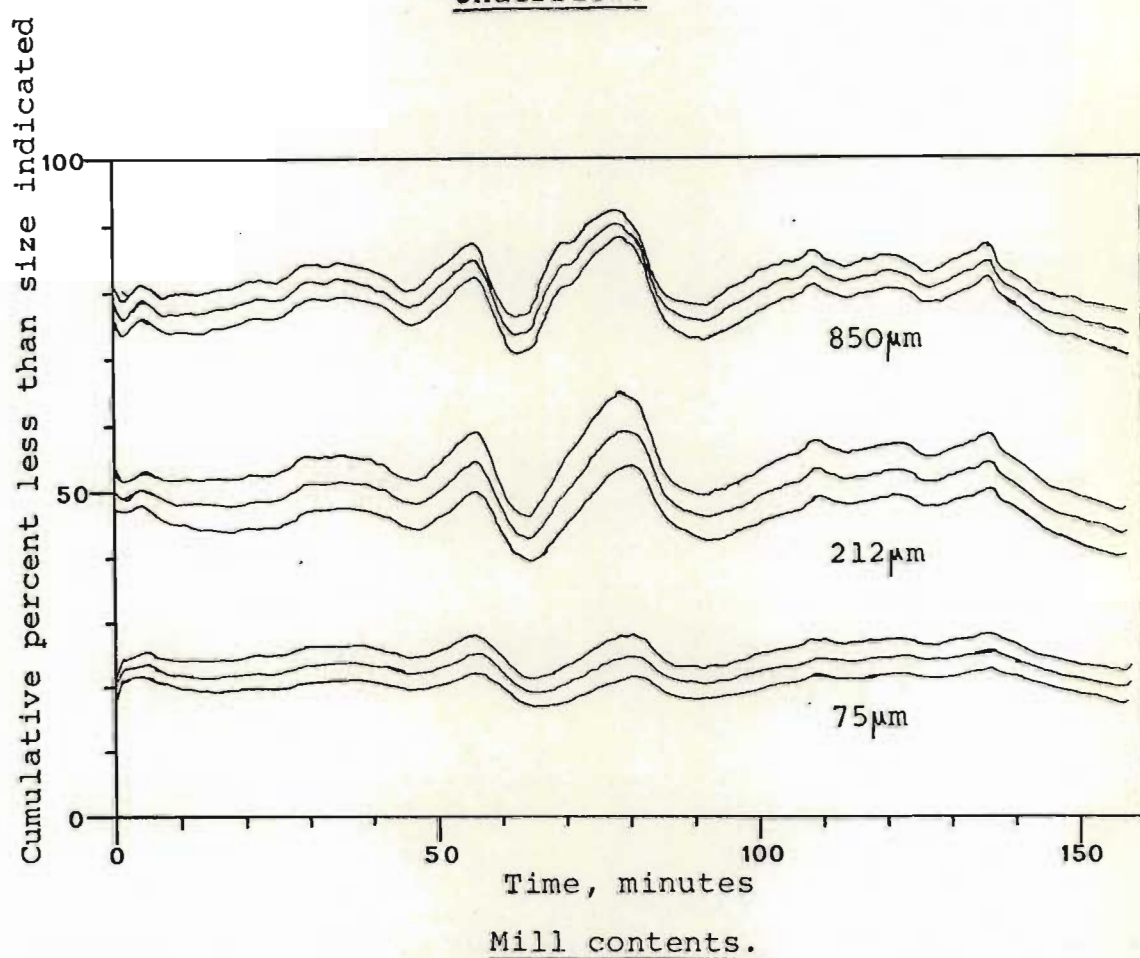
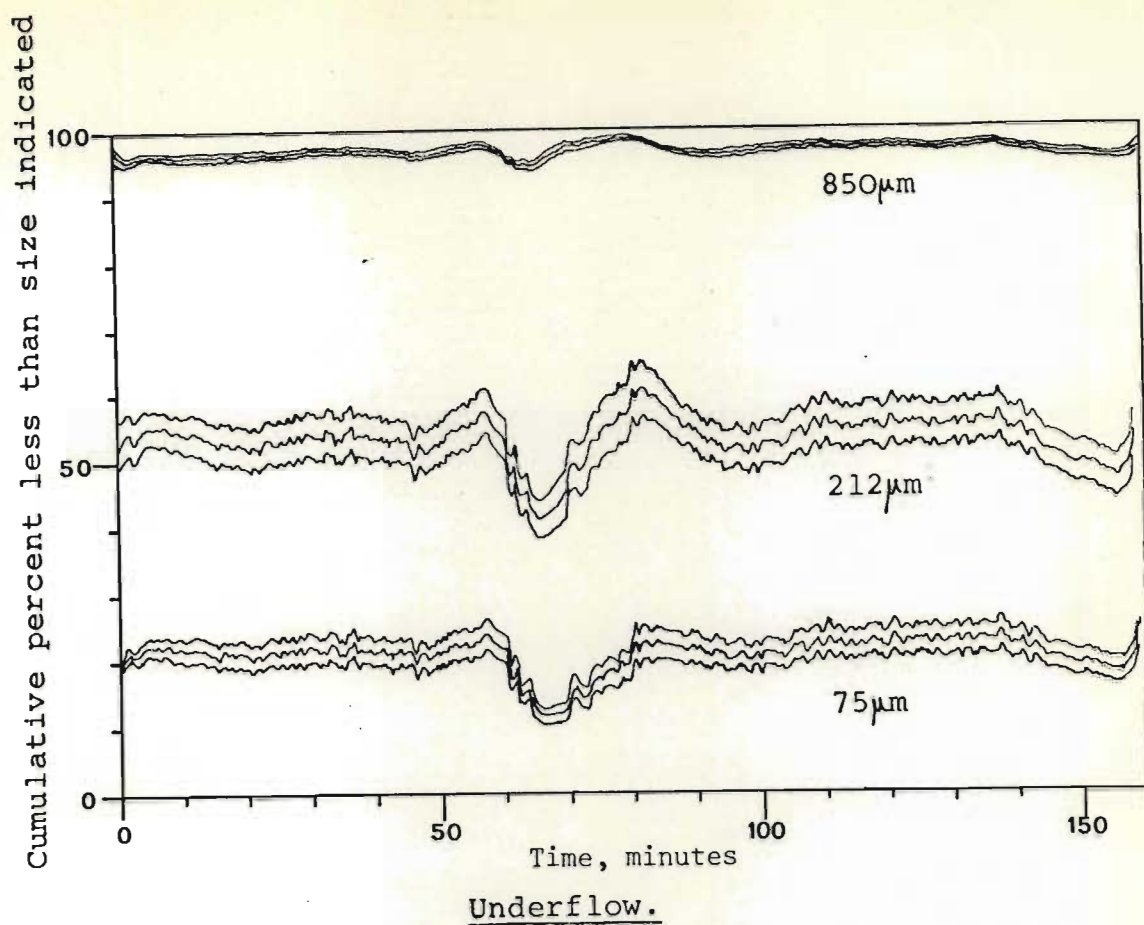


Figure 6.32 Run D - Filter predictions of particle size distributions in the cyclone underflow and mill contents as shown.

Each set of three lines is mean and mean \pm standard deviation.

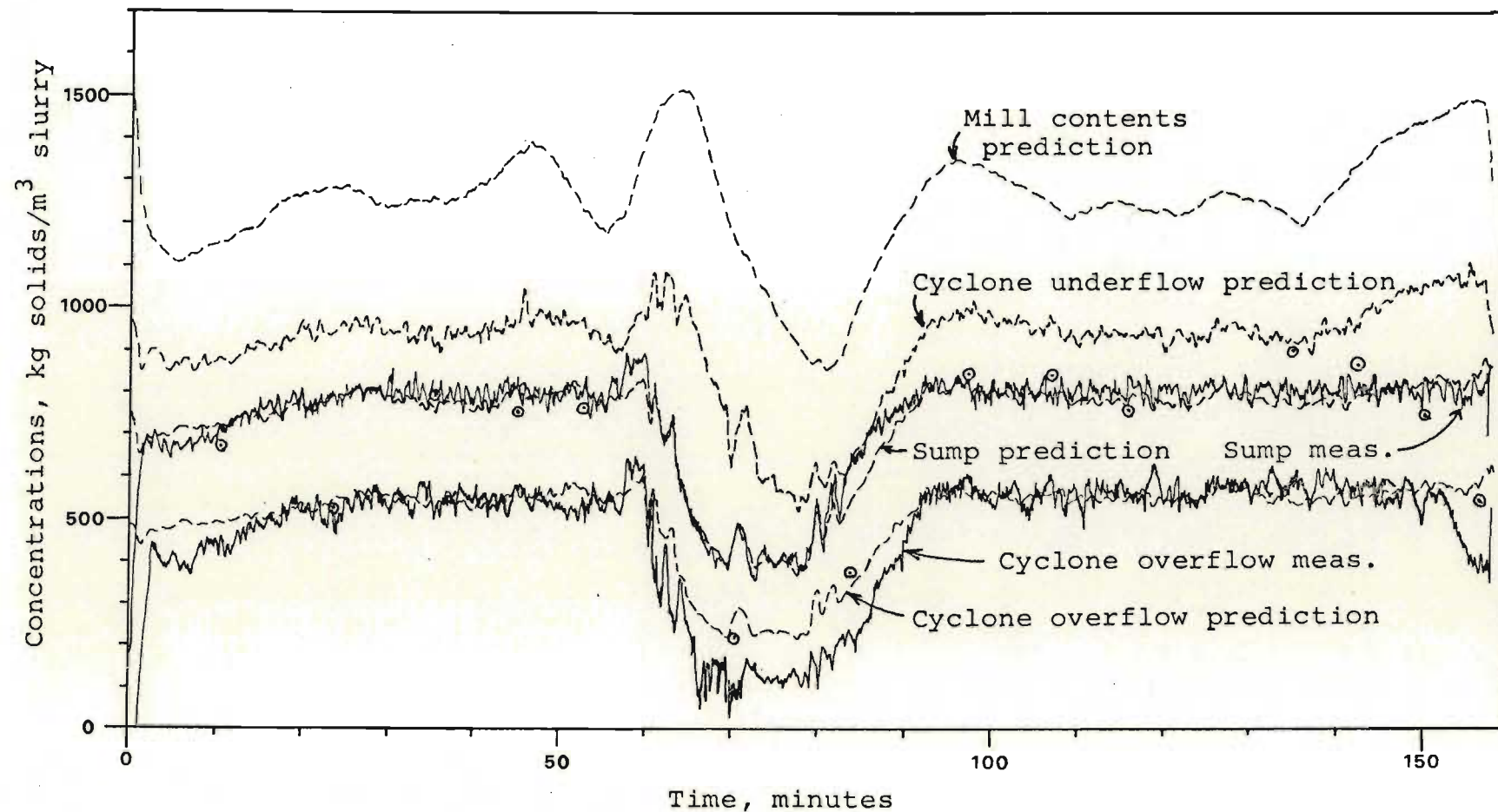


Figure 6.33 Run D - Filter predictions and measurements of concentrations.

Predictions shown dotted and instrument measurements shown continuous. Overflow samples = ⊙

of these, at 84 minutes, was soon after the upset and was probably caused by it. The second, at 157 minutes, was associated with a decrease in concentration, and may have been a poor sample, but was probably a result of an unmeasured decrease in rock softness, perhaps caused by a mill concentration change. Other than these, there were insufficient changes to show any trends, but the predictions were in the right range. Again the size distributions in the underflow and mill contents (Figure 6.32) could not be checked without samples for comparison.

The concentration predictions are shown in Figure 6.33. Here the predictions follow the measurements better than in run C, but the concentrations of cyclone overflow samples are again high. A noticeable drop in this concentration towards the end can be observed in the samples and measurements but not in the predictions. The reason for this is unknown.

6.8. Effects of various factors on the filter

The testing of the various factors discussed below was done firstly to determine what parts of the filter were more important in obtaining good results, and secondly to find the effects of each factor so that bad filter performance could be analysed and remedied. Although this particular part of the work was specific to a milling circuit filter, it would be a necessary part of any filter development.

Run B was used for all the tests done, and the standard filter with the parameter set given in Table 6.17 was used except where it was changed as needed. Most of the results in the following sections may be compared to the "standard" results for run B shown already in Figures 6.22 to 6.25.

6.8.1. Efficacy of checks in the volumetric filter

The only test done on the volumetric filter was to determine how effective the checks against upsets were. Early results had shown that the filter became unstable at the first upset because of integration difficulties caused

by a very low/...

by a very low sump volume. This led to improved integration, limits on the minimum sump volume, and checks to reduce the possibility of faulty data causing an upset. These checks were explained in the theory, Section 4.3.2.

The difference in the volumetric filter results with and without the checks is shown in Figures 6.22 and 6.34 respectively for run B. It is particularly noticeable during the upsets at 55, 100 and 150 to 180 minutes. Around 150 to 180 minutes, the sump pump was at the maximum of its range and the controller tried to push it higher. The filter was unable to see this directly, but the checks helped to reduce the effects.

The effects on the p.s.d. filter are shown in Figure 6.35. Here the p.s.d. filter was run without the observation step, so that errors in the model would show up more clearly on the predicted concentrations.

Figure 6.35 is interesting in that it shows both how the cyclone feed concentration behaves with no observations to correct it, and the effects of the volumetric filter checks on this prediction. The checks are again most noticeable at the upsets, and can be seen to make the predictions follow the measurements more closely. We can thus conclude that these checks would help during plant upsets in reducing the unwanted error incurred by the upset.

6.8.2. Effect of cyclone model parameter errors

In the classification model, \underline{cc}_0 and \underline{cc}_1 were the parameter vectors (see Section 4.2.2). The \underline{cc}_1 described the dependence of the classifier functions on the cyclone feed concentration, while \underline{cc}_0 was the value of the classifier functions at zero feed concentration. The effects of both these parameters were tested.

Figure 6.36 shows the effects on overflow size predictions of no feed concentration dependence, i.e. $\underline{cc}_1 = 0$ and \underline{cc}_0 was changed so that the model remained the same at the mean concentration of 665 kg/m³. These were the

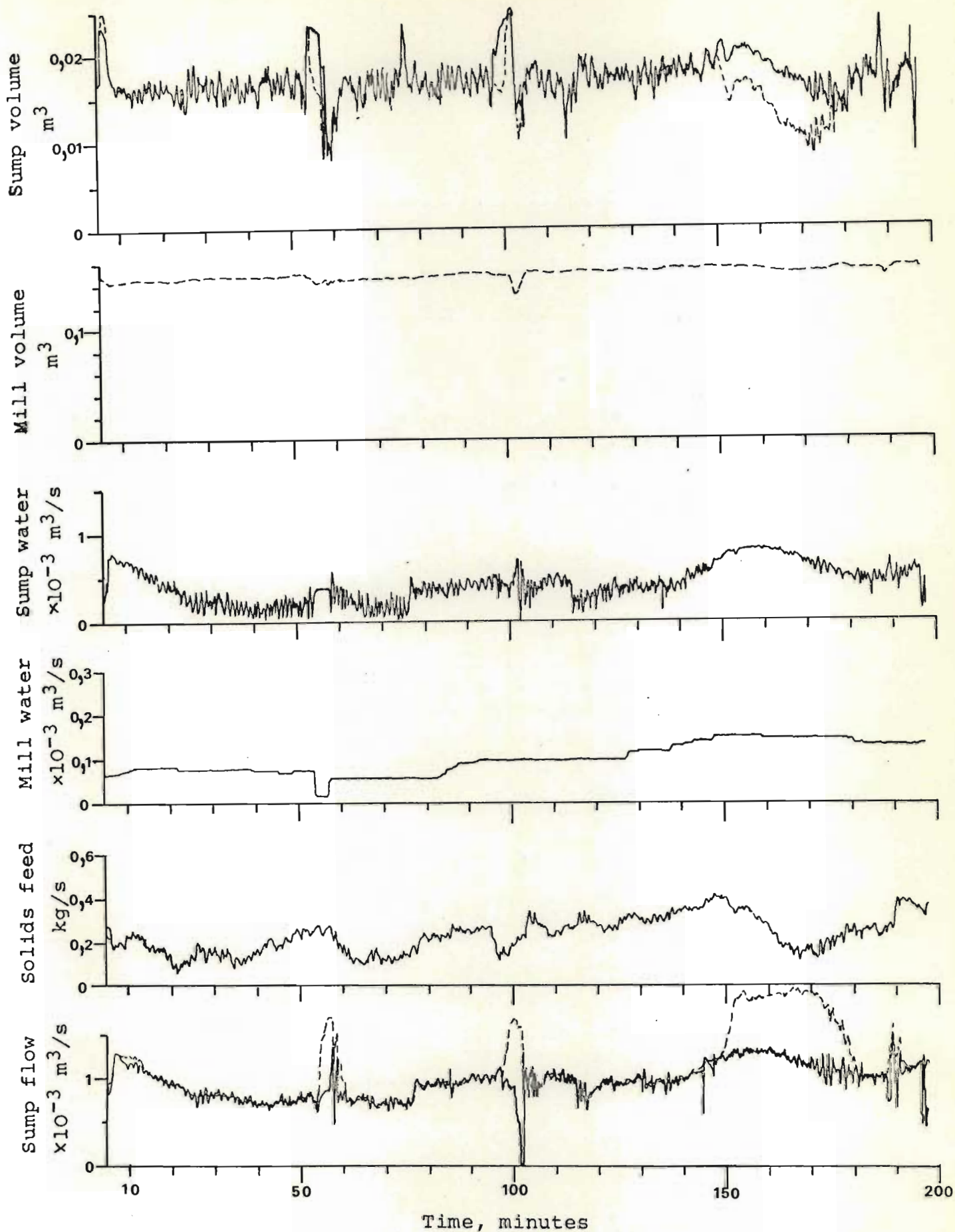


Figure 6.34 Volumetric filter without checks.

Run B data. Predictions shown dotted (---) and instrument measurements shown (—). Compare this with figure 6.22 which used checks

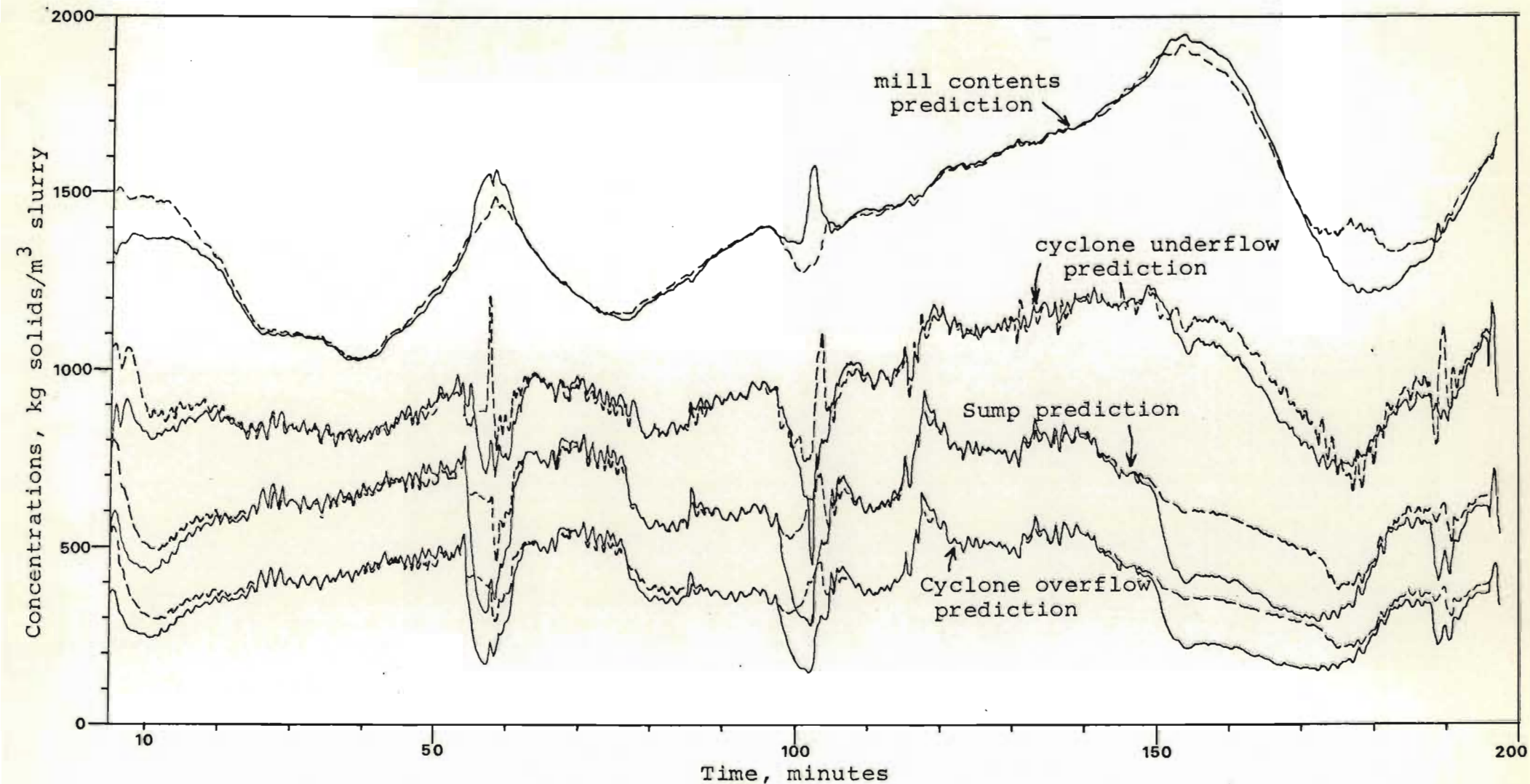


Figure 6.35 Effect of volumetric filter checks on p.s.d. filter predictions of concentrations.

Continuous lines are without checks, dashed lines are with checks. (Also different starting points.)

P.s.d. filter was run without observation step, as explained in text (section 6.8.1). See figure 6.25.

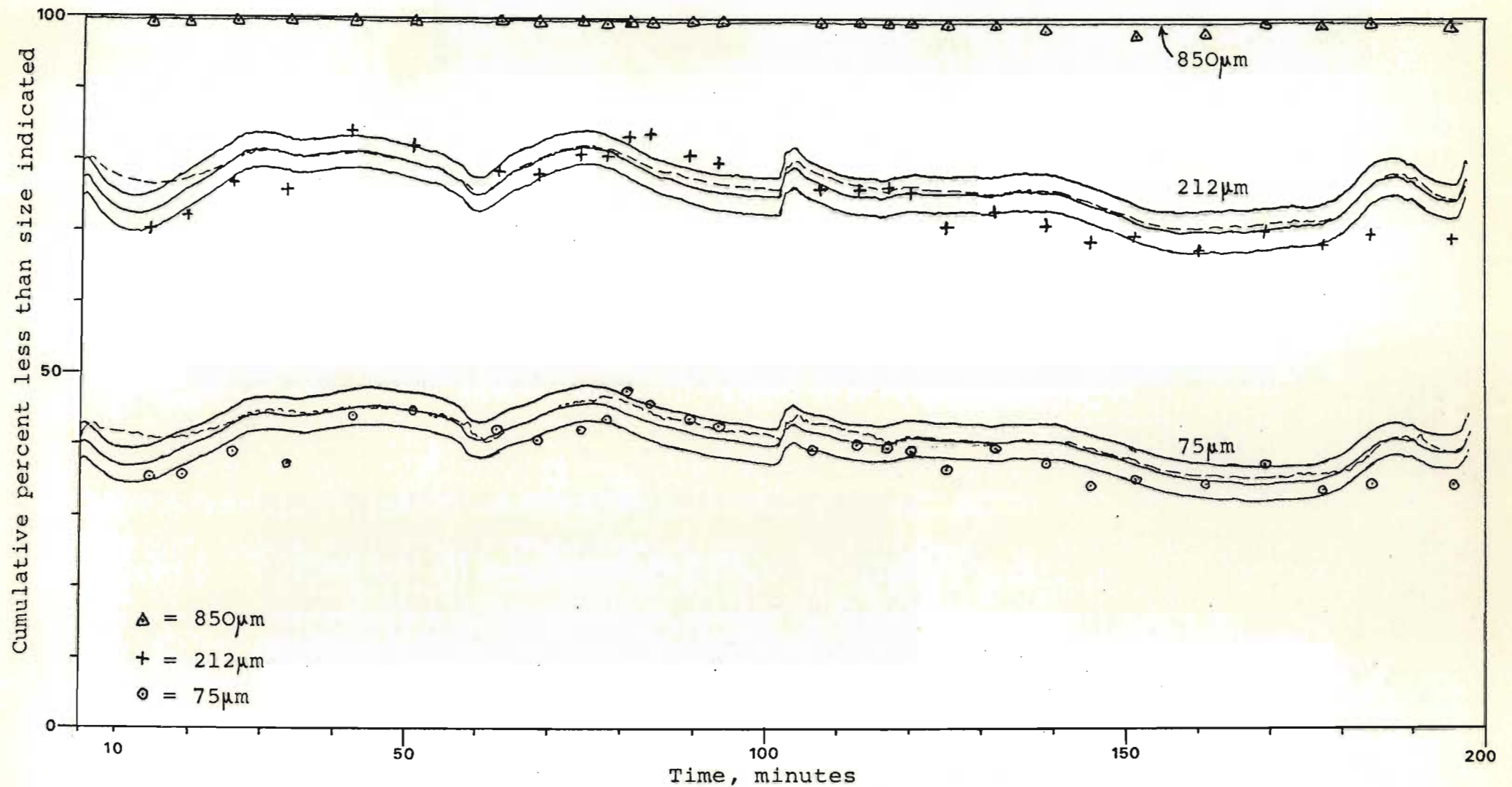


Figure 6.36 Effect of cyclone model changes.

Parameters $\underline{cc}_1 = \underline{0}$ and \underline{cc}_0 = values in column 2 of table 6.9. Prediction of particle size distribution of cyclone overflow for run B shown. Standard mean values (from fig 6.23) shown dotted.

values given in the second column in Table 6.9. There was little difference, although the lines were smoother. One should notice that the cyclone feed concentration only changed noticeably from 70 to 110 minutes and during some upsets, and the effects on the predictions were slight, though not negligible. The effects on other variables such as concentrations were small, and are not plotted here.

Figure 6.37 shows the effects on overflow size predictions of using offset values for the classification functions. The values given in Table 6.10 were used, and were greater than the standard values (i.e. a finer cut).

From graph 6.37 it can be seen that the size predictions for the $-75\text{ }\mu\text{m}$ and $-212\text{ }\mu\text{m}$ fractions were on average about 6% finer than the predictions under standard conditions. Using this result it was possible to estimate approximately the effect that errors in the cyclone model would have on the filter predictions of size, as follows.

The variance of the residuals between the actual classifier functions and the regressed cyclone model for the data used to prepare Table 6.9 are shown below in the second column. The differences between the classifier functions given by Table 6.9 (standard values) and by Table 6.10 (values used for Figure 6.37) at an average feed concentration of 600 kg/m^3 (a rounded average for run B) are shown in the fourth column, and their ratios to the standard deviations are given in the fifth column.

Size fraction	Variance of residuals	Standard deviation = $\sqrt{\text{variance}}$ "x"	Difference in classif. functions "y"	Ratio ($\frac{y}{x}$)
$-75\text{ }\mu\text{m}$	0,0045	0,067	0,0461	0,69
75 to $212\text{ }\mu\text{m}$	0,0130	0,114	0,1310	1,15
212 to $850\text{ }\mu\text{m}$	0,0081	0,090	0,1034	1,15
$+850\text{ }\mu\text{m}$	0,0012	0,034	0,0290	0,85

From this table/...

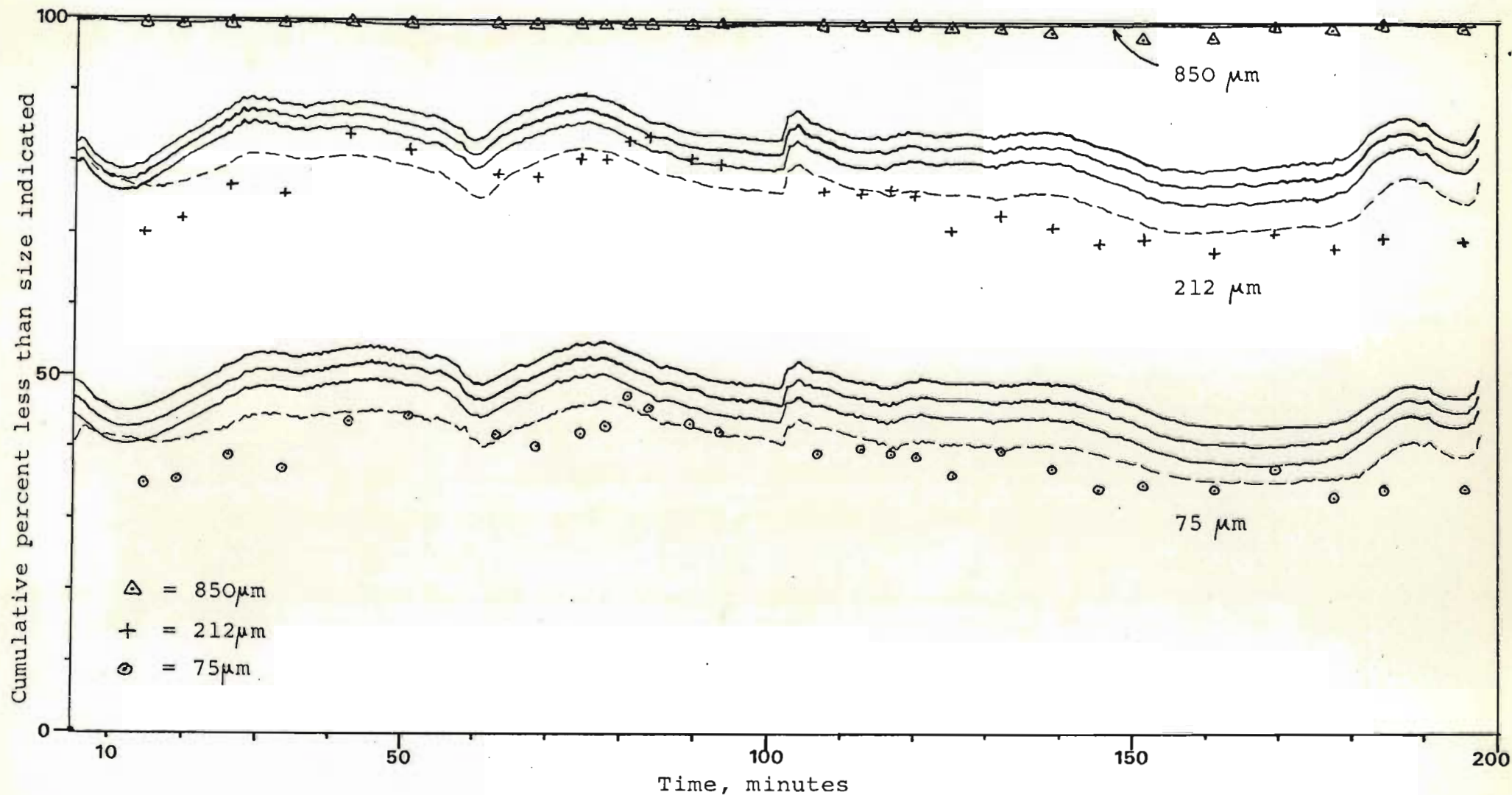


Figure 6.37 Effect of cyclone model changes.

Parameters used given in table 6.10. Prediction of particle size distribution of cyclone overflow for run B shown. Standard mean values (from figure 6.23) shown dotted.

From this table it can be seen that the classifier functions given by Table 6.10 were approximately one standard deviation finer than the values in Table 6.9. Thus the errors in the filter predictions of size could have a standard deviation of 6% for the -75 μm and -212 μm fractions, caused by the poor cyclone model. Fortunately, it appears that the cyclone behaviour fluctuates (it is not known exactly how) and that this is damped with a filter time constant of about 10 minutes (see Section 6.8.7). Although not shown here, the concentration predictions were also poor.

From these results, we see that the classification function is important, but its dependence on feed concentration is slight. This emphasizes the need to get good data for the cyclone, and the need for a better cyclone model.

6.8.3. Effects of errors in grinding model parameters (S and b)

To determine how exact the selection and breakage functions had to be, a constant selection function and Broadbent and Callcott's breakage model, i.e

$$B(y,x) = (1 - \exp (-x/y)) / (1 - \exp (-1/\sqrt{2}))$$

were tried. The selection function was given a value of 0,1 minutes⁻¹ for all sizes. These data were then reduced to the four size groups used in the filter, (see Sections 4.2.1 and 6.1) giving the figures shown in Table 6.19. (Compare these to the standard values shown in Table 6.5 for run 20/6.)

Table 6.19 Reduced data for simplified grinding model

<u>S</u>	=	(0,050262	0,070000	0,078789	0,0) ^T
<u>b</u>	=	$\begin{bmatrix} -1,0 & 0,70812 & 0,18495 & 0,10692 \\ 0 & -1,0 & 0,58762 & 0,41238 \\ 0 & 0 & -1,0 & +1,0 \\ 0 & 0 & 0 & 0 \end{bmatrix}$			
(units of <u>S</u> in minutes ⁻¹)					

When these parameters were tried on the filter, the results were too much in error to be satisfactory. The distributions were quite different (although of the same order of magnitude) and the predicted mill concentration was too high (up to 2050 kg/m³). This showed that the model was completely inadequate. We thus see that it was necessary to get reasonable values for the grinding model parameters, and that this involved doing batch tests off line.

6.8.4. Effect of feed distribution and softness of rock

A feed distribution with equal mass percentage in each size fraction (i.e. considerably finer than normal feed - see table below) was tested in the filter on both runs A and B.

Graph 6.38 shows the overflow size predictions for run B with this finer feed. The table below summarises the results from this graph:

	Feed size distribution, cumulative % less than			Nominal average predicted product size distribution, cumulative % less than		
	75 µm	212 µm	850 µm	75 µm	212 µm	850 µm
Standard filter for Run B	6,25%	11,5%	24,3%	41%	76%	99%
Filter with finer feed for Run B	25%	50%	75%	48%	85%	99%

The filter performed reasonably, and predicted a finer product, but the difference in product distributions can be seen in the table to be relatively much less than the difference in the feed distributions. This was probably the result of the correcting action of the concentration measurements. From Tables 6.1 and 6.2 it was possible to calculate the difference in feed distributions between batch runs 30/4 and 20/6, and estimate variances for the feed distribution. The standard deviations are shown below:

Feed size distribution/...

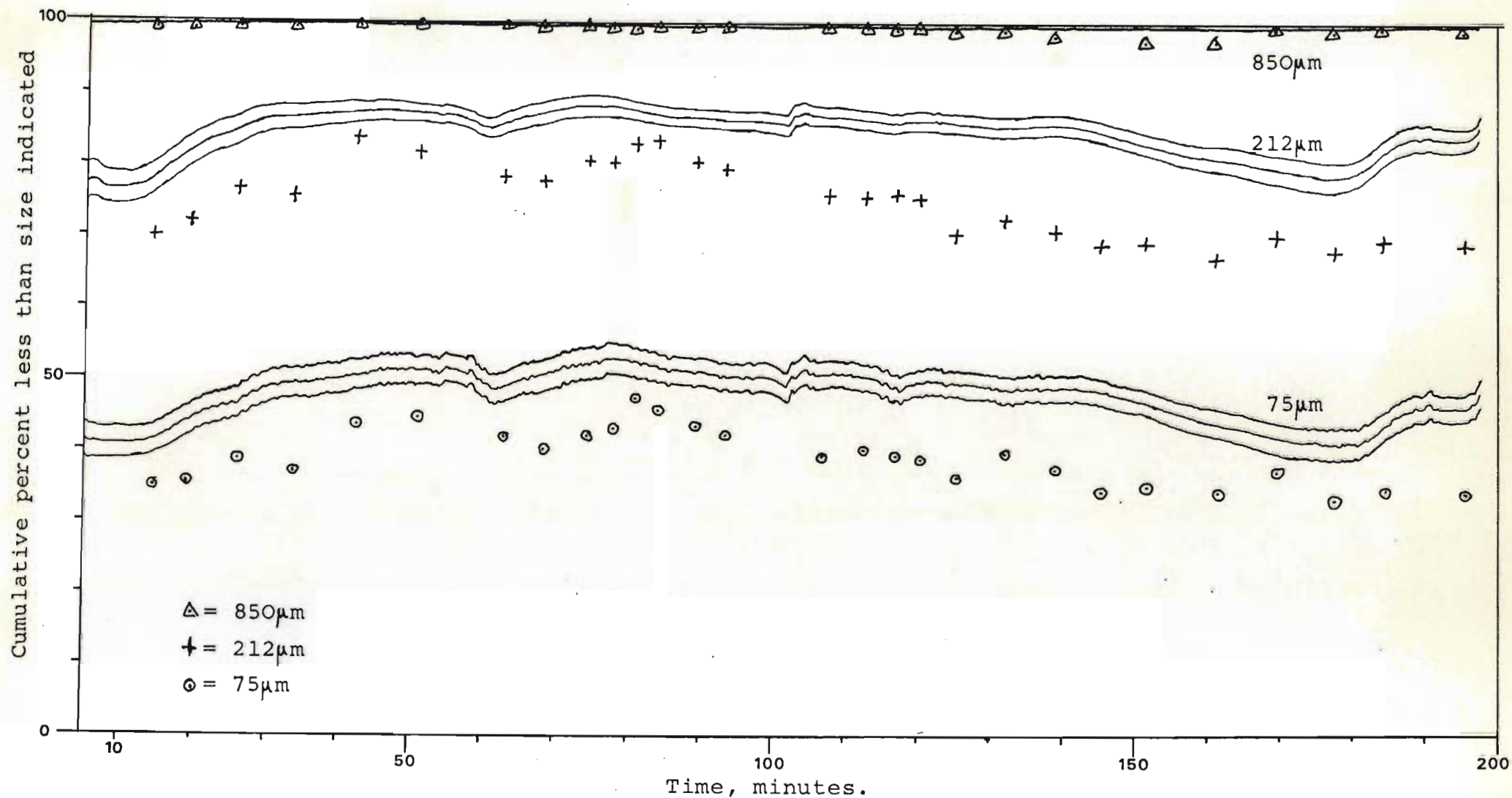


Figure 6.38 Effect of finer feed on cyclone overflow
particle size distribution predictions for run B.

	Feed size distribution, cumulative % less than:		
	75 μm	212 μm	850 μm
Mean	6,25	11,5	24,3
Standard deviation	0,98	2,5	5,2

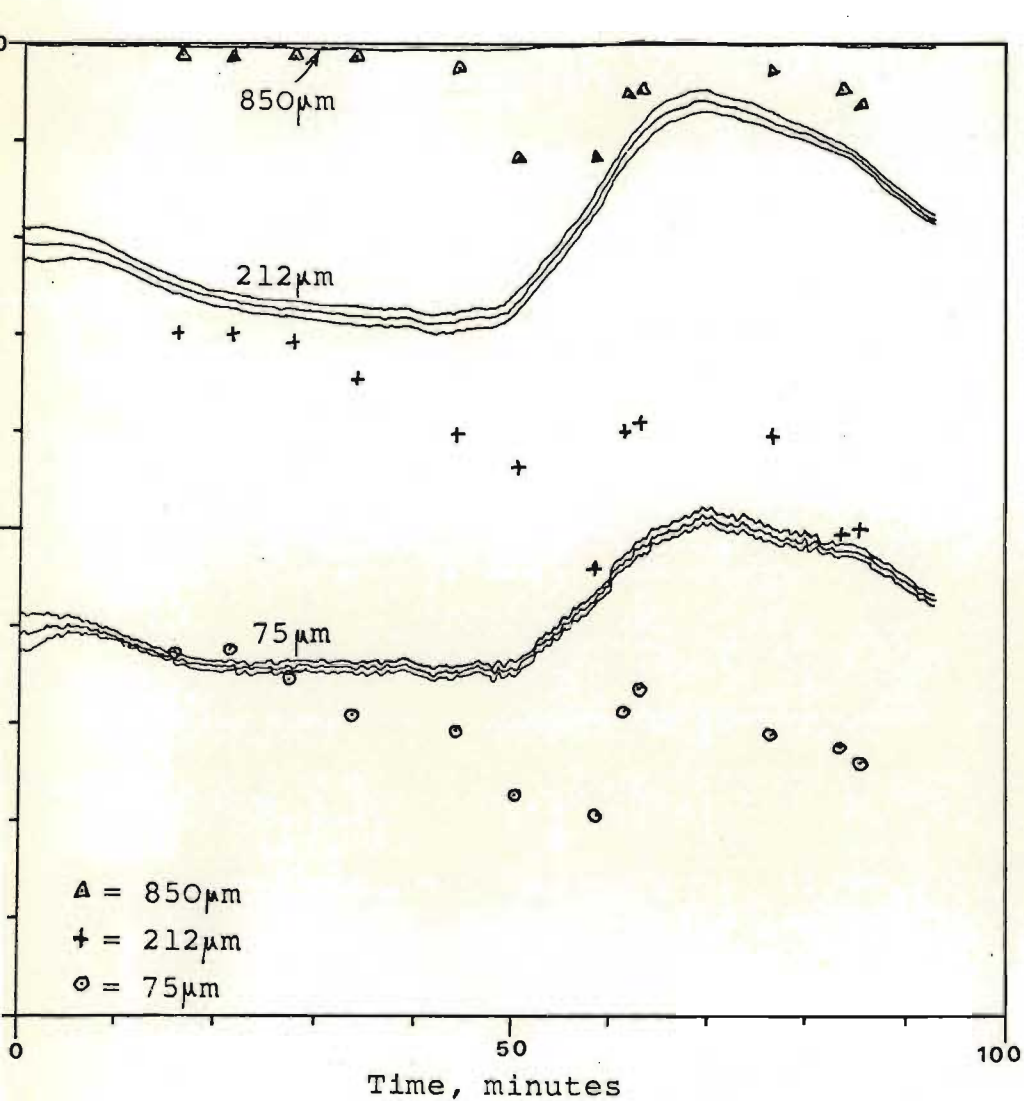
We can thus conclude that the effects of variations in feed size on the filter are not important. This is fortunate, as there are often fluctuations in feed size on an operating plant.

In run A, the finer feed was at times finer than the actual product, and so represented a severe test on the filter. The results for this run are shown in Figure 6.39 as the size predictions for the cyclone overflow and the mill contents. The results are again finer, but it can be seen that the coarsest fraction in the mill had a negative quantity for part of the run. This is a form of filter instability and is further discussed in section 6.8.9. The filter recovered after this, however, and continued normally. This shows us that gross errors in the parameters which are physically unrealisable can lead to filter instability. It is under circumstances like these that an understanding of the plant being used helps in filter development.

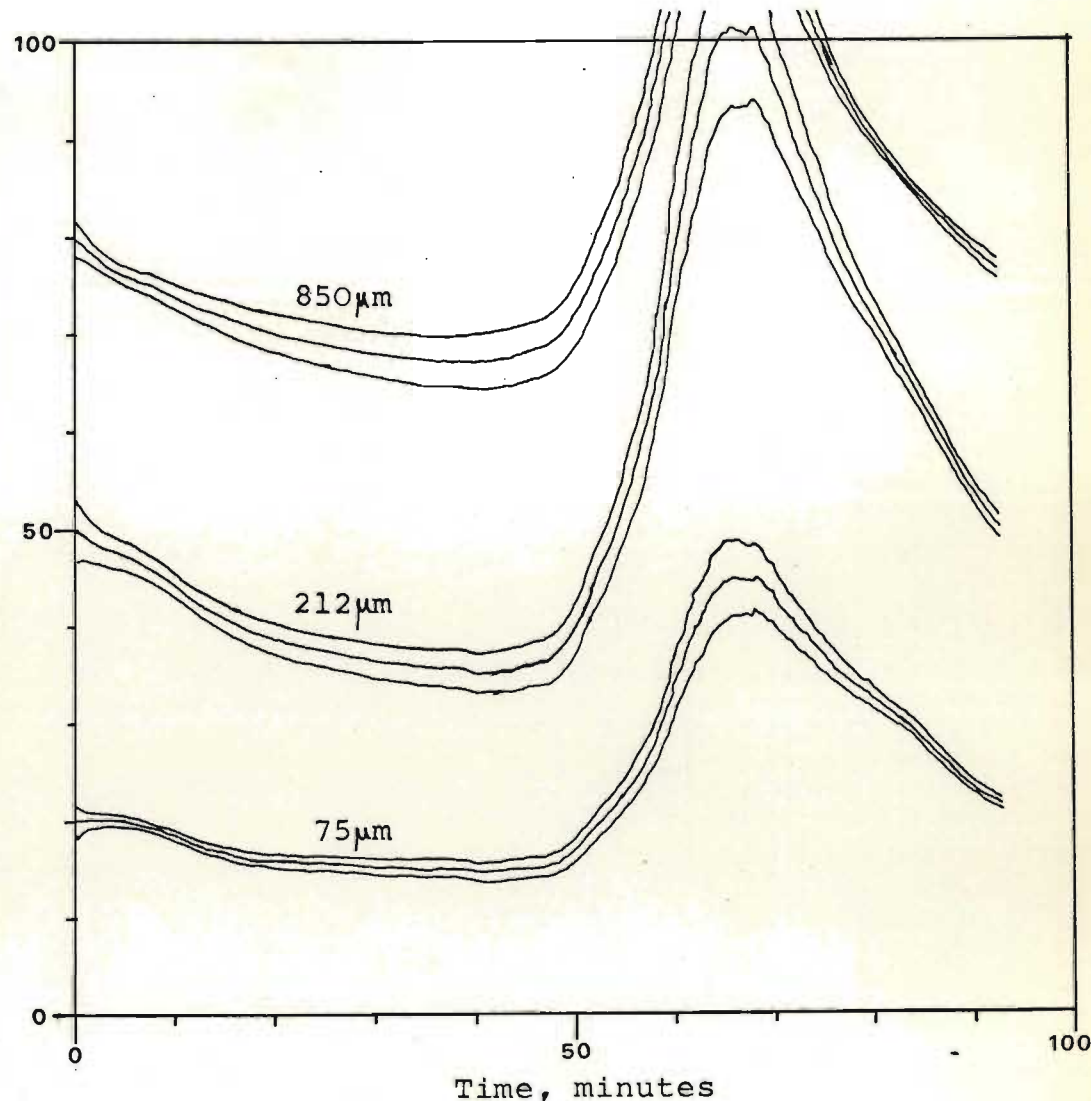
Austin proposed (private communication) that a change in feed rock softness could not be distinguished from an equivalent change in feed distribution (i.e. two feed distributions, the coarser of which can be ground to the finer using the given set of S and b functions). Although it may be difficult to observe, changes in a harder finer feed may appear in the product sooner than changes in a softer coarser feed. Thus this hypothesis is only a steady state one. The effects of different feed softnesses have been shown already in Figures 6.18 and 6.21, and are similar to the effects of a different feed size.

6.8.5. On-line regression of softness

As explained earlier, the filter could be made to estimate the softness parameter on line/...



Cyclone overflow.



Mill contents.

Figure 6.39 Effect of finer feed on run A data. Particle size distributions of cyclone overflow and mill contents. Note the overshoot in the mill contents prediction.

parameter on line, although this was not normally done. The p.s.d. filter formulation in Section 4.3.4. showed how this was done.

Figure 6.40 shows the overflow size predictions with simultaneous estimation of rock softness for run B. The estimated value of K_S is also plotted. The size predictions were all finer than the samples taken during the run. The estimated values for K_S shown on the graph also seem unreasonably high. This behaviour was probably caused by the actual concentration measurements being biased, as the gamma-ray slurry concentration gauges were found to drift slightly during runs. The cyclone model which was used may also have contributed to the poor results.

It is difficult to show precisely from the filter formulation why the on-line estimation of softness degraded the filter performance. The state estimates in a filter are affected by both the plant model (during the evolution), and the actual observations (through the observation model). Parameter estimates are only changed at the observation step (see equation 4.1.18). In a filter where only the states are estimated, the effects of unmodelled observation errors on the predictions would be reduced during the evolution step if they were contrary to the plant model. If, however, a parameter was also estimated, it would have an effect on the plant model without itself being corrected during the evolution. The parameter would continue to be changed by the observations until the plant model was forced to agree on average with the observations coming from the instruments.

These results seem to show that it is better to have a reasonably accurate model for the process with fixed parameters which are determined beforehand than to estimate parameters on line in a model where the parameters are not known initially. This would also save some computation in the filter.

In particular, on-line estimation of softness should not be included in future milling circuit filters.

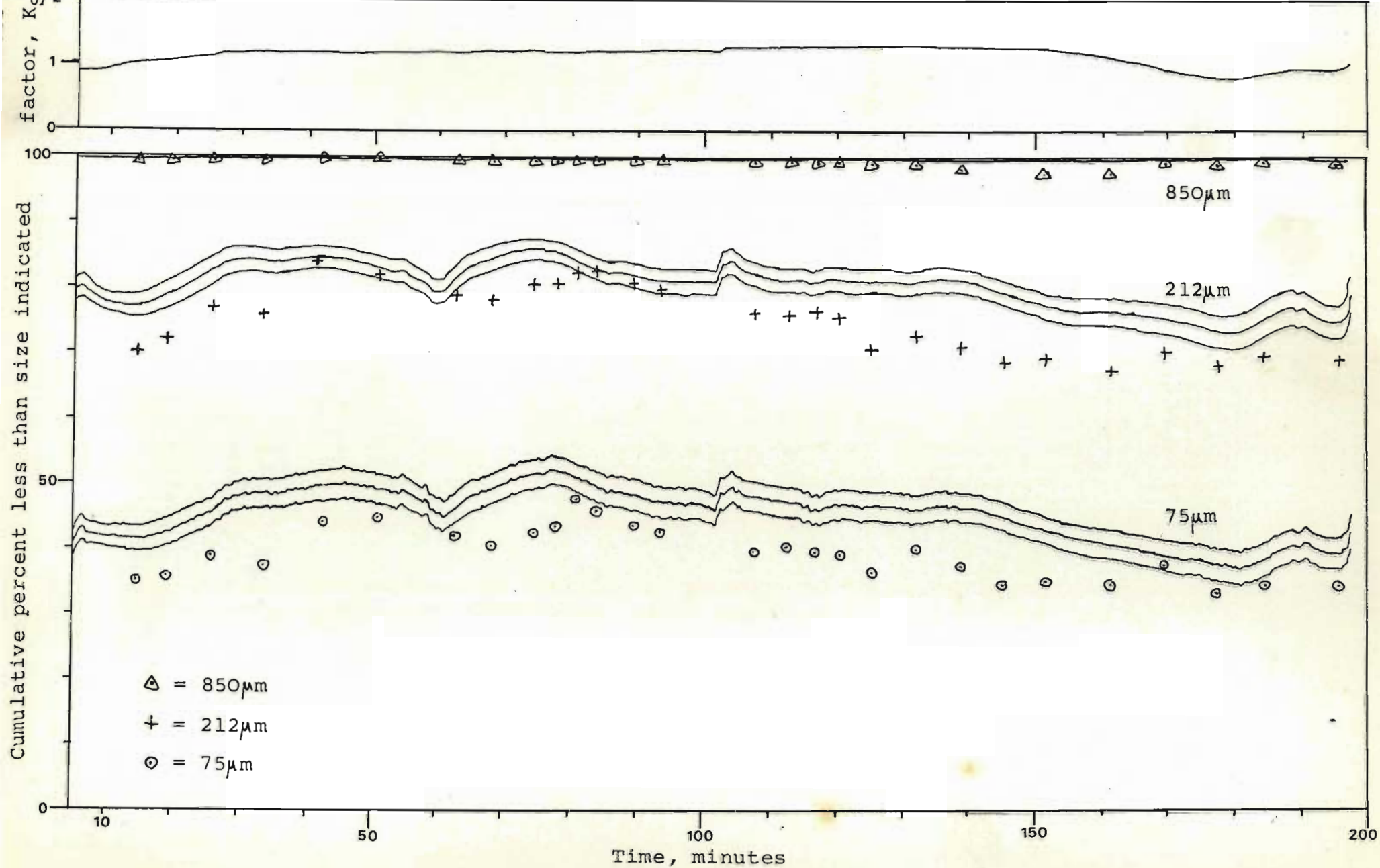


Figure 6.40 On-line regression of softness. Predictions of cyclone overflow size distribution shown below, and softness factor above. Compare to normal results for run B shown in figure 6.23.

6.8.6. Effects of observation errors

The usual standard deviations for the concentration measurement errors were 200 and 400 kg/m³ for the cyclone feed and overflow respectively. Three computations were done using different observation errors in the p.s.d. filter. The results of these on the cyclone overflow size predictions for run B are shown in Figures 6.41 to 6.43:

(1) Figure 6.41 shows the effect of an accentuated sensitivity to the overflow concentration measurement. The standard deviations used were 200 kg/m³ for both feed and overflow errors.

(2) Figure 6.42 shows the effect of an accentuated sensitivity to the cyclone feed concentration measurement. The standard deviations used were 100 kg/m³ for feed and 400 kg/m³ for overflow.

(3) Figure 6.43 shows the effect of overall reduced observation sensitivity. The standard deviations used were 400 kg/m³ for the feed and 800 kg/m³ for the overflow.

(The effects on the concentrations of having no observation step in the filter have been shown already in Figure 6.35.)

Figures 6.41 and 6.42 show that, when an observation was accentuated, the predictions became over-sensitive to noise fluctuations, and so were slightly poorer. Reduced sensitivity to observations (Figure 6.43) gave a smoother prediction, which was reasonably good compared to the "standard" graph in Figure 6.23. The predictions also drifted towards the end of the run, and had a slight bias. All concentration predictions were affected detrimentally by these tests. The effects on the concentration predictions of having no observation step as shown in Figure 6.35, were also detrimental.

Besides showing the individual effects, these results show again what was found with the volumetric filter: the estimates of noise levels have to

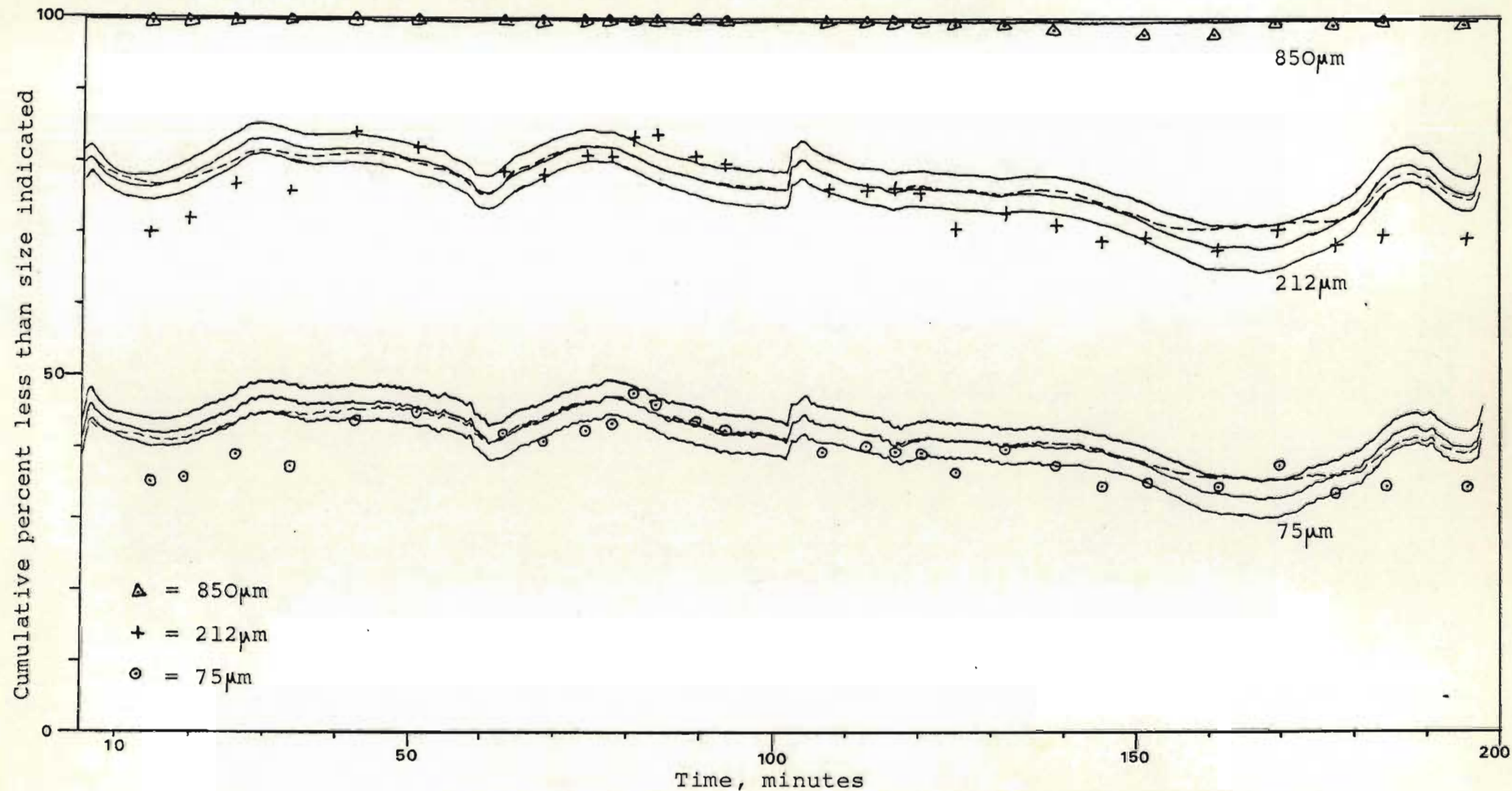


Figure 6.41 Effect of accentuated cyclone overflow concentration measurement.

Predictions of cyclone overflow size distribution for run B. Dashed lines are means under standard conditions. (Compare to figures 6.23, 6.42, 6.43.)

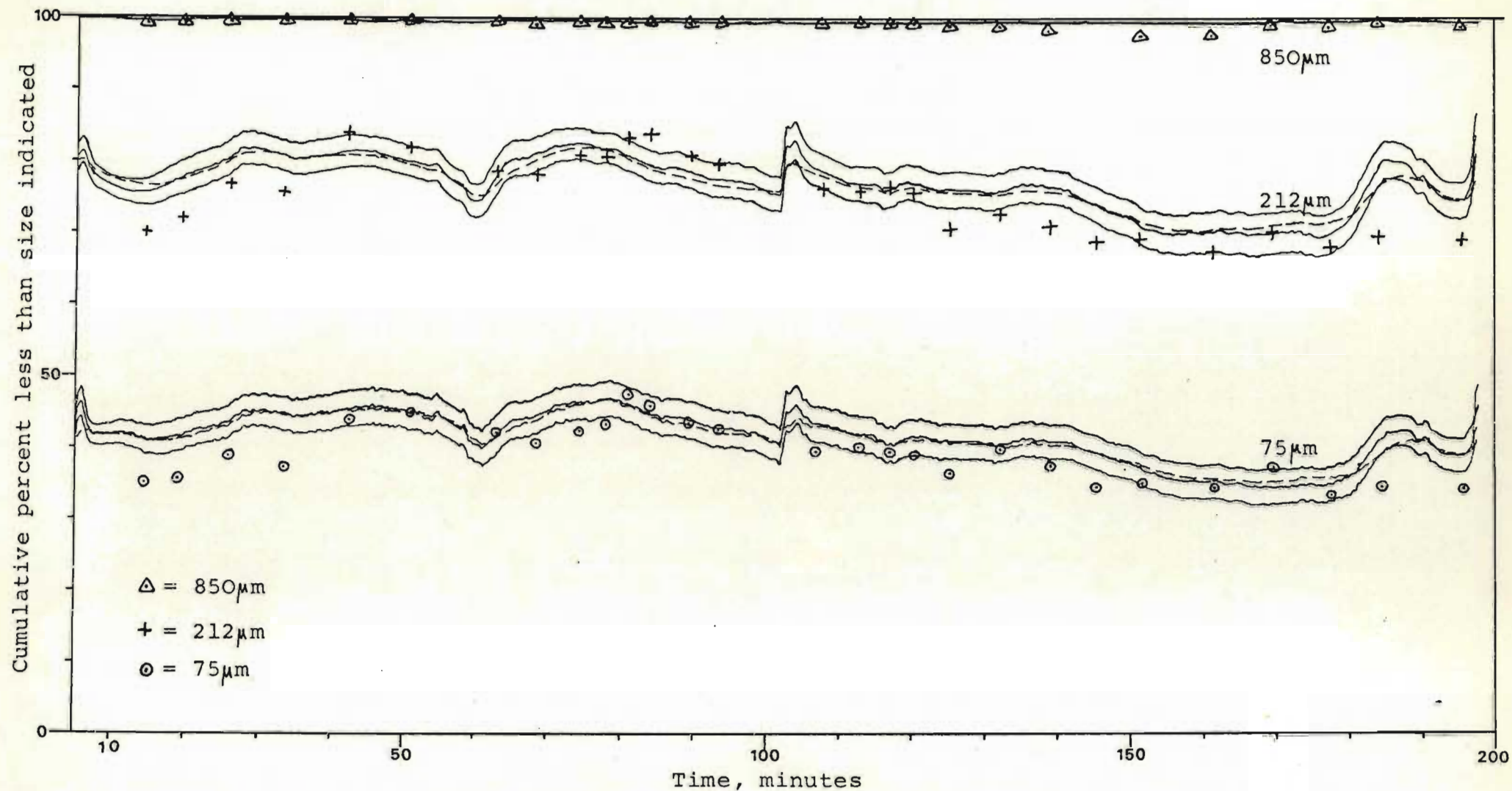


Figure 6.42 Effect of accentuated cyclone feed concentration measurement.

Predictions of cyclone overflow size distribution for run B. Dashed lines are means under standard conditions. (Compare to figures 6.23, 6.41, 6.43.)

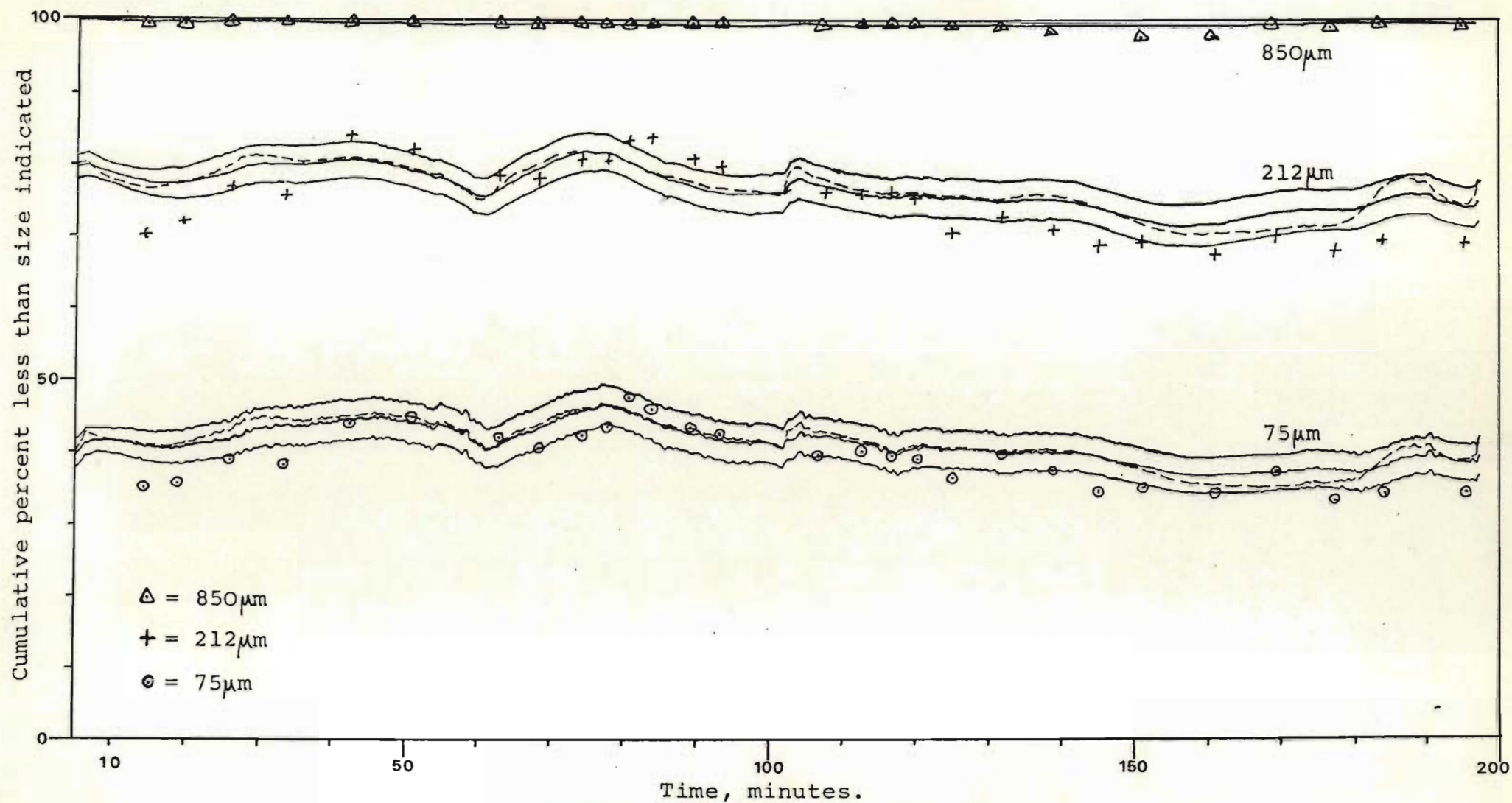


Figure 6.43 Effect of reduced observation sensitivity in p.s.d. filter.

Predictions of cyclone overflow size distribution for run B. Dashed lines are means under standard conditions. (Compare to figures 6.23, 6.41, 6.42.)

be close to the correct levels for the filter to work well. More accurate concentration measuring instruments would also help to obtain better predictions.

6.8.7. Effects of incorrect starting points

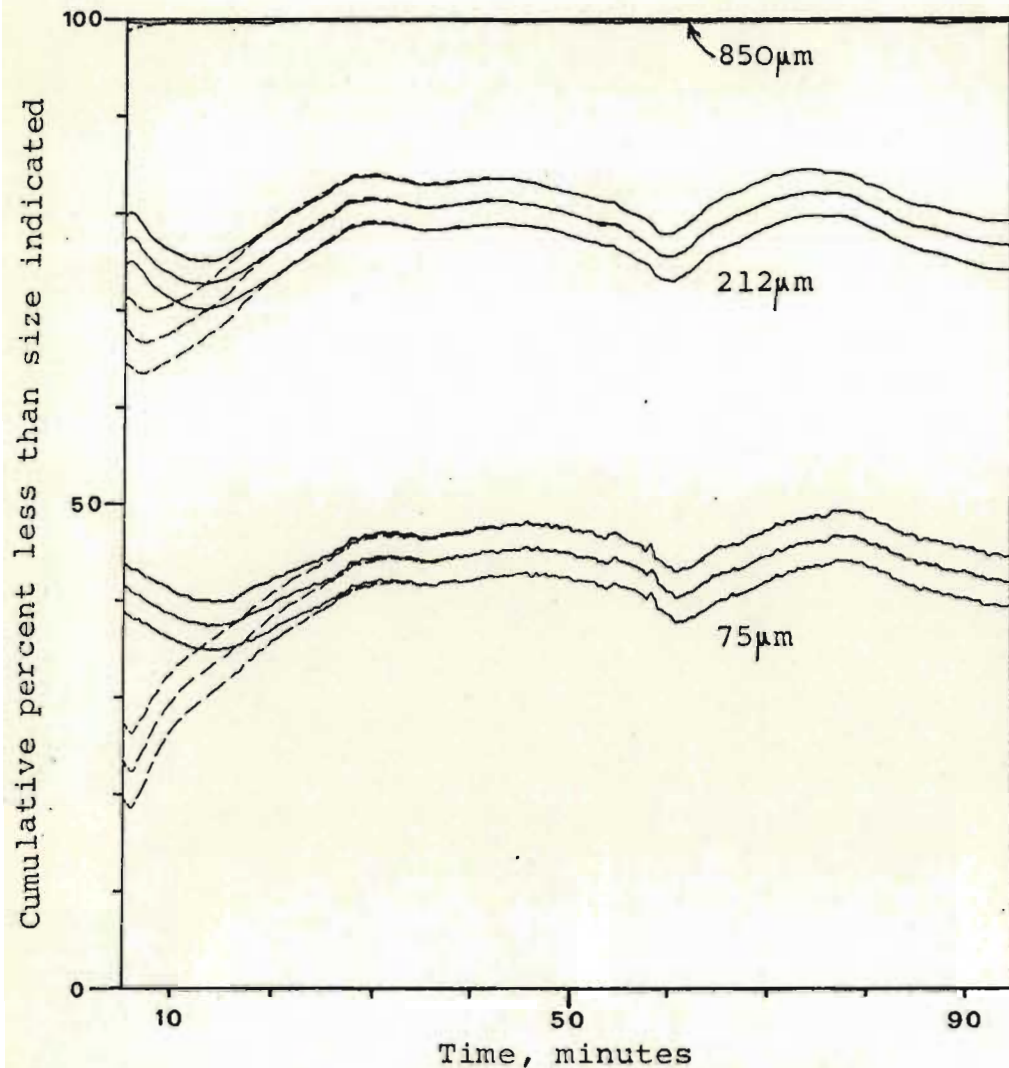
For most runs, the p.s.d. filter was started with a diagonal covariance matrix. This took about 10 to 20 minutes to change into the actual covariance matrix, but the filter remained stable. To test the effect of incorrect starting points, a suitable average covariance matrix was used from the start. The volumetric filter had a considerably faster response (the largest time constant was that of the mill overflow = $0,01 \text{ s}^{-1}$) than the p.s.d. filter, and so only the p.s.d. filter was examined in detail. The mass in each fraction in the mill and sump were changed for the different starting points.

Figure 6.44 shows how the two different starting points converged for the cyclone overflow size predictions and the concentration predictions in run B. Generally, it took the first 10 minutes or so to converge rapidly, and then the convergence slowed and took about 30 minutes more to complete. Any errors in the predictions caused by upsets or noise would have a similar response.

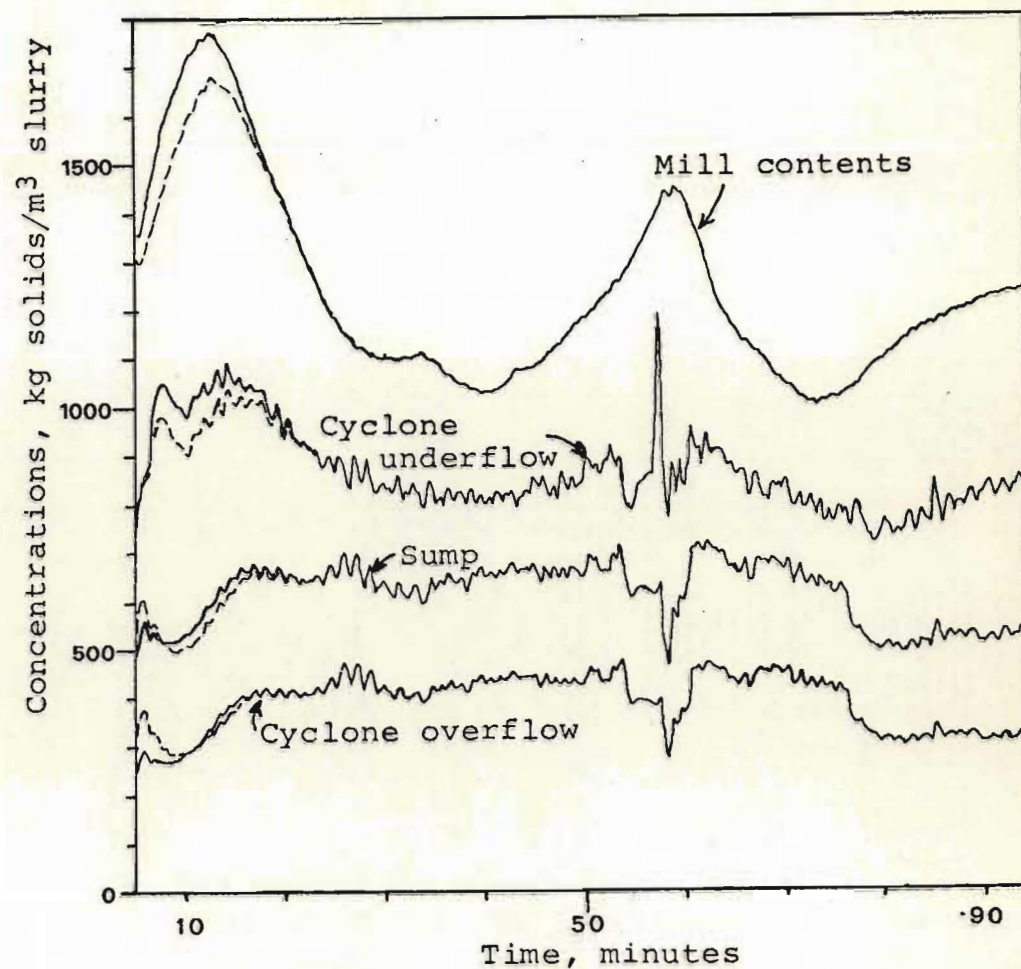
6.8.8. Frequency response of filter

The dynamic responses of the filter were tested for perturbations in the concentration measurements and total solids feed. This was done partly to get some idea of how fast the filter responded to unknown upsets, and partly to get some rough data for controller design. The standard filter and parameters were used, and tests were done on simulations on the Burroughs B5700 computer. Normal frequency testing was done over a range of frequencies, and the amplitude ratio and phase shift were noted. Conditions used were typical of average operation.

Figures 6.45 to 6.47/...



Cyclone overflow size distribution.



Concentrations.

Figure 6.44 Response from different starting points. Predictions of particle size distributions of cyclone overflow, and concentrations for run B data.

Figures 6.45 to 6.47 show the results of these tests. Each figure shows four Nyquist diagrams giving the transfer functions for the predictions of mill concentration, sump concentration, product -75 μm size fraction, and product -212 μm size fraction, as output, with the indicated perturbation as input, over a range of frequencies.

The responses to the cyclone feed concentration shown in Figure 6.45 were all nearly first order with a time constant of around 60 seconds. The overflow concentration perturbations (Figure 6.46) produced slow responses in the size predictions with time constants around 400 seconds, but faster, more complex responses in the concentration estimates with time constants around 60 seconds. The responses to the total solids feed perturbations in Figure 6.47 were not examined thoroughly, but were fairly complex with more than 2nd order dynamics. Here time constants were about 300 seconds. From the Nyquist stability criterion, Figure 6.47 shows that, if the solids feed to the circuit was controlled through a simple proportional controller from the size predictions at, say, -75 μm , instability could result if the gain was greater than $0,25 \text{ kg.s}^{-1}.\%^{-1}$, with a cycle of period 10 minutes.

6.8.9. Stability of filter

The filter was normally very stable and could take considerable upsets. There were three factors, however, that were found to cause upsets during the tests. These were

- (1) Integration difficulties with short time constants compared to step size. This occurred when the sump volume was low, and has been discussed already in Sections 4.3.2 and 6.8.1. Checks in the filter could prevent this.
- (2) Use of wrong parameter values that were physically impossible, in particular a feed distribution that was too fine. This has also been shown already in Section 6.8.4 (Figure 6.39). This is a situation which would not normally occur once the filter was running properly.

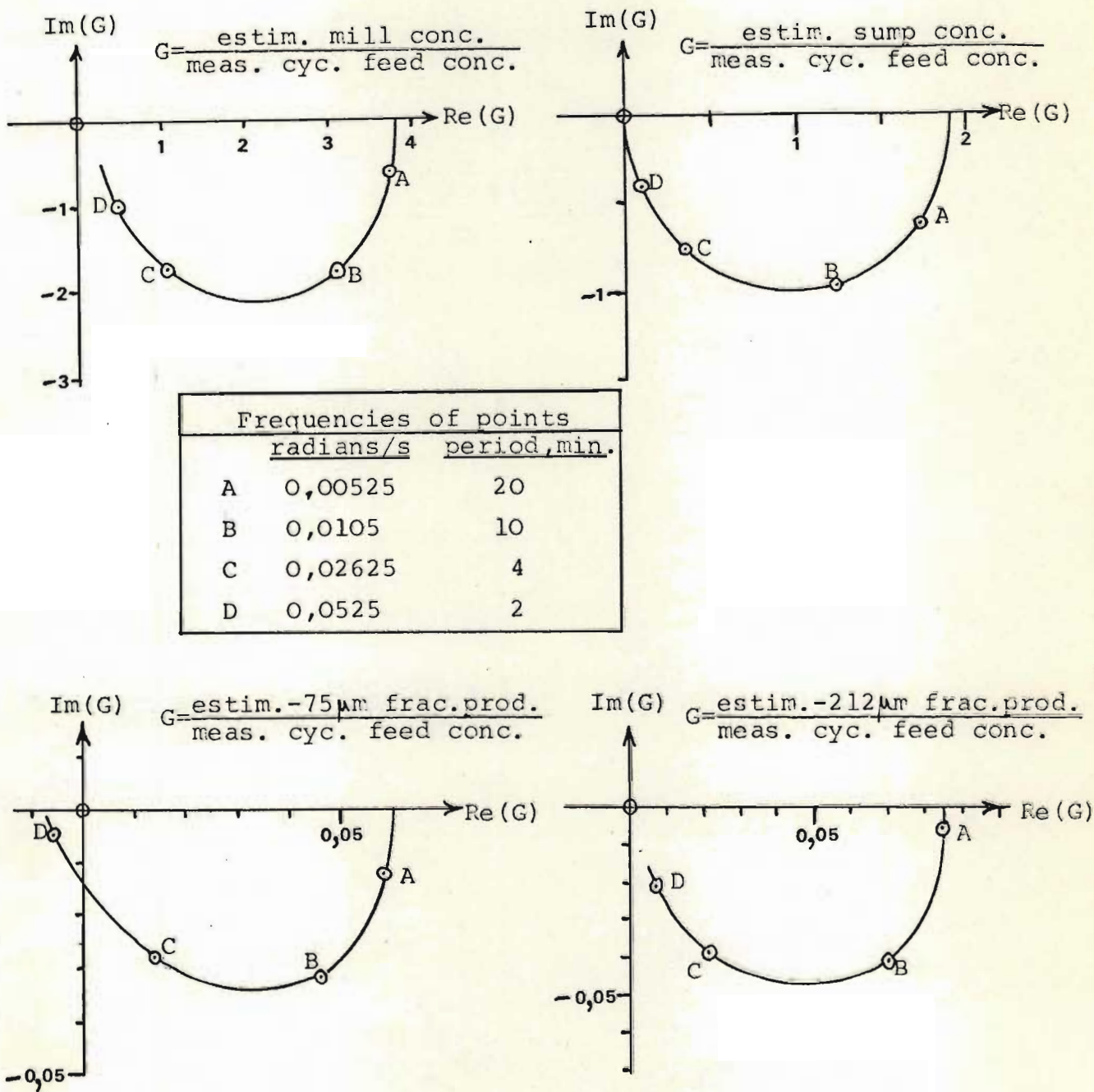
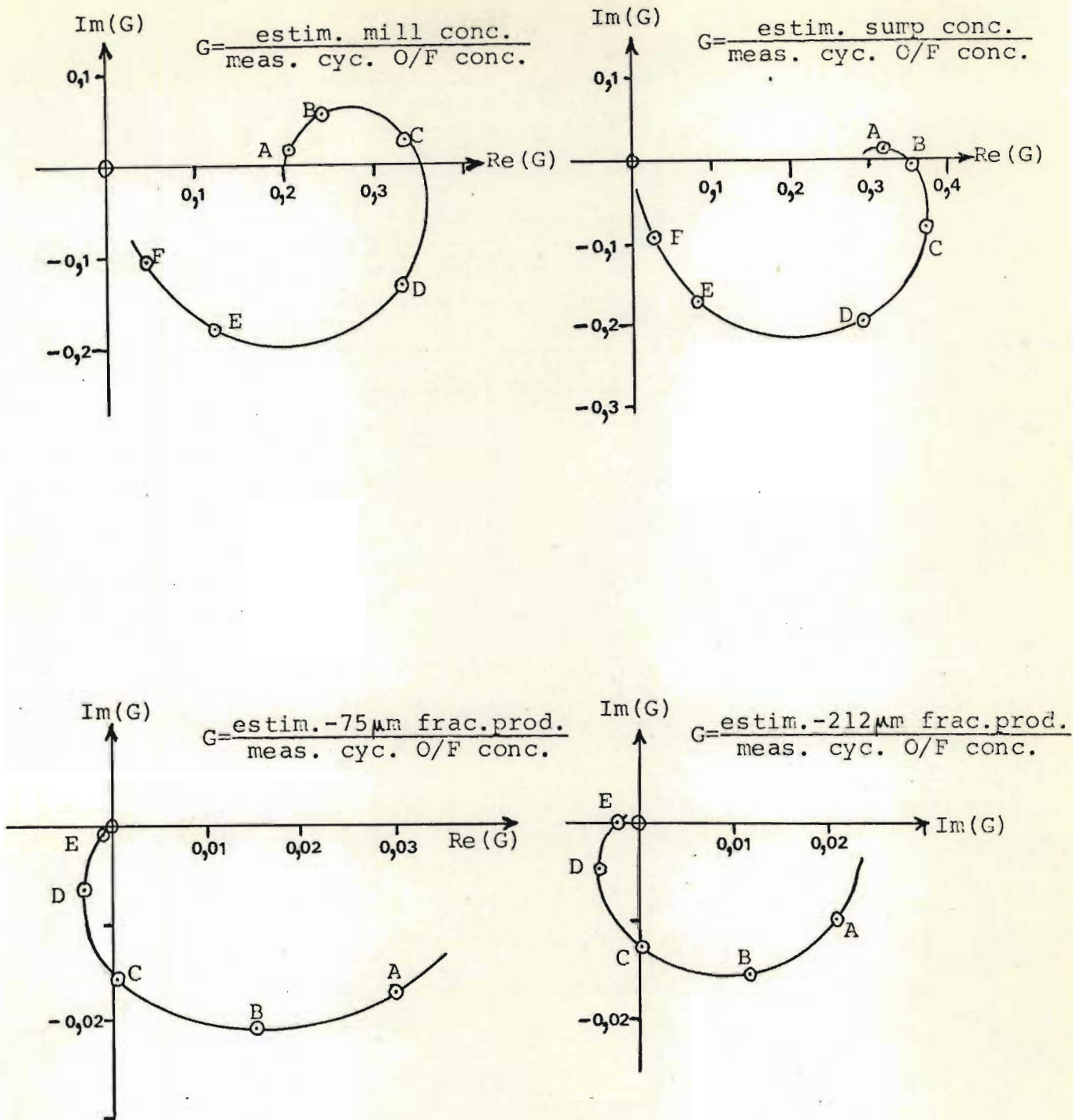


Figure 6.45 Frequency testing of filter.

Nyquist plots showing effects of perturbations in cyclone feed concentration measurement.



Frequencies of points		
	radians/s	period, min.
A	0,00105	100
B	0,002625	40
C	0,00525	20
D	0,0105	10
E	0,02625	4
F	0,0525	2

Figure 6.46 Frequency testing of filter.

Nyquist plots showing effects of perturbations in cyclone overflow concentration measurement.

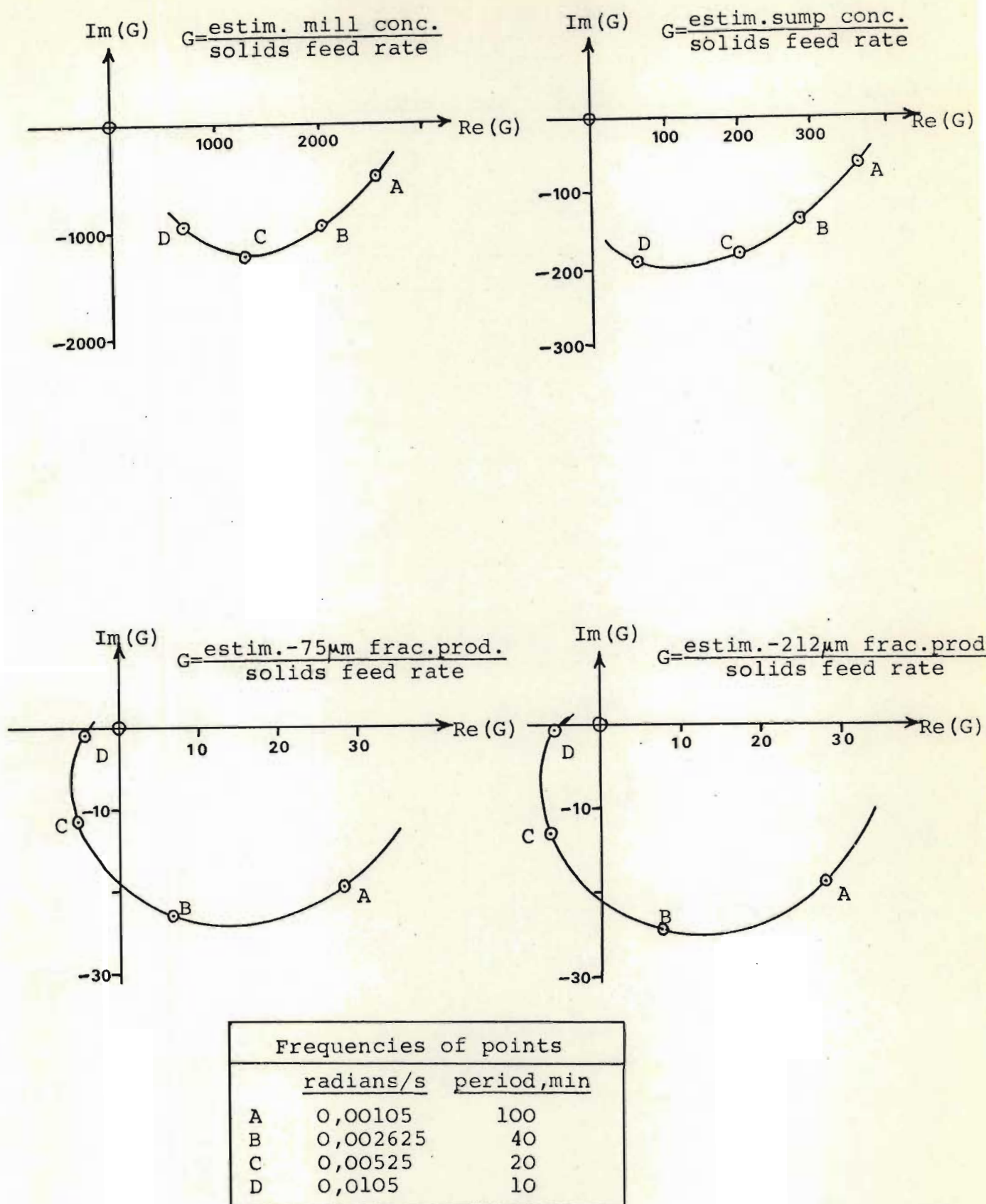


Figure 6.47 Frequency testing of filter.

Nyquist plots showing effects of perturbations in solids feed parameter.

(3) Use of the wrong covariance matrix for starting. It can be seen from equation 4.1.20 that the Kalman gain matrix cannot be calculated if $(m_x \cdot P_{Ak} - m_x^T + R)$ is singular. Under correct filter operation R and $m_x \cdot P_{Ak} - m_x^T$ are positive semidefinite matrices (because they are covariance matrices) and, provided at least one is nonsingular, the sum is nonsingular, and the Kalman gain can be calculated. It was found in the nonlinear p.s.d. filter that, as a result of the approximations used, it was possible to obtain a $m_x \cdot P_{Ak} - m_x^T$ matrix which was not positive definite and which made $(m_x \cdot P_{Ak} - m_x^T + R)$ singular. This was only a temporary occurrence, and resulted from a starting value for P_{Ak} which was outside the range of applicability for the approximations in the filter. This was discovered experimentally when the average matrix of covariances, P_{Ak} , for a softness of 0,9 was used to start a test having a softness factor of 0,2.

The effect is shown in Figure 6.48 with run A data. Here the filter appeared to work reasonably up to 7 minutes and then suddenly became unstable. Afterwards it took about 40 minutes to recover, but then carried on working normally. An interesting fact is that, during the recovery, each prediction went through a point of zero variance. It appears from the reason for this upset that this instability is not easy to see in advance, and can be caused by factors which are not immediately obvious. One can avoid this trouble by starting with a diagonal covariance matrix.

In each of the three cases of instability encountered, the filter was able to recover afterwards. This is useful for continuous plant applications, where the filter should be able to recover by itself if there is an upset.

6.8.10. Time requirements

The time requirements for various parts of the filter are shown in Table 6.20. These computation times were measured from the core clock for the CDC1700 computer in background mode. Times for calculations done with both hardware and software/...

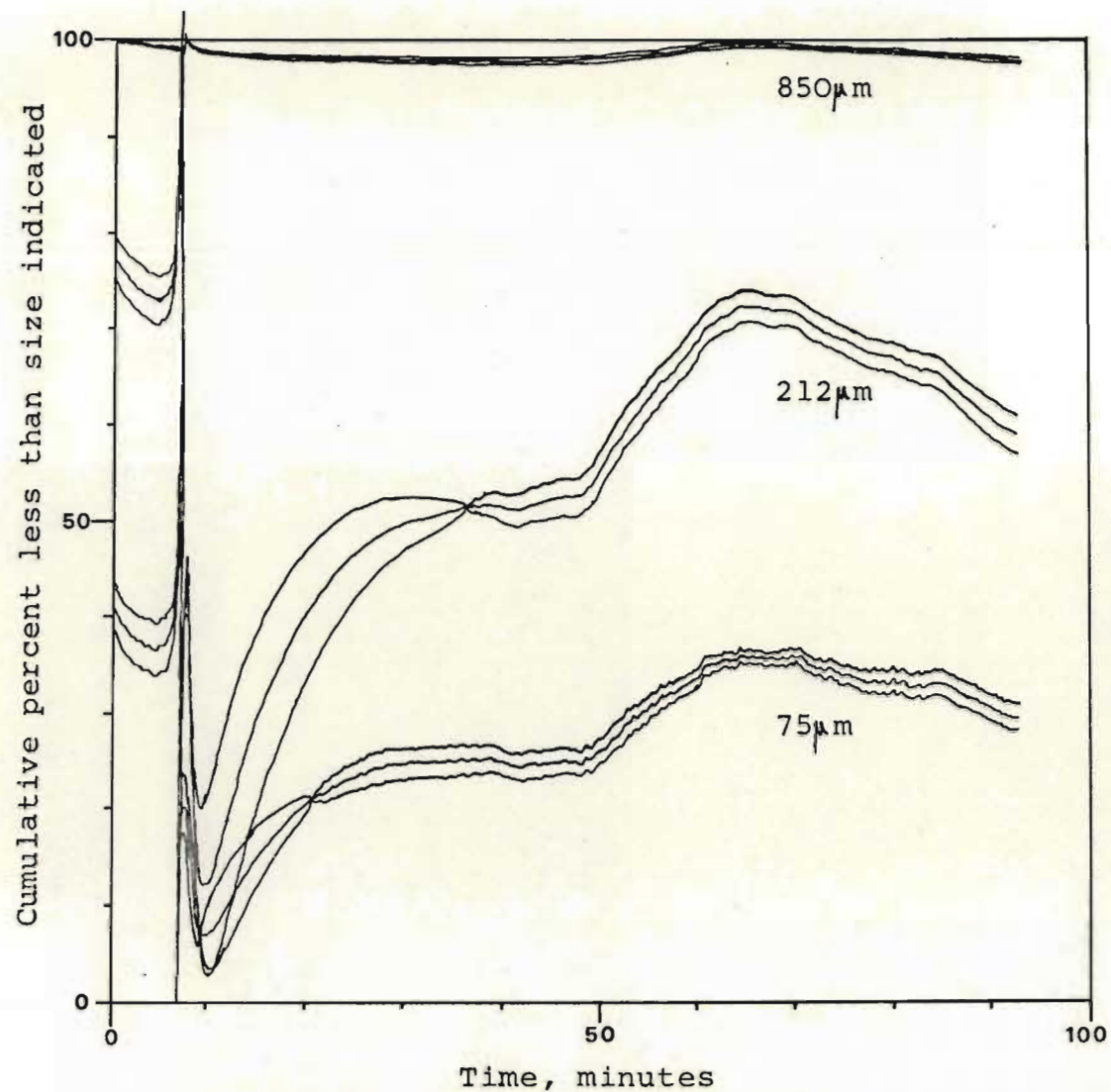


Figure 6.48 Instability caused by wrong starting values for the covariance matrix.

Predictions of particle size distributions of cyclone overflow for run A.

hardware and software floating point (f.p.) arithmetic are shown.

Table 6.20. Computation times

Operation	Time required, seconds	
	f.p. software	f.p. hardware
1) Reading disc file	0,10	0,105
2) Data conversion and "book-keeping"	0,10	0,026
3) Volumetric filter (call to IBSTST)	0,17	0,059
4) P.s.d. filter, observation step. (Call to IBPOBS)	0,50	0,126
5) P.s.d. filter, evolution step:		
a) Single step integration	0,86	-
b) Euler two step integration	1,72	0,460
6) Conversions to distributions and concentrations (call to IBPTOF)	4,03	0,968

6.8.11. Simplified calculations

Because the computer took longer to calculate the filter when using software arithmetic than the plant took to evolve, (run B took approximately 4 hours to calculate in background mode) the simplified calculations, explained in Section 4.35, were used for real time work. These cut the calculation time down to about 3 seconds per cycle, (see Section 6.9) mainly through the time saved in not using IBPTOF. (See Table 6.20.)

Basically, the subroutine IBSIMP calculated the concentrations and size distributions without taking variances into account (see Section 4.3.5). The results showed that the predicted concentrations were almost unaffected, while the size distributions differed by less than 0,25% of the mass in each fraction. This was because the nonlinearities in the filter were not very great. This accuracy is far greater than that of the filter, and is an example of an unnecessary refinement. It also means that the

term /...

term $\frac{1}{2} (P_{Ak} - \partial^2 m)$ in equation (4.1.18) is insignificant and could be neglected without much loss of accuracy, and with some saving in time and core.

6.9. Results from differential quadrature filter

The quadrature filter outlined in Section 4.1.2.5 was run on the data from run B. Results were not particularly successful, and so not much time was spent on it. The predictions of cyclone overflow size are shown in Figure 6.49. These predictions held very steady regardless of the plant behaviour, probably because of the limited range allowed by the grid size. The concentration predictions varied more than the size predictions, but were also far steadier than the actual variables on the plant. We may therefore conclude that discretisation in a large dimensional system is not a practical tool for solution.

The time requirements of this quadrature filter are of interest in assessing the time required by the method of moments. On the CDC 1700 computer, using software arithmetic, the times required for one complete observation cycle (which took 5 seconds in real time) for each filter are shown below.

(1) Quadrature filter	4,3 seconds
(2) Moments filter with IBPTOF (off-line)	6,0 "
(3) Moments filter with IBSIMP (on-line)	~ 3,0 "

(The time required for on-line computations in (3) depended on time sharing with other programmes.)

This shows us that the use of the quadrature filter required about as much time as the moments filter, even though the formulation was much simpler. This was found to be typical of matrix formulations, and is discussed in Chapter 7.

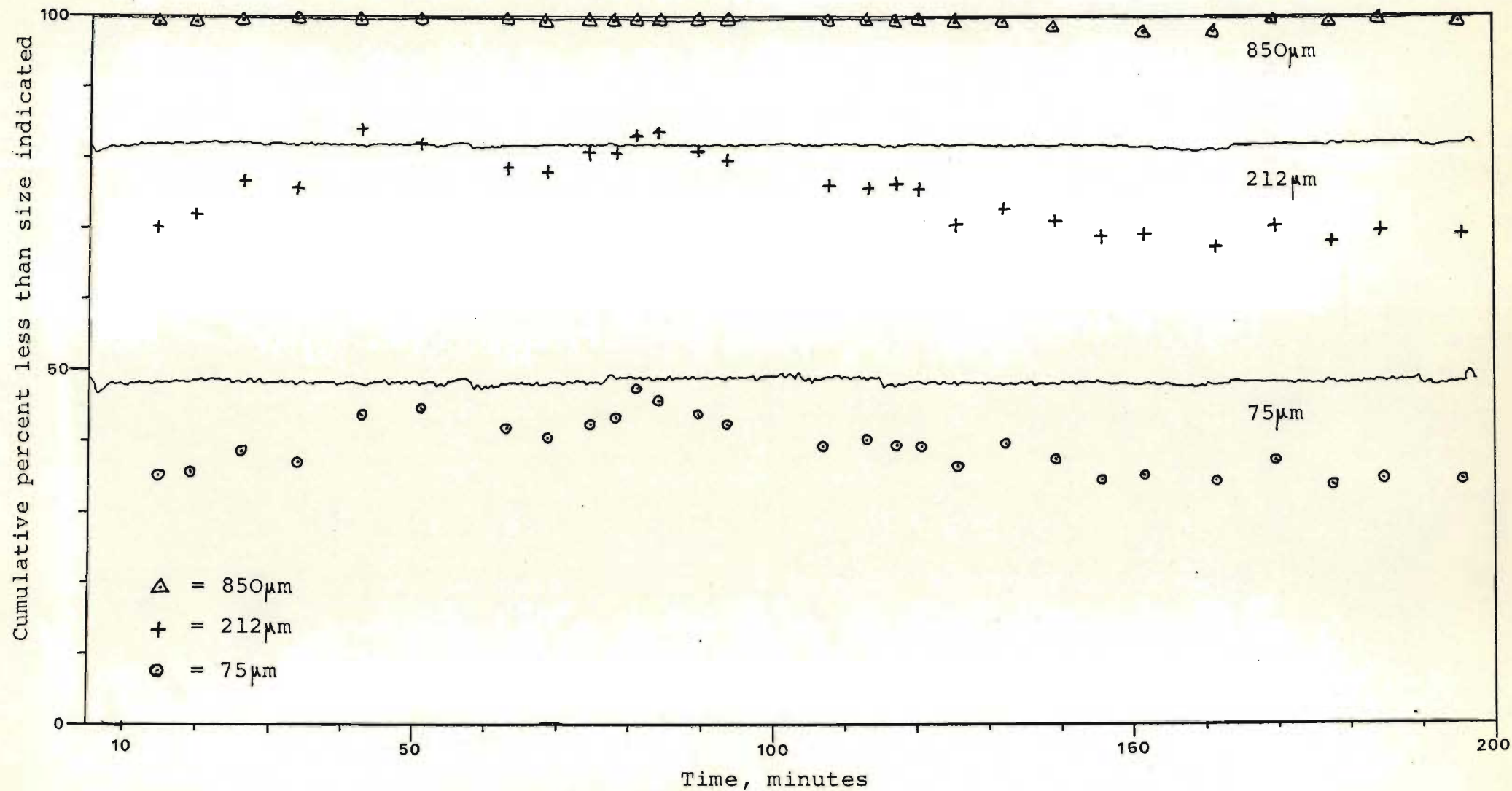


Figure 6.49 Quadrature filter predictions of means of particle size distributions in cyclone overflow for run B.

Chapter 7

DISCUSSION

The results of this investigation are discussed here firstly with regard to the milling circuit filter in particular, and secondly to filters in general.

7.1. Results of off-line tests

Before discussing the filter results, the results of the off-line tests should be briefly considered, as they give much useful information on how the filter could be expected to perform.

7.1.1. Selection and breakage functions from batch mill tests

The results from the batch milling tests gave reasonable estimates of the selection and breakage functions for the conditions examined. As is typical of wet ball milling, some of the assumptions of first order breakage were not well justified, particularly in the coarse size groups, although the overall fit was satisfactory. It was found during the regressions that the breakage function was less critical than the selection function. The shape of the curves and the difference between the two ball size distributions is of theoretical interest, but was not of use in this study.

The scale-up to a larger mill assumed that the selection function would be scaled uniformly over all size groups. It is known that the larger-size groups on the downward part of the curve usually scale by a larger factor, but the scaling factor was small, and there was little difference after data reduction to fewer size groups. The error incurred by assuming the ore to be homogeneous could not be easily estimated. The decay curves of the coarse size fractions did not have the typical "knee" of a mixed ore, but the circulating load rock had a higher measured specific gravity than the feed

rock. Also the filter/...

rock. Also the filter results showed that the rock in the continuous mill was definitely harder than the rock used for the batch tests, as the softness factor was less than 1,0.

7.1.2. Cyclone model

The flow model for the cyclone assumed that the total underflow volumetric flow rate was constant. The data showed that it was not noticeably dependent on either feed flow or concentration, but that there was scatter about the mean. The operation of a cyclone underflow is complicated by the air core, and the exact dependence of the underflow rate on the operating variables is not known well enough to propose more complex models. This is unfortunate, as the variation in the underflow rate was the largest error in the volumetric filter, and had a direct influence on the p.s.d. filter. The result was that the overflow volume rate from the cyclone could not be predicted with sufficient accuracy and so the estimates of concentrations were influenced.

Results from the cyclone tests showed that the performance of the cyclone can vary considerably. Tests done on the filter showed that the parameters used in the cyclone model had a considerable effect on the predictions, and so accurate values were needed for the parameters. It can be seen that the performance of the whole milling circuit was dependent on cyclone variables which were difficult to control to within the desired tolerances.

Overall, the cyclone contributed much error to the predictions by the filter. Both the flow model and the classification model were inadequate. A better understanding of cyclone operation, and improved models are still needed.

7.1.3. Mill overflow and transport

The overflow from the mill was not an important factor in the filter, as the

error in predicting the mill volume from the volumetric filter was not large enough to affect the p.s.d. filter results significantly. An assumption was made in developing the filter that the volumetric model was not influenced by the mass or size of solids present. In the case of mill overflow, the solids affected the flow because of viscosity, but this seemed a minor effect in the mill studied. Transport through the mill was more important, but models requiring more than a single stirred tank for the mill would increase the dimension of the p.s.d. filter. The filter was not sufficiently accurate to show up any errors in grinding caused by the transport model, but a difference in response time was noticeable.

Classification at the mill exit was affected by the solids present, particularly when the concentration was high. This phenomenon could easily be included in the p.s.d. filter model, but it would need much difficult experimentation to collect data for parameters.

7.1.4. Runs on milling circuit

Runs B, C and D all gave useful information for testing the filter under normal operation. Run A was too upset to give normal data, but it was useful for testing how the filter behaved under abnormal circumstances.

The control interval of 5 seconds was not varied. Earlier, a 10-second interval was tried, but the control on the sump was found to be too erratic. The 5-second interval was then tried as a balance between having good control and having enough time to do filter computations, and was found to be satisfactory.

The maximum throughput of the milling circuit seemed to be limited both by the cyclone underflow solids rate, and by the mill when it put out large stones when it was overloaded. As in run A, operation near the limits was found to be likely to give trouble.

7.2. Results from the filter tests

The performance of the filter is best evaluated by studying in detail the graphs 6.17 to 6.33 shown in the results, chapter 6. These results showed the following points.

- (1) A filter for predicting the state of a milling circuit could be written and made to operate successfully on an actual plant in real time. It gave reasonable predictions and tolerated plant upsets. In doing this, we achieved the main goal of this investigation.
- (2) The volumetric filter performed well in each case. It was simple to employ, and gave no trouble on its own. It followed measurements closely and recovered quickly after upsets. The built-in checks helped to prevent it causing instabilities or upsets in the p.s.d. filter when the plant was experiencing an upset, but it did not affect normal operation noticeably.
- (3) In the p.s.d. filter, the product or cyclone overflow size distribution was more accurately predicted than the underflow size distribution. All trends were followed well, although the predictions were slightly ahead. The concentration predictions were inaccurate because of the poor cyclone model in the volumetric filter. The actual softness of the rock appeared to vary slightly, although this was kept constant in the filter.

The predictions were observed to be slightly ahead of the samples. This was probably caused by two main factors. The first possibility was that we did not take any delays in the circuit into consideration, e.g., in the lines, the cyclone overflow tank, the mill residence time, the sump, the pump, and the cyclone. This would only explain about half the delay of approximately 8 minutes that was observed. The second possibility was that the use of only four size groups in the filter meant that the coarse material entering the

circuit would start to appear in the fine product too soon. In reality, it would have to break through considerably more intermediate sizes. The use of more than four size groups would help this, but must be balanced by the greater computational load. The results obtained indicate that the use of only four size groups is as good a compromise as possible.

7.3. Effects of factors on filter

Section 6.8 showed the effects of several factors on the filter performance, and discussed these. Some of these proved to be more important than others. These main results are discussed below.

(1) Variations in rock softness, feed size, and cyclone classification all produced similar results, particularly on the cyclone overflow size prediction. It was difficult to distinguish between the causes, and this raises the question of whether it was necessary to distinguish between the causes. Provided all the parameters are of the correct order and are as accurate as they can be conveniently determined, it might be easier to describe all variations in terms of changes in rock softness. The filter was found to be poor at regressing on rock softness, but this was mainly due to not having an adequate cyclone model, and was not helped by the poor instrumentation. If, on a larger scale, the predictions were found to drift slightly, then it may be better to let the filter regress on softness. The difficulties in this regression, which were pointed out earlier, should, however, be noted.

(2) The noise in the plant and on the instruments was not small. This gave larger than desired prediction errors. A larger scale plant might give better predictions, partly because it would probably be less prone to noise because of its scale, and partly because it would have better instrumentation, particularly on concentration measurements.

(3) Of the models used in the filter, the cyclone was the most inaccurate and one of the most critical, both for flow and classification. The cyclone

obviously needs further study. The cyclone model could have been made stochastic, except that this would have made it more difficult to develop a filter, as the same noise would appear in both the evolution equation 4.1.1 and the observation equation 4.1.2. This would require some modifications of the basic filter structure, and is a problem discussed by Jazwinski (1970) page 208. The performance would probably not differ much from that of the existing filter, as the basic cyclone model would still be the same. The grinding model was reasonably accurate over the normal operating range. A larger number of size groups would have helped both models. The ore used, being of mixed hardness and density, also produced some scatter.

(4) The use of differential quadrature is not suited to large dimensional systems. Although requiring a calculation time comparable with the method of moments, the results were inferior.

7.4. General use of real-time recursive filters

The results from the milling circuit filter have been discussed. This investigation also showed a number of matters and problems associated with real time use of filters in general. These are discussed below.

7.4.1. Determination of noise levels

Noise levels in a filter are difficult to determine precisely, and they are a source of uncertainty in a filter. Various methods are given in section 4.2.4, and the effects of varying noise levels are shown in section 6.8. To determine levels experimentally, if it were possible, would take a long time. The questions arise of how exact do they need to be and what are the effects of using incorrect levels.

Noise levels determine how much relative reliance is placed on each part of the filter process and observation models. For this it is the relative magnitudes which are important, rather than the absolute values. If a noise

level were increased by a factor of 2, i.e. the variance by a factor of 4, (as in section 6.8.6) then the effect of that part of the model would be reduced by a factor of almost 4. It appeared that the effects of such factors were not great under normal operation, as the plant and the filter evolutions did not differ widely, and new observations did not have to change the state predictions noticeably. Under a plant upset, however, the effects could usually be seen more easily.

Noise levels also determine the accuracy of the predictions. It has been found that the mean value of a prediction is the most useful and most easily understood statistic. In a multidimensional system, the variances of individual variables are used occasionally, but the full variance-covariance matrix, or the probability density function are seldom consulted. Noise levels usually have little effect on the mean. Thus the need for reliable noise levels is not as great as the need for a good model.

The response of the means in a linear filter is not affected by a uniform scaling of all the noise levels. This can easily be seen by applying a scalar factor, say b , to Q , U_k , C_U , P_{k+} , and P_{k+1-} in equation (4.1.12) and R , P_{k-} , and P_{k+} in (4.1.17), and noting that the Kalman gain K does not change while the other filter equations remain satisfied. In an actual plant situation where control actions will be taken on the basis of the filter output, greater accuracy would be required for estimates of the noise levels than those achieved in this study. As indicated in section 4.2.4, noise levels can be obtained with reasonably good precision and this does not appear to be a major difficulty in the industrial application of the modelling and filtering technique developed in this study.

7.4.2. Presentation of results

Presenting output from a filter is a problem. To judge the performance visually, it is necessary to have graphs which are not confusing but contain

all the relevant data. Raw data from a filter are generally meaningless, and they must be converted, as explained in section 4.3.5, to more meaningful quantities. Output in the form of numbers is only useful for checking, and uses an excessive amount of paper. Statistical checks are useful to quantify performance, but they do not convey how the filter actually worked. Perhaps on a larger scale of plant, most of the filter data would be used only for control, and output of only key variables to an operator would be by way of a chart or by a display on request.

7.4.3. Advantages of a noisy system

In developing a filter for a system such as a milling circuit, one has two particular advantages over systems tested previously, such as those for missile tracking.

The first advantage is that the milling circuit is inherently stable over a reasonable range, and so the filter is less likely to diverge through lack of good information. This has not been proved rigorously for a nonlinear system, but it follows intuitively because the evolution equations in the p.s.d. filter (appendix A), with reasonable parameter values, will tend to a fixed point with a finitely limited variance, as a result of the stability of the model. This was shown to be correct for a number of points (see sections 6.6(5) and 6.8.1) when developing the noise levels in the filter. For a linear system, any observations will decrease the variance of the estimates (from equation 4.1.17). Thus, provided any observations from the plant are not out of the operating range, the range of the estimates of the means and variances should remain bounded.

The second advantage is that the noise levels are high and the nonlinearities are slight. Thus simpler, more approximate methods of solution can be used provided the errors which they introduce are relatively smaller than the standard deviations of the estimates. This also means that there is less

likelihood of computational instability, as simpler methods are generally stable over a wider region.

With a practical filter, one has the advantage that the model of the plant will behave much like the actual plant. A "feel" for the plant is useful for understanding how the filter works, and for guessing parameters for use in the filter without actually measuring them.

A filter automatically reduces the error in the mass balance for the plant. It will not do an exact mass balance, but it will try to compromise between the errors which it holds in its model noise levels.

7.4.4. Updating a filter

It was found throughout this investigation that it was necessary to check calibrations continually, and make changes in parameter values as the plant changed. This would probably also be the same with any plant, and is a disadvantage in that it would always require attention.

7.5. Necessary considerations in designing a filter

With a large nonlinear system, the problem of what type of filter formulation to use is very important. The following factors are important in considering the method.

- (1) Speed of operation: Real time work allows a very limited amount of time for computations and there are considerable complications if this is exceeded even once during plant operation.
- (2) Accuracy of prediction: An approximate criterion is that the accuracy of the method must be better than the normal error in the predictions, but this may be difficult to determine. To be too accurate is a waste of time and computer capacity. An example of this was shown in section 6.8.11. Inaccuracy may make the results useless, as in the case of the

quadrature filter in section 6.9.

- (3) Difficulty in formulation: An intricate filter takes a long time to formulate, programme and test, and this is expensive in terms of man-hours. It might be advantageous to develop filters such as the one presented here before needing them on an industrial plant, as there may not be enough time to develop a new one from the beginning when commissioning a plant. Some filters are already available in this way, usually as part of a control scheme, e.g. for paper-making machines (see Åström 1970).
- (4) Computer requirements for (i) storage, (ii) processing: A long filter programme usually uses a large amount of both core and time. Methods which require a lot of storage for filter variables generally take a long time to compute, and are not usable. Storage for variables for most practical methods is not large compared to that available in a computer, and would probably only be important if the computer was on-line to several parallel plants simultaneously. The accuracy required for the arithmetic may also vary between methods. Typically, large matrix inversion requires high accuracy, often more than 32 bit floating point arithmetic (which is typical of present-day control computers) can provide.
- (5) Availability of data for parameter determination: In a model, the use of extra sections which have little effect on the result but which require much off-line experimentation, is inefficient. It would be better if time was limited to run the filter the first time on a simulation with assumed values for the parameters. Once the sensitivity to errors had been checked, the necessary parameters could be determined experimentally.

7.6. Comparison of methods for implementing a filter

This project studied a large and noisy system which was not linear, but not highly nonlinear. It is felt that this is typical of most metallurgical plants. The conclusions drawn here are based on this system, rather than the

more exact missile-tracking type of system.

- (1) Method of moments: This was the method used here, not to be confused with extensions to the linear Kalman-Bucy filters. This was found to be the best method for most problems where the dimension was large and the nonlinearities were small. It is more economical for computing time than the extensions of the linear filters, as less arithmetic is needed, but the programmes are not as general. It is also more difficult to write and programme than the equivalent extended filter.
- (2) Extensions to linear filtering theory: After the method of moments, this is the next most feasible method on present day machines. More core is required for storage of variables, and more time is required for computations. This is because of the time used in doing calculations on large parts of the matrices which have little effect on the results. The method is quicker for programming, and has been well developed in the literature, so that its behaviour is more easily understood.
- (3) Orthogonal series approximations: These approximations are usually only feasible on a small system, but give more information about the actual probability distribution, which the above methods do not give. They generally take time to formulate and programme, and are not very well developed in the literature for filters.
- (4) Discretised state space: This method is only suited to very low dimensions, and can give very detailed information. If differential quadrature is used, the formulation is simplified, and matrix arithmetic is all that is required for solution. The use of discretised state space for large dimensions was shown in this investigation to be unsuccessful.

Other possible methods, such as Gaussian sums, Monte-Carlo techniques, or deterministic observers, were not examined in detail in this study, as they did not appear to be suitable.

7.7. Recommended procedure for practical filters

The following procedure is recommended for developing a filter.

- (1) Draw up the simplest possible model for the process being studied.
A "feel" for the plant being studied is a great advantage here.
- (2) Develop a filter from the process model. This may require revising the model.
- (3) Collect whatever data can be collected easily from the plant or from literature. Estimate values for the parameters which cannot be measured, and run the filter to test it.
- (4) From the results of the tests, decide on what parameters need to be determined, and whether improvements are needed in the filter.
- (5) Perform the further work required and re-run the filter.

Some type of improvement to a filter is usually possible, and so (4) and (5) will be repeated several times. For this reason, it is essential to have some form of the filter operating as early as possible.

7.8. Comment on linear algebra

Linear algebra is often used in control theory. It is a convenient "shorthand" way of formulating problems, and the algebra has been well developed. It is not restricted to linear control theory. It is a well known fact, and it became increasingly obvious during this study, that the length of time required on most computers for doing matrix manipulations is too long. This makes the technique impractical in all but the smallest systems.

In recent years, computers with parallel processors have been built. These enable several similar computations to be done simultaneously and are suited

to doing matrix arithmetic quickly (see section 3.5 no.(9)). The use of small multiprocessor machines for real-time control work would revolutionise the use of advanced control theory on complicated industrial plants. The programmes would be both simpler to write and quicker in execution, and these are two of the greatest difficulties in present day control theory applications.

The use of matrix algebra in filtering theory has already been explained for extensions of the linear theory. In this investigation, the method of moments was chosen as it was the best method of solving the filter equations with the existing facilities, but it took a long time to prepare. If a matrix processor had been available, then the second order extended Kalman filter probably would have been a superior method. Other methods, such as differential quadrature, would also become feasible.

7.9. Estimation of a distribution

A problem that was encountered when first developing the filter for the milling circuit was the lack of fundamental mathematics available for handling the estimation of a distribution or distribution density. In this study (see section 4.3.3), the size distribution density, $p(d)$, was lumped at four points d_i , $i=1, \dots, 4$, and designated p_i , $i=1, \dots, 4$. These p_i were then treated as state variables, and the filter was written about their probability density function, $h_I(p_i, i=1, \dots, 4)$. No success was achieved when attempting to formulate the filter in terms of a continuous $p(d)$, although it seemed that this should have been possible. This is obviously an area where more basic research is still needed.

7.10 Advantages and disadvantages of practical use

A filter provides a knowledge of the state of a process in real time. This state is often otherwise unmeasurable, or not measurable as accurately as the filter can predict it. It is the availability of this knowledge for further use which is the main advantage in using a filter.

The implementation of a filter is complicated and time-consuming. A large computing facility is required as opposed to conventional DDC loops. Much off-line experimentation is needed to get data for the model, and these data must be continually updated as the plant changes. These are the main disadvantages in using a filter on a real plant.

In the case of the milling circuit filter developed here, the particle size distributions were calculated at three different sizes in the distribution curves. Most present day size monitoring instruments and estimation techniques give only one point on the distribution. The use of a size measuring instrument together with the filter could also be considered, as this should give more accurate predictions and more information than either could provide separately.

Chapter 8/...

Chapter 8CONCLUSIONS

In this investigation, a filter was developed and successfully tested in real time on a milling circuit. The following is a summary of the main conclusions drawn.

- (1) The use of Kalman filters is definitely feasible on a typical metallurgical process where the modelling is normally poor and the errors are large.
- (2) The predictions from the milling circuit filter agreed reasonably well with the samples taken. This showed that a simple model could be used, and that approximate methods of solution are sufficient.
- (3) The time of execution was not short, but the calculations could be done fast enough for the filter to be used in real time.
- (4) Of the methods of implementing a filter that were tried for the system, the method of moments was found to be the best.
- (5) The choice of noise levels in a filter is difficult. The need for good model parameters was greater than the need for accurate noise levels, but it was essential to give some effort to get reasonable estimates from the start.
- (6) The main advantage of a filter is briefly that it provides a knowledge of the state of a system which could not be obtained as accurately from direct measurements.
- (7) Disadvantages of a filter are the complexity and time required in development, and the need for continual updating of calibrations and parameters as the plant changes.

(8) Further work is needed in the following areas:

- (i) Development of suitable simple models. These should reflect a good understanding of the process rather than being very accurate. This applies particularly to the cyclone model in the milling circuit filter.
- (ii) On-line computing facilities. Use of small parallel processing machines would make matrix formulations of large filters feasible in real time. This would simplify filter design considerably.
- (iii) Filter development. Actual applications of filters to real plants are needed as there are still several difficulties to be overcome, particularly in the modelling and development of large filters. On the theoretical side, methods of implementation and more general methods of modelling (e.g. particle size distributions) are needed.
- (iv) Milling circuit filter. Improved cyclone models would improve filter performance. Given faster computing machinery, more complex models particularly with more size groups, might be tried with advantage.

APPENDIX A

EQUATIONS FOR THE EVOLUTION OF MOMENTS FOR THE PARTICLE

SIZE DISTRIBUTION FILTER.

The equations for the moments shown below were derived from the model for the p.s.d. filter (equations (4.3.26) and (4.3.27)), as explained in section 4.3.4, using the method of moments given in section 4.1.2.2. These equations were prepared as a subroutine, IBCDRV (see appendix C) for use in the evolution step of the filter.

Notation

State vector $\underline{x} = (p_{M1}, \dots, p_{M4}, p_{S1}, \dots, p_{S4})^T$

Softness parameter = K_S

First moment of $x_i = m_1(x_i) \quad (= \mu_1(x_i))$

Second central moment of x_i and $x_j = m_2(x_i, x_j) = \mu_2(x_i, x_j) - m_1(x_i) \cdot m_1(x_j)$

First Order Moments (means) $m_1(x_i)$, $i = 1, \dots, 8$.

Mill Contents -

$$\begin{aligned} \frac{dm_1(x_i)}{dt} = & q_{Fi} - \beta_i \cdot \frac{Q_M}{V_M} \cdot m_1(x_i) - S_{i0} K_L \cdot (m_2(x_i, K_S) + m_1(x_i) \cdot m_1(K_S)) \\ & + \sum_{j=1}^{i-1} S_{j0} K_L b_{ji} \cdot (m_2(x_j, K_S) + m_1(x_j) \cdot m_1(K_S)) \\ & + \gamma_i \cdot \frac{Q_S}{V_S} \cdot \left(c_{i0} m_1(x_{i+4}) + \frac{c_{i1}}{V_S} \cdot \sum_{j=1}^4 \gamma_j \cdot (m_2(x_{i+4}, x_{j+4}) + m_1(x_{i+4}) \cdot m_1(x_{j+4})) \right), \\ & i = 1, \dots, 4. \end{aligned}$$

(A4.1)

Sump Contents -

$$\frac{dm_1(x_i)}{dt} = \beta_{i-4} \cdot \frac{Q_M}{V_M} \cdot m_1(x_{i-4}) - \gamma_{i-4} \cdot \frac{Q_S}{V_S} \cdot m_1(x_i), \quad i = 5, \dots, 8 \quad (A4.2)$$

Note -

$$\frac{dm_1(K_S)}{dt} = 0,0 \quad \text{as it was assumed that the softness parameter would not change over an observation interval.}$$

Second Order Central Moments (Covariances) $m_2(x_i, x_j)$, $i = 1, \dots, 8$; $j = 1, \dots, 8$.Mill - Mill Covariances -

$$\begin{aligned} \frac{dm_2(x_i, x_j)}{dt} = & -(\beta_i + \beta_j) \cdot \frac{Q_M}{V_M} \cdot m_2(x_i, x_j) \\ & - S_{i0} K_L \cdot (m_2(x_i, x_j) m_1(K_S) + m_2(x_j, K_S) m_1(x_i)) \\ & - S_{j0} K_L \cdot (m_2(x_i, x_j) m_1(K_S) + m_2(x_i, K_S) m_1(x_j)) \\ & + \sum_{k=1}^{i-1} S_{k0} K_L b_{ki} \cdot (m_2(x_j, x_k) m_1(K_S) + m_2(x_k, K_S) m_1(x_j)) \\ & + \sum_{k=1}^{j-1} S_{k0} K_L b_{kj} \cdot (m_2(x_i, x_k) m_1(K_S) + m_2(x_k, K_S) m_1(x_i)) \\ & + \gamma_i \cdot \frac{Q_S}{V_S} \left\{ c_{i0} m_2(x_j, x_{i+4}) + \frac{c_{i1}}{V_S} \cdot \sum_{k=1}^4 \gamma_k \cdot (m_2(x_j, x_{i+4}) m_1(x_{k+4}) + m_2(x_j, x_{k+4}) m_1(x_{i+4})) \right\} \\ & + \gamma_j \cdot \frac{Q_S}{V_S} \left\{ c_{j0} m_2(x_i, x_{j+4}) + \frac{c_{j1}}{V_S} \cdot \sum_{k=1}^4 \gamma_k \cdot (m_2(x_i, x_{j+4}) m_1(x_{k+4}) + m_2(x_i, x_{k+4}) m_1(x_{j+4})) \right\} \\ & + \sum_{k=1}^{\min(i,j)} S_{k0}^2 K_L^2 b_{ki} b_{kj} \phi_k^2(\mu_4(x_k^2 K_S^2)) , \\ & i = 1, \dots, 4, \quad j = 1, \dots, 4 \end{aligned} \quad (A4.3)$$

where $\mu_4(x_k^2 K_S^2)$ = fourth order moment, assume

$$\mu_4(x_k^2 K_S^2) \approx m_1^2(x_k) m_1^2(K_S) + m_2^2(x_k) m_2^2(K_S) + 2 \cdot m_2^2(x_k K_S)$$

Sump - Sump Covariances -

$$\begin{aligned} \frac{dm_2(x_i x_j)}{dt} &= \beta_{i-4} \cdot \frac{Q_M}{V_M} \cdot m_2(x_{i-4} x_j) + \beta_{j-4} \cdot \frac{Q_M}{V_M} \cdot m_2(x_i x_{j-4}) \\ &\quad - (\gamma_i + \gamma_j) \cdot \frac{Q_S}{V_S} \cdot m_2(x_i x_j), \quad i = 5, \dots, 8, \quad j = 5, \dots, 8. \end{aligned} \quad (A4.4)$$

Mill - Sump Covariances -

$$\begin{aligned} \frac{dm_2(x_i x_j)}{dt} &= \beta_{j-4} \frac{Q_M}{V_M} \cdot m_2(x_i x_{j-4}) - \gamma_{j-4} \frac{Q_S}{V_S} \cdot m_2(x_i x_j) \\ &\quad - \beta_i \frac{Q_M}{V_M} \cdot m_2(x_i x_j) - S_{i0} K_L (m_2(x_i x_j) m_1(K_S) + m_2(x_j K_S) m_1(x_i)) \\ &\quad + \sum_{k=1}^{i-1} S_{k0} K_L b_{ki} (m_2(x_k x_j) m_1(K_S) + m_2(x_j K_S) m_1(x_k)) \\ &\quad + \gamma_i \frac{Q_S}{V_S} \cdot \left[c_{i0} m_2(x_{i+4} x_j) + \frac{c_{i1}}{V_S} \sum_{k=1}^4 \gamma_k (m_2(x_{i+4} x_j) m_1(x_k) + m_2(x_j x_k) m_1(x_{i+4})) \right], \\ &\quad i = 1, \dots, 4, \quad j = 5, \dots, 8 \end{aligned} \quad (A4.5)$$

Mill - Softness Covariances -

$$\begin{aligned} \frac{dm_2(x_i K_S)}{dt} &= - \beta_i \frac{Q_M}{V_M} \cdot m_2(x_i K_S) - S_{i0} K_L (m_2(x_i K_S) m_1(K_S) + m_2(K_S^2) m_1(x_i)) \\ &\quad + \sum_{k=1}^{i-1} S_{k0} K_L b_{ki} (m_2(x_k K_S) m_1(K_S) + m_2(K_S^2) m_1(x_k)) \\ &\quad + \gamma_i \frac{Q_S}{V_S} \cdot \left[c_{i0} m_2(x_{i+4} K_S) + \frac{c_{i1}}{V_S} \sum_{k=1}^4 \gamma_k (m_2(x_{i+4} K_S) m_1(x_k) + m_2(x_k K_S) m_1(x_{i+4})) \right], \\ &\quad i = 1, \dots, 4 \end{aligned} \quad (A4.6)$$

Sump - Softness Covariances -

$$\frac{dm_2(x_i K_S)}{dt} = \beta_i \frac{Q_M}{V_M} \cdot m_2(x_{i-4} K_S) - \gamma_i \frac{Q_S}{V_S} \cdot m_2(x_i K_S), \quad i = 5, \dots, 8. \quad (A4.7)$$

APPENDIX B

BIBLIOGRAPHY.

1. M. Abramowitz, I.A. Stegun, "Handbook of Mathematical Functions", Dover Publications, 1965, New York. (Nat. Bureau of Stds. 1964.)
2. D. L. Alspach "Dual Control Based on Approximate A Posteriori Density Functions" IEEE trans. automat. control, Vol. AC-17, No. 5, Oct. 1972, p.689-693.
3. D. L. Alspach, H. W. Sorenson "Nonlinear Bayesian Estimation Using Gaussian Sum Approximation" IEEE trans. automat. control, Vol. AC-17, No.4, Aug. 1972, p.439-448.
4. M.P. Amsden, C. Chapman, M. G. Reading "Computer Control of Flotation at the Ecstall Concentrator" 10th APCOM conf. 10-14 April 1972, Johannesburg. (paper 27)
5. B.D.O. Anderson, T. Kailath "The Choice of Signal-Process Models in Kalman Bucy Filtering" J. Math. Anal. and Appl. Vol. 35, No. 3, Sept. 1971, p.659-668.
6. K. J. Astrom "Introduction to Stochastic Control Theory" Academic Press, 1970.
7. K. J. Astrom "On a First-order Stochastic Differential Equation" Int. J. of Control, Vol. 1, no. 4, 1965, p.301-326.
8. A. R. Atkins, "Control of the Mill Classifier Process" Chamber of Mines of South Africa, Internal Report, 1973.
9. S. R. Atre, S.S. Lamba "Derivation of an Optimal Estimator for Distributed Parameter Systems via Maximum Principle" IEEE trans. automat. control. Vol. AC-17, No. 3, June 1972, p.388-390.
10. L. G. Austin "A commentary on the Kick, Bond and Rittinger Laws of Grinding" Powder Technol. Vol. 7, No. 6, June 1973 (a) p.315-317.
11. L. G. Austin "A Review: Introduction to the Mathematical Description of Grinding as a Rate Process" Powder Technol. Vol. 5 No. 1, 1971/72, p.1-17.

12. L. G. Austin "Understanding Ball Mill Sizing" Ind. Engng. Chem., Process. Des. Dev., Vol. 12, No. 2, 1973(b), p.121-129.
13. Y. Bar-Shalom "Optimal Simultaneous State Estimation and Parameter Identification in Linear Discrete-Time Systems" IEEE Trans. automat. control., Vol. AC-17, No. 3, June 1972 (a), p.308-319.
14. Y. Bar-Shalom "Redundancy and Data Compression in Recursive Estimation" IEEE trans. automat. control, Vol. AC-17, No. 5, Oct. 1972(b), p.684-9.
15. L. Basanez, R. M. Huber, J. Pages-Fita "Conversion and Averaging Processes in Stochastic Computation" 4th IFAC/IFIP Int. conf. on Dig. Comp. Applics. to Proc. Control, Zurich, March 19-22, 1974, Part 1, p.25-35.
16. J. H. Bassarear, G. R. McQuie "Onstream Analysis of Particle Size" Min. congress J., Vol. 58, No. 5, May 1972, p.36-42.
17. M. S. Beck, K. T. Lee, N.G. Stanley-Wood, "A New Method of Evaluating the Size of Solid Particles Flowing in a Turbulent Fluid" Powder Technol., Vol. 8, 1973, p.85-90.
18. A. K. Bejczy, R. Shridhar "Approximate Nonlinear Filters and Deterministic Filter gains" Trans. A.S.M.E., Series G (J. of Dynamic Systems, Meas. and Control) Vol. 94, No. 1, March 1972, p.57-63.
19. R. Bellman "Methods of Nonlinear Analysis, Vol. II" Academic Press, 1973, New York.
20. J. S. Bendat, A. G. Piersol, "Random Data: Analysis and Measurement Procedures", J. Wiley, 1971 (revised version of 1966 edition).
21. G. J. Bierman, "Sequential Square Root Filtering and Smoothing of Discrete Linear Systems" Automatica, Vol. 10, March 1974, p.147-158.
22. P. R. Birch, "An Introduction to the Control of Grinding Circuits Closed by Hydrocyclones" Miner. Sci. Engng. Vol. 4, No. 3, July 1972, p.55-66.

23. M.I.G. Bloor, D.B. Ingham "On the Efficiency of the Industrial Cyclone" Trans. Instn. Chem. Engrs., Vol. 51, No. 3, 1973(a), p. 173-176.
24. M.I.G. Bloor, D.B. Ingham "Theoretical Investigation of the Flow in a Conical Hydrocyclone" Trans. Instn. Chem. Engrs., Vol. 51, No. 2, 1973(b), p.36-41.
25. D. Bradley "The Hydrocyclone" Pergamon Press, 1965.
26. M. I. Brittan, E.J.J. van Vuuren "Computer Analysis, Modelling and Optimisation of Gold Recovery Plants of the Anglo-American Group" J.S.Afr. Inst. Min. Metall., Vol. 73, No. 7, Feb. 73, p.211-222.
27. S.R. Broadbent, T.G. Callcott, "Coal Breakage Processes. I.A. New Analysis of Coal Breakage Processes. I. A Matrix Representation of Breakage". J.Inst. Fuel, Vol. 29, Dec.1956, p.524-539.
28. G.F. Brookes, G.W. Cutting, D. Watson, "The Use of a Digital Controller in the Control of a Grinding/Classification Circuit". 9th Int. Miner. Proc. Congress, Prague, 1970, p.383-389.
29. G.F. Brookes, T.H. Hughes, D.Watson, D.J.A. Woodley "Control and Modelling of a Grinding/Classification Circuit", 9th Commonwealth Min. and Metall. Congress, London, Vol. 3, 1969.
30. R.S. Bucy, P.D. Joseph "Filtering for Stochastic Processes with Applications to Guidance" J. Wiley, 1968.
31. J.A. Camp "Kalman Filtering Simulation via Numerical Solution of the Associated Matrix Differential Equations". J. Comp. Phys. Vol. 8, No. 2, Oct. 1971, p.175-196.
32. B. Carnahan, H.A. Luther, J.O. Wilkes, "Applied Numerical Methods" J. Wiley, 1969.
33. K.G. Carr-Brion, P.J. Mitchell, "An 'On-Stream' X-ray Particle Size Sensor", J. Scient. Instrum., Vol. 44, 1967, p.611-614.

34. J.L. Center (Jr), "Practical Nonlinear Filtering of Discrete Observations by Generalised Least Squares Approximation of the Conditional Probability Distribution" 2nd Symp. on Nonlin. Estim. Theory, San Diego, Calif., Sept.13-15, 1971, p.88-99.
35. J.M.C. Clark, "The Representation of Nonlinear Stochastic Systems with Applications to Filtering". Ph.D. Thesis, Imperial College, Elec.Eng.Dept., April 1966.
36. B. Clarke, J.A. Kitchener, "The Influence of Pulp Viscosity on Fine Grinding in a Ball Mill", Br.Chem.Engng., Vol.13, No. 7 (July 1968), p.991-995.
37. H. Cramer, "The Elements of Probability Theory", J. Wiley, 1955.
38. T.C. Crosby, "Process Dynamics of Grinding Circuits and the Use of Automatic Control". Trans. Can. Inst. Min. Metall., Vol. 70, March 1967, p.54-59.
39. H.E. Cross "Automatic Mill Control System", American Min. Cong. 1966 Metal Mining and Industrial Minerals Convention, Salt Lake City, Utah, Sept. 11-14, 1966.
40. T.R. Crossley, B. Porter "Modal Theory of State Observers", Proc. IEE, Vol.118, No. 12, (Dec. 71), p.1835-1838.
41. P.W. Dart, J.A. Sand, "Benefits to be Expected from a Real-time Measurement of Particle Size" 1973 Conf. of Metallurgists, Can.Inst.Min.Metall., Quebec, Canada. August 29, 1973.
42. H.R. Dessau, "Dynamic Linearisation and Nonlinear Filtering with Application to a Tracking Problem", Inf. Sciences Vol. 4, no. 1, Jan.1972, p.51-63.
43. L. Diaz, P.M. Musgrove, "On-line Size Analysis in Grinding Circuit Control". A.I.M.E. Annual meet., Seattle, Sept. 22-24, 1971.
44. N. Draper, K.H. Dredge, A.J. Lynch, "Operating Behaviour of an Automatic Control System for a Mineral Grinding Circuit". Proc. 9th Commonwealth Min.Metall.Congr. Vol. 3, 1969, Paper 22, p.673-699.

45. T.I. Dubenko, "The Kalman Filter for Random Fields (Distributed Parameter Systems)", Automn. remote control, Vol. 33, No. 12, pt.1, Dec.1972, p.1945-8.
46. H.A. Fertik, "Simple Smoothing and Forecasting Methods for Use in Process Control", 12th Joint Auto. Control Conf., St. Louis, 1971. (IEEE) paper no. 6-E2, p.553-561.
47. J.H. Fewings, "Digital Computer Control of a Wet Mineral Grinding Circuit". Symp. on Auto. Control Sys. in Min.Processing Plants, Technical papers, Brisbane, May 71, p.333-357.
48. J.H. Fewings, J.D. Pitts, "Digital Computer Control Systems Application for the Grinding Circuits at the American Smelting and Refining Company's Silver Bell Concentrator." 11th APCOM conf., April 1973, Vol. 2, p.F1-F25.
49. A.F. Filippov "On the Distribution of the Sizes of Particles which Undergo Splitting". Theory of Prob. and its Applics., Vol. 6, No. 3 (1961), p.275-394.
50. D.G. Fisher, B.A. Jacobsen, "Computer Control of a Pilot Plant Evaporator", Chem. Engr. London, No. 279, Nov. 1973, p.552-558.
51. F.J. Fontein "Some Variables Influencing Sieve Bend Performance". A.I.Ch.E. - Instn. Chem. Engrs., London, Sympos. Series No. 1, 1965, p.122-130.
52. F.J. Fontein, J.G. van Kooy, H.A. Leniger "The Influence of Some Variables upon Hydrocyclone Performance". Br.Chem.Engr. Vol. 7, No. 6, June 1962, p.410-421.
53. R.D. Fournier "An observer for On-line Estimation of Flotation Rates" Master of Applied Science Thesis, Dept. of Elec.Engng., Univ. of Toronto, Oct. 1971.
54. R.D. Fournier, H.W. Smith "Experimental Parameter Identification for a Dynamic Model of a Continuous Rod Mill", Can.Min. Metall. Bull, Dec. 72.
55. E.J. Freeh, W.E. Horst, W.L. Adams, R.C. Kellner "Simulation and Analysis of Closed Circuit Grinding" E/MJ, Vol. 174, No. 8, Aug. 1973, p.86-91.

56. F.D. Galiana, F.C. Schweppe, A. Fiechter "Equivalences Among Model Reduction, Filter-Observer and Feedback Control Design" 4th IFAC/IFIP Int. Conf. on Dig. Comp. Applics. to Process Control, Zurich, March 19-22, 1974, p.208-220 of part II.
57. R.P. Gardner, K. Verghese "A Model with a Closed Form Analytic Solution for Steady State, Closed Circuit Comminution Processes" Powder Technol. Vol.II, 1975, p.87-89.
58. S.F. Goldman, R.W.H. Sargent "Applications of Linear Estimation Theory to Chemical Processes: a Feasibility Study". Chem. Engng. Sci. Vol. 26, Oct. 1971, p.1535-1553.
59. S.L. Goren "Distribution of Lengths in the Breakage of Fibres or Linear Polymers". Can.J. of Chem.Engng., Vol.46, June 68, p.185-188.
60. I.A. Gura, A.B. Bierman "On the Computational Efficiency of Linear Filtering Algorithms" Automatica, Vol. 7, No. 3, May 1971, p.299-314.
61. J.C. Hamilton, D.E. Seborg, D.G. Fisher "An Experimental Evaluation of Kalman Filtering" A.I.Ch.E.J., Vol. 19, No. 5, Sept. 1973, p.901-909, also A.I.Ch.E. 74th National Meeting, New Orleans, 1973.
62. J.M. Hammersley, D.C. Handscomb "Monte Carlo Methods" Methuen's Monographs on Applied Probability and Statistics, 1964.
63. V.R. Harvey "Control of Cement Plant Raw Material System" (An Investigation into the Application of Computer Control to a Cement Plant Raw Material Proportioning System) M.Sc. Thesis, Univ. of Natal, July 1972.
64. R.E. Hathaway "A Proven On-stream Particle Size Monitoring System for Automatic Grinding Circuit Control". 1972 Min. and Metall. Indust. group symp. and exhib. of the Instrum. Soc. of Am., Phoenix, Arizona, April 24-25, 1972. Also 7th Annual Symp. of Lake Superior Sect. of the Instrum. Soc. of Am., Duluth, Minnesota, June 15-16, 1972.
65. C. Hecht "Digital Realisation of Nonlinear Filters" 2nd Symp. on nonlin. estim. theory, San Diego, California, Sept. 13-15, 1971, p.152-158.

66. G. Heess "Application of State Space Statistical Linearisation to Optimal Stochastic Control of Nonlinear Systems" Int. J. Control, Vol. 2, No.4, 1970, p.697-701.
67. J.A. Herbst, D.W. Fuersteneau "Influence of Mill Speed and Ball Loading on the Parameters of the Batch Grinding Equation" Trans. S.M.E.-A.I.M.E., Vol. 252, June 1972, p.169-176.
68. J.A. Herbst, G.A. Grandy, T.S. Mika, D.W. Fuersteneau "An Approach to the Estimation of the Parameters of Lumped Parameter Grinding Models from On-line Measurements". Zerklienern, 3rd Europ. Symp. on Comminution. Edit. H. Rumpf and K.S. Schonert, Cannes, 1971. Dechema-Monographien, Vol. 69, 1972, part 1, p.475-514.
69. J.A. Herbst, T.S. Mika "Linearisation of Tumbling Mill Models Involving Nonlinear Breakage Phenomena", 11th APCOM sympos. April 1973, Vol.2, p.E78-E124.
70. J.A. Herbst, T.S. Mika "Mathematical Simulation of Tumbling Mill Grinding: An Improved Method". Proc. 9th Int. Min. Proc. Congr., Ustav Pro Vuyzkum Rud, Prague, 1970, Part III, p.27-37.
71. G.W. Heyes, D.F. Kelsall, P.S.B. Stewart "Continuous Grinding in a Small Wet Rod Mill" -
Part 1 "Comparison with a Small Wet Ball Mill" Powder Technol. Vol.7, No.6, June 1973(a) p.319-325.
Part 2 "Breakage of Some Common Ore Materials" Powder Technol. Vol.7, No.6, June 1973(b), p.337-341.
72. D.H. Himmelblau "Process Analysis by Statistical Methods" J. Wiley 1970.
73. A.B. Holland-Batt "Further Developments of the Royal School of Mines On-stream Particle Size Analyser" Trans. Inst. Min. Metall. Vol. 77, 1968, p.C185-C190.
74. J.H. Hughen, V. Vimolvanich "Recursive Nonlinear Estimation Using a Quasi-Moment Approximation" Proc. 5th Hawaii Int. Conf. on Syst. Science, Honolulu, Hawaii, 11-13 Jan. 1972, p.486-488.

75. Institute of Electrical and Electronic Engineers "Computer and Control Abstracts" Published Monthly by IEEE.
76. R. Iserman, V. Baur, W. Bamberger, P. Kneppo, H. Siebert "Comparison of Six On-line Identification and Parameter Estimation Methods" Automatica, Vol. 10, 1974, p.81-103.
77. A.H. Jazwinski "Stochastic Processes and Filtering Theory" Academic Press, 1970.
78. R.E. Kalman "A New Approach to Linear Filtering and Prediction Problems" J. Basic Engng., Vol. 82, March 1960, p.35-45.
79. R.E. Kalman, R.S. Bucy "New Results in Linear Filtering and Prediction Theory" J. Basic Engng., Vol. 83, March 1961, p.95-108.
80. T. Kaneko, B. Liu, "Effect of Coefficient Rounding in Floating Point Digital Filters". IEEE trans. Aerospace and Electronic Systems, Vol.AES-7, No.5, Sept. 1971, p.995-1003.
81. D. Kanungo, T.C. Rao "A Study on the Performance of a 3 Inch Hydrocyclone Classifier". Can. Min. Metall. Bull., Vol.66, No.735, July 1973, p.78-80.
82. I.E. Kazakov "Algorithm for Determining Probability Density Function of Phase Coordinates in a Nonlinear Stochastic System". Automation and Remote Control, Vol.30, No.5, May 1969, p.54-56.
83. F.J. Kelly "Operations Analysis, Process Design and Process Control" Can. Min. J., Vol.94, No.6, June 1973, p.43-44.
84. D.F. Kelsall "A Study of the Motion of Solid Particles in a Hydraulic Cyclone" Trans. Instn. Chem. Engrs. Vol.30, 1952, p.87-108.
85. D.F. Kelsall, K.J. Reid, C.J. Restarick, "Continuous Grinding in a Small Wet Ball Mill" -
 Part 1 "A Study of the Influence of Ball Diameter"
 Powder Technol. Vol.1, 1967/68, p.291-300.
 Part 2 "A Study of the Influence of Hold-up Weight"
 Powder Technol. Vol.2, 1968/69, p.162-168.
 Part 3 "A Study of the Distribution of Residence Time"
 Powder Technol. Vol.3, 1969/70, p.170-178.

D.F. Kelsall, P.S.B. Stewart, K.R. Weller ...

Part 4 "A Study of the Influence of Grinding Media Load and Density" Powder Technol. Vol.7, 1973(a), p.293-301.

Part 5 "A Study of the Influence of Media Shape" Powder Technol. Vol.8, 1973(b), p.77-83.

86. R.P. King "An Analytical Solution to the Batch Comminution Equation" J.S.Afr. Inst. Min. Metall., Vol.73, No.4, Nov.1972(a), p.127-131.
87. R.P. King "An Introduction to Stochastic Differential Equations: Abbreviated Lecture Notes" National Institute for Metallurgy, report no. 1025, 19 March 1971(a), Project C9/69 report 2. (Johannesburg).
88. R.P. King "Applications of Stochastic Differential Equations to Chemical Engineering Problems - An Introductory Review" Unpublished paper, 1972(b).
89. R.P. King "Continuous Flow Systems with Stochastic Transfer Functions" Part I - C.E.S., Vol.23, 1968, p.1035-1044.
Part II - C.E.S., Vol.26, 1971(b), p.729-737.
90. R.P. King "The Control of the Slurry Conditioning System in a Mineral Flotation Plant by On-line Digital Computer" IFAC 5th World Congress, Paris, June 1972(c).
91. R.P. King "Visit to University Departments and Flotation Plants in North America and Europe, May-June 72" National Institute for Metallurgy, Technical Memorandum, Project 009/71, 1972(d) (Johannesburg).
92. "The Kloof Concentrator" (no author given), Mining Mag., London, Vol. 128, No.2, Feb.73, p.76-87.
93. D.E. Knuth "The Art of Computer Programming, Vol. 2, Seminumerical Algorithms" Addison-Wesley 1969.
94. V.G. Lapa "Estimate of the Efficiency of Adaptive Prediction Algorithms" Eng. Cybern. Vol.8, No.6, Nov.1970, p.1176-1183.
95. R.E. Larson, E. Tse, "Modal Trajectory Estimation and Parallel Computers" 2nd Sympos. on non.lin. estim. theory, San Diego, California, Sept. 13-15, 1971, p.188-198.
96. M.J. Lees "A Further Study of the Hydrocyclone" B.Sc.Thesis, Fac.Sci., University of Queensland, Australia, 1968.

97. M.J. Lees "Small Digital Computers for the Control of Mineral Processing Plants" Australian Comp. J., Vol.3, No.4, Nov. 1971, p.146-149.
98. M.J. Lees, A.J. Lynch "Dynamic Behaviour of a High Capacity Multi-Stage Grinding Circuit" Trans.Instn. Min.Metall., Vol.81, No.793, Dec.1972.
99. T. Leskinen, H. Penttilä "Computer Control at Kotalahti" Min.Mag., London, Vol.128, No.4, April 1973, p.239,241,243.
100. C.L. Lewis "Application of a Computer to a Flotation Process" Can. Min.Metall.Bull., Jan.71, also 72nd Annual gen.meet. of the C.I.M., Toronto, April 70.
101. P.J. Lloyd, A.R. Atkins, A.L. Hinde "Measurement and Control of Particle Size in a Milling Circuit". Joint Symp. on Meas. and Control in the Chem. Proc. Ind., 11 Sept. 1974, (SAICHe and SAIM&C, Johannesburg.)
102. P.T. Luckie, L.G. Austin "A Review Introduction to the Solution of the Grinding Equations by Digital Computation" Miner. Sci.Engng., Vol.4, No.2, April 1972, p.24-51.
103. A.J. Lynch, T.C. Rao "The Operating Characteristics of Hydrocyclone Classifiers" Indian J. Technol., Vol.6, 1967, p.106-114.
104. A.J. Lynch, T.C. Rao, K.A. Prisbey "The Influence of Hydrocyclone Diameter on Reduced Efficiency Curves", Int.J.Miner. Proc., Vol. 1, 1974, p.173-181.
105. A.J. Lynch, G.G. Stanley "Automatic Control in Australian Mineral Processing Plants". World Mining, May 1971, p.24-29.
106. A.K. Mahalanabis "On Minimising the Divergence in Discrete Filters" IEEE Trans. auto.control, Vol.AC-17, No.2, April 1972, p.239-240.
107. A.K. Mahalanabis, M. Farooq "A Second-Order Method for State Estimation of Nonlinear Dynamical Systems" Int. J. Control, Vol. 14, No.4, 1971, p.631-639.
108. J.S. Meditch "Filtering and Smoothing of Boundary and Interior Measurement Data for Distributed Parameter Systems". Proc. 9th IEEE symp. on adaptive process. Texas, USA. 7-9 Dec. 1970, p.V.1.1-V.1.6.

109. J.S. Meditch "Least Squares Filtering and Smoothing for Linear Distributed Parameter Systems" Automatica, Vol.7, No.3, May 1971, p.315-322.
110. O. Molerus "Stochastisches Modell der Gleichgewichtssichtung" Chemie-Ing-Techn.39, Jahrg 1967/Hef 13, p.792-796.
111. A.L. Mular, W.R. Bull, "Mineral Processes: Their Analysis, Optimisation and Control". Notes for Summer School run by the authors, 1969; Univ. of Brit. Columbia, Vancouver, B.C., Canada, and Colorado School of Mines, Golden, Colorado, USA.
112. M.E. Muller, "A Comparison of Methods for Generating Normal Deviates on Digital Computers". J.Assoc. Comp. Machines, Vol.6, 1959, p.376-383.
113. T. Nomura, K. Nakamura, "Discrete Time Regulator of an Infinite Dimensional System" J. Franklin Inst., Vol. 293, No.4, April 1972, p.229-241.
114. A.R.M. Noton "Two Level Form of the Kalman Filter". IEEE trans. automat.control., Vol. AC-16, No.2, April 1971, p.128-133.
115. Yu Ya Ol'skii "Automated Control Systems". Soviet J. Non-ferrous Metals, Vol. 12, No.3, March 1971, p.12-22.
116. B.F. Osborne "A Complete System for On-Stream Particle Size Analysis" Can. Min. Metall. Bull., Sept.1972, p.97-107.
117. B.F. Osborne "A Practical On-Stream Particle Size Analysis System" Instrum. Soc. Am., 25th conf. on advances in instrumentation, Vol.25, pt.4, Oct.1970, p.844.1-844.8.
118. A. Papoulis "Probability, Random Variables and Stochastic Processes" McGraw-Hill, 1965.
119. J.H. Perry, "Chemical Engineers Handbook", McGraw-Hill, Tokyo, 1963.
120. T.H. Peterson, J.W. White, E.E. Krist "Off-line Development and Testing of a Minicomputer Process Control Program for an Industrial Grinding Circuit" SME-AIME 103rd annual meet., Dallas, Texas, Feb.24-28, 1974.
121. C.L. Philips "Instabilities Caused by Floating-Point Arithmetic Quantisation" IEEE trans. automat. control, Vol.AC-17, No.2, April 1972, p.242-243.

122. J.H. Pownall "Control Applications Grinding Circuit" Warren Spring Lab., Dept. Scientific and Indus. research, CRR/MP/69, Parc Mine proj., report 4.2, Feb.1964.
123. A. Ralston, H.S. Wilf "Mathematical Methods for Digital Computers" (Vols. 1 and 2) J. Wiley, 1967.
124. R.J. Ricci "A Method for Monitoring Particle Size Distribution in Process Slurries". Trans.Inst.Stand.Am., Vol.9, No.1, 1970, p.28-36, also Procedyne Corp. Bulletin no. PA-10.
125. E.A. Robinson "Multichannel Time Series Analysis with Digital Computer Programs" Holden-Day, Inc., San Francisco, 1967.
126. H.J. Rome "Finite Memory Batch Processing Smoother" IEEE trans. aerospace and electron. syst., Vol.AES-7, No.5, Sept. 1971, p.968-973.
127. C.A. Rowland "Automation of Grinding Circuits" Pit and Quarry, Vol. 56, July 1963, p.176-179.
128. J.E. Sacks, H.W. Sorenson "Nonlinear Extensions of the Fading Memory Filter". IEEE trans. automat.control, Vol.AC-16, No.5, Oct. 1971, p.506-7.
129. A.P. Sage, J.L. Melsa "Estimation Theory with Applications to Communications and Control" McGraw-Hill, 1971.
130. G. Sansone (translated by A.H. Diamond) "Orthogonal Functions" Interscience, New York, 1959.
131. G.N. Saridis "Comparison of Six On-line Identification Algorithms" Automatica, Vol. 10, 1974, p.69-79.
132. M. Schilder "A Power Series Expansion for Nonlinear Kalman-Bucy Filtering" 2nd symp. on nonlin. estim. theory, San Diego, California, 13-15 Sept. 1971, p.282-287.
133. K. Schonert "The Influence of Classifier Characteristics on the Stability of Closed Circuit Grinding". A Decade of Dig. comp. in the mineral indus. ed. A. Weiss, AIME, NY 1969, p.677-694.
134. D.E. Seborg, D.G. Fisher, J.C. Hamilton "An Experimental Evaluation of State Estimation in Multivariable Control Systems" 4th IFAC/IFIP Int. conf. on dig. comp. applics. to proc.contr., Zurich, March 19-22, 1974, Part I, p.144-155.

135. Yu A. Shreider "The Monte Carlo Method" Pergamon Press, 1966.
136. R.A. Singer, R.G. Sea "Increasing the Computational Efficiency of Discrete Kalman Filters" IEEE trans. automat. contr. Vol.AC-16, No.3, June 1971, p.254-257.
137. D.L. Slotnik "The Fastest Computer" Scient.Am., Feb.1971, p.76-87.
138. H.W. Smith, C.L. Lewis "Computer Control Experiments at Lake Dufault", Can.Min.Metall.Bull., Vol.62, No.682, Feb. 1969, p.109-115.
139. Yu. A. Solov'yev "Approximation of Multidimensional Linear Filters" Eng.Cybern., Vol.8, No.6, Nov.1970, p.1237-1241.
140. H.W. Sorenson, D.L. Alspach "Recursive Bayesian Estimation Using Gaussian Sums". Automatica, Vol.7, No.4, July 71, p.465-479.
141. P.S.B. Stewart "The Control of Wet Grinding Circuits", Austral. Chem.Proc.Engng., Vol.23, No.7, July 1970, p.22-33.
142. A.R. Stubberud, W.K. Masenten "Polynomial Estimators". Proc. 9th IEEE Symp. on adaptive procs.: decision and control, Austin, Tex., USA, 7-9 Dec. 1970, p.XIX.1.1-XIX.1.7.
143. A.A. Sveshnikov "Problems in Probability Theory, Mathematical Statistics and Theory of Random Variables". W.B. Saunders, 1968.
144. P. Swerling "Classes of Signal Processing Procedures Suggested by Exact Minimum Square Error Procedures" SIAM.J. of Appl. Math., Vol.14, No.6, Nov.1966(a), p.1199-1224.
145. P. Swerling "Note on a New Computational Data Smoothing Procedure Suggested by Minimum Mean Square Error Estimation". IEEE trans. inform. theory, Vol.12, No.1, Jan.1966(b) p.9-12.
146. P. Swerling, G.B. Goldstein, D.J. Arnold "Bayes' Nonlinear Estimation with a Fourth Order Series Approximation to the Logarithm of the Conditional Probability Density", 2nd symp. on nonlin. estim. theory, San Diego, California, 13-15 Sept. 1971, p.333-339.

147. E.C. Tacker, T.D. Linton "Digital and Hybrid Simulation of a Bayes-Optimal Nonlinear Filter" Project Themis, Tech. report no.40, LSU-T-TR-40, College of Egng., Louisiana State Univ., Sept. 1970.
148. A.F. Taggart "Handbook of Mineral Dressing" J. Wiley, New York, 1927.
149. L. Takacs "Stochastic Processes" Methuen Monographs on Applied Prob. & Stats., 1968.
150. D.T. Tarr "Practical Application of Liquid Cyclones in Mineral Dressing Problems". Krebs Engrs., 1205 Chrysler Drive, Menlo Park, California, 94025, 7 Oct.1965.
151. W.H.A. Timms, A.J. Williams "Grinding and Classification Control at Lake Dufault Mines, Ltd." AIME Ann.meet. Denver, Colorado, 15-19 Feb.1970(a), preprint no. 70-B-43.
152. W.H.A. Timms, A.J. Williams "Milling Practices and Process-Control Techniques Employed at Lake Dufault Mines, Ltd." AIME world symp. on min., metall. of lead & zinc, St. Louis, 1970(b), vol.1, p.616-641.
153. E. Tse "Parallel Computation of the Conditional Mean State Estimate for Nonlinear Systems" 2nd symp. on nonlin. estim. theory, San Diego, California, 13-15 Sept. 1971, p.385-394.
154. S.G. Tzafestas "Bayesian Approach to Distributed Parameter Filtering and Smoothing" Int. J. Control, Vol.15, No.4, April 1972, p.665-671.
155. M.T. Wasan "Parametric Estimation" McGraw-Hill, 1970.
156. D. Watson, R.W.G. Cropton, G.F. Brookes, "Modelling Methods for a Grinding/Classification Circuit and the Problem of Plant Control" trans.instn.min.metall., Vol.79, 1970, p.C112-C119.
157. C.C.B. Webber, L.S. Diaz, "Automatic Particle Size and Rod Mill Tonnage Control at Craigmont". Can. Min. J., Vol.94, No.6, June 1973, p.36-37, also Can. Min. Procs. Ann. meet., Ottawa, Ont., 23-25 Jan. 1973.
158. N. Weiss "Automatic Grinding Circuit Control by 'Water Balance' and 'Delta-T' ", Mining World, Vol.22, No.7, June 1960, p.30-33.

159. C.H. Wells "Application of Modern Estimation and Identification Techniques to Chemical Processes", A.I.Ch.E. J., Vol.17, No.4, July 1971, p.966-973.
160. J.W. White "Survey of Automated Controls Generates both Negative and Positive Feedback" E/MJ, Vol.175, No.2, Feb.1974, p.59-66.
161. R.C. White "A Survey of Random Methods for Parameter Optimisation" Simulation, Nov. 1971, p.197-205.
162. R.L. Wiegel "Progress Report on the Direct Digital Control of Cyclone Overflow Size in Taconite Processing" 11th APCOM conf., April, 1973, vol.2, p.F26-F67.
163. J.E. Williamson "The Automatic Control of Grinding Medium in Pebble Mills" J.S.Afr.Inst.Min.Metall., Vol.60, Feb.1960, p.333-345.
164. D.A. Wismer, C.H. Wells "A Modern Approach to Industrial Process Control", Automatica, Vol.8, No.2, March 1972, p.117-125.
165. E. Wong "The Construction of a Class of Stationary Markov Processes" Proc. Symp. on Appl. Maths. - Am.Math.Soc., Providence, Rhode Island, Vol.16, 1964, p.264-276.
166. E. Wong, J.B. Thomas "On Polynomial Expansions of Second-Order Distributions" J.Soc.Indust.Appl.Math., Vol. 10, No.3, Sept.1962, p.507-516.
167. E. Wong, M. Zakai "On the Relationship Between Ordinary and Stochastic Differential Equations" Int.J.Engng.Sci., Vol.3, 1965(a),p.213-229.
168. E. Wong, M. Zakai "On the Convergence of Ordinary Integrals to Stochastic Integrals" Annals of Math.Stats., Vol.36, 1965(b), p.1560-1564.
169. T. Yoshimura, T. Soeda "The Application of the Monte-Carlo Method to the Nonlinear Filtering Problem", 2nd symp. on nonlin. estim. theory, San Diego, California, 13-15 Sept. 1971, p.395-398.

APPENDIX CListing of Programmes Used in the Filter.

This appendix contains the relevant programmes used in the mill filter. They are all written in Fortran IV for the CDC 1700 computer. Each programme contains comments to guide the reader as to the purpose of each section, and these should be read in conjunction with the corresponding section in the main body of the thesis, as indicated below. (See also the CDC manuals on Fortran IV and Fortran in a multiprogramming environment, as well as the Departmental programming notes.)

	<u>Page</u>
(1) IBSTST. Used to perform volumetric filter calculations. (See section 4.3.7.)	C2
(2) IBCDRV. This calculates derivatives of the estimates of means and variances for use in the p.s.d. filter evolution step. (See section 4.3.6 and appendix A.)	C2
(3) IBPOBS. This performs the observation step in the p.s.d. filter. (See section 4.3.6.)	C4
(4) IBFVAR. Subroutine used by IBPTOF (see below).	C4
(5) IBPTOF. Calculates concentrations and size distributions from raw state variable estimates. (See section 4.3.5.)	C5
(6) IBSIMP. Simplified version of IBPTOF. (See section 4.3.5.)	C6
(7) IBMFLC. Main programme for running the filter off line on stored data. (See section 4.3.7.)	C6
(8) IBOLMF. Main programme for on-line filter operation. Communicates with control programme through communication block 9. (See sections 4.3.7 and 5.6)	C8
(9) IBPRPC. Prepares data for the filter. (Section 4.3.7.)	C9

IBSTST/...

BSTST

```

SUBROUTINE IBSTST(PHI,PSI,CON,M,AKALK,YMA,XMB,XAVER,UMA,UMB,
  UAUVER,DU,QUAV,YOBS,R,NS,NP,ND,PA,PB,PC,PD)
...SUBROUTINE TO HANDLE REAL-TIME EVOLUTION OF A STATIONARY FILTER FOR MEANS
...ONLY. STARTS AT OBS STEP. UPDATES MEANS OF STATE AND PARAMETERS BEFORE.
...OBSERVATIONS XMB & UMB, USING YOBS & AKALK, TO GET XMA & UMA AFTER (RSERV.
...THEN COMPUTES UMB AFTER CHANGES DU, AND AVERAGE CONTROLS OVER NEXT INTERVAL
...FROM UMA + QUAV. TAKES EVOL STEP TO GET NEW XMB AND COMPUTES AVERAGES OF
...STATE OVER NEXT INTERVAL, XAVER.
...IF OBSERVATIONS ARE NEARER STATE AT BEGINNING OF PREVIOUS INTERVAL (POSSIBLE
...PLANT MODEL FAILURE) THEN THOSE VALUES ARE USED FOR THE UPDATE. IF NORMAL=
...ISED OBSERVATION ERROR IS GREATER THAN CRITERION (POSSIBLE OBS MODEL FAIL)
...THEN OBSERVATION ERRORS ARE SCALED DOWN.
  DIMENSION PHI(1),PSI(1),CON(1),M(1),AKALK(1)
  DIMENSION XMA(1),XMB(1),XAVER(1),UMA(1),UMB(1),UAUVER(1)
  DIMENSION DU(1),QUAV(1),YOBS(1),R(1)
  DIMENSION PA(1),PB(1),PC(1),PD(1)
...DIMENSIONS OF PA,PB,PC, ALL .GT. NS+NP
... (X U)AUG A = (X U)AUG B + AKALK * (YOBS - AM * (X U)AUG B)
  DO 1 I=1,NS
    PC(I)=XMA(I)
  1 PA(I)=XMB(I)
  DO 2 I=1,NP
    II=I+NS
    PC(II)=UMA(I)
  2 PA(II)=UMB(I)
  NT=NS+NP
  FRA=0.0
  FRR=0.0
  DO 6 I=1,ND
    II=M(I)
    PD(I)=YOBS(I)-PC(II)
    PH(I)=YOBS(I)-PA(II)
    ERA=ERA+PD(I)**2/R(I)
    FRR=FRR+PB(I)**2/R(I)
  6 CONTINUE
...CHECK FOR PLANT MODEL FAILURE
  IF (ERR.LF.ERA) GO TO 7
  DO 8 I=1,NS
    XMR(I)=XMA(I)
  8 PA(I)=PC(I)
  DO 9 I=1,NP
    II=I+NS
    PA(II)=PC(II)
  DO 10 I=1,ND
    PH(I)=PD(I)
    FRR=FRR
  7 CRIT=4.0+1.4*FLOAT(ND)
...CHECK FOR OBS MODEL FAILURE
  IF (FRR.LT.CRIT) GO TO 11
  RAT=SQRT(CRIT/FRR)
  DO 12 I=1,ND
    PH(I)=RAT*PB(I)
  12 CONTINUE
  CALL MATMPY(AKALK,PB,PC,NT,ND,1)
  CALL MATADD(PA,PC,PA,NT,1)
...SEPARATE (X U)AUG AND COMPUTE UMB=UMA+DU, UAUVER=UMA+QUAV
  DO 3 I=1,NS
    XMA(I)=PA(I)

```

```

  II=I+NS
  UMA(I)=PA(II)
  UMR(I)=PA(II)+DU(I)
  4 UAUVER(I)=PA(II)+QUAV(I)
C... EVOLUTION OF STATE MEANS. XMR = PHI * XMA + PSI * UAUVER + CON
  CALL MATMPY(PSI,UAUVER,PA,NS,NP,1)
  CALL MATADD(PA,CON,XMR,NS,1)
  CALL MATMPY(PHI,XMA,PA,NS,NS,1)
  CALL MATADD(PA,XMR,XMR,NS,1)
  DO 5 I=1,NS
    XAVER(I)=0.5*(YMA(I)+XMB(I))
  RETURN
END

```

IBCDRV

```

SUBROUTINE INCDRV(PM,PVAR,PSV,SOFTV,SOFT,S,AKL,B,QMDVM,QSDVS,
  IRETA,GAMMA,PHI,CO,C1,V,S,FEED,DPM,DPVAR,DPSV)
C...SUBROUTINE TO CALCULATE DERIVATIVES OF MEANS AND VARIANCES FOR 4 SIZE GROUPS
C...IN SUMP AND MILL, USING IMPROVED CYCLONE MODEL, ROCK SOFTNESS, AND MATRICES
C...STORED IN SQUARE FORM
C---PM = VECTOR OF MEANS, PVAR = VARIANCE MATRIX OF MILL AND SUMP MASSES
C---PSV = VAR WITH SOFTNESS, SOFTV = VAR OF SOFTNESS, SOFT = SOFTNESS
C---S = SELECTION FUNCTION FUNCTION VECTOR, AKL = LOADING SCALING FACTOR FOR
C---S FUNCTION, B = BREAKAGE FUNCTION MATRIX
C---QMDVM = QM/VM, QSDVS = QS/VS BETA, GAMMA = CLASSIFICATION CONSTANTS
C---PHI = INTENS OF NOISE ON S, CO, C1 = CYCLONE CLASSIFICATION CONSTANTS
C---VS = SUMP VUL, FEED = MILL FRESH FEED VECTOR
C---DPM, DPVAR, DPSV = DERIVS TO BE CALCULATED BY THIS SUBROUTINE
  DIMENSION PM(8),PVAR(64),PSV(8),DPM(8),DPVAR(64),DPSV(8)
  DIMENSION S(4),B(16),BETA(4),GAMMA(4),PHI(4)
  DIMENSION CO(4),C1(4),FEED(4),HA(8)
  DIMENSION GQV(4),BOV(4),CGQV(4),CGQVV(4),SR(16)
C...CALCULATE TYPICAL TERMS
  DO 11 I=1,4
    GQV(I)=GAMMA(I)*QSDVS
    BOV(I)=BETA(I)*QMDVM
    CGQV(I)=GQV(I)*CO(I)
    CGQVV(I)=GQV(I)*C1(I)/VS
  11 CONTINUE
C...S MUST HAVE ZERO 4TH ELEMENT, AND B MUST BE
C...
C...
C...


|    |     |     |     |
|----|-----|-----|-----|
| -1 | B12 | B13 | B14 |
| 0  | -1  | B23 | B24 |
| 0  | 0   | -1  | 1   |
| 0  | 0   | 0   | 0   |


  DO 14 I=1,4
    II=I
    X=AKL*S(I)
    DO 14 J=1,4
      SR(II)=X*B(II)
    II=II+4
  14 CONTINUE
C...CYCLONE PART OF CHVAR MILL-MILL-SUMP, MILL-SOFTNESS, AND MILL MEANS.
  II=0
  DO 40 J=1,8
    HA(J)=0.0
    II=II+4
    DO 40 I=1,4
      II=II+1
      HA(J)=HA(J)+PVAR(II)*GAMMA(I)
  40 CONTINUE

```



```

MH=0.0
HC=0.0
DO 43 I=1.4
II=I+4
HC=HC+PSV(II)*GAMMA(I)
HR=HR+PM(II)*GAMMA(I)
43 CONTINUE
II=0
LOOP OVER PM ROW
DO 41 J=1.4
JJ=J+4
IK=J-4
X=CGQVV(J)*HR+CGQV(J)
Y=PM(JJ)*CGQVV(J)
DPSV(J)=PSV(JJ)*X+HC*Y
DPM(J)=PM(JJ)*X+HA(JJ)*CGQVV(J)
LOOP OVER PM, PS COLUMN
DO 41 K=1.8
II=II+1
IK=IK+8
DPVAR(II)=HA(K)*Y+X*PVAR(IK)
41 CONTINUE
..COVARS OF SUMP-SUMP AND SUMP-SOFTNESS, ALSO MEANS OF SUMP MASSES
IJ=32
J1=60
DO 60 J=1.4
JJ=J+4
IJ=IJ+4
JI=JI-31
DPM(JJ)=BQV(J)*PM(J)-GQV(J)*PM(JJ)
DPSV(JJ)=BQV(J)*PSV(J)-GQV(J)*PSV(JJ)
DO 61 I=1.4
IJ=IJ+1
JI=JI+8
IF (I-J) 62,63,64
64 X=GQV(I)+GQV(J)
DPVAR(IJ)=BQV(I)*PVAR(IJ-4)+BQV(J)*PVAR(JI-32)-X*PVAR(IJ)
GO TO 61
63 DPVAR(IJ)=2.0*(BQV(I)*PVAR(IJ-4)-GQV(I)*PVAR(IJ))
GO TO 61
62 DPVAR(IJ)=DPVAR(JI)
61 CONTINUE
60 CONTINUE
..GRINDING AND TRANSPORT SECTION. FINISHING OF COVARS OF MILL MASSES WITH
..SUMP AND SOFTNESS, ALSO EXTEND MILL-MILL COVARS
II=0
JJ=-4
IJ=-4
LOOP FOR PM ROW
DO 50 J=1.4
II=II+4
IJ=IJ+4
JJ=JJ+4
HB=0.0
HC=0.0
DO 51 K=1.4
JK=J+K
HB=HB+SB(JK)+PM(K)
HC=HC+SB(JK)*PSV(K)
HA(K)=SB(JK)*SOFT
51 CONTINUE
Y=FEED(J)=BQV(J)*PM(J)
DPM(J)=DPM(J)+Y+HC+HB*SOFT

```

```

Y=HA(J)-BQV(J)
C LOOP FOR PM AND PS COL
DO 53 I=1.4
II=II+1
IJ=IJ+1
KI=I+4
KJ=J
DPVAR(II)=DPVAR(II)+PSV(I+4)*HB+BQV(I)*PVAR(IJ)
DPVAR(IJ)=DPVAR(IJ)+PSV(I)*HB
HA(J)=X-GQV(I)
DO 52 K=1.4
DPVAR(II)=DPVAR(II)+HA(K)*PVAR(KI)
IF (K.F0.4) HA(J)=X
DPVAR(IJ)=DPVAR(IJ)+HA(K)*PVAR(KJ)
KI=KI+8
KJ=KJ+8
52 CONTINUE
53 CONTINUE
C COV OF PM WITH SOFTNESS
DPSV(J)=DPSV(J)+SOFTV*HB
DPSV(J)=DPSV(J)+HC*SOFT-BQV(J)*PSV(J)
50 CONTINUE
C...COPY SUMP-MILL INTO MILL-SUMP
JI=0
DO 42 I=1.4
JI=JI+4
IJ=I+24
DO 42 J=1.4
JI=JI+1
IJ=IJ+8
DPVAR(IJ)=DPVAR(JI)
42 CONTINUE
C...FINISH OFF COVARS OF MILL-MILL BY ADDING NOISE ON S FUNCTION TERMS
C PREPARE 4TH MOMENTS
X=SOFTV+SOFT*SOFT
II=-8
DO 30 I=1.4
II=II+9
Y=PVAR(II)+PM(I)*PM(I)
Z=PSV(I)*(2.0*PSV(I)+4.0*PM(I)*SOFT)
HA(I)=(X+Y+Z)*PH1(I)*PH1(I)
30 CONTINUE
C COMPUTE TERMS IN MILL-MILL COVARS
II=-4
IJ=24
JI=-4
DO 31 I=1.4
II=II+4
IJ=IJ-31
JI=JI+4
JJ=-4
DO 31 J=1.4
IJ=IJ+8
JI=JI+1
JJ=JJ+4
IF (I.G1.4) GO TO 33
KI=II
KJ=JJ
DO 34 K=1.4
KI=KI+1
KJ=KJ+1
DPVAR(KI)=DPVAR(KI)+DPVAR(IJ)+HA(K)*SB(KI)*SB(KJ)
GO TO 34

```



```

34 CONTINUE
31 CONTINUE
RETURN
END

```

BPOBS

```

SUBROUTINE IBPOBS(VAR,PSV,SOFTV,R,XM,SOFT,ORS,CO,C1,GAM,ETA,
1QS,VS,QU,PA,PB)
C...THIS SUBROUTINE HANDLES SLURRY CONCENTRATION MEASUREMENTS AROUND CYCLONE,
USING MODIFIED SECOND ORDER FILTER EQUATIONS
---VAR = VARIANCE OF STATE. PSV = STATE - SOFTNESS COVARIANCE
---SOFTV = VAR OF SOFTNESS. R = OBSERVATION VARIANCE
---XM = MEANS OF STATE. SOFT = SOFTNESS FACTOR. ORS = OBSERVATIONS OF CYCLON
---FEED AND OVERFLOW. CO, C1 = CLASSIFICATION FUNCTION PARAMETERS FOR CYCLON
---GAM = GAMMA, THE CLASSIFICATION ON LEAVING THE SUMP
---ETA = CLASSIFICATION IN CYC O/F TANK
---QS = SUMP WITHDRAWAL = CYCLONE FEED RATE. VS = SUMP VOLUME
---QU = UNDERFLOW TOTAL VOLUME FLOW. PA, PB = AREAS FOR INTERMEDIATE STORAGE
VAR64,PSV8,R4,XM8,ORS2,CO4,C14,GAM4,PA18,PB18
DIMENSION VAR(1),PSV(1),R(1),XM(1),ORS(1)
DIMENSION CO(1),C1(1),GAM(1),ETA(1),PA(1),PB(1)
DIMENSION VOBS(4),YD(2)
C...CALCULATE EXTRA TERM GIVING NONLINEARITY OF OBSERVATION
EXTRA=0.0
IJ=28
DO 1 I=1,4
IJ=IJ+8
DO 1 J=I,4
JJ=IJ+J
TERM=(C1(I)/ETA(I)+C1(J)/ETA(J))*GAM(I)*GAM(J)*VAR(JJ)
IF (I.EQ.J) TERM=0.5*TERM
1 EXTRA=EXTRA+TERM
QK=QS/(VS*(QS-QU))
EXTRA=-QK*EXTRA/VS
C...CALCULATE VAR*(LINEARISED OBSERVATION MATRIX)TRANS IN PA AND INITIALLY
PREDICTED OBSERVATIONS THEN OBSERVATION ERRORS IN YD
SA=0.0
SB=0.0
YD(1)=0.0
DO 2 I=1,4
X=GAM(I)*XM(I+4)
YD(1)=YD(1)+X
SA=SA+X*C1(I)/ETA(I)
SB=SB+X*(1.0-CO(I))/ETA(I)
2 CONTINUE
YD(1)=YD(1)/VS
YD(2)=ORS(2)-QK*(SB-YD(1)*SA)-EXTRA
SA=SA/VS
DO 3 I=1,18
3 PA(I)=0.0
IJ=32
DO 4 I=1,4
II=I+4
XA=GAM(I)/VS
XB=QK*GAM(I)*((1.0-CO(I)-C1(I)*YD(1))/ETA(I)-SA)
PA(9)=PA(9)+XA*PSV(II)
PA(18)=PA(18)+XB*PSV(II)
DO 5 J=1,4
IJ=IJ+1

```

```

JJ=JJ+9
PA(J)=PA(J)+XA*VAR(IJ)
PA(JJ)=PA(JJ)+XB*VAR(IJ)
5 CONTINUE
PB(I)=YA
PB(II)=XH
4 CONTINUE
YD(J)=ORS(1)-YD(1)
C...CALCULATE VOBS AND INVENT IT
DO 6 I=1,4
6 VOBS(I)=H(I)
DO 7 I=1,4
VOBS(1)=VOBS(1)+PB(I)*PA(I+4)
VOBS(2)=VOBS(2)+PB(I)*PA(I+13)
VOBS(4)=VOBS(4)+PB(I+4)*PA(I+13)
7 CONTINUE
DET=VOBS(1)*VOBS(4)-VOBS(2)*VOBS(2)
HOLD=VOBS(1)
VOBS(1)=VOBS(4)/DET
VOBS(4)=HOLD/DET
VOBS(2)=-VOBS(2)/DET
C...CALCULATE MEANS OF STATE AND PARAMETERS AND MULTIPLY VOBS BY PBTRANS
HOLD=YD(1)
YD(1)=VOBS(1)*HOLD+VOBS(2)*YD(2)
YD(2)=VOBS(2)*HOLD+VOBS(4)*YD(2)
DO 8 I=1,9
II=I+9
PB(I)=VOBS(1)*PA(I)+VOBS(2)*PA(II)
PB(II)=VOBS(2)*PA(I)+VOBS(4)*PA(II)
IF (I.EQ.9) GO TO 8
XM(I)=XM(I)+PA(I)*YD(1)+PA(II)*YD(2)
8 CONTINUE
SOFT=SOFT+PA(9)*YD(1)+PA(18)*YD(2)
C...CALCULATE NEW VARIANCES
IJ=0
DO 11 I=1,8
JI=I
DO 9 J=1,8
IJ=IJ+1
IF (I.GT.J) GO TO 10
VAR(IJ)=VAR(IJ)-PA(I)*PB(J)-PA(I+9)*PB(J+9)
GO TO 9
10 VAR(IJ)=VAR(JI)
9 JI=JI+8
PSV(I)=PSV(I)-PA(I)*PB(9)-PA(I+9)*PB(18)
11 CONTINUE
RETURN
END

```

IBFVAR

```

SUBROUTINE IBFVAR(AM,PVAR,FVAR,VT,VC)
C...THIS SUBROUTINE OPERATES WITH IBPTOF TO CALCULATE VAR-COVAR MATRIX OF PSDS
C... PVAR STARTING SUBSCRIPT MUST BE 1 FOR MILL COVARS AND 37 FOR SUMP COVARS
DIMENSION AM(1),PVAR(1),FVAR(1),V(1),VC(1)
C...CALCULATE FVAR = (AM)TRANS * PVAR * AM
IJ=0
DO 1 J=1,4
DO 1 I=1,4
IJ=IJ+1
ILL=4*I-I

```

```

KJ=4+J-4
DO 1 K=1,4
LK=K-K-8
S=0.0
IL=ILL
DO 2 L=1,4
IL=IL+1
LK=LK+1
S=S+AM(IL)*PVAR(LK)
2 CONTINUE
KJ=KJ+1
FVAR(IJ)=FVAR(IJ)+S*AM(KJ)
1 CONTINUE
...VI = VARIANCE OF INDIVIDUAL FRACTIONS = DIAG(FVAR)
...VC = VARIANCE OF CUMULATIVE FRACTIONS = SUM OF ALL VARS AND COVARS IN FVAR
FOR SIZES NOT GREATER THAN I
S=0.0
DO 3 K=1,4
I=5-K
II=5+I-4
VI(I)=FVAR(II)
DO 4 J=1,4
X=FVAR(II)
II=II+1
IF (J.NE.I) X=X*2.0
S=S+X
4 CONTINUE
VC(I)=S
3 CONTINUE
RETURN
END

```

BPTOF

```

SUBROUTINE IBPTOF(PM,PVAR,VM,VS,QS,QU,CO,C1,GAM,ETA,CONC,VCUNC,
1FIM,VFIM,FCM,VFCM,FIO,VFIO,FCO,VFCO,FIU,VFIU,FCU,VFCU,PA,PB,PC)
.....THIS SUBROUTINE CONVERTS PRIMARY STATE VARIABLES (PM & PS) INTO
CONCENTRATIONS AND PARTICLE SIZE DISTRIBUTIONS
DIMENSION PM(1),PVAR(1),CO(1),C1(1),GAM(1),ETA(1),CONC(1),VCUNC(1)
DIMENSION FIM(1),FCM(1),FIO(1),FCO(1),FIU(1),FCU(1)
DIMENSION VFIM(1),VFCM(1),VFIO(1),VFCO(1),VFIU(1),VFCU(1)
DIMENSION PA(1),PB(1),PC(1),AR(4)
...CONC VECTOR = 1 MILL, 2 SUMP, 3 CYC FEED, 4 CYC O/F, 5 CYC U/F
...DETERMINE CONCS IN MILL, SUMP AND CYCLONE FEED
DO 1 I=1,5
CONC(I)=0.0
1 VCUNC(I)=0.0
QK=QS/(VS*(QS-QU))
UK=QS/(VS*QU)
DO 2 I=1,4
CONC(1)=CONC(1)+PM(I)
II=I+4
CONC(2)=CONC(2)+PM(II)
CONC(3)=CONC(3)+PM(II)*GAM(I)
2 CONTINUE
CONC(3)=CONC(3)/VS
...DETERMINE COMMON TERMS AT FIRST LEVEL
IJ=0
DO 3 I=1,4
Y=GAM(I)*PM(I+4)

```

```

AR(I)=0.0
CONC(4)=CONC(4)+(1.0-X)*Y
CONC(5)=CONC(5)+X*Y
Z=PM(I)/(CONC(1)+CONC(1))
DO 4 J=1,4
IJ=IJ+1
PA(IJ)=-Z
IF (I.EQ.J) PA(IJ)=PA(IJ)+1.0/CONC(1)
AR(I)=AR(I)+GAM(J)*(C1(I)+C1(J))*PM(J+4)
4 CONTINUE
AR(I)=AR(I)/VS+CO(I)
3 CONTINUE
C...DETERMINE VARIANCES OF FEED DISTRIBUTION
CALL IHFVAR(PA,PVAR(1),PR,VFIM,VFCM)
C...DETERMINE COMMON TERMS AT SECOND LEVEL
JI=0
CUO=0.0
IJ=32
DO 5 I=1,4
IJ=IJ+4
RRM=2.0*PM(I)/(CONC(1)+3)
Y=GAM(I)*PM(I+4)
CC=CO(I)+C1(I)*CONC(3)
TIO=Y*(1.0-CC)
TIU=Y*CC
FIO(I)=TIO/CONC(4)
FIU(I)=TIU/CONC(5)
FIM(I)=PM(I)/CONC(1)
ZZZ=Y*C1(I)/VS
DO 6 J=1,4
IJ=IJ+1
GIJ=GAM(I)*GAM(J)
VCUNC(1)=VCUNC(1)+PVAR(IJ-36)
Y=PVAR(IJ)
VCUNC(2)=VCUNC(2)+Y
X=Y*GIJ
VCUNC(3)=VCUNC(3)+X
VCUNC(4)=VCUNC(4)+X*(1.0-AR(I))*(1.0-AR(J))
VCUNC(5)=VCUNC(5)+X*AR(I)*AR(J)
CUO=CUO+Y*(C1(I)+C1(J))
HOLDQ=GIJ*(1.0-CC)*(1.0-AR(J))/CONC(4)
JI=JI+1
PA(JI)=-GIJ*(C1(I)/VS+HOLDQ)*PM(I+4)/CONC(4)
HOLDU=GIJ*CC*AR(J)/CONC(5)
PB(JI)=(GIJ*C1(I)/VS+HOLDU)*PM(I+4)/CONC(5)
IF (I.NE.J) GO TO 11
PA(JI)=PA(JI)+GAM(I)*(1.0-CC)/CONC(4)
PB(JI)=PB(JI)+GAM(I)*CC/CONC(5)
11 CONTINUE
JK=8+J+28
DO 7 K=1,4
JK=JK+1
GJK=GAM(I)*GAM(K)
GJK=GAM(J)*GAM(K)
RRH=2.0*TIO*GJK*(1.0-AR(J))*(1.0-AR(K))/CONC(4)
RHH=2.0*TIU*GJK*AR(J)*AR(K)/CONC(5)
ZZ=Z*GJK*(C1(J)+C1(K))/VS
Z=ZZ+GJK
RRH=(RRH+TIU*ZZ+Z*(2.0-AR(J)-AR(K)))/CONC(4)
RHH=(RHH+TIU*ZZ+Z*(AR(J)+AR(K)))/CONC(5)
IF (I.NE.J) GO TO 8
Y=GJK*C1(I)/VS

```



```

RRU=RRU+Y-AR(K)*GK*CC/CONC(5)
BRM=BRM-2.0/(CONC(1)*CONC(1))
8 CONTINUE
IF (I.NE.K) GO TO 9
Y=GIJ*C1(I)/VS
RRU=RRU+Y-HOLDN
RRU=RRU+Y-HOLDU
9 CONTINUE
XX=0.5*PVAR(JK)
FIO(I)=FIO(I)+XX*BRU/CONC(4)
FIU(I)=FIU(I)+XX*BRU/CONC(5)
FIM(I)=FIM(I)+XX*BRM
7 CONTINUE
6 CONTINUE
5 CONTINUE

```

C...FINISH OFF CONCS MEANS AND VARS

```

CONC(1)=CONC(1)/VM
CONC(2)=CONC(2)/VS
CUO=0.5*CUO/VS
CONC(4)=OK*(CONC(4)-CUO)
CONC(5)=UK*(CONC(5)+CUO)
VCUNC(1)=VCUNC(1)/(VM+VM)
VCUNC(2)=VCUNC(2)/(VS+VS)
VCUNC(3)=VCUNC(3)/(VS+VS)
VCUNC(4)=VCUNC(4)*OK*OK
VCUNC(5)=VCUNC(5)*UK*UK

```

C...CALCULATE VARIANCES OF O/F AND U/F PSDS.

```

CALL IBFVAR(PA,PVAR(37),PC,VFIO,VFCO)
CALL IBFVAR(PH,PVAR(37),PC,VFIU,VFCU)

```

C...CALCULATE MEANS OF CUMULATIVE MASS FRACTIONS FROM INDIVIDUAL

```

FCM(4)=FIM(4)
FCO(4)=FIO(4)
FCU(4)=FIU(4)
DO 12 K=1,3
I=4-K
FCM(I)=FCM(I+1)+FIM(I)
FCO(I)=FCO(I+1)+FIO(I)
FCU(I)=FCU(I+1)+FIU(I)

```

```

12 CONTINUE
RETURN
END

```

IBSIMP

```

SUBROUTINE IBSIMP(PH,GAM,ACO,AC1,VS,QS,QU,FIO,FCO,DCONC,UC,FC)
C...SIMPLIFIED ROUTINE TO CALCULATE PRODUCT DISTRIB AND CONCS AROUND CYCLONE
C...DCONC = O/F CONC UC = U/F CONC FC = FEED CONC
C...FIO, FCO = PSDS (FRACTIONS) OF O/F, INDIV AND CUM RESPEC.
DIMENSION PM(1),GAM(1),ACO(1),AC1(1),FIO(1),FCO(1)
C...CALCULATE FEED CONC
FC=0.0
DO 1 I=1,4
FC=FC+GAM(I)*PM(I+4)
FC=FC/VS
C...CALCULATE CLASSIFIER FUNCTION THEN STREAMS FIO EACH SIZE GROUP
DCONC=0.0
DO 2 I=1,4
CC=1.0-ACO(I)-AC1(I)*FC
FIO(I)=PM(I+4)*GAM(I)*CC
DCONC=DCONC+FIO(I)

```

```

2 CONTINUE
C...CALCULATE DISTRIBUTIONS AND DCONC
DO 3 I=1,4
3 FIO(I)=FIO(I)/DCONC
FCO(4)=FIO(4)
DO 4 I=1,3
II=4-I
FCO(II)=FIO(II)+FCO(II+1)
4 CONTINUE
DCONC=QS*DCONC/(VS*(QS-QU))
UC=(QS*FC-(QS-QU)*DCONC)/QU
RETURN
END

```

IBMFLC

PROGRAM IBMFLC

C...THIS PROGRAM DOES FULL FILTERING (VOLUMETRIC AND PSD) ON STORED DATA

```

DIMENSION IHEAD(40),LG(475)
DIMENSION XM(2),UM(4),PHIV(4),PSI(8),CONST(2),GOG(4),M(5)
DIMENSION CO(4),C1(4),FEED(4),PM(8),PVAR(64),PSV(8)
DIMENSION S(4),R(15),HETA(4),GAMMA(4),ETA(4),PHIN(4),RP(4)
DIMENSION IN(95),HHSV(5),HRS(2),XMA(2),UMA(4),XAVER(2),UAVER(4)
DIMENSION DU(4),DIJAV(4),PA(64),PH(14),PC(14),CONC(5),VCUNC(5)
DIMENSION FEI(4),DPM(8),DPVAR(64),DPSV(8),AKALK(30),PD(6),RV(5)
DIMENSION FIM(4),FCM(4),FIO(4),FCO(4),FIU(4),FCU(4)
DIMENSION VFIM(4),VFIM(4),VFIO(4),VFIO(4),VFIU(4),VFCU(4)
DIMENSION ACO(4),AC1(4)
EQUIVALENCE (IHEAD(1),LG(1)),(XM(1),LG(41)),(UM(1),LG(45)),
1(PHIV(1),LG(53)),(PSI(1),LG(61)),(CONST(1),LG(77)),
2(GOG(1),LG(81)),(M(1),LG(89)),(AKALK(1),LG(94)),
3(RV(1),LG(154))
EQUIVALENCE (CO(1),LG(201)),(C1(1),LG(209)),(FEED(1),LG(217)),
1(PM(1),LG(225)),(PVAR(1),LG(241)),(PSV(1),LG(349)),
2(S(1),LG(395)),(R(1),LG(393)),(HETA(1),LG(425)),
3(GAMMA(1),LG(433)),(ETA(1),LG(441)),(PHIN(1),LG(449)),
4(RP(1),LG(493))
EQUIVALENCE (TINT,LG(461)),(FHRQ,LG(463)),(VMQ,LG(465)),
1(AKA,LG(467)),(QRQ,LG(469)),(SOFT,LG(471)),(SOFTV,LG(473))

```

C...OPEN FILES AND GET DATA

```

OPEN 1,5,1,0,2000
OPEN 2,1,500,0,1500
OPEN 3,1,3000,0,3000
READ (1(1)) (LG(I),I=1,475)
JOUT=3

```

WRITE (JOUT,100) (IHEAD(I),I=1,40)

100 FORMAT (19H1DATA USED --- ,40A2//)

C...SET VALUES

```

IFRACK=20
IORACK=33
IFWAT=1530
IHWAT=690
RMFCOIN=2000.0
RMQCOIN=640.0
RHQS=1.37E3
IINQC=-1
IMW=0
IWHQC=1
NS=2
NP=4
NQ=5

```



```

CONC(5)=0.0
...GET DATA FOR OBSERVATIONS FROM DISC
KREC=0
LL=95
3 CONTINUE
LL=LL+13
IF (LL.LT.70) GO TO 2
KREC=KREC+1
LL=0
READ (2(KREC)) (IN(I),I=1,95)
DO 1 I=1,95
IF (IN(I).NE.0) GO TO 2
1 CONTINUE
IS=ITIME+2
WRITE (3(IS)) (IN(I),I=1,95)
STOP
2 CONTINUE
ITIME=ITIME+1
TSEC=TINT*FLOAT(ITIME)
TMIN=TSEC/60.0
KP=ITIME-(ITIME/12)*12
...CONVERT DATA INTO OBSERVATIONS
SOLIDS FEED AND FEED BELT SPEED, KG/S AND M/S WITH GAP 1.5CM.
FBS=2.764E-4*(IN(LL+1)+930)
CONVER=0.927-2.2E-4*FLOAT(IN(LL+1))
OBSV(1)=FBS*CONVER
MILL WATER FEED SETTING, WATMIL, M3/S
ISD=(IMW-IN(LL+2))*IVDRC
IM=IN(LL+2)
IF (ISD.LT.194) GO TO 66
IVDRC=-IVDRC
GO TO 67
66 IF (ISD.GT.0) GO TO 68
67 IMW=IN(LL+2)
IF (IVDRC.LT.0) IM=IM+194
WATMIL=0.15E-4+9.89E-8*EXP(4.98E-3*IM)
68 CONTINUE
OBSV(2)=WATMIL
SUMP WATER FLOW, M3/S
IX=IN(LL+3)
IF (IX.LT.450) IX=450
OBSV(5)=0.02265E-3*SQR(FLOAT(IX-450))
CYC FEED CONC KG SOLIDS / M3 SLURRY
CONRCR=RMFCN*ALOG(FLOAT(IFWAT-IFBACK)/FLOAT(IN(LL+6)-IFBACK))
IF (CONRCR.GT.RHOS) CONRCR=0.0
IF (CONRCR.LT.-20.0) CONRCR=0.0
OBSP(1)=CONRCR
CYC O/F CONC KG SOLIDS / M3 SLURRY
CONPRD=RMDCN*ALOG(FLOAT(IDWAT-IDBACK)/FLOAT(IN(LL+7)-IDBACK))
IF (CONPRD.GT.RHOS) CONPRD=0.0
IF (CONPRD.LT.-20.0) CONPRD=0.0
OBSP(2)=CONPRD
CYC FEED RATE, M3/S, CORRECTED FROM CONCENTRATION
RECIRC=1.57E-6*(IN(LL+4)+3)
OBSV(3)=RECIRC/(1.0+4.0E-4*CONRCR)
SUMP VOLUME, M3, CORRECTED FROM CONC
SMPVOL=FLOAT(IN(LL+5)-436)/(1.0+0.715E-3*CONRCR)
SMPVOL=7.6621E-3+3.467E-5*SMPVOL
OBSV(4)=SMPVOL
...CONTROLLER CHANGES
TCC=60.0*TINT
ITC=IFIX(TCC)

```

```

TND=LL+1+9
IF (IN(IND).GT.ITC) IN(IND)=ITC
IF (IN(IND).LT.-ITC) IN(IND)=-ITC
14 CONTINUE
C SUMP PUMP
TRANGE=60.0+40.5
TMOVE=FLOAT(IN(LL+10))
DU(1)=2.0E-3*TMOVE/TRANGE
FRAC=TMOVE/TCC
DUAV(1)=DU(1)+0.5*(2.0-FRAC)
C SOLIDS FEED
TMOVE=FLOAT(IN(LL+11))
DU(2)=(2.764E-4*CONVER-2.2E-4*FBS)+0.191*TMOVE
FRAC=TMOVE/TCC
DUAV(2)=DU(2)+0.5*(2.0-FRAC)
C MILL WATER
IPDS=IN(LL+2)+IFIX(0.507*IN(LL+12))
ISD=(IMW-IPDS)*IVDRC
IF (ISD.LT.0) GO TO 10
IF (ISD.GT.194) GO TO 11
DU(3)=0.0
DUAV(3)=0.0
GO TO 12
11 IF (IVDRC.GT.0) IPDS=IPDS+194
GO TO 13
10 IF (IVDRC.LT.0) IPDS=IPDS+194
13 VAL=0.15E-4+9.89E-8*EXP(4.98E-3*IPDS)
DU(3)=VAL-WATMIL
DUAV(3)=0.5*DU(3)
12 CONTINUE
C SUMP WATER
TMOVE=FLOAT(IN(LL+13))
WIG=IN(LL+3)-450.0
DWIG=1.0/(1.3668+3.281E-3*WIG+3.3866E-6*WIG*WIG)
WIG=WIG+DWIG*TMOVE
IF (WIG.LT.0.0) WIG=0.0
DU(4)=0.02265E-3*SQR(WIG)-OBSV(5)
FRAC=TMOVE/TCC
DUAV(4)=DU(4)+0.5*(2.0-FRAC)
C...WRITE OUT DATA BEFORE OBSERVATION STEP
IF (KP.EQ.0) WRITE (IOUT,110) ITIME,TSEC,TMIN
110 FORMAT (12H OBSERV NO,14,8H TIME =,F8.1,7H SECS =,F8.2,5H MINS)
IF (KP.EQ.0) WRITE (IOUT,111) (XM(I),I=1,NS),(UM(I),I=1,NP)
111 FORMAT (37H VOLUMETRIC MEANS BEFORE OBS = STATE,2E12.4,
19H PARAMS,4E12.4)
IF (KP.EQ.0) WRITE (IOUT,112) (OBSV(I),I=1,NO),(OBSP(I),I=1,2)
112 FORMAT (23H OBSERVATIONS = VOLUM.,5E12.4,6H PSD,2E12.4)
C...VOLUMETRIC FILTER FOR COMPLETE STEP (STATIONARY FILTER)
CALL IBSTST(PHY,PSI,CONST,M,AKALK,XMA,XM,XAVER,UMA,UM,UAVR,
IDU,DUAV,OBSV,RV,NS,NP,NO,PA,PR,PC,PD)
IF (XMA(2).LT.0.008) XMA(2)=0.008
IF (XM(2).LT.0.008) XM(2)=0.008
IF (XAVER(2).LT.0.008) XAVER(2)=0.008
IF (KP.EQ.0) WRITE (IOUT,113) (XMA(I),I=1,NS),(UMA(I),I=1,NP)
113 FORMAT (36H VOLUMETRIC MEANS AFTER OBS = STATE,2E12.4,
19H PARAMS,4E12.4)
C...PSD FILTER OBSERVATION AND CALCULATION OF DISTRIBUTIONS AFTERWARDS
IFRAC=(OBSV(4)/UMA(1))*(RHOS-CONC(5))/(RHOS-CONC(3))
OFRAC=1.0-IFRAC
DO 43 I=1,4
ACO(I)=OFRAC*IFRAC*CO(I)
ACI(I)=OFRAC*CI(I)

```

```

CALL IRPQRS(PVAR,PSV,SOFTV,RP,PM,SOFT,NRSP,ACO,AC1,GAMMA,ETA,
1UMA(1),VS,QRO,PA,PB)
SOFT=0.9
CALL IBPTOF(PM,PVAR,XMA(1),VS,UMA(1),QRO,ACO,AC1,GAMMA,ETA
1,CONC,VCONC,FIM,VFIM,FCM,VFCM,FID,VFID,FCO,VFCO,FIU,VFIU,FCU,VFCU
2,PA,PB,PC)
IF (KP,EQ.0) WRITE (IOUT,114) (CONC(I),I=1,5)
114 FORMAT (27H FILTER CONCS. KG/M3 MILL,F7.1,7H SUMP,F7.1,
1 11H CYC FEED,F7.1,10H CYC O/F,F6.1,10H CYC U/F,F7.1)
IF (KP,EQ.0) WRITE (IOUT,115) (FCM(I),I=1,4), (FCO(I),I=1,4),
1(FCU(I),I=1,4)
115 FORMAT (26H PSDS. (CUM FRACS) MILL,4F6.3,7H O/F,4F6.3,
1 7H U/F,4F6.3)
...PSD FILTER EVOLUTION
QMDVM=AKA*(XMA(1)-VMO)/XMA(1)
VS=XMA(2)+0.02
QSDVS=UMA(1)/VS
UFRAC=(QRO/UMA(1))*(RHOS-CONC(5))/(RHOS-CONC(3))
OFRAC=1.0-UFRAC
DO 44 I=1,4
ACO(I)=UFRAC+UFRAC*CO(I)
AC1(I)=OFRAC*C1(I)
44 FE0(I)=FEED(I)*UMA(2)*5.0
AKL=1.0+10.0*(XMA(1)-0.1435)
CALL IBCDRV(PM,PVAR,PSV,SOFTV,SOFT,S,AKL,B,QMDVM,QSDVS,
1BETA,GAMMA,PHIN,ACO,AC1,VS,FE0,DPM,DPMVAR,DPSV)
THALF=0.5*TINT
DO 45 I=1,8
PB(I)=PM(I)+DPM(I)*THALF
45 PC(I)=PSV(I)+DPSV(I)*THALF
DO 46 I=1,64
PA(I)=PVAR(I)+DPMVAR(I)*THALF
QMDVM=AKA*(XAVER(1)-VMO)/XAVER(1)
VS=XAVER(2)+0.02
QSDVS=UAVER(1)/VS
UFRAC=(QRO/UAVER(1))*(RHOS-CONC(5))/(RHOS-CONC(3))
OFRAC=1.0-UFRAC
DO 40 I=1,4
ACO(I)=UFRAC+UFRAC*CO(I)
AC1(I)=OFRAC*C1(I)
40 FE0(I)=FEED(I)*UAVER(2)*5.0
AKL=1.0+10.0*(XAVER(1)-0.1435)
CALL IBCDRV(PB,PA,PC,SOFTV,SOFT,S,AKL,B,QMDVM,QSDVS,
1BETA,GAMMA,PHIN,ACO,AC1,VS,FE0,DPM,DPMVAR,DPSV)
DO 41 I=1,8
PM(I)=PM(I)+DPM(I)*TINT
41 PSV(I)=PSV(I)+DPSV(I)*TINT
DO 42 I=1,64
42 PVAR(I)=PVAR(I)+DPMVAR(I)*TINT
...WRITE TO DISC
IS=ITIME+1
WRITE (3(IS)) IS,(XMA(I),I=1,NS),(XMA(I),I=1,NS),(UM(I),I=1,NP),
1(URSV(I),I=1,NQ),URSP(1),OBSP(2),SOFT,(FCM(I),VFCM(I),FCO(I),
2VFCO(I),FCU(I),VFCU(I),I=1,4),(CONC(I),I=1,5),VCONC(1),VCONC(4)
GO TO 3
END

```

30LMF

```

C...ON LINE PROGRAM TO WORK WITH AMTEL, PROCESSING DATA TO TREDUC 1.0340
DIMENSION IWRBF(80),ITEMP(8),AMOVE(4),TLIM(4),JTEMP(8)
DIMENSION IHEAD(40),LG(475)
DIMENSION XM(2),UM(4),PHIV(4),PSI(8),CONST(2),GGG(4),M(5)
DIMENSION CO(4),C1(4),FFFD(4),PM(8),PVAR(64),PSV(8)
DIMENSION S(4),H(16),BETA(4),GAMMA(4),ETA(4),PHIN(4),RP(4)
DIMENSION IN(95),OHSV(5),NRSP(2),XMA(2),UMA(4),XAVER(2),UAVER(4)
DIMENSION DU(4),DUAV(4),PA(64),PR(18),PC(18),CONC(5),VCONC(5)
DIMENSION FED(4),DPM(8),DPMVAR(64),DPSV(8),AKALK(30),PD(6),RV(5)
DIMENSION FID(4),FCO(4)
DIMENSION ACO(4),AC1(4)
EQUIVALENCE (IHEAD(1),LG(1)),(XM(1),LG(41)),(UM(1),LG(45)),
1(PHIV(1),LG(53)),(PSI(1),LG(61)),(CONST(1),LG(77)),
2(GGG(1),LG(81)),(M(1),LG(89)),(AKALK(1),LG(94)),
3(RV(1),LG(154))
EQUIVALENCE (CO(1),LG(201)),(C1(1),LG(209)),(FEED(1),LG(217)),
1(PM(1),LG(225)),(PVAR(1),LG(241)),(PSV(1),LG(369)),
2(S(1),LG(385)),(B(1),LG(393)),(BETA(1),LG(425)),
3(GAMMA(1),LG(433)),(ETA(1),LG(441)),(PHIN(1),LG(449)),
4(RP(1),LG(193))
EQUIVALENCE (TINT,LG(461)),(ERR0,LG(463)),(VMO,LG(465)),
1(AKA,LG(467)),(QRO,LG(469)),(SOFT,LG(471)),(SOFTV,LG(473))
RELATIVE IBSTST,IBPORS,IBPTOF,IBCDRV,ALLOTS,IBSIMP
RELATIVE GETX,GETI,PUTX,PUTI,DEFREC,FINIO
RELATIVE MATADD,MATPHY
IOUT=17
C...SET TRAVEL LIMITS FOR CONTROLLERS, AND SUNDRY VARIABLES
TLIM(1)=0.123
TLIM(2)=0.0344
TLIM(3)=0.0546
TLIM(4)=0.163
NS=2
NP=4
NQ=5
HC=0.0
FC=0.0
RHOS=3.37E3
C...CYCLE, CHECKING FOR SIGNAL TO RUN
3 CONTINUE
IST=IGET(9,531,3)
IF (IST.NF.1) GO TO 7
CALL SETBFR(IWRBF,80)
WRITE (IOUT,101)
101 FORMAT (16H IBOLMF RELEASED)
CALL RELSPC(9)
CALL RELEASE(IBOLMF)
7 CONTINUE
ICYC=IGET(9,531,5)
IF (ICYC.NE.0) GO TO 2
ASSIGN 3 TO IRET
CALL TIMEP(IPET,30004,20,ITEMP)
CALL DISPAT
2 CONTINUE
C...GET DATA FROM COMMUNICATIONS BLOCK
OBSV(1)=XGET(9,531,22)
OBSV(2)=XGET(9,531,23)
OBSV(3)=XGET(9,531,25)
OBSV(4)=XGET(9,531,26)
OBSV(5)=XGET(9,531,24)
OBSV(1)=XGET(9,531,27)
OBSV(2)=XGET(9,531,28)
DO 5 I=1,4

```



```

      AMOVE(I)=XGET(9,531,I)
      FBS=XGET(9,531,35)
      CONVER=XGET(9,531,36)
      CALL INPUT(9,531,5,0)
C...CHECK AND IF NECESSARY, GET STARTING DATA FROM DISC
      IST=IGET(9,531,3)
      IF (IST.EQ.0) GO TO 6
      CALL DEFREC(515,422,1,5,1)
      DO 1 I=1,475
1    CALL GETI(LG(I))
      CALL FINIO(IER)
      CALL SETBFR(IWRBF,80)
      WRITE (IOUT,100) (IHEAD(I),I=1,40)
100  FORMAT(13H FILTER DATA ,40A2)
      CALL INPUT(9,531,3,0)
      6 CONTINUE
C...CONVERT CONTROL CHANGES
      DO 10 I=1,4
      IF (AMOVE(I).GT.TLIM(I)) AMOVE(I)=TLIM(I)
      IF (AMOVE(I).LT.-TLIM(I)) AMOVE(I)=-TLIM(I)
10  CONTINUE
C...SUMP PUMP
      DU(1)=2.0E-3*AMOVE(1)
C...SOLIDS FEED
      DU(2)=(2.908E-4*CONVER+2.31E-4*FBS)*AMOVE(2)+1581.0
C...MILL WATER
      DFBDP=5.29E-3*(OBSV(2)-0.15E-4)
      DPHDM=1217.0
      DU(3)=DFBDP*DPBDM*AMOVE(3)
C...SUMP WATER
      DU(4)=1.0E-3*AMOVE(1)
      DO 18 I=1,4
      FRAC=AMOVE(I)/TLIM(I)
      DUAV(I)=DU(I)*0.5*(2.0-FRAC)
18  CONTINUE
C...VOLUMETRIC FILTER
      CALL IBSTST(PHIV,PSI,CONST,M,AKALK,XMA,XM,XAVER,UMA,UM,UAVR,
1DU,DUAV,DHSH,RV,NS,NP,NU,PA,PR,PC,PD)
      IF (XMA(2).LT.0.008) XMA(2)=0.008
      IF (XM(2).LT.0.008) XM(2)=0.008
      IF (XAVER(2).LT.0.008) XAVER(2)=0.008
C...PSD QHS STEP
      UFRAC=(QRD/UMA(1))*(RHOS-UC)/(RHOS-FC)
      OFRAC=1.0-UFRAC
      DO 11 I=1,4
      ACO(I)=UFRAC+UFRAC*CO(I)
11  AC1(I)=OFRAC*C1(I)
      VS=XMA(2)+0.02
      CALL IBPHS(PVAR,PSV,SOFTV,RP,PM,SOFT,DRSP,ACO,AC1,GAMMA,ETA,
1UMA(1),VS,QRD,PA,PB)
C...PSD EVOLUTION
      QMDVM=AKA*(XMA(1)-VMD)/XMA(1)
      VS=XMA(2)+0.02
      QSDVS=UMA(1)/VS
      DO 12 I=1,4
12  FED(I)=FEED(I)*UMA(2)+5.0
      AKL=1.0+10.0*(XMA(1)-0.1435)
      CALL IBCDRV(PH,PVAR,PSV,SOFTV,SOFT,S,AKL,B,QMDVM,QSDVS,
1BETA,GAMMA,PHIN,ACO,AC1,VS,FED,DPH,DPVAR,DPSV)
      THALF=0.5*TINT
      DO 13 I=1,8
      PH(I)=PM(I)+DPH(I)*THALF

```

```

      DO 14 I=1,64
14  PA(I)=PVAR(I)+DPVAR(I)*THALF
      QMDVM=AKA*(XAVER(1)-VMD)/XAVER(1)
      VS=XAVER(2)+0.02
      QSDVS=UAVR(1)/VS
      UFRAC=(QMD/UAVR(1))*(RHOS-UC)/(RHOS-FC)
      OFRAC=1.0-UFRAC
      DO 15 I=1,4
      ACO(I)=UFRAC+OFRAC*CO(I)
      AC1(I)=OFRAC*C1(I)
15  FED(I)=FEED(I)+UAVR(2)+5.0
      AKL=1.0+10.0*(XAVER(1)-0.1435)
      CALL IBCDRV(PH,PA,PC,SOFTV,SOFT,S,AKL,B,QMDVM,QSDVS,
1BETA,GAMMA,PHIN,ACO,AC1,VS,FED,DPH,DPVAR,DPSV)
      DO 16 I=1,8
      PM(I)=PM(I)+DPH(I)*TINT
16  PSV(I)=PSV(I)+DPSV(I)*TINT
      DO 17 I=1,64
17  PVAR(I)=PVAR(I)+DPVAR(I)*TINT
C...CONVERT TO CMCS AND DISTRIBUTIONS
      UFRAC=(QRD/UM(1))*(RHOS-UC)/(RHOS-FC)
      OFRAC=1.0-UFRAC
      DO 20 I=1,4
      ACO(I)=UFRAC+OFRAC*CO(I)
20  AC1(I)=OFRAC*C1(I)
      CALL IBSIMPH(PH,GAMMA,ACO,AC1,XM(2),UM(1),QRD,FID,FCO,OC,UC,FC)
C...PUT FILTER DATA BACK INTO COMMUNICATIONS BLOCK
      CALL XPUT(9,531,41,FCO(4))
      CALL XPUT(9,531,42,OC)
      CALL XPUT(9,531,43,UC)
      CALL XPUT(9,531,44,FC)
      GO TO 3
      STOP
      END

```

IBPRPC

```

      PROGRAM IBPRPC
C...PREPARES DATA FOR VOLUMETRIC AND PSD FILTERS AND WRITES IT ON DISC
      DIMENSION IHEAD(40),LG(475)
      DIMENSION XM(2),UM(4),EVAL(4),EVAL(4),FINV(4),F(4),PHIV(4),G(8)
      DIMENSION PSI(8),CONST(2),GQG(4),M(5),RV(5),XVAR(4),COVSP(8)
      DIMENSION UVAR(16),AKALK(30),DUVAR(4)
      DIMENSION CO(4),C1(4),FEED(4),PM(8),PVAR(64),PSV(8)
      DIMENSION S(4),R(16),BFTA(4),GAMMA(4),ETA(4),PHIN(4),RP(4)
      DIMENSION PA(100),PB(100),PC(100),XMA(6),UAV(4),IR(5),IC(5)
      EQUIVALENCE (XMA(3),UAV(1))
      EQUIVALENCE (IHEAD(1),LG(1)),(XM(1),LG(41)),(UM(1),LG(45)),
1(PHIV(1),LG(53)),(PSI(1),LG(61)),(CONST(1),LG(77)),
2(GQG(1),LG(81)),(M(1),LG(89)),(AKALK(1),LG(94)),
3(RV(1),LG(154))
      EQUIVALENCE (CO(1),LG(201)),(C1(1),LG(209)),(FEED(1),LG(217)),
1(PM(1),LG(225)),(PVAR(1),LG(241)),(PSV(1),LG(369)),
2(S(1),LG(385)),(B(1),LG(393)),(BFTA(1),LG(425)),
3(GAMMA(1),LG(433)),(ETA(1),LG(441)),(PHIN(1),LG(449)),
4(RP(1),LG(493))
      EQUIVALENCE (TINT,LG(461)),(ERRR,LG(463)),(VMD,LG(465)),
1(AKA,LG(467)),(QRD,LG(469)),(SOFT,LG(471)),(SOFTV,LG(473))
C...READ AND WRITE HEADING
      TTN=1

```



```

WRITE (IOUT,101) (IHEAD(I),I=1,40)
100 FORMAT (40A2)
101 FORMAT (1H1,20X,40A2/)
NS=2
NP=4
C...READ AND WRITE STARTING VALUES
C... STATE. 1 = VM, 2 = VS. PARAMETERS 1 = QS, 2 = S, 3 = WM, 4 = WS
READ (IIN,102) (XM(I),I=1,NS),(UM(I),I=1,NP)
102 FORMAT (RE10,3)
WRITE (IOUT,103) (XM(I),I=1,NS),(UM(I),I=1,NP)
103 FORMAT (25H STARTING VALUES, STATE =,2E12,4,10H PARAS =,4E12,4/)
READ (IIN,102) TINT,ERRD,VMO,AKA,QRO
WRITE (IOUT,104) TINT,ERRD,VMO,AKA,QRO
104 FORMAT (17H TIME INT, SECS =,F6,2,13H ERROR ON QRO,E12,4,
U6H VMO =,F10,7,15H MILL N/F CONST,F12,4,6H QRO =,E12,4/)
C...READ IN EIGENVALUES AND (EIGENCOLUMNMATRIX)TRANS FOR F AND CHECK
DO 1 I=1,4
1 EVAL(I)=0.0
READ (IIN,102) VA,VB,(ECOL(I),I=1,4)
WRITE (IOUT,105) VA,VB,(ECOL(I),I=1,4)
105 FORMAT (19H EIGENVALUES OF F =,2E15,6/13H EIGENVECTS =,2E15,6,
110X,2E15,6/)
EVAL(1)=EXP(VA*TINT)
EVAL(4)=EXP(VB*TINT)
DET=ECOL(1)*ECOL(4)-ECOL(2)*ECOL(3)
EINV(1)=ECOL(4)/DET
EINV(2)=-ECOL(2)/DET
EINV(3)=-ECOL(3)/DET
EINV(4)=ECOL(1)/DET
CALL MATMPY(ECOL,EVAL,PA,NS,NS,NS)
CALL MATMPY(PA,EINV,PHIV,NS,NS,NS)
EVAL(1)=VA
EVAL(4)=VB
CALL MATMPY(ECOL,EVAL,PA,NS,NS,NS)
CALL MATMPY(PA,EINV,F,NS,NS,NS)
WRITE (IOUT,106) (F(I),I=1,4)
106 FORMAT (15H F MATRIX TRANS,2E15,6/15X,2E15,6/)
WRITE (IOUT,107) (PHIV(I),I=1,4)
107 FORMAT (17H PHIMATRIX TRANS,2E15,6/17X,2E15,6/)
C...READ IN G MATRIX (IN COLUMNS) AND CONST AND CALC PSI, CONST AND NOISE COVAR
DO 2 I=1,4,3
IF (EVAL(I).EQ.0) GO TO 3
EVAL(I)=(EXP(EVAL(I)*TINT)-1.0)/EVAL(I)
GO TO 2
3 EVAL(I)=TINT
2 CONTINUE
CALL MATMPY(ECOL,EVAL,PA,NS,NS,NS)
CALL MATMPY(PA,EINV,PB,NS,NS,NS)
READ (IIN,102) (G(I),I=1,8)
WRITE (IOUT,108) (G(I),I=1,7,2),(G(I),I=2,8,2)
108 FORMAT (9H G MATRIX,4E15,6/9X,4E15,6/)
CALL MATMPY(PB,G,PSI,NS,NS,NP)
WRITE (IOUT,109) (PSI(I),I=1,7,2),(PSI(I),I=2,8,2)
109 FORMAT (11H PSI MATRIX,4E15,6/11X,4E15,6/)
READ (IIN,102) PA(1),PA(2)
CALL MATMPY(PB,PA,CUNST,NS,NS,1)
WRITE (IOUT,110) PA(1),PA(2),CONST(1),CONST(2)
110 FORMAT (19H DIFFERENTIAL CONST,2E15,6,10X,16HDIFFERENCE CONST,
12E15,6/)
ERRD=ERRD*ERRD
GGG(1)=ERRD*PB(1)*PB(1)

```

```

GGG(3)=GGG(2)
GGG(4)=ERRD*PB(2)*PB(2)
WRITE (IOUT,111) (GGG(I),I=1,4)
111 FORMAT (19H NOISE COVAR MATRIX,2E15,6/19X,2E15,6/)
C...READ IN OBSERVATION INDEX VECTOR
NO=5
READ (IIN,112) (M(I),I=1,NO)
112 FORMAT (16I5)
WRITE (IOUT,113) (M(I),I=1,NO)
113 FORMAT (21H OBSERV. INDEX VECTOR,5I5/)
C...READ OBSERVATION ERRORS (STD.DEVS.) AND CONVERT TO COVAR MATRIX
READ (IIN,102) (RV(I),I=1,5)
WRITE (IOUT,114) (RV(I),I=1,5)
114 FORMAT (20H STD DEVS OF OBSRV,5E12,4/)
DO 4 I=1,NO
4 RV(I)=RV(I)*RV(I)
C...READ IN CONTROL CHANGE ERRORS
READ (IIN,102) (DUVAR(I),I=1,NP)
WRITE (IOUT,117) (DUVAR(I),I=1,NP)
117 FORMAT (24H CONTROL CHANGE STD DEVS,4E12,4/)
DO 5 I=1,NP
5 DUVAR(I)=DUVAR(I)**2
C...START WITH INPUT FOR PSD FILTER
C...READ CONSTANTS TO START
READ (IIN,102) SOFT,SOFTV
WRITE (IOUT,116) SOFT,SOFTV
116 FORMAT (11H SOFTNESS =,F7,4,16H SOFT VARIANCE =,E12,4/)
C...READ S AND B
C...READ AND WRITE S AND B
READ (IIN,102) (S(I),I=1,4)
WRITE (IOUT,204) (S(I),I=1,4)
204 FORMAT (14H SELEC. FUNC =,4F14,8/24H BREAKAGE MATRIX IS =)
DO 10 I=1,4
S(I)=S(I)/60.0
II=I+12
READ (IIN,102) (B(J),J=I,II,4)
WRITE (IOUT,205) (B(J),J=I,II,4)
10 CONTINUE
C...READ AND WRITE BETA, GAMMA, ETA, PHI, CO, C1
205 FORMAT (1X,8F14,5)
READ (IIN,102) (BETA(I),I=1,4)
WRITE (IOUT,206) (BETA(I),I=1,4)
206 FORMAT (1X//7H BETA =,4F10,5/)
READ (IIN,102) (GAMMA(I),I=1,4)
WRITE (IOUT,207) (GAMMA(I),I=1,4)
207 FORMAT (8H GAMMA =,4F10,5/)
READ (IIN,102) (ETA(I),I=1,4)
WRITE (IOUT,217) (ETA(I),I=1,4)
217 FORMAT (6H ETA =,4F10,5/)
READ (IIN,102) (PHIN(I),I=1,4)
WRITE (IOUT,208) (PHIN(I),I=1,4)
208 FORMAT (6H PHI =,4F10,5/)
READ (IIN,102) (CO(I),I=1,4)
WRITE (IOUT,209) (CO(I),I=1,4)
209 FORMAT (5H CO =,4F10,5/)
READ (IIN,102) (C1(I),I=1,4)
WRITE (IOUT,210) (C1(I),I=1,4)
210 FORMAT (5H C1 =,4F10,8//)
C...READ AND WRITE FEED
READ (IIN,102) (FEED(I),I=1,4)
FT=FEED(1)+FEED(2)+FEED(3)+FEED(4)
WRITE (IOUT,211) (FEED(I),I=1,4),FT

```

```

C...READ AND WRITE OBSERVATIONS AND OBSERVATION ERROR MATRIX
  READ (IIN,102) (RP(I),I=1,4)
  WRITE (IOUT,216) (RP(I),I=1,4)
216 FORMAT(21H OBS ERROR COVARIANCE,2F12.2/21X,2F12.2//)
C...READ AND WRITE STARTING VALUES
  WRITE (IOUT,212)
212 FORMAT (20H STARTING VALUES =/)
  READ (IIN,102) (PM(I),I=1,8)
  WRITE (IOUT,213) (PM(I),I=1,8)
213 FORMAT (17H MEANS OF STATE =,8F12.3//12H VARIANCES =)
  DO 11 I=1,8
  II=I+56
  READ (IIN,102) (PVAR(J),J=1,II,8)
  WRITE (IOUT,205) (PVAR(J),J=1,II,8)
11 CONTINUE
  READ (IIN,102) (PSV(I),I=1,8)
  WRITE (IOUT,214) (PSV(I),I=1,8)
214 FORMAT (1X/24H STATE-SOFTNESS COVARS =,8F12.3//)
C...FIND STATIONARY KALMAN GAIN
C...CREATE STARTING COVARIANCES
  IJ=0
  DO 20 I=1,2
  DO 20 J=1,2
  IJ=IJ+1
  XVAR(IJ)=0.0
  IF (I.EQ.J) XVAR(IJ)=XM(I)*XM(I)*0.01
20 CONTINUE
  DO 21 I=1,8
  DO 21 J=1,4
  IJ=IJ+1
  UVAR(IJ)=0.0
  IF (I.EQ.J) UVAR(IJ)=UM(I)*UM(I)*0.01
21 CONTINUE
C...LOOP TO GET STATIONARY STATE
  WRITE (IOUT,300) (XVAR(I),I=1,4,3),(UVAR(I),I=1,16,5)
  KL=0
  DO 30 KOUNT=1,240
  DO 32 I=1,NS
32 XMA(I)=XM(I)
  DO 33 I=1,NP
33 UAV(I)=UM(I)
  CHECK=XVAR(1)+XVAR(4)
  DO 31 I=1,NO
  MM=M(I)
  RR=RV(I)
  OBS=XMA(MM)
  CALL IBKFAC(PA,FINV,XVAR,COVSP,UVAR,RR,MM,NS,NP)
  CALL IBONEQ(XMA,UAV,XVAR,COVSP,UVAR,PA,FINV,OBS,MM,NS,NP)
31 CONTINUE
  KREM=KOUNT-(KOUNT/12)*12
  IF(KREM.EQ.0)WRITE(IOUT,300)(XVAR(J),J=1,4,3),(UVAR(J),J=1,16,5)
300 FORMAT(20H DIAG OF VAR. MATRIX,6E15.7)
  DO 35 J=1,NP
  JJ=5*J-4
  UVAR(JJ)=UVAR(JJ)+OUVAR(J)
35 CONTINUE
  CALL IBEVOL(PHIV,PSI,CONST,XMA,UAV,GQG,XVAR,UVAR,COVSP,NS,NP,PA
1,PR)
  CHANGE =XVAR(1)+XVAR(4)-CHECK

```

```

  IF (KL.EQ.36) GO TO 34
30 CONTINUE
34 CONTINUE
  WRITE (IOUT,300) (XVAR(I),I=1,4,3),(UVAR(I),I=1,16,5)
C...FORM P * MTRANS IN PA
  IJ=0
  DO 40 I=1,NO
  MM=M(I)
  IF (MM.LE.NS) GO TO 41
  K=(MM-NS-1)*NS
  DO 42 J=1,NS
  IJ=IJ+1
  K=K+1
42 PA(IJ)=COVSP(K)
  K=(MM-NS-1)*NP
  DO 43 J=1,NP
  IJ=IJ+1
  K=K+1
43 PA(IJ)=UVAR(K)
  GO TO 40
41 CONTINUE
  K=(MM-1)*NS
  DO 44 J=1,NS
  IJ=IJ+1
  K=K+1
44 PA(IJ)=XVAR(K)
  K=MM
  DO 45 J=1,NP
  IJ=IJ+1
  PA(IJ)=COVSP(K)
45 K=K+NS
40 CONTINUE
C...FORM M * P * MTRANS + R IN PB
  NT=NS+NP
  IJ=0
  DO 46 I=1,NO
  MM=M(I)
  DO 46 J=1,NO
  IJ=IJ+1
  PB(IJ)=PA(MM)
  MM=MM+NT
  IF (I.EQ.J) PB(IJ)=PB(IJ)+RV(I)
46 CONTINUE
C...PUT DIAG OF OBS/STATE COVAR MATRIX IN RV
  II=1
  DO 48 I=1,NO
  RV(I)=PB(II)
  II=II+NO+1
48 CONTINUE
  WRITE (IOUT,303) (RV(I),I=1,NO)
303 FORMAT (26H OBS-GIVEN-STATE VARIANCES,5E12.4//)
C...DETERMINE K MATRIX = PA * (PB)INV AND WRITE OUT
  CALL MATINC(PB,NO,DET,IR,IC)
  CALL MATMPY(PA,PB,AKALK,NT,NO,NO)
  WRITE (IOUT,301) DET
301 FORMAT(14H DETERMINANT =,E12.4/20H KALMAN GAIN MATRIX=)
  DO 47 I=1,NT
  II=I+(NO-1)*NT
  WRITE (IOUT,302) (AKALK(J),J=I,II,NT)
302 FORMAT(10X,5E15.6)
47 CONTINUE
C...WRITE TO DISC
  OPEN 1,5,1,8,2000
  WRITE (1(1)) (LG(I),I=1,475)
  STOP
  END

```


Appendix D

Nomenclature and Symbols Used.

$a_i(t)$	coefficients in orthogonal expansion, equation (4.1.23)
b_{ji}, B_{ji}	breakage functions (individual and cumulative, respectively)
\underline{c}	constant vector for discrete linear processes
\underline{c}'	constant vector for continuous linear processes
c_i	actual classifier function for size group i
c_{0i}, c_{1i}	coefficients for actual classifier function
cc_i	corrected classifier function for size group i
cc_{0i}, cc_{1i}	coefficients for corrected classifier function
C	concentration, kg/m ³
\underline{C}_u	covariance matrix between state and parameters
\underline{D}	parameter matrix for continuous linear processes
\underline{f}	function in equation (4.1.1)
f_i	individual mass fractions in each size group
$f_i(x)$	orthogonal function in equation (4.1.23)
\underline{F}	state transition matrix for continuous linear processes
F_i	cumulative mass fractions in each size group
\underline{g}	function in equation (4.1.1)
\underline{G}	noise matrix for continuous linear processes
h_I, h_C	probability density functions for individual and cumulative p.s.d.'s
H_I, H_C	probability function for individual and cumulative p.s.d.'s
k_1	mill overflow constant
\underline{K}	Kalman gain matrix
K	normalising factor in (4.1.24)
\underline{K}_i	vector defined in equation (4.1.26)
K_C	concentration factor on rate of grinding
K_L	volume load factor on rate of grinding

K_S	softness factor on rate of grinding
m_i	i th central moment
\underline{m}	observation function
\underline{M}	observation matrix
n_p	number of particle sizes
n_s	dimension of state
n_u	dimension of control parameters
n_W	dimension of noise vector
\underline{N}	uncertain error vector in volumetric filter
p	individual particle size distribution
$p(.)$	probability density function
p_x	$= p(x(t))$, probability density of state
p_i	mass in size group i in p.s.d. filter
P	cumulative particle size distribution
\underline{P}	covariance matrix of state
q_i	mass flow in size group i in p.s.d. filter
Q	volumetric flow rate, m^3/s
\underline{Q}	noise covariance matrix for plant model
Q_U	underflow volume rate
Q_{U0}	mean underflow volume rate
\underline{R}	covariance matrix of observation noise
S	error measure in volumetric filter checks
S_i	selection function for size group i (tabulated here as mins^{-1} , but used as s^{-1} in filter)
t	time
t_e	equivalent grinding time (in minutes) in equation (4.2.6)
t_{ci}	time for controller change to be implemented
T	observation interval
\underline{T}	transition matrix in differential quadrature

\underline{u}	control vector
\underline{U}	covariance matrix of parameters
\underline{v}	random noise vector
V	volume, m^3
V_{MO}	mill zero volume (no overflow)
\underline{W}	Wiener process vector
\underline{x}	state vector
\underline{y}	observation vector
Y_k	set of observations up to time t_k
$\alpha_1, \alpha_2, \alpha_3$	coefficients in breakage function, equation (4.2.5)
α_{1j}, α_{2j}	coefficients in Kolmogorov equation (4.1.4)
β_i	mill classification parameters as in figure 4.4
γ_i	sump classification parameters as in fig. 4.4
$\underline{\Gamma}$	noise matrix for discrete linear processes
δ_{im}	Kroeneker delta
∂^2_m	operation defined by equation (4.1.21)
Δu	change in controls
$\underline{\Delta U}$	covariance of control changes
ϵ_u	error in underflow volume rate
η_i	cyclone overflow tank classification parameters in fig. 4.4
θ	differential quadrature coefficients
μ_i	i th moment (not control)
ρ_s	solids density, kg/m^3
σ^2_{ϵ}	variance of ϵ_u
ϕ_i	noise attenuation factor in mill model
$\underline{\Phi}$	state transition matrix for discrete linear processes
$\underline{\Psi}$	parameter matrix for discrete linear processes
ω	random symbol in a random variable

Subscripts, superscripts and symbols

Subscripts i , j , k , l , m , and n were used for indexing.

Subscripts M , V , O , U , and F refer to the mill, sump, cyclone overflow, cyclone underflow and cyclone feed respectively.

k as in t_k is the time at observation k

$k+$ = time immediately after observation k

$k-$ = time immediately before observation k

$-$ = mean value

\wedge = estimate of mean

$-$ = vector

$=$ = matrix

Superscript T refers to matrix transpose.